Vibration, Buckling and Parametric Instability of Delaminated Composite Panels in Hygrothermal Environment

A thesis submitted

for the award of the degree of

Doctor of Philosophy

in

Engineering

by

Himanshu Sekhar Panda

under the supervision of

Prof. Shishir Kumar Sahu

Department of Civil Engineering

National Institute of Technology,

Rourkela, India

In sweet memory

of

our beloved little angel

Chinu

(Born: 15th June 2001)
(Passed away: 24th January 2013)

Twadiyam bastu Govinda tubhyameba samarpaye
Tena twadanghri kamale ratim me yachha saaswatim

Department of Civil Engineering

National Institute of Technology Rourkela

Rourkela-769 008, Odisha, India. www.nitrkl.ac.in

Prof. Shishir Kumar Sahu

Professor and Head

29 Feb, 2016

Certificate

This is to certify that the thesis entitled ***Vibration, Buckling and Parametric Instability of Delaminated Composite Panels in Hygrothermal Environment*** being submitted to the National Institute of Technology, Rourkela , India by ***Himanshu Sekhar Panda*** is a record of an original research work carried out by him under my supervision and guidance towards fulfilment of the requirements for the award of the degree of *Doctor of Philosophy* in *Engineering*.The results embodied in this thesis have not been submitted to any other university or institute for the award of any degree.

(Prof. Shishir Kumar Sahu)

Acknowledgements

Contributions from many persons in numerous ways helped this research work and they deserve special thanks. It is a pleasure to convey my gratitude to all of them.

I would like to express my deep sense of gratitude and indebtedness to my supervisor **Prof. Shishir Kumar Sahu** for his advice and guidance from early stage of this research and providing me extraordinary experiences throughout the work.

I am grateful to **Prof. Sarat Kumar Das, Prof. K. C. Biswal, Prof. K. C. Patra, Prof. N. Roy, Prof. P. Sarkar, Prof. R. Davis, Prof. P. K. Bhuyan** of Civil Engineering Department, **Prof. B. C. Roy, Prof. B. B. Verma** of Metallurgy and Minerals Engineering Department, **Prof. S. K. Sahoo, Prof. S. C. Mohanty, Prof. Alok Satpathy** of Mechanical Engineering Department, NIT, Rourkela for their kind support and concern regarding my academic requirements. I express my thankfulness to the faculty and staff members of the Civil Engineering Department for their continuous encouragement and suggestions. Among them, **Samir, Lugun, Garnaik, Tutu, Hembram** deserve special thanks for their kind cooperation in laboratory and non-academic matters during the research work.

I am indebted to **Deba, Meena, Kuppu, Venky, Krishna, Satish, Naveen, Srilatha, Patel, Partha, Bikash, Chary, Manoj, Vishal, Prashant, Sambit, Karan, Sailesh, Mangal, Bunil, Biplab, Somen, Biraja and Rabi** for their support and co-operation which is difficult to express in words. The time spent with them will remain in my memory for years to come.

Thanks are also due to my co-scholars at NIT, Rourkela, for their whole hearted support and cooperation during the duration of this work.

My **Mommy, Nana, Bou, Tuku** and little masters **Munu and Kunu** deserve special mention for their inseparable support and prayers. The completion of this work came at the expense of my long hours of absence from home.

Words fail to express my appreciation to my **Master J. K. Dash**, elder brothers **P.K. Parhi, P. K. Rautray, R. K. Galgali, M. K. Roul** for being supportive and caring throughout the course of my doctoral dissertation. Apart from the above mentioned names, there are a lot of well-wishers who stretched their heads and hands

towards the Almighty for successful completion of my work. This work is dedicated to all of them.

Lastly, I must mention here the two names: my maternal uncle **late Kailash Chandra Panda** and my father **late Harekrushna Panda**, who would have been the happiest men in this universe if they would have seen this day. My holy prostrations to both of them.

The two poems, namely **A psalm of life by H. W. Longfellow and All things shall pass away by Theodore Tilton** echoed from my memories of adulthood frequently to bring back to normalcy from the sorrowful moods during the research work. I owe a lot to both the poets. This is the beginning and miles to go before I sleep.

I am really indebted to **Prof. Manoranjan Barik**, the LaTeX lover and an outstanding programmer in all the recent languages, for teaching me MATLAB and LaTeX unhesitatingly, whenever I have approached him.

On several occasions, I have faced many challenges from all sorts of *people having negative mentalities*, that reinforced me to tread in the *bivoucs of life*. I am thankful to all of them.

Finally, I surrender myself to the **Omnipresent *BABAJI*** for guiding me at every footstep during the course of this research work.

(**Himanshu Sekhar Panda**)

About the Author

Himanshu Sekhar Panda graduated in Civil Engineering with first class (Hons.) from University College of Engineering, Burla, Sambalpur in 1992. He then worked in several construction companies for ten years and joined Water Resources Department, Government of Odisha in 2003. He left the govt. job in 2008 and continued post graduate programme in structural engineering specialisation at College of Engineering and Technology, Bhubaneswar. He received the Masters degree in 2010 having been topped in the list of successful candidates in the university. In 2011, he joined the doctoral programme in the Department of Civil Engineering, National Institute of Technology, Rourkela. He is a member of American Society of Civil Engineers (ASCE), charter member of Structural Engineering Institute (SEI) and life member of Indian Society of Technical Education (ISTE).

The authors research interests lie in Computational and Experimental Mechanics of Composite Structures using Finite Element Method.

LIST OF PUBLICATIONS

<u>International Journals</u>

- **H. S. Panda, S. K. Sahu and P.K. Parhi (2013)**: Hygrothermal effects on free vibration of delaminated woven fiber composite plates - Numerical and experimental results, *Composite Structures*, Vol.**96**, pp. 502-513.

- **H. S. Panda, S. K. Sahu, P.K. Parhi and A.V. Asha (2015)**: Vibration of woven fiber composite doubly curved panels with strip delamination in thermal field, *Journal of Vibration and Control*, Vol.**21** (15), pp.3072-3089.

- **H. S. Panda, S. K. Sahu and P.K. Parhi (2014)**: Effects of moisture on the frequencies of vibration of woven fiber composite doubly curved panels with strip delaminations, *Thin Walled Structures*, Vol.**78**, pp.79-86.

- **H. S. Panda, S. K. Sahu and P.K. Parhi (2015)**: Buckling behavior of bidirectional composite flat panels with delaminations in hygrothermal field, *Acta Mechanica*, Vol.**226** (6), pp.1971-1992.

- **H. S. Panda, S. K. Sahu and P.K. Parhi (2015)**: Hygrothermal response on parametric instability of delaminated bidirectional composite flat panels, *European Journal of Mechanics A/Solids*, Vol.**53**, pp.268-281.

- **H. S. Panda, S. K. Sahu and P.K. Parhi (2015)**: Thermal effects on parametric instability of delaminated woven fabric composite curved panels, *International Journal of Structural Stability and Dynamics*, In Press.

<u>International Conferences</u>

- **S. K. Sahu, H. S. Panda and P.K. Parhi (2013)**: Numerical and experimental studies on free vibration of delaminated woven fiber composite plates at elevated temperatures, *Fourth International Conference on Recent Advances in Composite Materials (ICRACM - 2013)*, February 18-21 at Goa, India.

- **S. K. Sahu, H. S. Panda and P.K. Parhi (2013)**: Thermal effects on vibration of delaminated composite doubly curved panels, *Seventh International*

Conference on Materials for Advanced Technologies (ICMAT 2013), June 30-July 05 at Singapore.

- **H. S. Panda, S. K. Sahu and P.K. Parhi (2013)**: Modal analysis of delaminated woven fiber composite plates in moist environment, *International conference on Structural Engineering and Mechanics (ICSEM 2013)*, December 20-22, India.

Abstract

The present investigation deals with free vibration, static and dynamic stability performance of bidirectional delaminated composite flat and curved panels with in-plane periodic loading in hygrothermal environment.

The dynamic instability under in-plane periodic forces for delaminated woven fiber composite panels are studied in varying environmental conditions of temperature and moisture using finite element method (FEM). Numerical analysis by FEM and experimental studies are conducted on free vibration and buckling response of bidirectional delaminated composite panels in hygrothermal environment. The influences of various parameters such as hygrothermal conditions, area and strip delaminations, boundary conditions, ply orientations, stacking sequence, curvatures, static and dynamic load factors on the free vibration, static and parametric instability characteristics of bidirectional composite panels are considered in the present study.

A finite element model is developed having 8-noded isoparametric element with 5 degrees of freedom (DOF) per node for the vibration, static and dynamic instability characteristics of delaminated bidirectional composite flat and curved panels under hygrothermal environment utilizing first order shear deformation theory (FSDT). Principal instability zones are located by solutions of Mathieu-Hill equations using Bolotins approach. Based on principle of minimum potential energy, the elastic stiffness matrix, geometric stiffness matrix due to hygrothermal and applied loads, mass matrix and load vectors are formulated. Provision for area and strip delamination modeling is also made in the numerical analysis using multi-point constraint algorithm. A general formulation for vibration, buckling and dynamic stability characteristics of bidirectional delaminated composite flat and curved panels under in-plane periodic forces is presented.The materials utilised for casting of specimens are bidirectional Glass fiber, epoxy as resin, hardener, polyvinyl alcohol as a releasing agent and Teflon film for introducing artificial delaminations. The material constants are calculated from the tensile tests of coupons under varying temperature and moisture conditions as per appropriate ASTM standards. For free vibration testing, FFT analyzer with PULSE Labshop software is used. A test set up is fabricated for vibration

test of composite plates under different boundary conditions.The Universal testing machine INSTRON 8862 is used for determination buckling loads experimentally.

A good matching is observed between predicted and test results for free vibration and buckling of delaminated composite panels in hygrothermal field. The natural frequencies and buckling loads are observed to decrease with increase in delamination at elevated temperature and moisture conditions under different boundary conditions. However, an increment in the fundamental frequencies is found at sub-zero temperatures up to cryogenic range as against ambient conditions because of development of compressive residual stresses at sub-zero temperatures. Numerical results of finite element analysis (FEA) on instability study of delaminated composite panels conclude that dynamic instability regions (DIR) tend to move towards lesser excitation frequencies due to the static load factor of in-plane load. The onset of instability occurs earlier and the width of dynamic instability regions increases at elevated temperature and moisture contents for several parameters. It is observed that the ply stacking considerably affects the onset of instability region for delaminated composite panels in hygrothermal field for various boundary conditions. This property can be made use of tailoring the design of delaminated composite panels exposed to hygrothermal environment.

Key words: Bidirectional fiber, delamination, hygrothermal field, natural frequency, buckling, excitation frequency, parametric instability.

List of Symbols

The principal symbols used in this thesis are presented for easy reference. A single symbol is used for different meanings depending on the context and defined in the text as they occur.

English

a, b	dimensions of plate/shell
h	thickness of plate/shell
$[B]$	strain matrix for the element
$[D]$	Matrix of stiffnesses
E_{11}, E_{22}	modulus of elasticity
G_{12}, G_{13}, G_{23}	shear modulus of rigidity
$\|J\|$	jacobian
$[K]$	global elastic stiffness matrix
$\left[K_\sigma^N\right]$	global geometric stiffness matrix due to hygrothermal loads
$[K_\sigma^a]$	global geometric stiffness matrix due to applied loads
$[M]$	global consistent mass matrix
N_x, N_y, N_{xy}	in-plane stress resultants of the plate/shell
M_x, M_y, M_{xy}	bending moments of the plate/shell
$\{P\}$	global load vector
R_x, R_y, R_{xy}	radii of curvature of shell
u, v	in-plane displacements
w	out of plane displacement
L_S, L_D	static and dynamic load factors
T, T_0	elevated and reference temperatures respectively

C, C_0	elevated and reference moisture contents respectively
$N(t)$	in-plane harmonic load
N_S	static portion of the load N(t)
N_D	dynamic portion of the load N(t)
k	shear correction factor
$\{q\}$	vector of degrees of freedom
N_{cr}	critical load

Greek

$\sigma_x, \sigma_y, \tau_{xy}$	stresses at a point
$\epsilon_x, \epsilon_y, \gamma_{xy}$	bending strains
ν	Poisson´s ratio
$\frac{\partial}{\partial x}, \frac{\partial}{\partial y}$	partial derivatives with respect to x and y
ρ	mass density of the material
θ_x, θ_y	slopes normal and transverse to the boundary
$\kappa_x, \kappa_y, \kappa_{xy}$	curvatures of the plate/shell
ω, Ω	frequencies of vibration and forcing function
ω	natural frequency in rad/sec
ϖ	non-dimensional frequency
Ω	excitation frequency in rad/sec
$\bar{\Omega}$	non-dimensional excitation frequency
α_1, α_2	thermal coefficients along 1 and 2 axes of lamina respectively
β_1, β_2	moisture coefficients along 1 and 2 axes of lamina respectively
ξ, η	natural coordinate axes system of element

Mathematical Operators

$[\,]^{-1}$	inverse of the matrix
$[\,]^T$	transpose of the matrix

List of Abbreviations

The abbreviations used in this thesis are presented for easy reference.

DIR	Dynamic Instability Region
FEM	Finite Element Method
FEA	Finite Element Analysis
$FSDT$	First Order Shear Deformation Theory
BC	Boundary Condition
FRF	Frequency Response Function
$C-C-C-C$	All four sides clamped
$S-S-S-S$	All four sides simply supported
$C-F-F-F$	One side clamped and other three sides free
$C-F-C-F$	Two opposite sides clamped and two other sides free
$C-S-C-S$	Two opposite sides clamped and two other sides simply supported

Contents

List of Figures

List of Tables

Chapter - 1

Introduction

1.1 Background

Fiber reinforced composites are considered as a group of engineering materials that have better utilization as structural components in aerospace industry, automotive panels, turbine blades, marine structures, medical equipment along with roofs of auditoriums, airports and many more due to the exceptional specific strength, specific stiffness and prospect for tailoring the properties to boost structural behavior. Besides military aircraft, noteworthy applications are reported to the tune of more than 50% composites in Airbus 350/ Airbus 380, Boeing 787 dreamliner and BMW Oracle sailboat, pressure vessels in which significant temperature and moisture variations are encountered. A significant temperature gradient is observed during flight and landing conditions of aircraft. Moisture variations are observed for naval, sailboat and other applications. These structures are vulnerable to delamination damage, which are generally prompted by fabrication defect, low velocity impact, structures- free edge effect or by reversal of stresses during transportation to operation. The combination of above two influences becomes critical, which finally affects the free vibration, buckling response and dynamic stability of composite panels due to introduction of residual stresses.

1.2 Importance of present structural stability study

Structural elements are frequently subjected to in-plane periodic loading during service and become unstable dynamically with increase in amplitude of transverse vibration for certain combination of load and disturbing frequency parameters. Above phenomenon is known as dynamic instability or parametric resonance or parametric instability. This dynamic instability can take place at much lower than critical load of structure under compressive loading over a series of excitation frequencies. Several means of combating dynamic instability such as damping and vibration isolation may be inadequate and sometimes dangerous with reverse results. Apart from principal resonance, the dynamic instability can occur not merely at a single excitation frequency but even for small excitation amplitudes and combination of frequencies. The division between good and bad vibration systems of a structure under in-plane periodic forces can be known from an analysis of dynamic instability region (DIR) spectra. Again the presence of delamination and hygrothermal conditions may increase the complicacies linked to parametric resonance of the laminated composite panels. So, the evaluation of these parameters with sufficiently high precision is an integral part of dynamic instability analysis of delaminated composite panels in hygrothermal field. The wide range of practical applications demands a vital understanding of vibration, static and dynamic stability characteristics of delaminated composite panels under hygrothermal conditions.

1.3 Objectives of present research

The present research work mainly focuses on the study of vibration, static and dynamic stability of industry driven bidirectional Glass/Epoxy delaminated composite flat and curved panels in hygrothermal environment. The objectives of the present research is dynamic characterization of delaminated composite panels under hygrothermal environment. A thorough review of earlier works done in this field is an important requirement to arrive at the objective and scope of the present investigation.

Chapter - 2

Literature Review

2.1 Introduction

Increasing demand of composite panels is the subject of research for many years. Although, the present investigations are mainly focused on dynamic stability analysis of delaminated composite panels in hygrothermal environment, some relevant research works on free vibration and buckling of delaminated composite panels in hygrothermal field are also considered for the sake of its relevance and completeness. Some of the relevant studies done recently are reviewed elaborately and critically discussed to identify the lacunae in existing literature. The literature reviewed in this chapter is divided into three major aspects as:

- Vibration of delaminated composite panels in hygrothermal field.
- Buckling of delaminated composite panels in hygrothermal field.
- Parametric instability of delaminated composite panels in hygrothermal field.

The literature for each problem above is discussed in terms of lamination (i.e. laminated or delaminated), geometry (i.e. plates and shells) and consideration of hygrothermal environment (i.e. ambient condition, temperature or moisture effects) etc. for completeness.

2.2 Vibration of delaminated composite panels in hygrothermal field

Plenty of studies are available on vibration of laminated composite plates under ambient temperature and moisture conditions by using different theories and reviewed by Leissa [1987], and Zhang and Yang [2009]. The natural frequency and mode shapes of a number of CFRP plates were experimentally determined by Cawley and adams [1978]. The First order Shear Deformation Theory (FSDT) was considered more efficient for the prediction of the global responses, i.e., the transverse displacements, the free vibration frequencies, and the buckling loads as reported by Reddy [1979]. Higher order Shear Deformation Theory (HSDT) was developed by Kant and Mallikarjuna [1989] to improve the predictions of laminate static and dynamic behavior. Reddy [1990] presented a layer wise theory for the analysis of free vibration of laminated plates. Narita and Leissa [1992] developed an analytical method for the free vibration of cantilevered rectangular plates. An experimental and numerical investigation into the structural behavior of symmetrically laminated carbon fiber-epoxy composite rectangular plates subjected to vibration was studied by Chai et al. [1993]. Raleigh-Ritz method was employed by Chai [1994] to study the free vibration behavior of laminated plates with various edge support conditions in addition to experiments performed using TV-holography technique to verify the predicted results for composite laminates. Linear vibration analysis of laminated rectangular plates was reported by Han and Petyt [1996]. Chakraborty and Mukhopadhyay [2000] presented a combined experimental and numerical study of free vibration behavior of composite unidirectional plates for determining the frequency response functions for extracting modal parameters based on finite element method.

However, delamination related researches on composite plates are few. The delamination problem of composite panels is generally more complex which involve material discontinuities. Due to its practical applications, some researchers have shown significant interest in determining the natural frequencies of delaminated composite panels.

Della and Shu [2007] presented a detailed review on different mathematical models for vibration of composite panels having delaminations. DiScivua [1986] proposed a displacement model based on a piece wise linear displacement field to predict the vibration frequencies of three layered symmetric cross ply square composite plates with simply supported boundary condition only. The impact of delaminations on natural frequencies of vibration of composite plates was studied by Tenek et al. [1993] using FEM based on three dimensional theory of linear elasticity. Based on Mindlin´ s plate theory, Ju et al. [1995] used finite element formulation for calculation of natural frequencies of vibration of unidirectional composite panels with delaminations. Finite element approach was presented by Ju et al. [1995] for analyzing free vibration behavior of square and circular composite plates with delaminations around internal cut outs. A finite element model was developed by Krawezuk et al. [1997] to study the dynamic behaviour of cracked composites. Chang et al. [1998] investigated the vibration of composite plates on elastic foundation with delaminations under axial load only based on the concept of continuous analysis. Zak et al. [2000] presented the natural frequencies of unidirectional composite beams and plates with delaminations using FSDT and two dimensional finite element modeling. Parhi et al. [2000] extended the two dimensional model proposed by Gim [1994] for single delamination to investigate the dynamic characteristics having single and multiple delaminations of composite panels using FEM for unidirectional fibers only.

Cho and Kim [2001] proposed higher order layer wise zig-zag theory for predicting the dynamic behavior of laminated composites with multiple delaminations. Zak et al. [2001] studied the effects of the delamination on changes in vibration characteristics of the unidirectional composite panels by finite element method. Ostachowicz and Kaczmarczyk [2001] predicted the effects of delaminations on the natural frequencies of vibration of composite plates with SMA fibers using a finite element model. Higher order plate theory was used by Hu et al. [2002] for determining the effects of delamination on natural frequencies of delaminated composite plates with FEM. Thornburg and Chattopadhyay [2003] used finite element method to analyze the vibration behavior of composite laminates having delaminations. Kim et al. [2003]

utilized first order layer wise zig-zag theory for the dynamic analysis of composite plates with through-width delaminations. Suzuki et al. [2004] used multilayered finite element numerical analysis for non-linear vibration and damping characterization of delaminated CFRP composite laminates. A finite element model for prediction of dynamic characteristics of delaminated composite plates was proposed by Yam et al. [2004]. A numerical analysis based on FEM was presented by Chen et al. [2004] to study the dynamic response characteristics of delaminated composite plates with two dimensional models using FSDT. A four-noded finite element formulation based on high-order zig-zag plate theory for delaminated composite plates to predict the vibration characteristics was developed by Oh et al. [2005]. Based on higher order zig-zag theory, Jinho et al. [2005] reported the dynamic behavior of laminated composite plates with multiple delaminations using FEM. Kumar and Shrivastava [2005] used a finite element model based on higher order shear deformation theory and Hamilton's principle for studying the free vibration characteristics of square composite plates having delaminations around central rectangular cut out. Alnefaie [2009] presented three dimensional finite element models for calculation of natural frequencies and modal displacements of delaminated fiber reinforced composite plates. Shiau and Zeng [2010] investigated on the effect of delamination on free vibration of a simply supported rectangular homogeneous plate with through-width delamination by the finite strip method. Radial point interpolation method (RPIM) in Hamilton system was used by Li et al. [2011] for predicting the free vibration frequencies of composite laminates with interfacial imperfections. Gallego et al. [2013] developed a method for damage detection of delaminated CFRP plates by Ritz/2-d wavelet analysis using the vibration modes obtained from finite element analysis. Using fracture mechanics principles, Panigrahi [2013] dealt with the structural design of single lap joints with delaminated FRP composite adherends. Marjanovic and Vuksanovic [2014] utilized Reddy's layer wise plate theory extending it to include delaminations for predicting the natural frequencies of delaminated composite and sandwich plates. Using FEM, Kumar et al. [2014] studied the free mode vibration of delaminated composite plates with variable kinematic multi-layer elements.

Modal testing is a versatile technique and is used recently by many investigators including Muggleton et al. [2014] for detection of buried infrastructures. However, very little amount of literature related to experimental results on vibration of composite plates with delaminations are witnessed. Champanelli and Engblom [1995] determined vibration results of unidirectional delaminated Graphite/PEEK composite plates and compared with numerical counterparts using FEM. Modal analysis experiments on cantilever composite plates with strip delaminations were conducted by Luo and Hanagud [1996]. Hou and Jeronimidis [1999] made experimental tests on composite plates with delaminations which are induced by impact.

But the behaviour of composite structures under varying temperature and moisture is of practical interest. Few researchers have shown interest in investigating the environmental effects on frequencies of vibration of composite plates. Tauchert [1991] reviewed the investigations on the vibration of thick plates exposed to temperature. Vibration of thick laminated composite plates in hygrothermal field was investigated by Gandhi et al. [1988]. Chen and Lee [1988] reported the vibrations of a simply supported orthotropic plate induced by thermal parameters using differential equation. Chen and Chen [1989] studied the free vibration response of laminated composite plates under hygrothermal environment by finite element method. Using FEM, Sairam and Sinha [1992] presented the effects of temperature and moisture on the natural frequencies of laminated unidirectional composite plates for simply supported and clamped boundary conditions only. Analytical three dimensional solutions for the free vibrations of thermally stressed laminated composite plates were presented by Noor and Burton [1992]. Liu and Huang [1995] investigated the natural frequencies of laminated composite plates exposed to temperature using finite element method. Vibrations of composite plates exposed to temperature and moisture was studied by Eslami and Maerz [1995] using finite element method. Lai and Young [1995] reported the natural frequencies of free vibration of graphite/epoxy composites having delamination in environmental conditions.

Patel et al. [2000] investigated vibration characteristics of composite laminates under hygrothermal field using finite element method. Rao and Sinha [2004] pre-

sented the influences of temperature and moisture on free vibration and transient response of laminated composites using 3D finite element analysis. Effects of hygrothermal conditions on the dynamic characteristics of shear deformable laminated plates on elastic foundations was studied by Shen et al. [2004] using a micro-mechanical analytical model. Vibrations of shear deformable laminated plates in hygrothermal field were examined by Huang et al. [2004] based on higher-order shear deformation theory. Abot et al. [2005] reported the moisture absorption process of woven fiber carbon-epoxy composites experimentally and its effect on visco-elastic properties. Matsunaga [2007] presented the free vibration characteristics of laminated composite sandwich plates under thermal loading using power series expansion method.

Vibration responses of laminated composite plates in thermal exposure were described by Jeyaraj et al. [2009], using FEM. Lal and Singh [2010] investigated the free vibration behavior of laminated composite plates under thermal environment using finite element method. Fakhari and Ohadi [2010] examined the large amplitude vibration of functionally graded material (FGM) plates under thermal gradient and transverse mechanical loads using finite element method. Lo et al. [2010] proposed global-local higher order theory to study the response of laminated composite plates in varying hygrothermal environment pertaining to the material properties.

All the above studies deal with numerical analysis of vibration characteristics of unidirectional laminates exposed to hygrothermal environment. But the experimental investigations on this topic are rare in literature. Natural frequencies of laminated composite plates were determined by Anderson and Nayfeh [1996] using experimental modal analysis and compared with FEM prediction.

The widespread use of shell structures in aerospace applications has stimulated many researchers to study various aspects of their structural behaviour. In the present study an attempt is made to the reviews on shells in the context of the present work but discussions are limited to vibration and stability. Studies of vibration of laminated composite curved panels of different geometry, boundary conditions having different models were reviewed by Liew et al. [1997] through 1992 and Qatu et al. [2010] through 2009. Leissa and Narita [1984] used Ritz method to calculate the

frequencies of vibration of free-free shells with rectangular planform. The free vibration characteristics of laminated composite shells are studied using an isoparametric doubly curved quadrilateral shear flexible element by Chandrashekhara [1989] using shear deformable Sanders´ theory. Vibrations of thin laminated composite shallow shells with two adjacent edges clamped and remaining free were analyzed by Qatu [1993] by Ritz technique. Ding and Tang [1999] suggested a three dimensional theory for free vibration of thick laminated cylindrical shells with clamped edges. Qatu [1999] studied the vibration response of composite laminated barrel thin shells.

Using a layerwise B-spline finite strip method, Zhang et al. [2006] presented the frequencies of vibration of rectangular composite laminates. Asadi and Qatu [2012] used general differential quadrature method for calculating the frequencies of vibration of thick laminated cylindrical shells with different boundary conditions. Viola et al. [2013] determined frequencies of free vibration of completely doubly curved laminated shells using general higher order shear deformation theory. Kumar et al. [2013] used FEM with higher order shear deformation theory (HSDT) to calculate the fundamental frequencies of vibration of laminated composite skew hypar shells. Fazzolari and Carrera [2013] investigated the free vibration response of doubly curved anisotropic laminated composite shallow and deep shells by advanced Ritz technique. Applying Sanders' theory, Strozzi and Pellicano [2013] examined the nonlinear natural frequencies of vibrations of functionally graded cylindrical shells.

Very few studies are available on vibration of delaminated composite shell panels. Karmakar et al. [2005] presented a numerical approach for determination of natural frequencies of composite pre-twisted shallow shells with delaminations. Acharya et al. [2007] investigated the free vibration characteristics of composite cylindrical shells with delaminations. Jansen [2007] studied the vibration behavior of anisotropic cylindrical shells with geometric imperfections. Using FEM, Lee and Chung [2010] determined the natural frequencies of composite spherical shell panels with delaminations around central cutouts. Acharyya [2010] calculated the natural frequencies of delaminated composite shallow cylindrical shells based on FEM. Hadi and ameen [2011] characterized the embedded delamination on the dynamic response of com-

posite laminated structures by finite element modeling for geometrically nonlinear large amplitude vibration of shallow cylindrical and delamination shells. Dey and Karmakar [2012] used FEM for computation of natural frequencies of vibration of multiple delaminated angle ply composite conical shells. Nanda and Sahu [2012] determined the natural frequencies of delaminated composite shells in finite element technique using different shell theories. Based on Mindlin's theory, Dey and Karmakar [2012] studied the effects of rotational speed on free vibration behavior of twisted cross ply composite delaminated conical shells employing FEM. Based on Sanders' third order shear deformation theory, Noh and Lee [2012] presented natural frequencies of vibration of composite laminated spherical shells only with embedded rectangular delaminations. Based on Mindlin's theory, Dey and Karmakar [2013] studied the delamination effects on free vibration characteristics of quasi-isotropic conical shells. The above studies are on the free vibration behavior of composite shells with delaminations under ambient conditions only.

A handful of researchers have shown interest in the field of dynamic behavior of composite panels in hygrothermal environments without considering the effects of delaminations. The vibration response of flat and curved panels subjected to thermal and mechanical loads are presented by Librescu and Lin [1996]. The dynamic analysis of laminated cross-ply composite noncircular thick cylindrical shells subjected to thermal/mechanical load are carried out based on higher-order theory was studied by Ganapathi et al. [2002]. Liew et al. [2006] presented linear and nonlinear numerical vibration frequencies of coating-FGM-substrate cylindrical panels subjected to a temperature gradient by using first order shear deformation theory. The nonlinear free vibration behavior of laminated composite shells subjected to hygrothermal environment was investigated by Naidu and Sinha [2007]. Geometrically nonlinear vibrations of linear elastic composite laminated shallow shells under the simultaneous action of thermal fields and mechanical excitations are analyzed by Ribeiro and Jansen [2008]. The vibration characteristics of pre and post-buckled hygro-thermo-elastic laminated composite doubly curved shells were investigated by Kundu and Han [2009].

Considering the effects of delaminations, some studies on vibration of unidirec-

tional composite shells in hygrothermal field are also available in open literature. Parhi et al. [2001] investigated the effect of moisture and temperature on the natural frequencies of composite laminated plates and shells with and without delaminations. Nanda et al. [2010] studied the effects of delaminations on the nonlinear transient behavior of composite shells in hygrothermal environment. Frostig and Thomsen [2011] examined the geometrically nonlinear behavior of debonded curved sandwich panels subjected to thermal and mechanical loading. Nanda and pradyumna [2011] presented the results of free vibration frequencies of laminated shells with geometric imperfections in hygrothermal environments. Alijani et al. [2011] used multi modal energy approach for study of thermal effects on vibration of functionally graded doubly curved shells. All these researchers studied the response of delaminations on dynamic characteristics of composite panels having unidirectional fibers only.

A combined attempt to have a numerical solution and experimental verification of numerical results of vibration of delaminated bidirectional composite panels exposed to hygrothermal environment is an important task.

2.3 Buckling of delaminated composite panels in hygrothermal field

Related research papers on buckling characteristics of laminated and delaminated composite panels under ambient as well as hygrothermal environments are presented in a chronological manner. The laminated ambient cases are presented for completeness on the subject.

Plenty of research papers are available in open literature on buckling behavior of laminated composite plates at ambient conditions. A detailed review of buckling of laminated composite plates was reported by Leissa [1987]. The characteristics and parameters related to buckling analysis of laminated composite plates, both from mathematical and physical points of view that provides perspective and organization on the subject were considered by Leissa [1983].The buckling loads for laminated

plates under unidirectional loading were investigated by Chai and Khong [1993] using LVDT. Salim et al. [1998] studied the effect of material parameter randomness on the initial buckling load of composite laminates based on classical laminate theory.

Shukla et al. [2005] proposed a formulation based on the first-order shear deformation theory to estimate the buckling loads of laminated composite rectangular plates under in-plane uniaxial and biaxial loadings. Numerical and experimental studies were conducted by Baba [2007] to study the influence of boundary conditions on the buckling load for laminated composite rectangular plates. Baba and Baltaci [2007] carried out numerical and experimental studies to determine the buckling behavior of laminated composite plates with central cut out by taking the help of ANSYS code for theoretical calculations. Buckling load of laminated composites plate with different boundary conditions using FEM and analytical methods was presented by Ozben [2009]. Buckling analysis of laminated composite plates was presented by Ovesy et al. [2010] using higher order semi-analytical finite strip method. Pietropaoli and Riccio [2012] discussed various issues related to linear and non-linear buckling analysis of composite structures attempting to bridge the gap between current researchers and already published literature. Buckling analysis of laminated composite plate assemblies based on higher order shear deformation theory was used by Fazzolari and Carrera [2013] using Wittrick-Williams algorithm as a solution technique for computation of critical buckling loads.

Few researchers studied the buckling behavior of delaminated composite flat panels in ambient conditions. Sallam and Simitses [1985] presented results on buckling of composite laminates with delaminations using one-dimensional model. Pavier and Chester [1990] studied the compressive failure of carbon fiber-reinforced laminates with delaminations. Kutlu and Chang [1992] performed a combined analytical and experimental investigation on unidirectional laminates to study the buckling of delaminated composites. Suemasu [1993] determined the buckling characteristics of delaminated composite panels experimentally and analytically, using Rayleigh-Ritz approximation technique. The buckling behavior of delaminated plates under uniaxial compressive loading was examined experimentally and analytically by Yeh and

Tan [1994]. A finite element model to study buckling behavior of delaminated composite shells was reported by Kim and Hong [1997]. Gu and Chattopadhyay [1999] presented experimental investigations on buckling behavior of delaminated composite plates. Kim and Kedward [1999] presented an analytical method for predicting local and global buckling initiation of composite plates with delaminations. Based on Mindlin plate theory, buckling analysis of composite laminates with embedded delaminations was carried out by Hu et al. [1999] employing FEM.

Hwang and Mao [2001] predicted the buckling loads of unidirectional carbon/epoxy composites having strip delaminations. The buckling behavior of delaminated composites was experimentally and numerically studied by Hwang and Liu [2002]. Shan and Pelegri [2003] proposed an approximate analytical method for predicting the buckling behavior of delaminated composites. A 3D finite element model of delaminated plates to study the buckling loads was utilized by Kucuk [2004]. Zor et al. [2005] used a 3D finite element model to study the effects of the delamination on buckling loads of composite panels. Based on Mindlin's first order shear deformation theory, Li et al. [2005] utilized a semi analytical method for predicting the bucking behavior of rectangular delaminated plates. Cappello and Tumino [2006] examined the buckling response of unidirectional composite delaminated plates. ANSYS and experimental results on the buckling of strip delaminated composite panels were carried out by Pekbey and Sayman [2006]. Buckling characteristics of delaminated composite panels were investigated by Lee and Park [2007] using 3D FEM. Tuumino et al. [2007] studied the buckling load of delaminated composite panels by FEM. Buckling characteristics of delaminated composite panels was examined analytically by Kharazi and Ovesy [2008]. Effects of delamination size on buckling characteristics of E-glass/epoxy composite plates with triangular delaminations was reported by Aslan and Sahin [2009].

Numerical analysis of buckling characteristics of composite delaminated flat panels was done by Mohsen and Amin [2010] using a differential quadrature method. Using FEM, the post buckling behavior of composite laminates containing embedded delaminations was studied by Hosseini-Toudeshky et al. [2010]. Buckling characteristics

of delaminated plates under compression was investigated by Obdrzalek and Vrbka [2010] through FEM. Damghani et al. [2011] studied the critical buckling caharacteristics of through-the-length delaminated composite plates using an exact stiffness analysis and compared with results of FEM. Buckling and post-buckling characteristics of an axially loaded delaminated beam-plate was examined by Chattopadhyay and Murthy [2011]. Kang et al. [2011] utilized a numerical procedure to study the buckling behaviour of delaminated composite panels. Tsouvalis and Garganidis [2011] made the buckling strength parametric study of delaminated composite plates. Hajlaoui et al. [2012] proposed an enhanced assumed strain (EAS) hexahedral solid-shell finite element to study the buckling behavior of delaminated composite plates. Liu and Zheng [2013] utilized FEM to predict the buckling characteristics of delaminated composite panels. Using an exact stiffness analysis with Wittrick-Williams algorithm and smearing method, Damghani et al. [2014] proposed global buckling analysis of composite plates with rectangular delaminations only.

Hygrothermal effects on buckling behavior of laminated composite flat panels have been the area of research for a handful of researchers. Based on theorem of minimum potential energy, Flaggs and Vinson [1978] reported the buckling behavior of symmetrically laminated graphite/epoxy composite plates under hygrothermal loading. Chen and Chen [1987] reported the thermal buckling of laminated composite plate subjected to a temperature change using Galerkin's method. Sairam and Sinha [1992] used FEM to determine the buckling response of laminated composite plates under hygrothermal conditions. A refined higher order finite element models for thermal buckling of laminated composite and sandwich plates was proposed by Babu and Kant [2000].

Zor [2003] investigated the buckling loads of the simply supported delaminated composite plates using 3D FE model. Jones [2005] presented the thermal buckling effects of unidirectional and symmetric cross ply laminated composite rectangular plates under simply supported boundary conditions only. Kumar and Singh [2008] studied the thermal buckling analysis of laminated composite plates subjected to uniform temperature distribution using finite element method. Singh and Verma

[2009] investigated the hygrothermal effects on the buckling of laminated composite plates with random geometric and material properties using finite element method. Lal et al. [2009] examined the effects of random system properties on thermal buckling load of laminated composite plates under uniform temperature rise using finite element method.

Lal and Singh [2010] presented the effect uncertain system properties thermoelastic stability of laminated composite plates under nonuniform temperature distribution using finite element method. Post buckling behavior of functionally graded materials in hygrothermal environment was studied by Lee and Kim [2013] using first order shear deformation theory. Zhang et al. [2013] predicted the compressive failure of unidirectional laminates with moisture and temperature effects. Using FEM, Natarajan et al. [2014] reported the effects of moisture concentration and thermal gradient on vibration and buckling of laminated composite plates.

A handful of studies are available on buckling of unidirectional composite shells at ambient conditions with embedded delaminations. Based on higher order zig-zag theory, Oh et al. [2008] studied the buckling behavior of multiple delaminated composite shells using a three noded triangular shell element. Wang et al. [2014] reported an analytical method to study the non-linear buckling characteristics of fiber reinforced piezoelectric laminated shells having rectangular local delamination near the surface. An analytical method was presented by Yang et al. [2014] to investigate the non-linear buckling behavior of functionally graded laminated piezoelectric composite shells having delaminations near the surface. Gaiot et al. [2014] proposed a high order mixed interpolation tensorial components (MITC) shell element approach for predicting the buckling behavior of composite shells with delaminations.

Very few researchers have shown interest in determining the buckling behavior of laminated composite shell panels in ambient as well as hygrothermal conditions. Hygrothermoelastic buckling behaviour of laminated composite shells were numerically simulated using geometrically nonlinear finite element method was studied by Kundu and Han [2009]. Effect of random system properties on the post buckling load of geometrically nonlinear laminated composite cylindrical shell panel subjected

to hygro-thermo-mechanical loading is investigated byLal et al. [2011]. Kumar et al. [2013] investigated the buckling characteristics of laminated curved composite stiffened panels using finite element method(FEM). Buckling behaviour of cracked laminated composite cylindrical shells subjected to combined loading using FEM technique was studied by Allahbakhsh and Shariati [2013].

All the above studies are based on unidirectional composite panels. However, a combined numerical and experimental attempt to investigate the buckling characteristics of delaminated bidirectional composite panels under hygrothermal conditions is an essential assignment.

2.4 Parametric instability of delaminated composite panels in hygrothermal field

Parametric instability related literature on laminated and delaminated composite panels at ambient and hygrothermal conditions are presented in a chronological manner.

The investigations on dynamic stability analysis of structures are much less in comparison to static stability and got a boost after Bolotin [1964] contribution to the literature. A comprehensive review of early developments in the dynamic instability of structural elements including plates was presented in the review article by Simitses [1987]. Recently, an extensive bibliography of earlier works on dynamic stability of plates and shells was presented by Sahu and Datta [2007] from 1987-2005.

Bert and Birman [1987] investigated the dynamic instability of shear deformable antisymmetric angle ply plates. Nguyen et al. [1989] performed experiments to investigate the dynamic stability responses of four rectangular plates subjected to periodic in-plane loads and under four different sets of boundary conditions. Using FSDT, the dynamic stability of laminated composite plates due to periodic in-plane loads was investigated by Chen and Yang [1990]. The dynamic stability of shear deformable plates was studied by Moorthy et al. [1990] using finite element method.

The dynamic stability of laminated composite plates under in-plane periodic loads was studied by Cederbaum [1991] based on higher order shear deformation theory. Kwon [1991] investigated the dynamic instability of composite laminates following finite element method. Mond and Cederbaum [1992] presented the dynamic stability of anti-symmetric laminated plates by using the method of multiple scales. Prabhakara and Datta [1993] reported the parametric instability characteristics of rectangular plates subjected to in-plane periodic load using finite element method, considering shear deformation. Liao and Cheng [1994] studied the dynamic instability characteristics of stiffened isotropic and composite square plate. Deolasi and Datta [1995] examined the parametric instability characteristics of rectangular plates subjected to localized tension and compression edge loading using Bolotin's approach. Deolasi and Datta [1997] experimentally investigated the parametric vibration response characteristics of aluminum plates subjected to tensile edge loading. Ganapathi [1998] proposed the dynamic instability of composite plates subjected to thermal loads using first order shear deformation theory.

Chattopadhyay and Radu [2000] examined the dynamic instability of composite laminates by finite element method using higher-order theory. The dynamic stability characteristics of rectangular composite plates was investigated by Wang and Dawe [2002]. Dynamic stability of composite skew plates under in-plane periodic load was investigated by Dey and Singha [2006]. Chakrabarty and Sheikh [2006] presented the dynamic instability of laminated sandwich plates subjected to in-plane partial edge loading by using finite element method. Lanhe and Hangjur [2007] studied the dynamic stability analysis of FGM plates by the moving least squares differential quadrature method. The dynamic instability analysis of composite laminated thin walled structures was carried out by Fazilati and Ovesy [2010] by using two versions of finite strip method (FSM). Lee [2010] presented finite element dynamic stability of laminated composite skew plates containing cutouts based on higher order shear deformation theory (HSDT). Dynamic stability of shear deformable composite plates subjected to non-uniform loading was examined by Ramchandra and Panda [2012] using Ritz technique. Chen et al. [2013] studied the dynamic stability of laminated

composite plates subjected to arbitrary periodic loads based on first order shear deformation plate theory.

A small amount of literature is available on dynamic instability of delaminated composite plates. Higher order theory was used by Chattopadhyay et al. [2000] for dynamic stability analysis of composite plates having delaminations. Radu and Chattopadhyay [2002] analyzed the dynamic stability of composite plates including delamination using higher order theory with transformation matrix approach. Yeh and Tung [2006] investigated the dynamic instability behavior of delaminated composite plates under transverse excitation experimentally and analytically. Based on higher order shear deformation theory, Noh and Lee [2014] examined the effects of various parameters on dynamic stability of delaminated composite skew plates under various periodic in-plane loads.

A handful of researchers have studied the dynamic stability of laminated composite shells at ambient temperature and moisture conditions. The dynamic stability of circular cylindrical shells under both static and periodic compressive forces was examined by Nagai and Yamaki [1988], based on the Donnell's shell equations. The dynamic stability of laminated anisotropic circular cylindrical shells under axial loading using perturbation technique was examined by Argento and Scott [1993]. The dynamic stability of thin cross-ply laminated composite cylindrical shells under combined static and periodic axial force was investigated by Ng et al. [1998] using Love's classical theory of thin shells. Lam and Ng [1998] presented the dynamic stability analysis of laminated cylindrical shells subjected to conservative periodic axial loads using Loves theory.

Sahu and Datta [2001] used FEM to study parametric instability characteristics of doubly curved panels subjected to various in-plane static and periodic compressive edge loadings. Dynamic stability of laminated composite curved panels under non-uniform loading was investigated by Sahu and Datta [2001] using FEM. Srivastava et al. [2003] investigated the dynamic instability of stiffened plates subjected to non-uniform harmonic edge loading. The research work of Ravi Kumar et al. [2003] dealt with the study of buckling, vibration and dynamic stability of multilaminated curved

panels using FEM. A numerical technique is developed for the dynamic stability analysis of composite laminated cylindrical shell under static and periodic axial forces by mesh-free Ritz method by Liew et al. [2006]. Udar and Datta [2007] investigated the dynamic instability of laminated doubly curved panels with centrally located circular cutout subjected to non-uniform compressive in-plane harmonic edge loading. Numerical technique via kp-Ritz method was utilized by Liew et al. [2007] for dynamic stability analysis of thin composite cylindrical panels.

Pradyumna and Bandyopadhyay [2011] studied the dynamic instability behavior of laminated hypar and conoid shells using higher order shear deformation theory. Asha and Sahu [2011] examined the vibration, buckling and parametric instability characteristics of general laminated cross ply pre twisted cantilever flat and curved panels. Qinkai and Fulei [2013] studied the parametric instability of rotating truncated conical shells by generalized differential quadrature (GQD) method. Ovesy and Fazilati [2014] investigated parametric instability regions of laminated composite plates and cylindrical shells subjected to non-uniform in-plane axial end loading. Dey and Ramachandra [2014] studied the postbuckling and dynamic instability behavior of simply supported composite cylindrical shell panels subjected to dynamic partial edge loadings. Sofiyev [2015] reported the dynamic instability of sandwich cylindrical shells using shear deformation theory.

Few researches are available on parametric instability of composite shells considering delaminations under ambient temperature conditions. An extensive research in the field of delamination mechanics and related defects in laminate and fiber composites was discussed by Bolotin [1996]. Using FEM, Sahu and Datta [2003] studied the dynamic stability characteristics of laminated composite curved panels having cut outs under in-plane static and periodic compressive loads. Yang and Fu [2007] examined the dynamic stability for composite cylindrical panels with delaminations using Raleigh-Ritz method. Park and Lee [2009] investigated parametric instability of delaminated composite spherical shells subjected to in-plane pulsating forces. The dynamic instability of moderately thick laminated cylindrical shell panels having internal cutouts was presented by Fazilati and Ovesy [2012] using the developed finite

strip methods (FSM).

In recent past, a very little amount studies are available on dynamic stability analysis of laminated composite plates and shells in hygrothermal conditions. Chatterjee and Kulkarni [1979] studied the flutter type instability of laminated fiber composite panels based on piston theory aerodynamics and shear deformable laminated plate theory taking into account the environmental factors like temperature and moisture contents. Alijani and amabili [2013] studied the non-linear dynamic instability characteristics of functionally graded plates in thermal environments.

Applying FEM, Lee and Yen [1989] investigated the moisture and temperature effects on the stability of cylindrical composite shell panel subjected to axial or in-plane shear loading. Birman and Bert [1990] presented the dynamic stability analysis of thin multilayered shells reinforced by axial and ring stiffeners in thermal field. Wu and Chiu [2002] presented thermally induced dynamic instability of laminated composite conical shells by means of perturbation method. Pradyumna and Gupta [2011] reported the non-linear dynamic stability characteristics of laminated composite cylindrical and spherical shells integrated with piezoelectric layers using FEM in thermal environment.

However, a combined attempt to study the parametric resonance characteristics of delaminated bidirectional composite panels exposed to hygrothermal environment is an important task.

2.5 Critical Discussions

On the whole, the focus of the research is changing from vibration to buckling effects and then to parametric instability of composite panels. Currently, more studies are conducted on woven fiber composites than unidirectional composites. As regards to the methodology, the focus is shifted from numerical method to experimental method for free vibration and buckling effects of composite plates and shells with delamination exposed to hygrothermal field.

The study shows that the investigators are now concentrating on analysis of com-

plicated aspects of different parameters including delamination and hygrothermal conditions of composite panels. From the above review of literature, the intrinsic lacunae of earlier investigations which need further attention of future researchers are summarized below.

2.5.1 Vibration of delaminated composite panels in hygrothermal field

The review of literature for recent works points out that an ample amount of numerical analytical models was presented for vibration of unidirectional laminated composite panels at ambient conditions. Some studies are available on vibration of delaminated composite panels in ambient temperature and moisture conditions. Ju et al. [1995], Zak et al. [2001] and Yam et al. [2004] investigated the free vibration of delaminated composites by using the FEM. The natural frequencies of composite plates with multiple delaminations were presented by Oh et al. [2005] following a finite element formulation with four node elements based on high-order zig-zag theory. Alnefaie [2009] presented three dimensional finite element model for calculation of natural frequencies of delaminated composite plates. Shiau and Zeng [2010] reported on the effect of delamination on free vibration of a simply supported rectangular homogeneous plate with through-width delamination by the finite strip method.

However, experimental results on vibration of delaminated composite plates are seldom found in literature. Luo and Hanagud [1996] made experimental investigation to study natural frequency of delaminated graphite/PEEK composite plates. Experimental investigation on delaminated composite plates for vibration was made by Hou and Jeronimidis [1999]. Both the tests are restricted to unidirectional fibers only.

The investigations involving free vibrations of bidirectional laminated flat panels exposed to hygrothermal environment are rare in literature. Tauchert [1991] reviewed the reports on the vibration plates under raised temperatures. The free vibration of laminated composite plates in hygrothermal environment by using finite

element method has been investigated by Chen and Chen [1989] and Sairam and Sinha [1992]. Almost all previous reports deal with numerical analysis of vibration characteristics of unidirectional composites exposed to hygrothermal environments. Natural frequencies of laminated unidirectional composite plates were determined by Anderson and Nayfeh [1996] by experimental modal analysis and FEM.

The effect of delamination on free vibration characteristics of composite pretwisted cylindrical shallow shells of different stacking sequences and involving delamination as a parameter was presented by Karmakar et al. [2005].

The free vibration of composite shells in hygrothermal environment has been studied by Librescu and Lin [1996], Parhi et al. [2001], Naidu and Sinha [2007] & Ribeiro and Jansen [2008]. Nonlinear free vibration response of single and doubly curved shell panels was investigated by Kundu and Han [2009]. All the above studies deal with numerical analysis of free vibration response of unidirectional composite shell panels exposed to hygrothermal conditions.

However, combined numerical and experimental investigations on the vibration response of bidirectional composite panels including delaminations exposed to hygrothermal field are not available in open literature and is a subject of present research work for practical interest.

2.5.2 Buckling of delaminated composite panels in hygrothermal field

The studies related to the buckling response of delaminated composite flat panels unser in plane load at ambient conditions are scarce in literature. Sallam and Simitses [1985] followed one one-dimensional model to describe the buckling problem of delaminated composites. Numerical and experimental techniques were developed by some researchers for predicting the buckling load of delaminated composite flat panels (Yeh and Tan [1994], & Gu and Chattopadhyay [1999]).

Kutlu and Chang [1992] studied the buckling behavior of unidirectional delaminated composites by analytical and experimental investigation. A three-dimensional

FEM model was developed by Kucuk [2004], Zor et al. [2005], & Lee and Park [2007] to study the effects of delamination on the buckling loads. Buckling load of multi-delaminated composite panels was studied by Tuumino et al. [2007] using FEM. Liu and Zheng [2013] utilized FEM to predict the buckling and post buckling behavior of symmetric and asymmetric composite laminates having through-the-width multiple delaminations.

Sufficient amount of literature is available on buckling behavior of composite flat panels under ambient environmental conditions. Leissa [1987] reviewed the works on buckling a characteristics associated at elevated temperatures of thin and thick plates. Many investigators worked on buckling analysis of laminated composite plates in thermal environment using different methods by Flaggs and Vinson [1978], & Chen and Chen [1987]. Sairam and Sinha [1992] investigated the effects of moisture and temperature on the buckling of laminated composite plates using finite element method. Studies were also conducted for composite flat panels in thermal field using finite element method by Kumar and Singh [2008], Singh and Verma [2009], Lal et al. [2009], & Lal and Singh [2010]. All the above studies deal with numerical analysis of buckling effects of unidirectional composite flat panels under hygrothermal environment.

However, experimental studies on the buckling effects are scarce in literature. So, the buckling characteristics of bidirectional delaminated composite flat panels under hygrothermal environments are of tremendous technical importance, for which it is a theme for present research.

2.5.3 Parametric instability of delaminated composite panels in hygrothermal field

In comparison to vibration studies, parametric instability of composite structures are less in literature. Bert and Birman [1987] investigated the dynamic instability of shear deformable antisymmetric angle ply plates. Dynamic stability of laminated composite plates due to periodic in-plane loads is investigated by Chen and Yang

[1990]. The dynamic stability of shear deformable plates was studied by Moorthy et al. [1990] using finite element method. Mond and Cederbaum [1992] presented the dynamic stability of anti-symmetric laminated plates by using the method of multiple scales. The dynamic stability of composite plates has been studied using FEM by Liao and Cheng [1994], & Chakrabarty and Sheikh [2006]. Kwon [1991], & Chattopadhyay and Radu [2000] examined the dynamic instability of composite plates by finite element method using higher-order theory. The dynamic stability characteristics of rectangular composite plates were investigated by Wang and Dawe [2002]. The parametric study on dynamic instability behaviour of laminated composite plate was performed by using FEM Lee [2010].Studies were also conducted for the dynamic stability of rectangular plates due to periodic in-plane load by using finite strip method by Fazilati and Ovesy [2010].

However, the studies of dynamic instability behavior of composite plates subjected to delamination are scarce in literature. Radu and Chattopadhyay [2002], Yeh and Tung [2006],Park and Lee [2009], & Noh and Lee [2014] investigated the dynamic instability behavior of delaminated composite plates under transverse excitation.

Ganapathi [1998] proposed the dynamic instability of composite plates subjected to thermal loads using first order shear deformation theory and Lagrange's equation.

No studies are available on parametric instability of bidirectional delaminated composite plates in hygrothermal environment and thus it becomes the subject of present investigation.

The parametric resonance characteristics of composite shells are studied by few investigators without considering the hygrothermal effects. Based on the donnell's shell equations, the dynamic stability of circular cylindrical shells under both static and periodic compressive forces was examined by Nagai and Yamaki [1988]. The dynamic stability of layered anisotropic circular cylindrical shells under axial loading using perturbation technique was investigated by Argento and Scott [1993]. The dynamic stability of thin cross-ply laminated composite cylindrical shells under combined static and periodic axial force was investigated by Ng et al. [1998] using Love's classical theory of thin shells.

In recent past, a very little amount of literature are available on dynamic stability analysis of laminated composite panels in hygrothermal conditions. Wu and Chiu [2002] studied dynamic instability of laminated composite conical shells by means of perturbation method under thermal conditions. Alijani and amabili [2013] presented the dynamic instability behavior of functionally graded plates in thermal field.

Since, the combined influence of delamination and hygrothermal conditions on parametric instability of bidirectional composite panels are not available in literature, the topic is of significant importance for current research.

2.6 Novelty of current research

Vibration, buckling and parametric instability of bidirectional composite flat and curved panels having area and strip delaminations in hygrothermal environment are studied in the present research. So far, no experimental work is reported in open literature on vibration of delaminaed bidirectional composite flat panels subjected to hygrothermal conditions. The author utilises for the first time a combined numerical (by FEM) and experimental (by modal testing) approach for determination of natural frequencies of industry driven woven fabric delaminated composite plates at elevated temperature and moisture conditions. Studies related to the dynamic characteristics of woven fibre composite doubly curved panels having mid plane strip delaminations in thermal field considering sub-zero temperatures up to cryogenic range and elevated moist environment are conducted numerically using FEM as a debut attempt by the author. Open literature lacks research on buckling response of bidirectional composite flat panels under combined influence of delamination and hygrothermal conditions. Numerical and experimental test results on buckling behaviour of delaminated composite plates (symmetric, asymmetric, cross ply as well as angle ply) with different boundary conditions are studied as a first attempt in literature. Investigations related to parametric instability of bidirectional delaminated composite flat and curved panels subjected to hygrothermal environment are not available in open literature, which is of current research interest. The results of numerical analysis by FEM on

parametric instability of delaminated composite plates and shells under hygrothermal influence are new. The results presented in this research work will be of great help for future researchers and designers of composite stressed skin structures (i.e. plates and shells) considering delaminations with environmental effects combinedly.

2.7 Scope of present investigation

A broad literature review shows that a good amount of work is done on vibration and buckling of unidirectional composite panels considering delaminations and environmental effects separately. However, bidirectional composite is a recent class of textile composite that has many industrial applications. A handful of work is done on parametric instability of unidirectional composite panels considering separately the influences of delaminations and hygrothermal field. The present study focusses at filling some of the lacunae that exist in the proper understanding of the dynamic stability of industry driven bidirectional delaminated composite panels in hygrothermal environment. Based on literature review, the various examples identified for the present study are as:

- Vibration of delaminated composite plates in hygrothermal field
- Buckling of delaminated composite plates in environmental field
- Parametric instability of delaminated composite panels in hygrothermal field

Vibration and buckling of delaminated composite plates are conducted both numerically and experimentally. The effects of different parameters on natural frequency and critical buckling loads are studied. The present investigation mainly focuses on the vibration, buckling and dynamic stability behaviour of delaminated bidirectional composite panels in hygrothermal field. The influence of various parameters such as static and dynamic load factors, delamination size, stacking sequence, ply orientations, temperature, moisture and boundary conditions on the instability behaviour of delaminated composite panels are examined numerically using Bolotin's approach and finite element method.

Chapter - 3

Mathematical Formulation

3.1 The Basic Problem

This chapter represents the theory and finite element formulation (FEM) for free vibration, buckling and parametric instability of the composite panels of various geometry with delamination under hygrothermal environment. The basic configuration of the problem considered here is a composite panel with mid plane area as well as strip delaminations under in-plane harmonic loading in hygrothermal field as shown in Figure 3.1 and Figure 3.2. The choice of the doubly curved panel geometry as a basic configuration has been made so that depending on the value of curvature parameter, composite plates and different doubly curved shell panels with reference to curvatures may be considered as special cases.

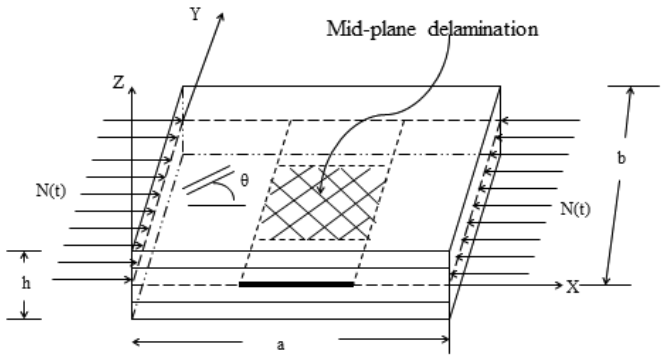

Figure 3.1: Area delamination of composite flat panel

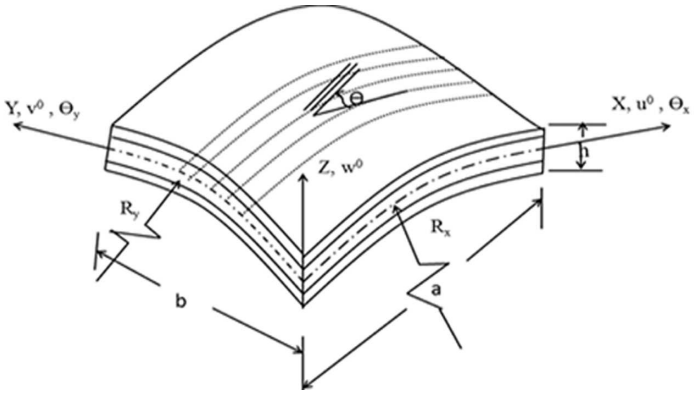

Figure 3.2: Strip delamination of composite doubly curved panel

The percentages of area and strip delaminations considered in the present study are shown in Figure 3.3 through Figure 3.5 and Figure 3.6 respectively. Single mid plane strip delamination of four different sizes i.e. 12.5% (d1), 25% (d1+d2), 37.5% (d1+d2+d3) and 50% (d1+d2+d3+d4) of the total panel area are considered in the study.

Mathematical formulation for free vibration, buckling and dynamic stability characteristics of delaminated composite doubly curved panels subjected to moisture and temperature are presented. Consider a laminated panel of uniform thickness 'h' consisting of a number of thin laminae, each of which may be arbitrarily oriented at an angle 'θ' with reference to the X-axis of the co-ordinate system as shown in Figure 3.7 and Figure 3.8.

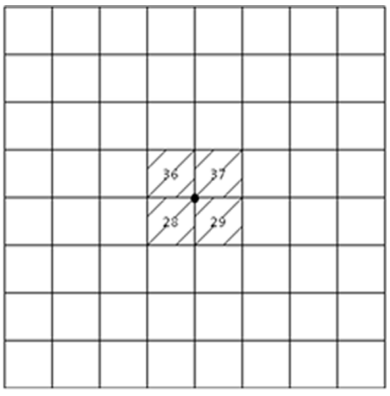

Figure 3.3: Area delamination of 6.25%

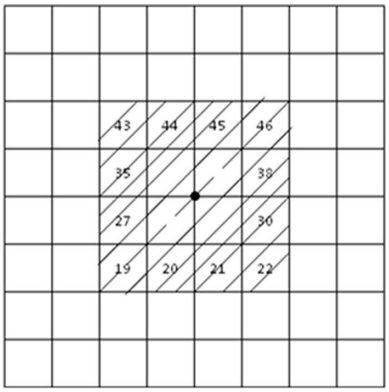

Figure 3.4: Area delamination of 25%

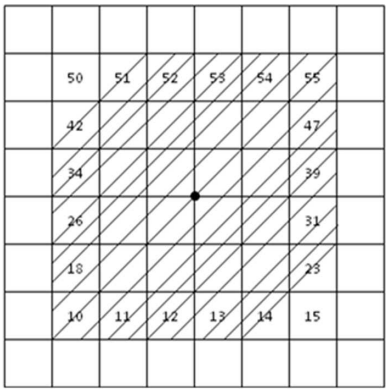

Figure 3.5: Area delamination of 56.25%

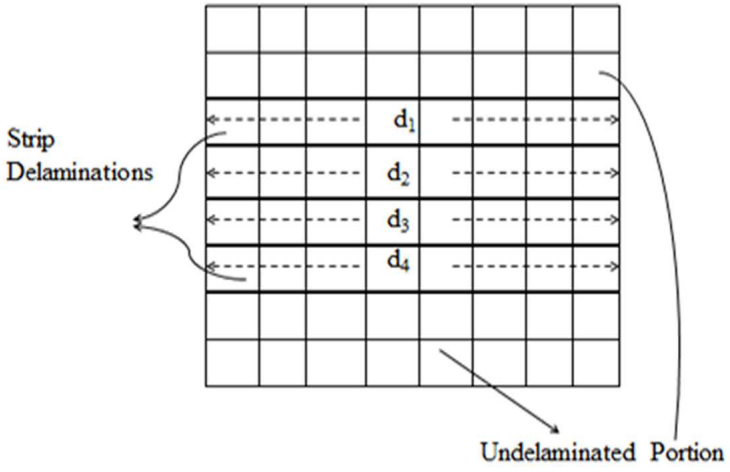

Figure 3.6: Planform showing mid plane strip delaminations

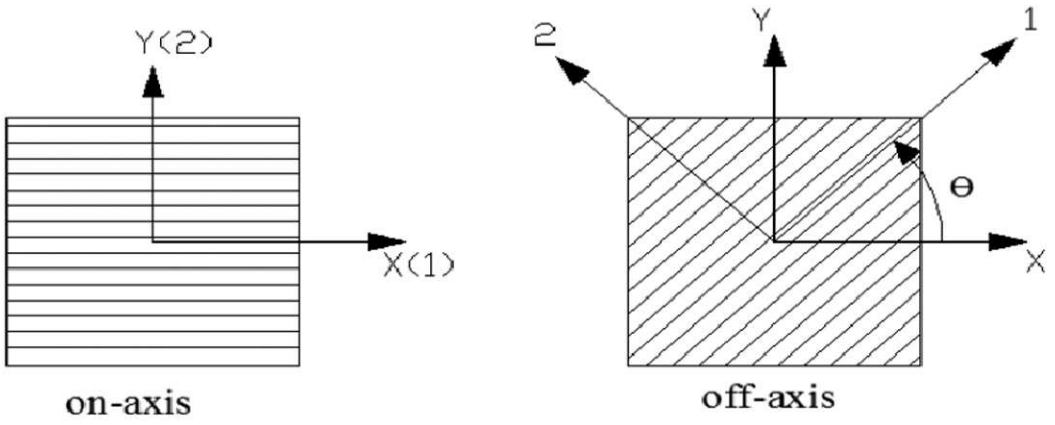

Figure 3.7: Arbitrary oriented laminated panel

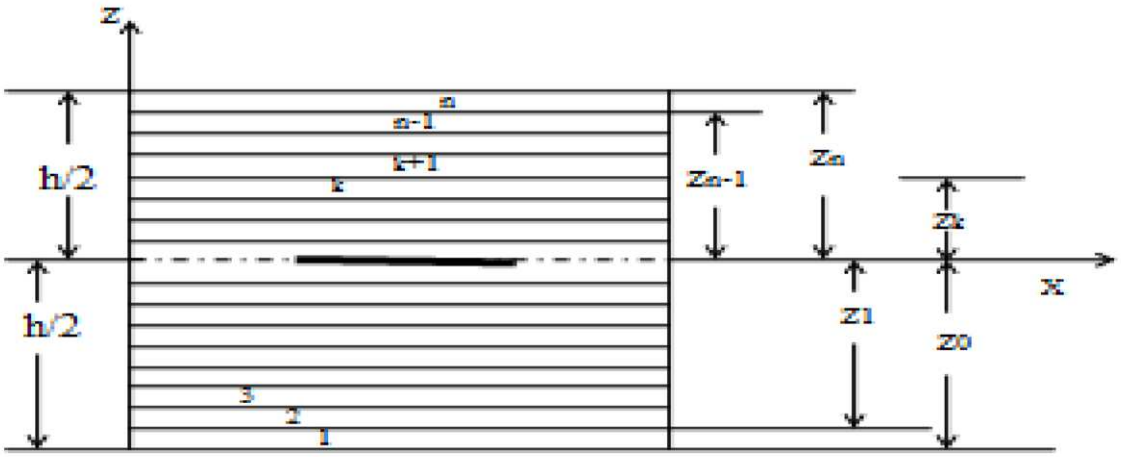

Figure 3.8: Geometry of an n-layered laminate

3.2 Proposed Analysis

The governing equations for the dynamic stability of delaminated composite doubly curved panels subjected to hygrothermal loading are developed. The presence of hygrothermal loading in the panel induces an in-plane stress field in the structures. This necessitates the determination of stress field as a prerequisite to the solution of the problem like vibration, buckling and dynamic stability behavior of composite plates and shells at different temperature and moisture concentrations. As the thickness of the structure is relatively smaller, the determination of stress field reduces to the solution of a plane stress problem. Due to the in-plane harmonic load the equation of motion represents second order Mathieu-Hill type. The development of the regions of instability arises and the solution is obtained on Bolotin's approach using finite element method (FEM). The governing differential equations have been developed using first order shear deformation theory (FSDT). The assumptions made in this analysis are summarized as follows:

3.2.1 Assumptions in the Analysis

- The analysis is linear, in line with previous studies on the dynamic stability of panels (Bert and Birman [1988]; Sahu and Datta [2003]) with a few exceptions. This implies both linear constitutive relations (generalized Hooke's law for the material and linear kinematics) and small displacement to accommodate small deformation theory.

- The delaminated curved panels are of various shapes with no initial imperfections. The considerations of imperfections are less important for dynamic loading and is consistent with the work of Bert and Birman [1988].

- This theory can be considered to be an extension of Sanders' theory to doubly curved panels, considering transverse shear and rotary inertia. The straight line that is perpendicular to the neutral surface before deformation remains straight

but not normal after deformation (FSDT). The thickness of the shell is small compared with the principal radii of curvature. Normal stress in Z - direction is neglected.

- The loading on the delaminated composite curved panel is considered axial with a simple harmonic fluctuation with respect to time.
- All damping effects are neglected.

3.3 Governing Differential Equations

The governing differential equations of the composite panels in hygrothermal environment are presented below.

$$\frac{\partial N_x}{\partial x} + \frac{\partial N_{xy}}{\partial y} + \frac{Q_x}{R_x} + \frac{Q_y}{R_{xy}} = I_1 \frac{\partial^2 u}{\partial t^2} + I_2 \frac{\partial^2 \theta_x}{\partial t^2} \tag{3.3.1}$$

$$\frac{\partial N_{xy}}{\partial x} + \frac{\partial N_y}{\partial y} + \frac{Q_y}{R_y} + \frac{Q_x}{R_{xy}} = I_1 \frac{\partial^2 v}{\partial t^2} + I_2 \frac{\partial^2 \theta_y}{\partial t^2} \tag{3.3.2}$$

$$\begin{aligned} \frac{\partial Q_x}{\partial x} + \frac{\partial Q_y}{\partial y} - \frac{N_x}{R_x} - \frac{N_y}{R_y} - 2\frac{N_{xy}}{R_{xy}} + N_x^N \frac{\partial^2 w}{\partial x^2} + N_y^N \frac{\partial^2 w}{\partial y^2} + N_{xy}^N \frac{\partial^2 w}{\partial x \partial y} \\ + N_x^a \frac{\partial^2 w}{\partial x^2} + N_y^a \frac{\partial^2 w}{\partial y^2} + N_{xy}^a \frac{\partial^2 w}{\partial x \partial y} = I_1 \frac{\partial^2 w}{\partial t^2} \end{aligned} \tag{3.3.3}$$

$$\frac{\partial M_x}{\partial x} + \frac{\partial M_{xy}}{\partial y} - Q_x = I_2 \frac{\partial^2 u}{\partial t^2} + I_3 \frac{\partial^2 \theta_x}{\partial t^2} \tag{3.3.4}$$

$$\frac{\partial M_{xy}}{\partial x} + \frac{\partial M_y}{\partial y} - Q_y = I_2 \frac{\partial^2 v}{\partial t^2} + I_3 \frac{\partial^2 \theta_y}{\partial t^2} \tag{3.3.5}$$

$$\text{where, } (I_1, I_2, I_3) = \sum_{k=1}^{n} \int_{z_{k-1}}^{z_k} (\rho)_k (1, z, z^2) dz$$

and N_x, N_y, N_xy are in-plane stress resultants per unit length; M_x, M_y, M_xy are moment resultants per unit length; Q_x, Q_y are transverse shear resultants. The terms with superscript $(^N)$ represents the corresponding non-mechanical in-plane stress re-

sultants due to moisture and temperature. The terms with superscript (^{a}) represents the corresponding in-plane stress resultants due to applied in-plane forces.

3.4 Energy Expressions

The delaminated composite panel is subjected to initial in-plane edge loads N_x^0, N_y^0 and N_{xy}^0. These in-plane loads cause in-plane stresses of σ_x^0, σ_y^0 and σ_{xy}^0 inducing a plane stress problem. The delaminated composite panels with the initial stresses undergo small lateral deformations. The total stress at any layer is the sum of the initial stresses plus the stresses due to bending and shear deformation.

The strain energy stored due to bending and shear deformation in the presence of initial stresses due to hygrothermal load and in-plane axial load (neglecting higher order terms) is given by Asha and Sahu [2011]:

$$U = U_1 + U_2 + U_3 \tag{3.4.1}$$

where

U_1 = Strain energy associated with bending with transverse shear

U_2 = Work done by the initial in-plane axial stresses and the nonlinear strain

U_3 = Work done due to non-mechanical loads from hygrothermal conditions

$$U_1 = \frac{1}{2}\int\int\int \left[\{\varepsilon_l\}^T[D]\{\varepsilon_l\}\right] dV \tag{3.4.2}$$

where, the strains can be expressed in terms of deformations as

$$\{\varepsilon_l\} = [B]\{q^0\} \tag{3.4.3}$$

The strain energy due to in-plane axial stresses and non-linear strains

$$U_2 = \frac{1}{2}\int\int\int \left[\{\sigma^0\}^T\{\varepsilon_{nl}\}\right] dV \tag{3.4.4}$$

and the strain energy due to non-mechanical loads from htgrothermal conditions

$$U_3 = \frac{1}{2}\int\int\int \left[\{\sigma^N\}^T\{\varepsilon_{nl}\}\right] dV \tag{3.4.5}$$

where, $\{\sigma^N\}$ are the stresses due to non-mechanical hygrothermal loads.

The method of explicit integration is performed through the thickness of the composite panel and thus the generalized force and moment resultants can directly be related to the strain components through the laminate stiffness. The kinetic energy 'V' of the composite panel can be derived as:

$$V = \frac{1}{2}\int\int \rho\left[h\left\{\frac{\partial\bar{u}^2}{\partial t} + \frac{\partial\bar{v}^2}{\partial t} + \frac{\partial\bar{w}^2}{\partial t}\right\} + \frac{h^3}{12}\left\{\frac{\partial{\theta_x}^2}{\partial t} + \frac{\partial{\theta_y}^2}{\partial t}\right\}\right] dxdy \tag{3.4.6}$$

Now, the various energies can be expressed in matrix form as

$$U_1 = \frac{1}{2}\{q\}^T[K]\{q\} \tag{3.4.7}$$

$$U_2 = \frac{1}{2}\{q\}^T[K_\sigma^a]\{q\} \tag{3.4.8}$$

$$U_3 = \frac{1}{2}\{q\}^T[K_\sigma^N]\{q\} \tag{3.4.9}$$

$$V = \frac{1}{2}\{\dot{q}\}^T[M]\{\dot{q}\} \tag{3.4.10}$$

where,

$[K]$ = Bending stiffness matrix with shear deformation

$[K_\sigma^a]$= Geometric stiffness matrix due to applied in-plane load

$[K_\sigma^N]$= Geometric stiffness matrix due to hygrothermal load

$[M]$ = Consistent mass matrix

3.5 Dynamic Stability Studies

The equation of motion for vibration of a laminated composite panel in hygrothermal environment, subjected to generalized in-plane load, may be expressed in the matrix form as (Ng et al. [1999]):

$$[M]\{\ddot{q}\} + [[[K] + [K_\sigma^N]] - N(t)[K_\sigma^a]]\{q\} = 0 \tag{3.5.1}$$

Where, $\{q\}$ is the vector of degree of freedoms $(u_i, v_i, w_i, \theta_{xi}, \theta_{yi})$. The in-plane load $N(t)$ may be harmonic and can be expressed in the form:

$$N(t) = N_S + N_D \cos \Omega t \tag{3.5.2}$$

Where, N_S the static portion of load $N(t)$, N_D the amplitude of the dynamic portion of $N(t)$ and Ω is the frequency of the excitation in rad/sec. The stress distribution in the panel may be periodic. The static elastic buckling load of the composite panel N_{cr} is a measure of magnitudes of N_S and N_D,

$$N_S = L_S N_{cr}, \qquad N_D = L_D N_{cr} \tag{3.5.3}$$

Where L_S and L_D are the static and dynamic load factors respectively. Using Eq. 3.5.2, the equation of motion for composite panel in hygrothermal environment under periodic loads in matrix form is reduced to:

$$[M]\{\ddot{q}\} + [[[K] + [K_\sigma^N]] - L_S N_{cr}[K_\sigma^a] - L_D N_{cr}[K_\sigma^a] \cos \Omega t]\{q\} = 0 \tag{3.5.4}$$

The above Eq. 3.5.4 represents a system of differential equations with periodic coefficients of the Mathieu-Hill type. The development of regions of instability arises from Floquet's theory which establishes the existence of periodic solutions of periods T and $2T$. The boundaries of the primary instability regions with period $2T$, where, $T = 2\pi/\Omega$ are of greater practical importance as the widths of these unstable regions are usually larger than those associated with the solutions having period T. Using

Bolotins (1964) first approximation, the periodic solutions with period 2T can be achieved in the form of the trigonometric series:

$$\{q(t)\} = \sum_{k=1.3.5}^{\infty} \left[\{a\}_k \sin \frac{k\Omega t}{2} + \{b\}_k \cos \frac{k\Omega t}{2} \right] \tag{3.5.5}$$

Substituting the value of $\{q(t)\}$ from Eq. 3.5.5 into Mathieu-Hill expression Eq. 3.5.4, we have:

$$\begin{aligned} &[M] \sum_{k=1.3.5}^{\infty} - \left(\frac{k\Omega}{2}\right)^2 \left(\{a\}_k \sin \frac{k\Omega t}{2} + \{b\}_k \cos \frac{k\Omega t}{2} \right) + [[[K] + [K_\sigma^N]] \\ &-L_S N_{cr}[K_\sigma^a] - L_D N_{cr}[K_\sigma^a] \cos \Omega t] \left(\{a\}_k \sin \frac{k\Omega t}{2} + \{b\}_k \cos \frac{k\Omega t}{2} \right) = 0 \end{aligned} \tag{3.5.6}$$

Equating coefficients of $\sin \frac{\Omega t}{2}$ and $\cos \frac{\Omega t}{2}$, a set of linear homogeneous algebraic equations in terms of $\{a\}_k$ and $\{b\}_k$ is obtained. For non-trivial solutions, the infinite determinants of the coefficients of the groups of homogeneous equations are equal to zero. Approximate solutions can be obtained by truncating the determinants. Principal instability region, which is of practical importance, corresponds to $k = 1$ and for this the instability conditions leads to two matrix equations, where the only difference in the matrix term is a minus sign.

$$\left[[[K] + [K_\sigma^N]] - \alpha N_{cr}[K_\sigma^a] \pm \beta N_{cr}[K_\sigma^a] - \frac{\Omega^2}{4}[M] \right] \{q\} = 0 \tag{3.5.7}$$

The determinant of the matrix term in Eq. 3.5.7 represents an eigenvalue problem for known values of L_S, L_D and N_{cr}. The two conditions under the plus and minus sign correspond to two boundaries (upper and lower) of the dynamic instability region. The above eigenvalue solutions give values of Ω, which are the boundary frequencies of the instability regions for the given values of L_S and L_D. In this analysis, the computed static buckling load of the panel is considered as the reference load. Before solving the above equations, the stiffness matrix $[K]$ is modified through imposition of boundary conditions. The equation reduces to other problems as follows:

(1)Free Vibration: $L_S = 0, L_D = 0$ and $\omega = \Omega/2$

$$\left[[K] + [K_\sigma^N]] - \omega_n^2[M]\right] \{q\} = 0 \tag{3.5.8}$$

(2)Buckling: $L_S = 1, L_D = 0$ and $\Omega = 0$

$$\left[[K] + [K_\sigma^N]] - \lambda[K_\sigma^a]\right] \{q\} = 0 \tag{3.5.9}$$

3.6 Finite Element Formulation

An eight nodded isoparametric element is used for present analysis of woven fiber composite panels subjected to hygrothermal environment. Five degrees of freedom u^0, v^0, w^0, θ_x and θ_y are considered at each node. The element is modified to accommodate hygrothermal conditions of the panel, based on first order shear deformation theory (FSDT).

3.6.1 The isoparametric element

An eight noded isoparametric element is employed in the present analysis with five degrees of freedom $u_i, v_i, w_i, \theta_{xi}$ and θ_{yi} per node as shown in fig. 3.9. but the in-plane deformations are considered for initial plane stress analysis. The isoparametric element shall be oriented in natural coordinate systems and shall be transferred to the Cartesian coordinate systems using the Jacobian matrix [Cook et al. [2007]].

The element has four corner nodes and four mid side nodes as shown in 3.9. In the displacement model, simple functions are assumed to approximate the displacements for each element.

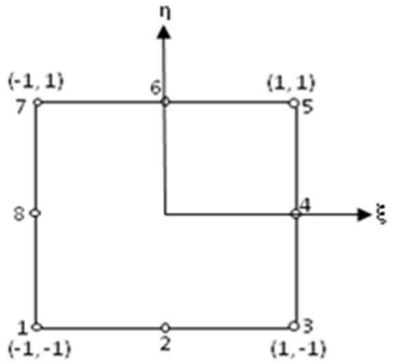

Figure 3.9: The element in natural coordinate system

The shape function of the element is derived using the interpolation polynomial as follows:

$$u(\xi,\eta) = \alpha_1 + \alpha_2\xi + \alpha_3\eta + \alpha_4\xi^2 + \alpha_5\xi\eta + \alpha_6\eta^2 + \alpha_7\xi^2\eta + \alpha_8\xi\eta^2 \tag{3.6.1}$$

The element geometry and displacement field are expressed by the shape functions N_i.

$$x = \sum_{i=1}^{8} N_i\, x_i, \quad y = \sum_{i=1}^{8} N_i\, y_i \quad u = \sum_{i=1}^{8} N_i\, u_i, \quad v = \sum_{i=1}^{8} N_i\, v_i,$$
$$w = \sum_{i=1}^{8} N_i\, w_i \quad \theta_x = \sum_{i=1}^{8} N_i\, \theta_{xi}, \quad \theta_y = \sum_{i=1}^{8} N_i\, \theta_{yi} \tag{3.6.2}$$

Where, x_i, y_i are the coordinates of i^{th} node and u_i^0, v_i^0, w_i, θ_{xi}, θ_{yi} are the displacement functions for different nodes.

.

N_i for different nodes as shown in Fig. 3.9 is defined as,

At corner nodes (i.e. for node 1, 3, 5, 7)

$$N_i \;=\; \frac{1}{4}\,(1+\xi\xi_i)\,(1+\eta\eta_i)\,(\xi\xi_i \;+\eta\eta_i \;-1)$$

At middle nodes (i.e. for nodes 2, 6)

$$N_i \;=\; \frac{1}{2}\,(1-\xi^2)\,(1+\eta\eta_i)$$

At middle nodes (i.e. for nodes 4, 8)

$$N_i \;=\; \frac{1}{2}\,(1+\xi\xi_i)\,(1-\eta^2) \tag{3.6.3}$$

where, ξ, η are the local natural coordinates of the element and ξ_i, η_i are the respective values at node i. The correctness of the shape function N_i is checked from the relations:

$$\sum N_i \;=\; 1,\;\; \sum N_i,\, \xi \;=\; 0,\;\; \sum N_i,\, \eta \;=\; 0 \tag{3.6.4}$$

The derivatives of the shape functions N_i with respect to x and y are expressed in terms of their partial derivatives with respect to ξ and η by the relationships:

$$\frac{\partial N_i}{\partial x} \;=\; \frac{\partial N_i}{\partial \xi}\frac{\partial \xi}{\partial x} \;+\; \frac{\partial N_i}{\partial \eta}\frac{\partial \eta}{\partial x}$$

$$\frac{\partial N_i}{\partial y} \;=\; \frac{\partial N_i}{\partial \xi}\frac{\partial \xi}{\partial y} \;+\; \frac{\partial N_i}{\partial \eta}\frac{\partial \eta}{\partial y}$$

$$\begin{Bmatrix} \dfrac{\partial N_i}{\partial x} \\ \dfrac{\partial N_i}{\partial y} \end{Bmatrix} = \begin{bmatrix} \dfrac{\partial \xi}{\partial x} & \dfrac{\partial \eta}{\partial x} \\ \dfrac{\partial \xi}{\partial y} & \dfrac{\partial \eta}{\partial y} \end{bmatrix} \begin{Bmatrix} \dfrac{\partial N_i}{\partial \xi} \\ \dfrac{\partial N_i}{\partial \eta} \end{Bmatrix}$$

$$\begin{Bmatrix} N_{i,x} \\ N_{i,y} \end{Bmatrix} = [J]^{-1} \begin{Bmatrix} N_{i,\xi} \\ N_{i,\eta} \end{Bmatrix} \tag{3.6.5}$$

where, the Jacobian,

$$[J] = \begin{bmatrix} \dfrac{\partial x}{\partial \xi} & \dfrac{\partial y}{\partial \xi} \\ \dfrac{\partial x}{\partial \eta} & \dfrac{\partial y}{\partial \eta} \end{bmatrix}$$

The composite panels with initial stresses undergo small lateral deformations. First order shear deformation theory is employed and the shear correction factor accounts for the non-linear distribution of the thickness shear strains through the total thickness. The displacement field assumes that midplane normal remains straight before and after deformation, but not necessarily normal after deformation so that

$$u(x, y, z) = u^0(x, y) + z\,\theta_x(x, y) \tag{3.6.6}$$

$$v(x, y, z) = v^0(x, y) + z\,\theta_y(x, y) \tag{3.6.7}$$

$$w(x, y, z) = w^0(x, y) \tag{3.6.8}$$

Where, u, v and w are displacements in the X, Y, and Z directions respectively for any point and the superscript $(^0)$ corresponds to the mid-plane values of the composite panel. θ_x, θ_y are the rotations of the cross section normal to the Y and X axis respectively. The middle plane of the composite panel is considered as the reference plane of the panel.

3.6.2 Strain Displacement Relations

Green-Lagrange's strain displacement relations are presented in general throughout the analysis. The linear part of the strain is used to derive the elastic stiffness matrix and the non-linear part of the strain is used to derive the geometric stiffness matrix.

The mid plane strains of the laminate are given by

$$\begin{aligned}
\varepsilon^0_{xx} \;=\; u^0_{,x},\; \varepsilon^0_{yy} \;=\; v^0_{,y},\; \gamma^0_{xy} \;=\; u^0_{,y} \;+\; v^0_{,x},\\
\gamma^0_{xz} \;=\; \theta_x \;+\; w_{,x},\; \gamma^0_{yz} \;=\; \theta_y \;+\; w_{,y}\\
\kappa_x = \theta_{y,x}, \kappa_y = -\theta_{x,y},\; \kappa_{xy} = \theta_{y,y} - \theta_{x,x},\\
\varphi_x = \theta_y + w_x, \varphi_y = -\theta_x + w_y
\end{aligned} \tag{3.6.9}$$

Where, $u^0_{,x}$, $v^0_{,y}$ etc. are the derivatives of the variable with respect to the subscript.

Assuming small deformations, the generalized linear in-plane strains of the laminate at a distance z from the mid-surface are expressed as

$$\{\varepsilon_{xx},\; \varepsilon_{yy},\; \gamma_{xy},\; \gamma_{xz},\; \gamma_{yz}\}^T \;=\; \{\varepsilon^0_{xx},\; \varepsilon^0_{yy},\; \gamma^0_{xy},\; \gamma^0_{xz},\; \gamma^0_{yz}\}^T + z\; \{\kappa_{xx},\; \kappa_{yy},\; \kappa_{xy},\; \kappa_{xz},\; \kappa_{yz}\}^T \tag{3.6.10}$$

where,

$$\{\varepsilon^0_{xx}, \varepsilon^0_{yy}, \gamma^0_{xy}, \gamma^0_{xz}, \gamma^0_{yz}\}^T = \left\{ \frac{\partial u^0}{\partial x} + \frac{w}{R_x}, \frac{\partial v^0}{\partial y} + \frac{w}{R_y}, \frac{\partial u^0}{\partial y} + \frac{\partial v^0}{\partial x} + \frac{2w}{R_{xy}}, \theta_x + \frac{\partial w}{\partial x}, \theta_y + \frac{\partial w}{\partial y} \right\}^T$$

$$\{\kappa_{xx},\; \kappa_{yy},\; \kappa_{xy},\; \kappa_{xz},\; \kappa_{yz}\}^T \;=\; \left\{ \frac{\partial \theta_x}{\partial x},\; \frac{\partial \theta_y}{\partial y}, \frac{\partial \theta_x}{\partial y} + \frac{\partial \theta_y}{\partial x},\; 0,\; 0 \right\}^T$$

and, R_x, R_y and R_{xy} are the three radii of curvature of the composite panel element. All the dynamic equations of equilibrium reduce to that of the plate, when the values of R_x, R_y and R_{xy} become infinity (∞). ε^0_{xx}, ε^0_{yy} ,γ^0_{xy},γ^0_{xz} and γ^0_{yz} are the mid-plane strains and κ_{xx}, κ_{yy}, and κ_{xy} are the curvatures of the laminate.

The total strain is given by

$$\varepsilon \;=\; \varepsilon_l \;+\; \varepsilon_{nl} \tag{3.6.11}$$

The linear generalized shear deformable strain displacement relations are

$$\varepsilon_{xl} \;=\; \frac{\partial u}{\partial x} \;+\; \frac{w}{R_x} \;+\; z\,\kappa_x \tag{3.6.12}$$

$$\varepsilon_{yl} \;=\; \frac{\partial v}{\partial y} \;+\; \frac{w}{R_y} \;+\; z\,\kappa_y \tag{3.6.13}$$

$$\gamma_{xyl} \;=\; \frac{\partial u}{\partial y} + \frac{\partial v}{\partial x} \;+\; \frac{2w}{R_{xy}} \;+\; z\,\kappa_{xy} \tag{3.6.14}$$

$$\gamma_{xzl} \;=\; \frac{\partial w}{\partial x} \;+\; \theta_x \;-\; \frac{u}{R_x} \;-\; \frac{v}{R_{xy}} \tag{3.6.15}$$

$$\gamma_{yzl} \;=\; \frac{\partial w}{\partial y} \;+\; \theta_y \;-\; \frac{v}{R_y} \;-\; \frac{u}{R_{xy}} \tag{3.6.16}$$

where, the bending strains κ_{ij} are expressed as,

$$\kappa_x \;=\; \frac{\partial \theta_x}{\partial x}, \quad \kappa_y \;=\; \frac{\partial \theta_y}{\partial y}$$

$$\kappa_{xy} \;=\; \frac{\partial \theta_x}{\partial y} \;+\; \frac{\partial \theta_y}{\partial x} \;+\; \frac{1}{2}\left(\frac{1}{R_x} - \frac{1}{R_y}\right)\left(\frac{\partial v}{\partial x} - \frac{\partial u}{\partial y}\right) \tag{3.6.17}$$

$$\varepsilon_{xnl} \;=\; \frac{1}{2}\left(\frac{\partial u}{\partial x}\right)^2 \;+\; \frac{1}{2}\left(\frac{\partial v}{\partial x}\right)^2 \;+\; \frac{1}{2}\left(\frac{\partial w}{\partial x} - \frac{u}{R_x}\right)^2 \;+\; \frac{1}{2}\,z^2\left[\left(\frac{\partial \theta x}{\partial x}\right)^2 \;+\; \left(\frac{\partial \theta y}{\partial x}\right)^2\right] \tag{3.6.18}$$

$$\varepsilon_{ynl} \;=\; \frac{1}{2}\left(\frac{\partial u}{\partial y}\right)^2 \;+\; \frac{1}{2}\left(\frac{\partial v}{\partial y}\right)^2 \;+\; \frac{1}{2}\left(\frac{\partial w}{\partial y} - \frac{v}{R_y}\right)^2 \;+\; \frac{1}{2}\,z^2\left[\left(\frac{\partial \theta x}{\partial y}\right)^2 \;+\; \left(\frac{\partial \theta y}{\partial y}\right)^2\right] \tag{3.6.19}$$

$$\gamma_{xynl} = \frac{\partial u}{\partial x}\left(\frac{\partial u}{\partial y}\right) + \frac{\partial v}{\partial x}\left(\frac{\partial v}{\partial y}\right) + \left(\frac{\partial w}{\partial x} - \frac{u}{R_x}\right)\left(\frac{\partial w}{\partial y} - \frac{v}{R_y}\right)$$

$$+ z^2\left[\left(\frac{\partial \theta x}{\partial x}\right)\left(\frac{\partial \theta x}{\partial y}\right) + \left(\frac{\partial \theta y}{\partial x}\right)\left(\frac{\partial \theta y}{\partial y}\right)\right] \quad (3.6.20)$$

3.6.3 Constitutive Relations for Hygrothermal Analysis

The constitutive relations for the composite panels subjected to hygrothermal field are given by

$$\{F\} = [D]\{\varepsilon\} - \{F^N\} \quad (3.6.21)$$

Where,

$$\{F\} = \{N_x,\ N_y,\ N_{xy},\ M_x,\ M_y,\ M_{xy},\ Q_x,\ Q_y\}^T$$

The non-mechanical loads due to hygrothermal conditions are,

$$\{F^N\} = \{N_x^N,\ N_y^N,\ N_{xy}^N,\ 0,\ 0,\ 0,\ 0,\ 0\}^T$$

$$\{\varepsilon\} = \{\varepsilon_{xx}^0,\ \varepsilon_{yy}^0,\ \gamma_{xy}^0,\ \kappa_x,\ \kappa_y,\ \kappa_{xy},\ \gamma_{xz},\ \gamma_{yz}\}^T$$

$$[D] = \begin{bmatrix} A_{11} & A_{12} & A_{16} & B_{11} & B_{12} & B_{16} & 0 & 0 \\ A_{12} & A_{22} & A_{26} & B_{12} & B_{22} & B_{26} & 0 & 0 \\ A_{16} & A_{26} & A_{66} & B_{16} & B_{26} & B_{66} & 0 & 0 \\ B_{11} & B_{12} & B_{16} & D_{11} & D_{12} & D_{16} & 0 & 0 \\ B_{12} & B_{22} & B_{26} & D_{12} & D_{22} & D_{26} & 0 & 0 \\ B_{16} & B_{26} & B_{66} & D_{16} & D_{26} & D_{66} & 0 & 0 \\ 0 & 0 & 0 & 0 & 0 & 0 & A_{44} & A_{45} \\ 0 & 0 & 0 & 0 & 0 & 0 & A_{45} & A_{55} \end{bmatrix}$$

$[D]$ is the matrix of stiffnesses.

The extensional, bending-stretching and bending stiffnesses of the laminate are expressed in the usual form as

$$(A_{ij},\ B_{ij},\ D_{ij}) = \sum_{k=1}^{n} \int_{z_{k-1}}^{z_k} (\bar{Q_{ij}})_k \left(1,\ z,\ z^2\right) dz \qquad i,j = 1,2,6 \qquad (3.6.22)$$

Similarly, the shear stiffness is expressed as

$$(A_{ij}) = \sum_{k=1}^{n} \int_{z_{k-1}}^{z_k} \boldsymbol{k}\ (\bar{Q_{ij}})_k\ dz, \qquad i,j = 4,5 \qquad (3.6.23)$$

$\boldsymbol{k}$, the shear correction factor, is assumed as 5/6 in line with the previous studies (Wang and Dawe [2002]). It accounts for the non-uniform distribution of transverse shear strain across the thickness of the laminate.

$(\bar{Q_{ij}})_k$ in Eq. 3.6.22 and Eq. 3.6.23 are the off-axis stiffness values defined as

$$(\bar{Q_{ij}})_k = \begin{bmatrix} m^2 & n^2 & -2mn \\ n^2 & m^2 & 2mn \\ mn & -mn & m^2 - n^2 \end{bmatrix} (Q_{ij})_k \begin{bmatrix} m^2 & n^2 & mn \\ n^2 & m^2 & -mn \\ -2mn & 2mn & m^2 - n^2 \end{bmatrix}, \quad i,j = 1,2,6$$

$$(\bar{Q_{ij}})_k = \begin{bmatrix} m & -n \\ n & m \end{bmatrix} (Q_{ij})_k \begin{bmatrix} m & n \\ -n & m \end{bmatrix}, \quad i,j = 4,5 \qquad (3.6.24)$$

Where, $(Q_{ij})_k$ are the on-axis stiffness coefficients in the material direction given by

$$(Q_{ij})_k \;=\; \begin{bmatrix} Q_{11} & Q_{12} & 0 \\ Q_{12} & Q_{22} & 0 \\ 0 & 0 & Q_{66} \end{bmatrix},\; i,j = 1,2,6 \text{ and } (Q_{ij})_k \;=\; \begin{bmatrix} Q_{44} & 0 \\ 0 & Q_{55} \end{bmatrix},\; i,j = 4,5 \tag{3.6.25}$$

$(Q_{ij})_k$ are calculated in the conventional manner from the values of elastic and shear moduli and the Poisson's ratio values.

The non-mechanical in-plane stress and moment resultants due to hygrothermal environment are given by,

$$\{N_x^N,\; N_y^N,\; N_{xy}^N\}^T \;=\; \sum_{k=1}^{n} \int_{z_{k-1}}^{z_k} (\bar{Q_{ij}})_k \;\; (e)_k \; dz$$

Here, $\{e\} \;=\; \{e_x,\; e_y,\; e_{xy}\}_k^T$ the non-mechanical strains of the k^{th} lamina, oriented at an arbitrary angle θ_k, expressed as

$$\{e\}_k \;=\; [\boldsymbol{T}]\; \{\beta_1,\; \beta_2\}_k^T\; (C - C_0) \;+\; [\boldsymbol{T}]\; \{\alpha_1,\; \alpha_2\}_k^T\; (T - T_0) \tag{3.6.26}$$

where, the transformation matrix,

$$[\boldsymbol{T}] \;=\; \begin{bmatrix} m^2 & n^2 \\ n^2 & m^2 \\ -2mn & 2mn \end{bmatrix}, \qquad m \;=\; \cos\,\theta_k \; and \; n \;=\; \sin\,\theta_k$$

$\beta_1,\; \beta_2$ are the moisture coefficients of the lamina in longitudinal and lateral directions, and their values considered here are 0 and 0.44 respectively. $\alpha_1,\; \alpha_2$ are the thermal coefficients of the lamina in longitudinal and lateral directions, and their values considered here are $-0.3 \times 10^{-6}/K$ and $28.1 \times 10^{-6}/K$. C_0 and T_0 are the reference moisture content in % and temperature in Kelvin(K) respectively and here their values assumed are 0 and $300K$ respectively. C and T are elevated moisture concentration and temperature respectively.

3.6.4 Delamination modeling

Composite laminated flat panel having n layers with s number of arbitrary located delaminations has been chosen for finite element programming. The mid plane displacements in each sub-laminate are stated in form of mid-plane displacements (u^0, v^0) of the original panel having no delaminations. Let, z_i^0 is the distance between the mid-plane of the original laminated panel and the mid plane of the i^{th} sub-laminate. Considering the sub laminate i as a separate plate, the displacement field within it is expressed as:

$$\begin{aligned} u_i &= u_i^0 + (z - z_i^0)\,\theta_x \\ v_i &= v_i^0 + (z - z_i^0)\,\theta_y \end{aligned} \tag{3.6.27}$$

where, u_i^0 and v_i^0 are the mid plane displacements of the i^{th} sub-laminate. The mid plane strains of the sub-laminate are

$$\begin{Bmatrix} \varepsilon_{xx}^0 \\ \varepsilon_{yy}^0 \\ \gamma_{xy}^0 \end{Bmatrix}_i = \begin{Bmatrix} \frac{\partial u_i^0}{\partial x} \\ \frac{\partial v_i^0}{\partial y} \\ \frac{\partial u_i^0}{\partial y} + \frac{\partial v_i^0}{\partial x} \end{Bmatrix} \tag{3.6.28}$$

From Eq. 3.6.27, the strain components within the sub-laminate, i can be expressed as

$$\begin{aligned} \begin{Bmatrix} \varepsilon_{xx} \\ \varepsilon_{yy} \\ \gamma_{xy} \end{Bmatrix}_i = \begin{Bmatrix} \frac{\partial u_i}{\partial x} \\ \frac{\partial v_i}{\partial y} \\ \frac{\partial u_i}{\partial y} + \frac{\partial v_i}{\partial x} \end{Bmatrix} &= \begin{Bmatrix} \frac{\partial u_i^0}{\partial x} \\ \frac{\partial v_i^0}{\partial y} \\ \frac{\partial u_i^0}{\partial y} + \frac{\partial v_i^0}{\partial x} \end{Bmatrix} + (z - z_i^0) \begin{Bmatrix} \frac{\partial \theta_x}{\partial x} \\ \frac{\partial \theta_y}{\partial y} \\ \frac{\partial \theta_x}{\partial y} + \frac{\partial \theta_y}{\partial x} \end{Bmatrix} \\ &= \begin{Bmatrix} \varepsilon_{xx}^0 \\ \varepsilon_{yy}^0 \\ \gamma_{xy}^0 \end{Bmatrix}_i + (z - z_i^0) \begin{Bmatrix} \kappa_{xx} \\ \kappa_{yy} \\ \kappa_{xy} \end{Bmatrix} \end{aligned} \tag{3.6.29}$$

Appropriate restraints are enforced between two adjacent plies for ensuring struc-

tural intactness; i.e. for avoiding mutual penetration, contact conditions are enforced in the delaminated region and for ensuring continuity of displacement, binding constraints are utilized outside the delaminated region Zheng and Sun [1998]. Any delamination boundary has three sub-laminates including the original laminate, where the lateral displacements and rotations have equal values for a common node. Applying these multipoint constraint conditions, the mid plane displacements of the sub laminate can be expressed in the form of mid plane displacements (u^0, v^0) of the original undelaminated laminate as:

$$\begin{aligned} u_i^0 &= u^0 + z_i^0\,\theta_x \\ v_i^0 &= v^0 + z_i^0\,\theta_y \end{aligned} \tag{3.6.30}$$

From Eq. 3.6.30, the mid plane strains of the sub-laminate can be generalized as a function of the mid plane displacements of the original undelaminated laminate as:

$$\begin{Bmatrix} \varepsilon_{xx}^0 \\ \varepsilon_{yy}^0 \\ \gamma_{xy}^0 \end{Bmatrix}_i = \begin{Bmatrix} \varepsilon_{xx}^0 \\ \varepsilon_{yy}^0 \\ \gamma_{xy}^0 \end{Bmatrix} + z_i^0 \begin{Bmatrix} \kappa_{xx} \\ \kappa_{yy} \\ \kappa_{xy} \end{Bmatrix} \tag{3.6.31}$$

Substituting Eq. 3.6.31 in Eq. 3.6.29, the strain components within the sub laminate can be rewritten as:

$$\begin{aligned} \begin{Bmatrix} \varepsilon_{xx} \\ \varepsilon_{yy} \\ \gamma_{xy} \end{Bmatrix}_i &= \begin{Bmatrix} \varepsilon_{xx}^0 \\ \varepsilon_{yy}^0 \\ \gamma_{xy}^0 \end{Bmatrix}_i + (z - z_i^0) \begin{Bmatrix} \kappa_{xx} \\ \kappa_{yy} \\ \kappa_{xy} \end{Bmatrix} \\ &= \begin{Bmatrix} \varepsilon_{xx}^0 \\ \varepsilon_{yy}^0 \\ \gamma_{xy}^0 \end{Bmatrix} + z_i^0 \begin{Bmatrix} \kappa_{xx} \\ \kappa_{yy} \\ \kappa_{xy} \end{Bmatrix} + (z - z_i^0) \begin{Bmatrix} \kappa_{xx} \\ \kappa_{yy} \\ \kappa_{xy} \end{Bmatrix} \end{aligned} \tag{3.6.32}$$

For any lamina of the i^{th} sub-laminate, the in plane and shear stresses are found

from the relation as

$$\begin{Bmatrix} \sigma_{xx} \\ \sigma_{yy} \\ \tau_{xy} \end{Bmatrix} = \begin{bmatrix} \overline{Q_{11}} & \overline{Q_{12}} & \overline{Q_{16}} \\ \overline{Q_{12}} & \overline{Q_{22}} & \overline{Q_{26}} \\ \overline{Q_{16}} & \overline{Q_{26}} & \overline{Q_{66}} \end{bmatrix} \begin{Bmatrix} \varepsilon_{xx} \\ \varepsilon_{yy} \\ \gamma_{xy} \end{Bmatrix}_i \tag{3.6.33}$$

$$\begin{Bmatrix} \tau_{xz} \\ \tau_{yz} \end{Bmatrix} = \begin{bmatrix} \overline{Q_{44}} & \overline{Q_{45}} \\ \overline{Q_{45}} & \overline{Q_{55}} \end{bmatrix} \begin{Bmatrix} \gamma_{xz} \\ \gamma_{yz} \end{Bmatrix}_i \tag{3.6.34}$$

Here, $\{\gamma_{xz}, \gamma_{yz}\}_i^T$ are assumed to be same as $\{\gamma_{xz}, \gamma_{yz}\}^T$ of the undelaminated plate.

Now, the respective rows in Eq. 3.6.33 and Eq. 3.6.34 can be multiplied with sub laminate strain terms $\{\varepsilon_{xx}, \varepsilon_{yy}, \gamma_{xy}\}_i^T$ and $\{\gamma_{xz}, \gamma_{yz}\}_i^T$ to get the corresponding stress terms.

For illustration,

$$\sigma_{xx} = \begin{bmatrix} \overline{Q_{11}}, & \overline{Q_{12}}, & \overline{Q_{16}} \end{bmatrix} \begin{Bmatrix} \varepsilon_{xx} \\ \varepsilon_{yy} \\ \gamma_{xy} \end{Bmatrix}_i \tag{3.6.35}$$

Substituting the values of $\{\varepsilon_{xx}, \varepsilon_{yy}, \gamma_{xy}\}_i^T$ from Eq. 3.6.32 in Eq. 3.6.35, σ_{xx} can be rewritten as

$$\sigma_{xx} = \begin{bmatrix} \overline{Q_{11}}, & \overline{Q_{12}}, & \overline{Q_{16}} \end{bmatrix} \left[\begin{Bmatrix} \varepsilon_{xx}^0 \\ \varepsilon_{yy}^0 \\ \gamma_{xy}^0 \end{Bmatrix} + z_i^0 \begin{Bmatrix} \kappa_{xx} \\ \kappa_{yy} \\ \kappa_{xy} \end{Bmatrix} + (z - z_i^0) \begin{Bmatrix} \kappa_{xx} \\ \kappa_{yy} \\ \kappa_{xy} \end{Bmatrix} \right] \tag{3.6.36}$$

From Eq. 3.6.36, integrating σ_{xx} over the sub-laminate thickness, h_i, the stress resultant, N_x can be expressed as

$$
\begin{aligned}
N_{xi} &= \int_{-\frac{h_i}{2}+z_i^0}^{\frac{h_i}{2}+z_i^0} \sigma_{xx} dz = \int_{-\frac{h_i}{2}+z_i^0}^{\frac{h_i}{2}+z_i^0} \left[\overline{Q_{11}}, \overline{Q_{12}}, \overline{Q_{16}}\right] \begin{Bmatrix} \varepsilon_{xx}^0 \\ \varepsilon_{yy}^0 \\ \gamma_{xy}^0 \end{Bmatrix} dz \\
&+ z_i^0 \int_{-\frac{h_i}{2}+z_i^0}^{\frac{h_i}{2}+z_i^0} \left[\overline{Q_{11}}, \overline{Q_{12}}, \overline{Q_{16}}\right] \begin{Bmatrix} \kappa_{xx} \\ \kappa_{yy} \\ \kappa_{xy} \end{Bmatrix} dz + \int_{-\frac{h_i}{2}+z_i^0}^{\frac{h_i}{2}+z_i^0} \left[\overline{Q_{11}},\ \overline{Q_{12}},\ \overline{Q_{16}}\right] (z - z_i^0) \begin{Bmatrix} \kappa_{xx} \\ \kappa_{yy} \\ \kappa_{xy} \end{Bmatrix} dz \\
&= [A_{11}\ A_{12}\ A_{16}]_i \begin{Bmatrix} \varepsilon_{xx}^0 \\ \varepsilon_{yy}^0 \\ \gamma_{xy}^0 \end{Bmatrix} + z_i^0 [A_{11}\ A_{12}\ A_{16}]_i \begin{Bmatrix} \kappa_{xx} \\ \kappa_{yy} \\ \kappa_{xy} \end{Bmatrix} + [B_{11}\ B_{12}\ B_{16}]_i \begin{Bmatrix} \kappa_{xx} \\ \kappa_{yy} \\ \kappa_{xy} \end{Bmatrix}
\end{aligned}
\tag{3.6.37}
$$

Similarly, M_x for the sub laminate can be written as

$$
\begin{aligned}
M_{xi} &= \int_{-\frac{h_i}{2}+z_i^0}^{\frac{h_i}{2}+z_i^0} \sigma_{xx}\ (z - z_i^0)\ dz = \int_{-\frac{h_i}{2}+z_i^0}^{\frac{h_i}{2}+z_i^0} \left[\overline{Q_{11}},\ \overline{Q_{12}},\ \overline{Q_{16}}\right] \begin{Bmatrix} \varepsilon_{xx} \\ \varepsilon_{yy} \\ \gamma_{xy} \end{Bmatrix}_i (z - z_i^0)\ dz \\
&= \int_{-\frac{h_i}{2}+z_i^0}^{\frac{h_i}{2}+z_i^0} \left[\overline{Q_{11}},\ \overline{Q_{12}},\ \overline{Q_{16}}\right] \left[\begin{Bmatrix} \varepsilon_{xx}^0 \\ \varepsilon_{yy}^0 \\ \gamma_{xy}^0 \end{Bmatrix} + z_i^0 \begin{Bmatrix} \kappa_{xx} \\ \kappa_{yy} \\ \kappa_{xy} \end{Bmatrix} + (z - z_i^0) \begin{Bmatrix} \kappa_{xx} \\ \kappa_{yy} \\ \kappa_{xy} \end{Bmatrix} \right] (z - z_i^0) dz \\
&= [B_{11}\ B_{12}\ B_{16}]_i \begin{Bmatrix} \varepsilon_{xx}^0 \\ \varepsilon_{yy}^0 \\ \gamma_{xy}^0 \end{Bmatrix} + z_i^0 [B_{11}\ B_{12}\ B_{16}]_i \begin{Bmatrix} \kappa_{xx} \\ \kappa_{yy} \\ \kappa_{xy} \end{Bmatrix} + [D_{11}\ D_{12}\ D_{16}]_i \begin{Bmatrix} \kappa_{xx} \\ \kappa_{yy} \\ \kappa_{xy} \end{Bmatrix}
\end{aligned}
\tag{3.6.38}
$$

where,

$$[A_{ij}]_i = \int_{-\frac{h_i}{2}+z_i^0}^{\frac{h_i}{2}+z_i^0} \left[\overline{Q_{ij}}\right]_i \, dz, \; [B_{ij}]_i = \int_{-\frac{h_i}{2}+z_i^0}^{\frac{h_i}{2}+z_i^0} \left[\overline{Q_{ij}}\right]_i \, (z - z_i^0) dz$$
$$= \int_{-\frac{h_i}{2}+z_i^0}^{\frac{h_i}{2}+z_i^0} \left[\overline{Q_{ij}}\right]_i \, z \, dz \; - \; z_i^0 \, [A_{ij}]_i$$

and

$$[D_{ij}]_i = \int_{-\frac{h_i}{2}+z_i^0}^{\frac{h_i}{2}+z_i^0} \left[\overline{Q_{ij}}\right]_i \, (z - z_i^0)^2 \, dz$$
$$= \int_{-\frac{h_i}{2}+z_i^0}^{\frac{h_i}{2}+z_i^0} \left[\overline{Q_{ij}}\right]_i \, z^2 \, dz \; - \; 2 \, z_i^0 \int_{-\frac{h_i}{2}+z_i^0}^{\frac{h_i}{2}+z_i^0} \left[\overline{Q_{ij}}\right]_i \, z \, dz \; + \; (z_i^0)^2 \, [A_{ij}]_i, \; i, j = 1, 2, 6$$

Similarly,

$$N_{y_i} = [A_{12} \; A_{22} \; A_{26}]_i \begin{Bmatrix} \varepsilon_{xx}^0 \\ \varepsilon_{yy}^0 \\ \gamma_{xy}^0 \end{Bmatrix} + z_i^0 \, [A_{12} \; A_{22} \; A_{26}]_i \begin{Bmatrix} \kappa_{xx} \\ \kappa_{yy} \\ \kappa_{xy} \end{Bmatrix} + [B_{12} \; B_{22} \; B_{26}]_i \begin{Bmatrix} \kappa_{xx} \\ \kappa_{yy} \\ \kappa_{xy} \end{Bmatrix}$$

$$N_{xy_i} = [A_{16} \; A_{26} \; A_{66}]_i \begin{Bmatrix} \varepsilon_{xx}^0 \\ \varepsilon_{yy}^0 \\ \gamma_{xy}^0 \end{Bmatrix} + z_i^0 \, [A_{16} \; A_{26} \; A_{66}]_i \begin{Bmatrix} \kappa_{xx} \\ \kappa_{yy} \\ \kappa_{xy} \end{Bmatrix} + [B_{16} \; B_{26} \; B_{66}]_i \begin{Bmatrix} \kappa_{xx} \\ \kappa_{yy} \\ \kappa_{xy} \end{Bmatrix}$$

$$M_{y_i} = [B_{12}\ B_{22}\ B_{26}]_i \begin{Bmatrix} \varepsilon^0_{xx} \\ \varepsilon^0_{yy} \\ \gamma^0_{xy} \end{Bmatrix} + z^0_i\ [B_{12}\ B_{22}\ B_{26}]_i \begin{Bmatrix} \kappa_{xx} \\ \kappa_{yy} \\ \kappa_{xy} \end{Bmatrix} + [D_{12}\ D_{22}\ D_{26}]_i \begin{Bmatrix} \kappa_{xx} \\ \kappa_{yy} \\ \kappa_{xy} \end{Bmatrix}$$

$$M_{xy_i} = [B_{16}\ B_{26}\ B_{66}]_i \begin{Bmatrix} \varepsilon^0_{xx} \\ \varepsilon^0_{yy} \\ \gamma^0_{xy} \end{Bmatrix} + z^0_i\ [B_{16}\ B_{26}\ B_{66}]_i \begin{Bmatrix} \kappa_{xx} \\ \kappa_{yy} \\ \kappa_{xy} \end{Bmatrix} + [D_{16}\ D_{26}\ D_{66}]_i \begin{Bmatrix} \kappa_{xx} \\ \kappa_{yy} \\ \kappa_{xy} \end{Bmatrix}$$

The above in-plane stress and moment resultants for the i^{th} sub-laminate can be expressed in a generalized manner as:

$$\begin{Bmatrix} N_x \\ N_y \\ N_{xy} \\ M_x \\ M_y \\ M_{xy} \end{Bmatrix} = \begin{bmatrix} A_{11} & A_{12} & A_{16} & Z^0_i A_{11} + B_{11} & Z^0_i A_{12} + B_{12} & Z^0_i A_{16} + B_{16} \\ A_{12} & A_{22} & A_{26} & Z^0_i A_{12} + B_{12} & Z^0_i A_{22} + B_{22} & Z^0_i A_{26} + B_{26} \\ A_{16} & A_{26} & A_{66} & Z^0_i A_{16} + B_{16} & Z^0_i A_{26} + B_{26} & Z^0_i A_{66} + B_{66} \\ B_{11} & B_{12} & B_{16} & Z^0_i B_{11} + D_{11} & Z^0_i B_{12} + D_{12} & Z^0_i B_{16} + D_{16} \\ B_{12} & B_{22} & B_{26} & Z^0_i B_{12} + D_{12} & Z^0_i B_{22} + D_{22} & Z^0_i B_{26} + D_{26} \\ B_{16} & B_{26} & B_{66} & Z^0_i B_{16} + D_{16} & Z^0_i B_{26} + D_{26} & Z^0_i B_{66} + D_{66} \end{bmatrix} \begin{Bmatrix} \varepsilon^0_x \\ \varepsilon^0_y \\ \gamma^0_{xy} \\ \kappa_x \\ \kappa_y \\ \kappa_{xy} \end{Bmatrix} \tag{3.6.39}$$

and the transverse shear forces for the i^{th} sub-laminate are presented as:

$$\begin{Bmatrix} Q_{xz} \\ Q_{yz} \end{Bmatrix}_i = \begin{bmatrix} A_{44} & A_{45} \\ A_{45} & A_{55} \end{bmatrix}_i \begin{Bmatrix} \gamma_{xz} \\ \gamma_{yz} \end{Bmatrix} \tag{3.6.40}$$

where,

$$[A_{ij}]_i = \int_{-\frac{h_i}{2}+z^0_i}^{\frac{h_i}{2}+z^0_i} \begin{bmatrix} \overline{Q_{44}} & \overline{Q_{45}} \\ \overline{Q_{45}} & \overline{Q_{55}} \end{bmatrix}_i dz, \quad i,j = 4,5$$

After finding the elastic stiffness matrices separately for each sub-laminate along the thickness, the sum of all the sub-laminate stiffnesses represents the resultant stiffness matrix of the delaminated composite panel.

3.6.5 Element Elastic Stiffness Matrix

The linear strain matrix is expressed as

$$\{\varepsilon\}_{8\times1} \;=\; [B]_{8\times40}\,\{\delta_e\}_{40\times1} = [[B_1]....[B_8]]\,\{\delta_e\} \tag{3.6.41}$$

$$\text{where, } \{\delta_e\}_{40\times1} \;=\; \{u_1^0,\; v_1^0,\; w_1,\; \theta_{x1},\; \theta_{y1}\;\ldots\; u_8^0,\; v_8^0,\; w_8,\; \theta_{x8},\; \theta_{y8}\}^T \tag{3.6.42}$$

$[B]$ is called the strain displacement matrix and is defined as:

$$[B] \;=\; \begin{bmatrix} N_{i,x} & 0 & \dfrac{N_i}{R_x} & 0 & 0 \\ 0 & N_{i,y} & \dfrac{N_i}{R_y} & 0 & 0 \\ N_{i,y} & N_{i,x} & 0 & 0 & 0 \\ 0 & 0 & 0 & N_{i,x} & 0 \\ 0 & 0 & 0 & 0 & N_{i,y} \\ N_{i,y} & -N_{i,x} & 0 & N_{i,y} & N_{i,x} \\ \dfrac{-N_i}{R_x} & 0 & N_{i,x} & N_i & 0 \\ 0 & \dfrac{-N_i}{R_y} & N_{i,y} & 0 & N_i \end{bmatrix}_{8\times40}$$

The element stiffness matrix is given by

$$[K_e]_{40\times 40} \;=\; \int_{-1}^{+1}\int_{-1}^{+1} [B]^T_{40\times 8}\,[D]_{8\times 8}\,[B]_{8\times 40}\,|J|\;d\xi\;d\eta \tag{3.6.43}$$

3.6.6 Element geometric stiffness matrix due to hygrothermal loading

The non-linear strains are expressed in matrix form

$$\{\varepsilon_{nl}\} \;=\; \{\varepsilon_{xnl},\;\varepsilon_{ynl},\;\varepsilon_{xynl}\}^T \;=\; [R]\,\{d\}\;/\;2 \tag{3.6.44}$$

where, $[R]$ is a multiplier matrix and

$$\{d\} \;=\; \{u_x,\;u_y,\;v_x,\;v_y,\;w_x,\;w_y,\;\theta_{x,x},\;\theta_{x,y},\;\theta_{y,x},\;\theta_{y,y},\;\theta_x,\;\theta_y\}^T \tag{3.6.45}$$

$\{d\}$ may be expressed as:

$$\{d\} \;=\; [G]\,\{\delta_e\} \tag{3.6.46}$$

The element geometric stiffness matrix due to non-mechanical (hygrothermal) forces is expressed in the form

$$[K^N_{\sigma e}]_{40\times 40} \;=\; \int_{-1}^{+1}\int_{-1}^{+1} [G]^T_{40\times 10}[S]_{10\times 10}[G]_{10\times 40}|J|\;d\xi\;d\eta \tag{3.6.47}$$

$$\text{where, } [G] = \sum_{i=1}^{8} \begin{bmatrix} N_{i,x} & 0 & N_i/R_x & 0 & 0 \\ N_{i,y} & 0 & 0 & 0 & 0 \\ 0 & N_{i,x} & 0 & 0 & 0 \\ 0 & N_{i,y} & N_i/R_y & 0 & 0 \\ -N_i/R_x & 0 & N_{i,x} & 0 & 0 \\ 0 & -N_i/R_y & N_{i,y} & 0 & 0 \\ 0 & 0 & 0 & N_{i,x} & 0 \\ 0 & 0 & 0 & N_{i,y} & 0 \\ 0 & 0 & 0 & 0 & N_{i,x} \\ 0 & 0 & 0 & 0 & N_{i,y} \end{bmatrix}_{10\times 40}$$

$$\text{and, } [S] = \begin{bmatrix} N_x^N & & & & & & & & & \\ N_{xy}^N & N_y^N & & & & & & & & \\ 0 & 0 & N_x^N & & & & & & & \\ 0 & 0 & N_{xy}^N & N_y^N & & & Sym. & & & \\ 0 & 0 & 0 & 0 & N_x^N & & & & & \\ 0 & 0 & 0 & 0 & N_{xy}^N & N_y^N & & & & \\ 0 & 0 & 0 & 0 & 0 & 0 & S_1 & & & \\ 0 & 0 & 0 & 0 & 0 & 0 & S_3 & S_2 & & \\ 0 & 0 & 0 & 0 & 0 & 0 & 0 & 0 & S_1 & \\ 0 & 0 & 0 & 0 & 0 & 0 & 0 & 0 & S_3 & S_2 \end{bmatrix}_{10\times 10}$$

In the above matrix, $S_1 = \dfrac{N_x^N h^2}{12},\ S_2 = \dfrac{N_y^N h^2}{12},\ S_3 = \dfrac{N_{xy}^N h^2}{12}$

3.6.7 Element geometric stiffness matrix due to applied load

The non-linear strains are expressed in matrix form

$$\{\varepsilon_{nl}\} \;=\; \{\varepsilon_{xnl},\; \varepsilon_{ynl},\; \varepsilon_{xynl}\}^T \;=\; [U]\;\{f\}\;/\;2 \tag{3.6.48}$$

where, $[U]$ is a multiplier matrix and

$$\{f\} \;=\; \{u_x,\; u_y,\; v_x,\; v_y,\; w_x,\; w_y,\; \theta_{x,x},\; \theta_{x,y},\; \theta_{y,x},\; \theta_{y,y},\; \theta_x,\; \theta_y\}^T \tag{3.6.49}$$

$\{f\}$ may be expressed as:

$$\{f\} \;=\; [H]\;\{\delta_e\} \tag{3.6.50}$$

$$\text{where, } [H] \;=\; \begin{bmatrix} N_{i,x} & 0 & N_i/R_x & 0 & 0 \\ N_{i,y} & 0 & 0 & 0 & 0 \\ 0 & N_{i,x} & 0 & 0 & 0 \\ 0 & N_{i,y} & N_i/R_y & 0 & 0 \\ -N_i/R_x & 0 & N_{i,x} & 0 & 0 \\ 0 & -N_i/R_y & N_{i,y} & 0 & 0 \\ 0 & 0 & 0 & N_{i,x} & 0 \\ 0 & 0 & 0 & N_{i,y} & 0 \\ 0 & 0 & 0 & 0 & N_{i,x} \\ 0 & 0 & 0 & 0 & N_{i,y} \end{bmatrix}_{10\times 40}$$

The element geometric stiffness matrix due to non-mechanical (hygrothermal)forces is expressed in the form

$$[K^a_{\sigma e}]_{40\times 40} \;=\; \int_{-1}^{+1}\int_{-1}^{+1} [H]^T_{40\times 10}[E]_{10\times 10}[H]_{10\times 40}\;|J|\;d\xi\;d\eta \tag{3.6.51}$$

where,

$$[E] = \begin{bmatrix} N_x^a & & & & & & & & & \\ N_{xy}^a & & & & & & & & & \\ 0 & 0 & N_x^a & & & & & & & \\ 0 & 0 & N_{xy}^a & N_y^a & & & & Sym. & & \\ 0 & 0 & 0 & 0 & N_x^a & & & & & \\ 0 & 0 & 0 & 0 & N_{xy}^a & N_y^a & & & & \\ 0 & 0 & 0 & 0 & 0 & 0 & E_1 & & & \\ 0 & 0 & 0 & 0 & 0 & 0 & E_3 & E_2 & & \\ 0 & 0 & 0 & 0 & 0 & 0 & 0 & 0 & E_1 & \\ 0 & 0 & 0 & 0 & 0 & 0 & 0 & 0 & E_3 & E_2 \end{bmatrix}_{10\times 10}$$

In the above matrix, $E_1 = \dfrac{N_x^a h^2}{12},\ E_2 = \dfrac{N_y^a h^2}{12},\ E_3 = \dfrac{N_{xy}^a h^2}{12}$

3.6.8 Element mass matrix

The element mass matrix is obtained from the integral

$$[M_e]_{40\times 40} = \int_{-1}^{+1}\int_{-1}^{+1} [N]_{40\times 5}^T [P]_{5\times 5} [N]_{5\times 40} |J|\, d\xi\, d\eta \tag{3.6.52}$$

$$\text{where, } [N] = \sum_{i=1}^{8} \begin{bmatrix} N_i & 0 & 0 & 0 & 0 \\ 0 & N_i & 0 & 0 & 0 \\ 0 & 0 & N_i & 0 & 0 \\ 0 & 0 & 0 & N_i & 0 \\ 0 & 0 & 0 & 0 & N_i \end{bmatrix}_{5\times 40}$$

$$\text{and, } [I] \;=\; \sum_{i=1}^{8} \begin{bmatrix} I_1 & 0 & 0 & 0 & 0 \\ 0 & I_1 & 0 & 0 & 0 \\ 0 & 0 & I_1 & 0 & 0 \\ 0 & 0 & 0 & I_3 & 0 \\ 0 & 0 & 0 & 0 & I_3 \end{bmatrix}_{5\times 5}$$

in which

$$I_1 \;=\; \sum_{k=1}^{n} \int_{z_{k-1}}^{z_k} \rho \; dz$$

and

$$I_3 \;=\; \sum_{k=1}^{n} \int_{z_{k-1}}^{z_k} z^2 \; \rho \; dz$$

ρ is the mass density.

3.6.9 Element Load vector

The element load vector due to hygrothermal forces and moments is given by

$$[P_e^N] \;=\; \int_{-1}^{+1} \int_{-1}^{+1} [B]^T \; \{F^N\} \; |J| \; d\xi \; d\eta \tag{3.6.53}$$

3.6.10 Solution process

The element elastic stiffness matrix, the element geometric stiffness matrix due to hygrothermal load, the element geometric stiffness matrix due to applied loads, element mass matrix and the load vectors of the element are evaluated by expressing the integrals in local Natural co-ordinates ξ and η of the element and then performing numerical integration by using Gaussian quadrature. Then the initial stress resultants N_x^i, N_y^i, N_{xy}^i, M_x^i, M_y^i, M_{xy}^i, Q_x^i and Q_y^i are obtained. Then the element matrices

are assembled to obtain the respective global matrices $[K]$, $[K_\sigma^N]$, $[K_\sigma^a]$ and $[M]$. The next part of the solution involves determination of natural frequencies, buckling loads and excitation frequencies from the eigenvalue solution of the equations Eq 3.5.7 through Eq.3.5.9.

3.6.11 Computer program

A computer program based on MATLAB environment is developed to perform all necessary computations as per the flow chart attached (Figure 3.10). The composite panel is divided into a two-dimensional array of rectangular elements. The element elastic stiffness and mass matrices are obtained with 2×2 gauss points. The geometric stiffness matrix is essentially a function of the in-plane stress distribution in the element due to applied load and residual stress distribution due to hygrothermal load. The overall element stiffness and mass matrices are obtained by assembling the corresponding element matrices. Reduced integration technique is adopted in order to avoid possible shear locking.

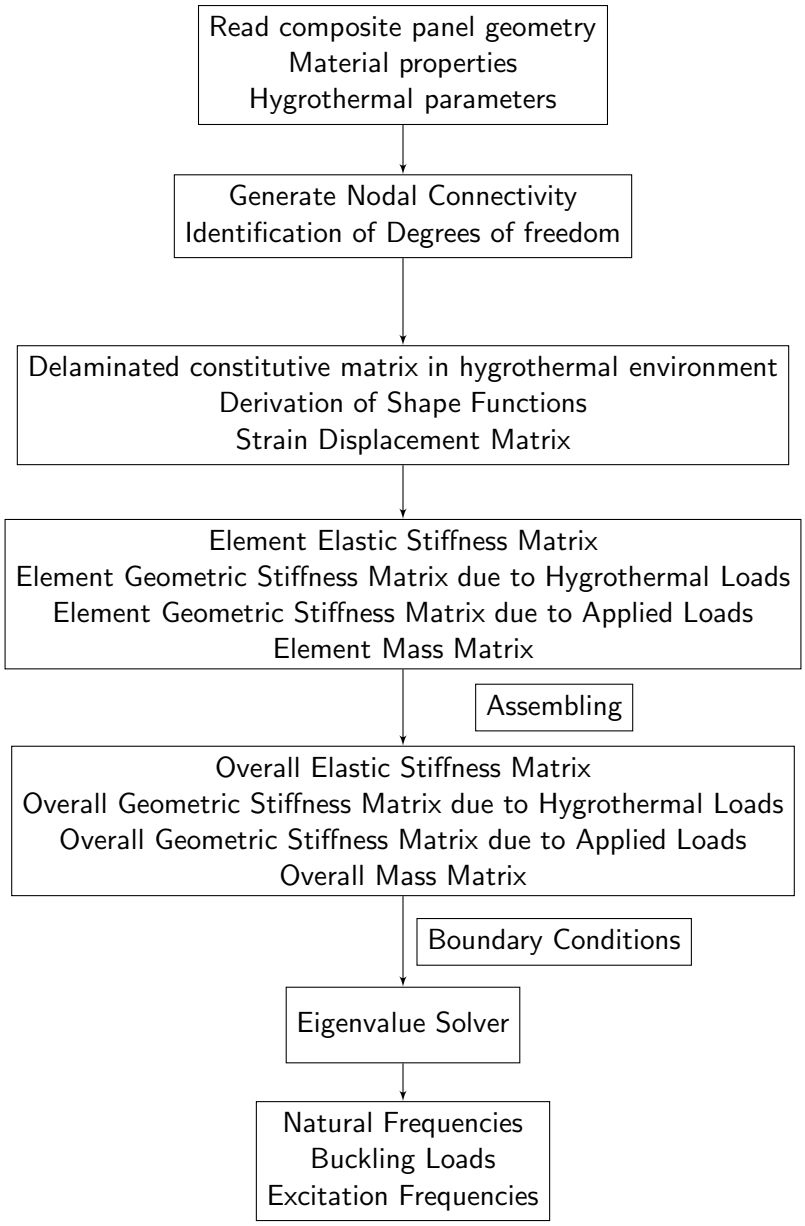

Figure 3.10: Flow chart of program in MATLAB for instability of delaminated composite panels in hygrothermal environment subjected to in-plane periodic loading

Chapter - 4

Experimental Programme

4.1 Introduction

This chapter highlights the experimental works conducted on the free vibration and buckling of industry driven woven roving delaminated composite plates in hygrothermal environment. Composite plates are fabricated for the aforementioned experimental works and the material properties are found out by tensile test as per ASTM Standard: D3039/D 3039 M [2008] guidelines to characterize the delaminated composite plates in thermal and moist environments. The experimental results are compared with the analytical or numerical predictions. The experimental work performed is categorized in three sections as follows:

- Determination of material constants
- Vibration of delaminated composite plates in hygrothermal environment
- Buckling of delaminated composite plates in hygrothermal environment

4.2 Materials required for fabrication of plates

The following materials are used for fabricating the glass/epoxy fiber plate:

- Woven roving E-Glass fibers (WR 360/100, Owens Corning-360 grams/m^2)

- Epoxy as resin matrix
- Hardener as catalyst (Ciba-Geigy, Araldite LY556 and Hardener HY951)
- Polyester resin (MEKP-Methyl Ethyl Ketone Peroxide)
- Polyvinyl alcohol as a releasing agent

4.3 Fabrication of woven roving composite plates

Glass fiber, Epoxy composite plate specimens were fabricated using weight fraction of 55 : 45 by hand layup method. Woven roving E-Glass fibers were cut into required size according to number of specimens required for testing. For the present numerical and experimental study, composite laminates of 16 layers of fibers in balanced form as per ASTM Standard: ASTM Standard: D5687/D5687M-07 [2007] specifications, were chosen. For preparation of Epoxy resin matrix, Hardener 8% of the weight of Epoxy was used. A flat ply wood rigid platform was selected. A plastic sheet, i.e. a mould releasing sheet was kept on the ply wood platform and a thin film of polyvinyl alcohol was applied as a releasing agent. Laminating was done with the application of a gel coat (mixture of Epoxy and Hardener) deposited on the mould by brush, whose main purpose was to provide a smooth external surface and to protect the fibers from direct exposure to the environment. Layers of reinforcements were placed on the mould at top of the gel coat and hand rolling was done by serrated steel roller to minimize the void content in the samples. Gel coat was applied again by brush (Fig. 4.1) and the process of hand layup was continued for all 16 layers of reinforcement before the gel coat had fully hardened (Fig. 4.2). After completion of all the layers, again a plastic sheet was covered at the top of last ply by applying polyvinyl alcohol inside the sheet as a releasing agent. Again one flat ply board and a heavy flat metal rigid platform were kept on the top of the plate for compression purpose. The laminates were cured at normal temperature (25^0C and 55% Relative Humidity) under a pressure of 0.2 MPa for 3 days. After proper curing of laminates, the release films were detached. The specimens were cut for free vibration and buckling testing into $235mm \times 235mm$

size. The average thickness of 16 layered laminate was measured by digital slide calipers and was found to be $6mm$.

Figure 4.1: Application of gel coat

Figure 4.2: Placing fibers on gel coat and removal of air entrapment by roller

4.3.1 Delamination procedure

Teflon film was embedded (Fig. 4.3) in the laminate simulating the presence of delamination. For the present finite element analysis (FEA), 8×8 mesh size is chosen. Accordingly, while preparing the specimen, teflon film was embedded in the mid plane of the laminate, i.e. on the 8^{th} layer, dividing the entire laminate into two sub-laminates. Square size teflon films were inserted as per the mesh division in three different areas such as $6.25\%, 25\%$ and 56.25% of the total area of the laminate. Complete care was taken in casting of the plates with presence of delamination.

Figure 4.3: Fixing Teflon film to introduce delamination

4.3.2 Hygrothermal treatment

The composite specimens were hygrothermally conditioned in Temperature Bath and Temperature/Humidity chamber separately before testing to know the effects of elevated moisture concentrations and temperature on natural frequency of free vibration.

The oven dried samples were kept in humidity chamber maintaining specified temperatures and Relative Humidity as per requirement of ASTM Standard: D5229/D5229M-04 [2004] for moisture absorption. To record moisture uptake, the samples were periodically removed from the temperature/humidity chamber, allowed to cool in a sealed,

humid environment (Fig. 4.4); weighed; and then quickly kept back in the chamber, if the required moisture content was not gained. The formula used for calculation of moisture content is as per ASTM Standard: D5229/D5229M-04 [2004].

$$M = [(W_i - W_0) / W_0] * 100$$

Where, M is in %, W_i = Current specimen mass in grams, and W_0 = Oven-dry specimen mass in grams.

For elevated temperature treatment of composite plates, three different temperatures as $325K, 350K, 375K$ and $400K$ were chosen for the experimental as well as numerical evaluation of natural frequencies. The samples were kept in the temperature bath (Fig. 4.5) for a period of 6-8 hrs and then removed, allowed to cool at room temperature before testing.

4.4 Determination of material constants

The material elastic constants were found experimentally by performing unidirectional tensile tests on specimens cut in longitudinal and transverse directions and at 45^0 to the longitudinal directions as described in ASTM Standard ASTM Standard: D3039/D 3039 M [2008]. At least three replicate sample specimens hygrothermally treated at elevated temperatures and moisture concentrations were loaded in INSTRON 1195 universal testing machine monotonically to failure (Fig.4.6)with a recommended rate of extension of 0.1 mm per minute for measuring Young's modulus (E_1 is same as E_2 in this case) and the mean values adopted.

Figure 4.4: Composite plates in humidity chamber

Figure 4.5: Composite plates in temperature bath

Figure 4.6: Failure of test coupon on INSTRON 1195 UTM

For determination of Poisson's ratio (ν_{12}), a different set of specimens were used, along with a pair of strain gages bonded over the gage length of the sample in two mutually perpendicular directions. The strains were recorded simultaneously in longitudinal and transverse directions with the help of two strain indicators. The ratio of transverse to longitudinal strain directly gives the Poisson's ratio within the elastic range. The shear modulus (G_{12}) was determined similarly with 45^0 coupons using the following standard formula.

$$G_{12} = \frac{1}{\frac{4}{E_s} - \frac{2(1-\nu_{12})}{E_1}}$$

Where E_s is the tensile modulus as obtained in 45^0 tensile test.

The values of material constants finally obtained experimentally for different temperature and moisture concentrations are presented in **Tables 5.1 and 5.2**.

4.5 Vibration of delaminated composite plates in hygrothermal field

In order to achieve the right combination of material properties and service performance, the dynamic behavior is the main point to be considered. It is important to determine natural frequency of the structure for design purposes. Due to the advancement in computer aided data acquisition systems and instrumentation, experimental modal analysis has become an extremely important tool in the hands of an experimentalist.

4.5.1 Test set up:Vibration

- Modal hammer. (B&K 2302-5)
- Accelerometer. (B&K 4507)
- FFT Analyzer. (Model B&K 3560-C)
- Notebook with PULSE lab shop software.
- Specimens to be tested (Composite plate size $0.235m \times 0.235m \times 0.006m$)

4.5.2 Vibration of delaminated composite plates under hygrothermal load

Hygrothermally treated delaminated composite test specimens were fitted properly to the prefabricated iron frame as shown in Fig. 4.7. The five different boundary conditions ($B.C.$) adopted for the present numerical analysis as well as experimental work are as follows: All four sides clamped ($C-C-C-C$), all sides simply supported ($S-S-S-S$), one side clamped and other sides free i.e. cantilever, ($C-F-F-F$), two opposite sides clamped and other two sides free ($C-F-C-F$) and two opposite

sides clamped with other two sides simply supported ($C-S-C-S$) shown in Figs. 4.8 through 4.12.

Figure 4.7: Frame to fit different boundary conditions

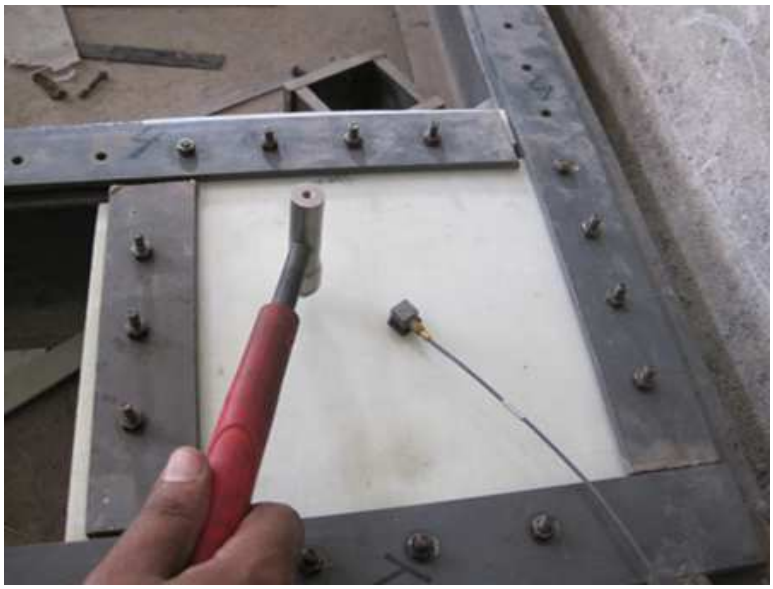

Figure 4.8: Plate with $C-C-C-C$ boundary condition

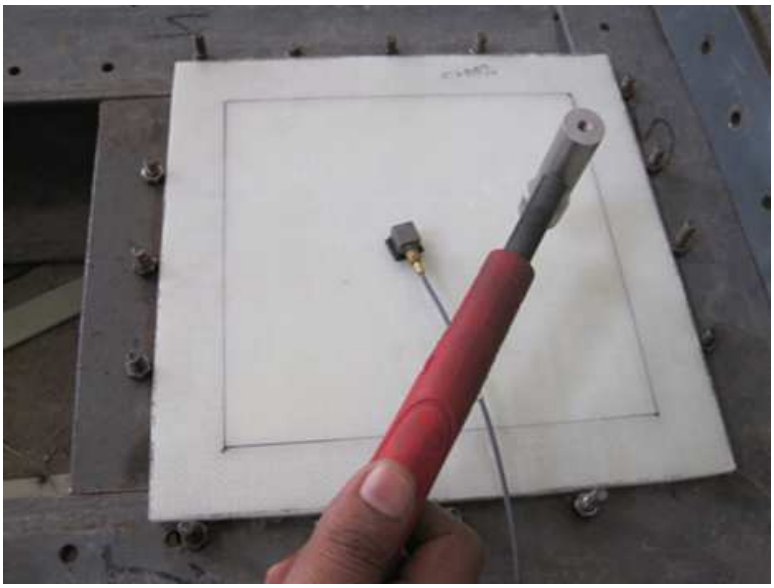

Figure 4.9: Plate with S-S-S-S boundary condition

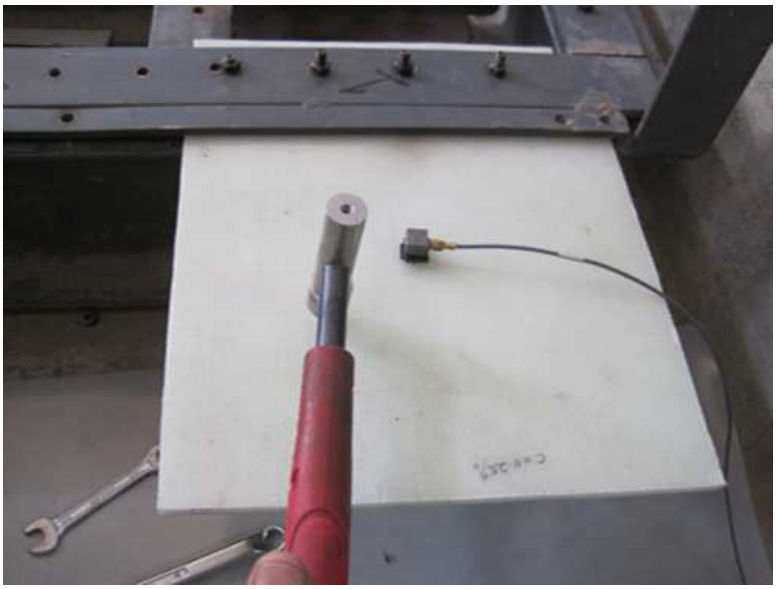

Figure 4.10: Plate with C-F-F-F boundary condition

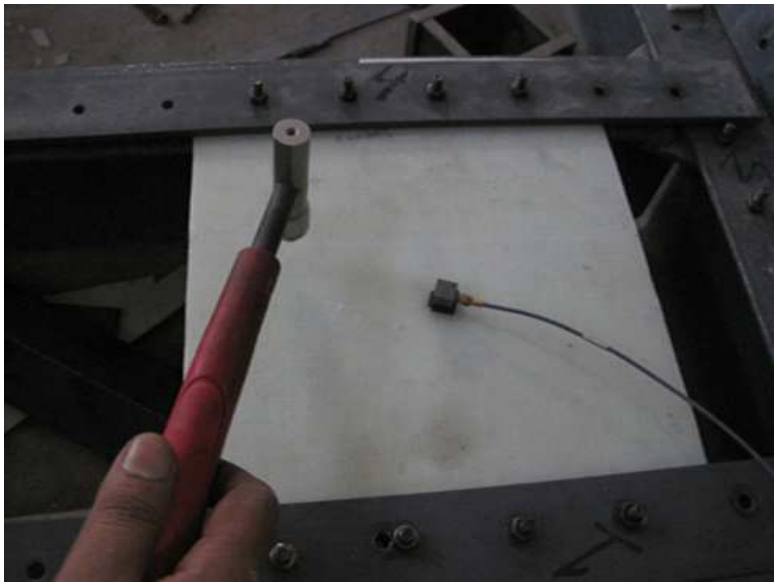

Figure 4.11: Plate with C-F-C-F boundary condition

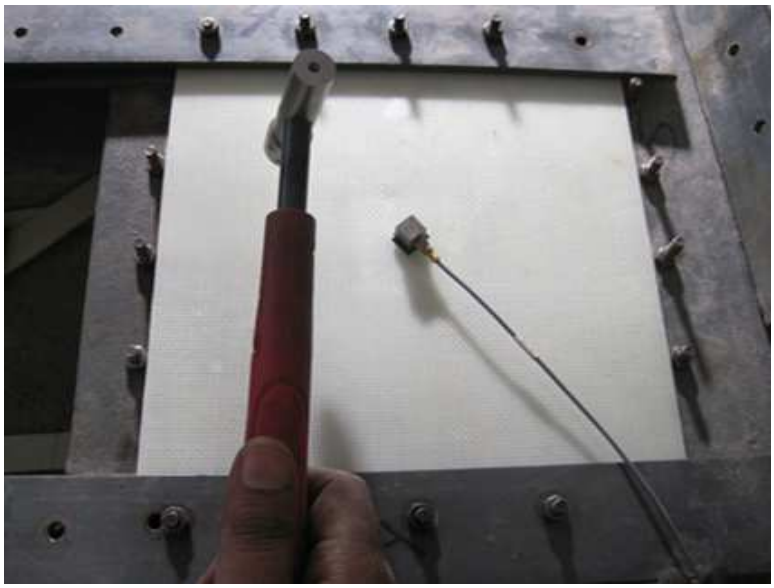

Figure 4.12: Plate with C-S-C-S boundary condition

The FFT (Fast Fourier Transform) analyzer (Model B&K3560 – C) as shown in Fig. 4.13, B&K4507 transducers, B&K2302 – 5 modal hammer and cables to the system were connected. PULSE Lab shop software was used during the vibration measurement. Composite plate was excited at selected points by means of impact hammer (Model 2302 – 5) and this resulting vibration of the specimens was picked up by the accelerometer. The accelerometer (B&K 4507) was mounted on the specimen

by means of bees wax. An arrangement of high sensitivity, light mass and insignificant physical dimensions make the accelerometer ideal for modal measurements. The signal was then subsequently led to the FFT analyzer, where its frequency spectrum was also obtained using the PULSE software. Various forms of Frequency Response Functions (FRFs) are directly measured. The FRF contains information regarding the system frequency and a collection of FRFs contain information regarding the mode shape of the system at the measured locations. This is the most important measurement related to experimental modal analysis. The coherence was observed for each set of measurement. The coherence function is used as a data quality assessment tool which identifies how much of output signal is related to the measured input signal. A typical FRF (PULSE report) of the measurement from the FFT analyzer along with the coherence curve is shown in Fig. 4.14 and Fig. 4.15 respectively. As per Fig. 4.14, the different peaks of FRF shows the different modes of vibrations and the coherence value of nearly 1 (one) in Fig. 4.15 shows the accuracy of the measurement. The output from the analyzer was displayed on the Lab shop screen as shown in Fig. 4.16. The present work calculates only the natural frequencies of the delaminated woven fiber composite plates in hygrothermal environment. For FRF, at each single point the modal hammer was struck five times and the average value of the response was displayed on the screen of the display unit as shown in Fig. 4.16. At the time of striking with modal hammer to the points on the specimen precautions were taken for making the stroke to be perpendicular to the surface of the plates. Then by moving the cursor to the peaks of the FRF graph the frequencies were measured by 'peak-picking' method.

Figure 4.13: FFT analyzer B&K 3560-C test set up

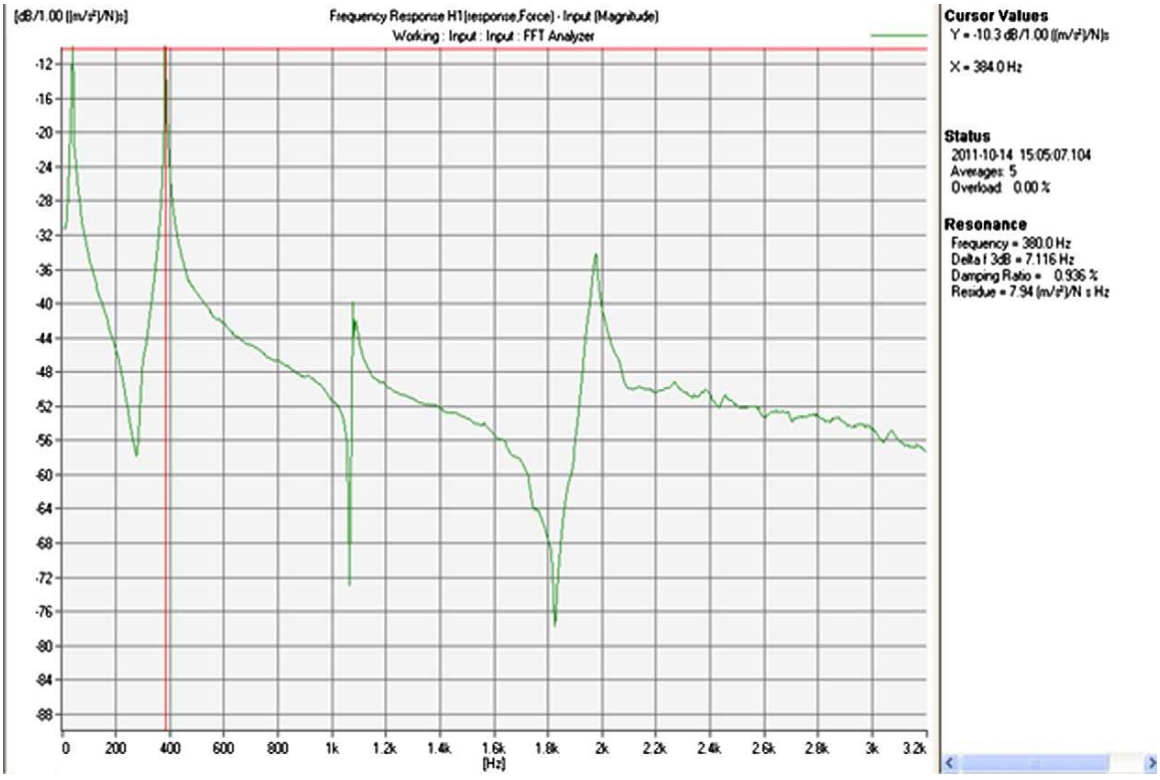

Figure 4.14: Typical FRF of test specimen

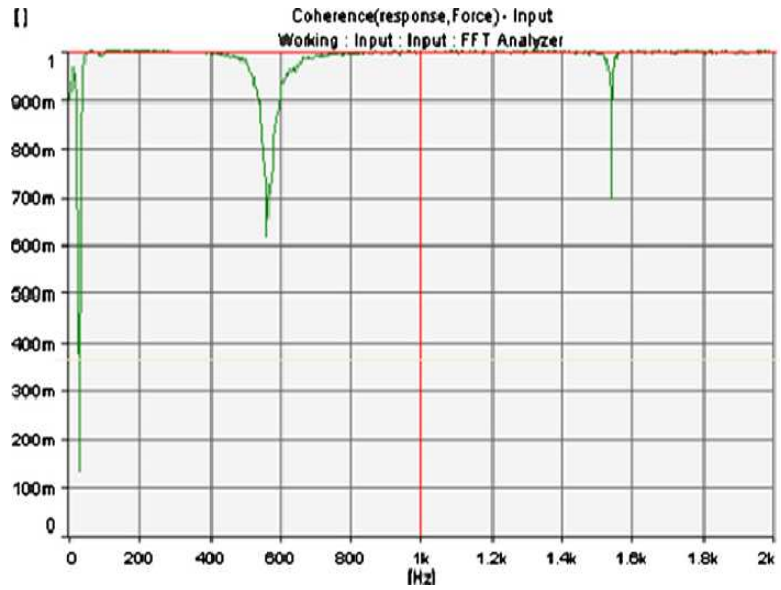

Figure 4.15: Typical coherence of test specimen

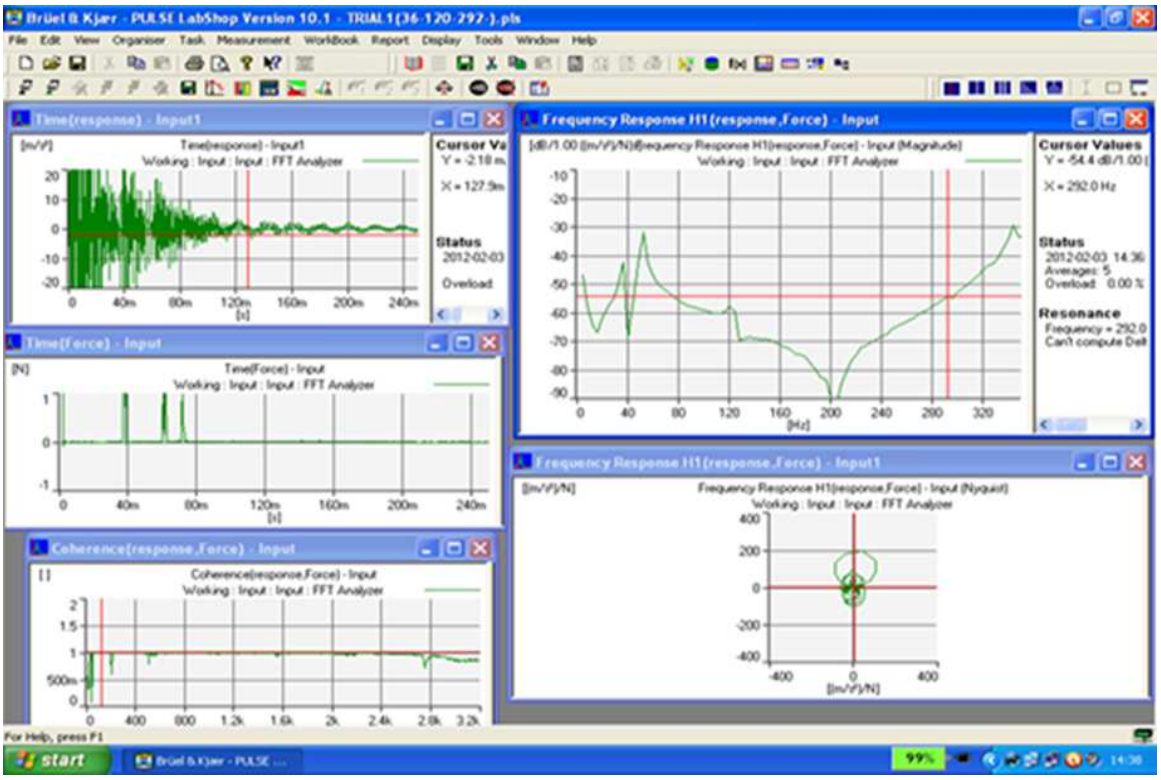

Figure 4.16: Various Pulse output windows on the display unit

4.6 Buckling test of woven fiber delaminated composite plates

The complex behavior of woven fabric composite laminates under compressive loading conditions is still not well understood and requires further experimental investigations in order to better understand their behavior especially buckling load. Studies of buckling analysis of woven fabric or bi-directional composite laminates are limited. Therefore, woven fabric glass/epoxy composites were used in this study to demonstrate the capability of the static stability analysis of woven fiber composite panels. In the present study, buckling loads of woven fabric composite plates were determined and compared to the numerical solutions using present FEM based formulation.

4.6.1 Test set up:Buckling

In view of actual real time behavior of delaminated composite plates, experimental methods have become important in solving the buckling problem of laminated composite plates. Hygrothermally treated delaminated composite plates were tested on INSTRON 8862 Universal testing machine (UTM) (Fig. 4.17) to determine the critical buckling loads. The INSTRON 8862 testing systems feature a single screw electromechanical actuator that has been developed for slow speed static, slow strain rate and quasi-dynamic cyclic testing. The systems are completed with high stiffness, precision aligned, two-column load frames to give unparalleled testing performance. The test space is configurable to suit the application requirements. For increased usability, the higher capacity 8862 machine can be equipped with the actuator mounted in the lower table or upper crosshead, and coupled with the option of hydraulic lifts. Combined with the advanced features of the INSTRON digital controller, and INSTRON's advanced fatigue-rated load cell technologies, the machine is ideally suited to low cycle fatigue, thermo-mechanical fatigue, high temperature static, creep fatigue, slow strain rate and ceramics testing.

Some typical features of INSTRON 8862 UTM:

- Integrated with digital controller servo-electric testing systems
- High accuracy load cell
- Capable of testing speeds down to 1 micron/hour
- Excellent waveform fidelity
- Low mechanical noise
- Wide variety of system options, grips, fixtures and accessories available
- A comprehensive range of applications available

Two types of boundary conditions were used with the frame shown in Fig. 4.18. First type is $C-F-C-F$, which shows the vertical faces of the plate free and the top and bottom faces of the plate as clamped. The second type is $C-C-C-C$ having all the sides of the composite plate clamped.

Figure 4.17: Buckling test set up of INSTRON 8862

4.6.2 Buckling test of delaminated composite plates under hygrothermal load

All specimens were loaded slowly unless buckling takes place. Clamped boundary conditions were simulated along top and bottom edges, restraining 2.5cm length. For axial loading, the test specimens were placed on INSTRON 8862 UTM between the two extremely stiff machine heads, of which the lower one was fixed during the test; whereas the upper head was moved downwards by servo hydraulic cylinder. All plates were loaded at constant cross-head speed of 0.5mm/min. The shape of the specimen after buckling is as shown in Fig. 4.18. The measurements were recorded on a computer from which the load vs deformation curve was drawn for each test. The load which is the initial part of the curve deviated linearity, is taken as the critical buckling load in KN in line with previous investigators.

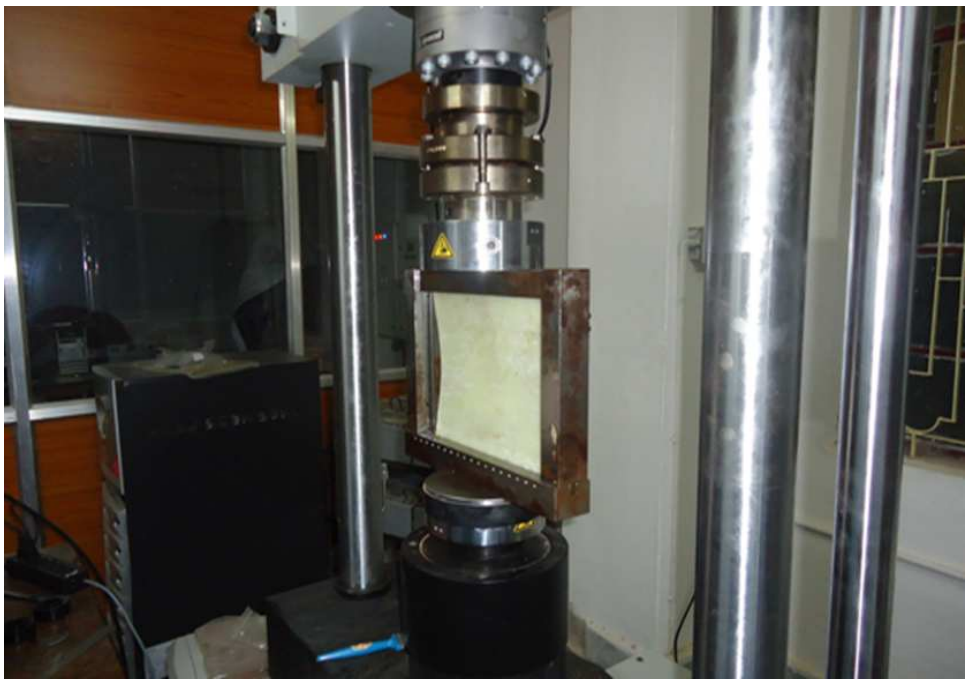

Figure 4.18: Composite plate buckling test with INSTRON 8862

Chapter - 5

Results and Discussions

5.1 Introduction

The present chapter deals with the determination of natural frequency, buckling load and excitation frequency of delaminated composite flat and doubly curved panels in hygrothermal environment. The vibration, buckling and parametric resonance characteristics of delaminated composite plates and shells are numerically investigated by using the FEM formulation given in the Chapter 3. The influence of various parameters like delamination size, fiber orientation, stacking sequence, boundary conditions, hygrothermal effects on vibration, buckling and parametric resonance characteristics of woven fiber composite plates and shells are presented using numerical model. The experimental results on vibration and buckling of bidirectional delaminated composite flat panels in hygrothermal field are also used to support the numerical predictions. Parametric instability studies are carried out for woven fiber delaminated composite flat and curved panels subjected to in-plane periodic loads in hygrothermal environment. The studies in this chapter are presented separately for composite flat and curved panels as follows:

- Vibration of delaminated composite panels in hygrothermal environment
  - i. Comparison with previous studies
  - ii. Numerical and experimental results

- Buckling of delaminated composite panels in hygrothermal environment
  - i. Comparison with previous studies
  - ii. Numerical and experimental results
- Parametric instability of delaminated composite panels in hygrothermal field
  - i. Comparison with previous studies
  - ii. Numerical results

The parameters of composite flat and doubly curved panels in the above studies (unless otherwise mentioned) are:

$$\text{a} = 235 \text{ mm, b} = 235 \text{ mm, h} = 6 \text{ mm,}$$
$$E_{11} = E_{22}, G_{12} = G_{13} = G_{23},$$
$$\textbf{mass density } `\rho' = 1660 \text{ Kg/m}^3,$$
$$\textbf{Poisson's ratio } `\nu' = 0.43$$

The composite doubly curved panels of various geometry considered in the present study are:

$$\textbf{cylindrical } (R_x = \infty, R_y = R, R_{xy} = \infty),$$
$$\textbf{spherical } (R_x = R_y = R, R_{xy} = \infty),$$
$$\textbf{hyperbolic paraboloidal } (R_x = -R_y = R, R_{xy} = \infty),$$
$$\text{and } \textbf{elliptic paraboloidal } (R_x \neq R_y, R_{xy} = \infty).$$

The different boundary conditions for the present study (unless otherwise mentioned)such as - all four sides clamped ($C-C-C-C$), all sides simply supported ($S-S-S-S$), one side clamped and other sides free i.e. cantilever ($C-F-F-F$), two opposite sides clamped and other two sides free ($C-F-C-F$) and two opposite sides clamped with other two sides simply supported ($C-S-C-S$), are considered.The displacement based boundary conditions considered in simply supported and clamped delaminated composite panels are:

$$\text{Simply supported: } u_i = w_i = \theta_{yi} = 0 \text{ at } x = 0, a$$

$$\text{and } v_i = w_i = \theta_{xi} = 0 \text{ at } y = 0, b.$$

$$\text{Clamped : } u_i = v_i = w_i = \theta_{xi} = \theta_{yi} = 0.$$

The non-dimensional parameters used in free vibration, buckling and dynamic stability analysis are presented in Table 5.1.

Table 5.1: Non-dimensional parameters of composite panels

Sl No.	Parameter	Non-dimensional equation
1	Free Vibration Frequency (ϖ)	$\omega a^2\sqrt{\rho h^2/E_2}$
2	Buckling Load (λ)	$N_x a^2/E_2 h^3$
3	Frequency of Excitation ($\bar{\Omega}$)	$\Omega a^2\sqrt{\rho h^2/E_2}$

where, ω and Ω are in rad/sec.

5.2 Vibration Analysis

Delamination in the composite panels greatly affects the dynamic behavior of structures. Also, the environmental effects pose a challenge to the designer due to loss of stiffness in the dynamic analysis and design of composite structures. The combination of the above two effects become critical which finally affects the free vibration characteristics of composite laminates because of degraded properties of composites and the residual stresses due to hygrothermal environment and poses a challenge to the designer of composite structures.

In the present investigation, natural frequencies of delaminated industry driven woven fiber glass/epoxy composite panels in hygrothermal field were determined both numerically and experimentally. The effects of various parameters like delamination area, boundary conditions, temperature, moisture concentrations and geometry on free vibration of woven fiber composite panels were studied critically.

5.2.1 Delaminated composite flat panels in hygrothermal field

The present study takes into account a combined numerical and experimental investigation on free vibration behavior of industry driven woven fabric delaminated composite plates under elevated temperature and moisture concentrations. Numerical (FEM) and experimental results of frequencies of vibration for $[0/0]_{8s}$ woven fiber Glass/Epoxy composite plates are obtained with elevated temperatures and moisture concentrations for different delamination areas as well as for different boundary conditions. In the present dynamic analysis in hygrothermal environment, moisture concentration is varied from 0% to 0.75% and temperature (T) from $3000K$ to $3750K$. For computing the results, centrally located single mid plane delamination of three different sizes like 6.25%, 25% and 56.25% of the total plate area is considered for composite plates. A mesh of 8×8 has been considered throughout the study for convergence and for ease of these percentages of delamination. The details of convergence study is presented in Appendix.

The geometry and material properties of the composite plates at elevated temperatures and moisture concentrations used in the present study are shown in Table 5.2 and Table 5.3 respectively.

Table 5.2: Elastic moduli of Glass/Epoxy lamina at different temperatures

Elastic	Temperature, T (K)			
Moduli(GPa)	300	325	350	375
E_1	15.4	15.39	14.93	13.21
G_{12}	3.56	3.54	3.51	3.48

Table 5.3: Elastic moduli of Glass/Epoxy lamina at different moisture contents

Elastic	Moisture concentration, C (%)			
Moduli(GPa)	0	0.25	0.5	0.75
E_1	15.4	15.38	14.69	13.17
G_{12}	3.56	3.53	3.49	3.47

5.2.1.1 Comparison with previous studies

The accuracy of the present finite element formulation is verified by comparing the frequencies of vibration of the 8 layer laminated composite plate example solved by Ju et al. [1995] using FEM. As shown in Table 5.4, the present FEM results compare well with the previous study. The results on vibration of composite plates subjected to hygrothermal loading based on present formulation are compared with the results of Whitney and Ashton [1971] using Ritz method and FEM results of Sairam and Sinha [1992] as shown in Table 5.5. There exists excellent agreement between the results involving different methods with the present FEM.

Table 5.4: Comparison of results of natural frequency (Hz) of 8-layer square $[0/90/45/90]_s$ laminated composite plate for different boundary conditions

$a = 0.25m, h = 0.00212m$
$E_1 = 132\ GPa$, $E_2 = 5.35\ GPa$, $G_{12} = 2.79\ GPa$,
mass density $\rho = 1446.2\ kg/m^3$, **Poisson's ratio** $\nu = 0.291$

Mode No	$S-S-S-S$		$C-C-C-C$		$C-F-F-F$	
	Ju et al.[1999]	Present FEM	Ju et al.[1999]	Present FEM	Ju et al.[1999]	Present FEM
1	164.37	163.97	346.59	346.13	41.347	41.265
2	404.38	404.01	651.51	651.24	60.663	60.354
3	492.29	491.93	781.06	780.93	221.52	220.997
4	658.4	658.72	1017.2	1016.87	258.72	259.036

Table 5.5: Comparison of results of non-dimensional frequency $\varpi = \sqrt{[\omega a^2(\rho/E_2h^2)]}$ of simply supported [0/90/90/0] laminated Graphite/Epoxy plate

$a/b = 1, a/h = 100$
$E_1 = 130\ GPa$, $E_2 = 9.5\ GPa$, $G_{12} = 6.0\ GPa$,$G_{12} = G_{13}$, $G_{23} = 0.5G_{12}$

Mode No	$C = 0.1\%$			$T = 325\ K$		
	Sai Ram and Sinha[1992]	Whitney and Ashton[1971]	Present FEM	Sai Ram and Sinha[1992]	Whitney and Ashton[1971]	Present FEM
1	9.429	9.411	9.391	8.088	8.068	8.041
2	20.697	19.911	19.892	19.196	18.378	18.354
3	40.068	39.528	39.353	39.324	38.778	38.597

For authentication of the formulation, natural frequencies for mid-plane delaminated composite plate is compared with the result by Ju et al. [1995] for different boundary conditions as shown in Table 5.6. The present finite element results show good agreement with the results of previous studies.

Table 5.6: Natural frequencies(Hz.) of square delaminated composite $[0/90/45/90]_s$ plates

Boundary Condition	Delamination Percentage %	Mode 1		Mode 2	
		Present FEM	Ju et al. [1995]	Present FEM	Ju et al. [1995]
$S-S-S-S$	0%	164.08	164.37	403.99	404.38
	25%	161.35	161.58	347.93	348.27
$C-C-C-C$	0%	346.07	346.59	650.89	651.51
	25%	333.98	334.67	578.86	579.43

After validation with previous studies, new examples dealing with vibration of delaminated composite panels subjected to varieties of temperature and moisture effects are observed experimentally and compared with the FEM results. These outputs can be used as bench mark results for future researchers in this area for validation purposes.

5.2.1.2 Delaminated plates at elevated temperatures

The variation of frequencies of vibration of simply supported woven fiber $[0/0]_{8s}$ Glass /Epoxy composite plates are computed using the present formulation and are plotted with temperatures in Kelvin (K) for different delamination areas as shown in Fig. 5.1 . There is good agreement between FEM and experimental results. As observed, the lowest mode frequencies of the S-S-S-S composite plates decrease by $10\%, 14\%, 24\%$ and 34% for different delaminations i.e. $0\%, 6.25\%, 25\%$ and 56.25% respectively with rise in temperature from 300^0K to 375^0K due to reduction of stiffness. At 300^0K, the frequencies decrease with increase in percentage of delaminations in the range $12\%, 29\%$ and 39% for the corresponding $6.25\%, 25\%$ and 56.25% delamination area

as shown in Fig. 5.1. There is significant reduction in frequencies of vibration of composite plates due to delamination than the effects of temperature.

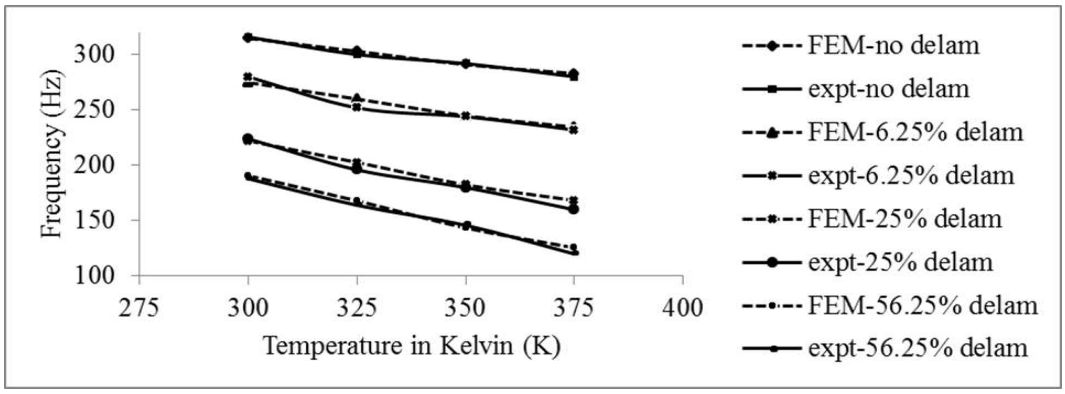

Figure 5.1: Effect of temperature on fundamental frequencies of vibration for composite plates with different delamination areas under $S-S-S-S$ boundary condition.

A comparative study of FEM and experimental results of frequencies of free vibration of fully clamped woven fiber $[0/0]_{8s}$ Glass /Epoxy composite plates with temperature in Kelvin (K) is as shown in Fig. 5.2. The C-C-C-C boundary condition

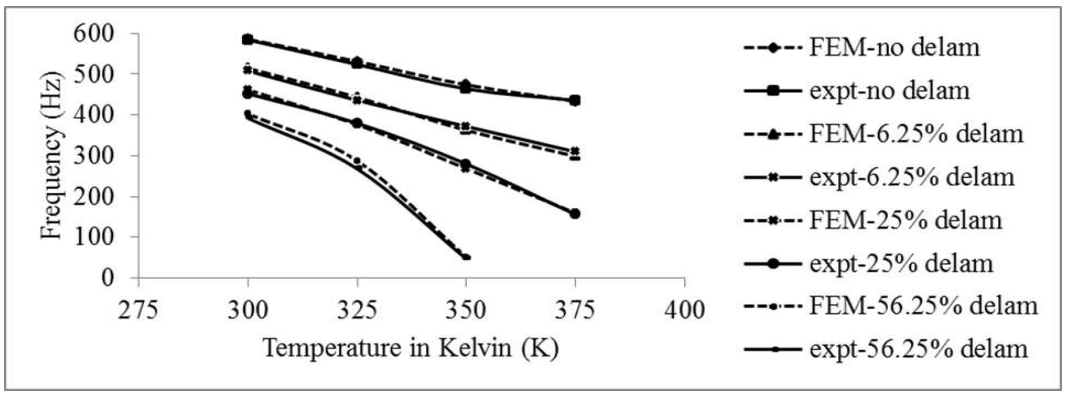

Figure 5.2: Effect of temperature on fundamental frequencies of vibration for composite plates with different delamination areas under $C-C-C-C$ boundary condition.

gives the highest values of frequencies among all boundary conditions considered. FEM and experimental results match well as seen from Fig. 5.2. In this case, the reduction in fundamental frequencies is 29% for 0% delamination, 42% for 6.25% delamination and 65% for 25% delamination area with temperature increment from 300^0K to 375^0K in each case. For 56.25% delamination, the frequency reduces drastically up to 84% with increase of temperature from 300^0K to 350^0K due to reduction in

stiffness and the variation is non-linear. At the reference temperature, the variation in frequencies is in range 12%, 21% and 31% for 6.25%, 25% and 56.25% delamination areas respectively from that of the intact plate. Here, the temperature effects play an important role in reduction of frequencies than that of the delamination size.

FEM and experimental results of frequencies of vibration for cantilever woven fiber $[0/0]_{8s}$ Glass /Epoxy composite plates are shown in Fig. 5.3 with temperature variations. Cantilever plates show the lowest frequencies among all boundary conditions and increase in temperature for different delamination areas does not affect the frequencies much as seen from Fig. 5.3 . But, at reference temperature, the reduction in frequencies is in the range of 2% for 6.25% delamination, 10% for 25% delamination and 26% for 56.25% delamination area from that of the intact plate. Here, the delamination size of the composite plate plays the dominant role in decreasing the frequencies than the temperature increment.

With rise in temperature, the results of present formulation and their counterparts are plotted for woven fiber $[0/0]_{8s}$ Glass /Epoxy composite plates with C-F-C-F boundary conditions in Fig. 5.4. Plates with C-F-C-F boundary conditions are the worst affected among all, as the variation in frequencies of free vibration of delaminated composite plates is greatly dependent on the boundary conditions. As seen from Fig. 5.4 , the first mode frequencies reduce drastically up to 45% for the intact plates with rise of temperature from 300^0K to 375^0K. With increase in delamination areas, the plates become unstable at higher temperatures due to much reduction in stiffness. At the reference temperature, the frequencies of 6.25%, 25% and 56.25% delaminated plates reduce from that of the intact plate in the range 4%, 10% and 21% respectively. There is a good correlation between the FEM and experimental results. In this case, the frequency reduction is more governed by the increase in temperature than the delamination area.

Variations between the frequencies of free vibration obtained from the present formulation and from the experiments for woven fiber $[0/0]_{8s}$ Glass /Epoxy composite plates with C-S-C-S boundary conditions and different delamination areas are shown in Fig. 5.5. Reduction in frequencies of the composite plates with increase

in temperature from 300^0K to 375^0K under C-S-C-S boundary conditions is in the range $26\%, 40\%$ and 63% for the delamination sizes of $0\%, 6.25\%$ and 25% respectively. When the delamination area becomes 56.25% of the total plate area, there is a sudden reduction in frequency up to 87% with temperature rise from 300^0K to 350^0K as marked from Fig. 5.5 and the variation is non-linear. In contrast to the above, at reference temperature, $12\%, 21\%$ and 31% decrease in frequency is seen for $6.25\%, 25\%$ and 56.25% delamination areas from that of the intact plate. In this case, rise in temperature plays important role for reduction in frequencies of vibration than the delamination size of the composite plates.

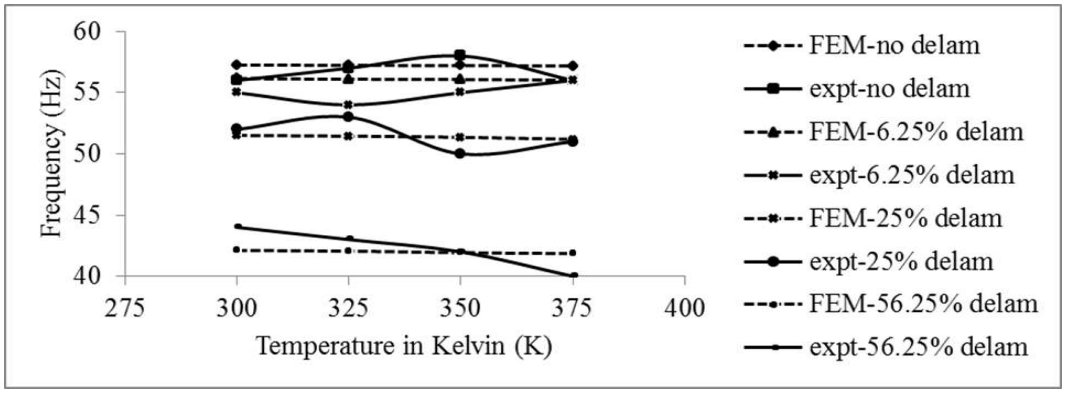

Figure 5.3: Effect of temperature on fundamental frequencies of vibration for composite plates with different delamination areas under $C-F-F-F$ boundary condition.

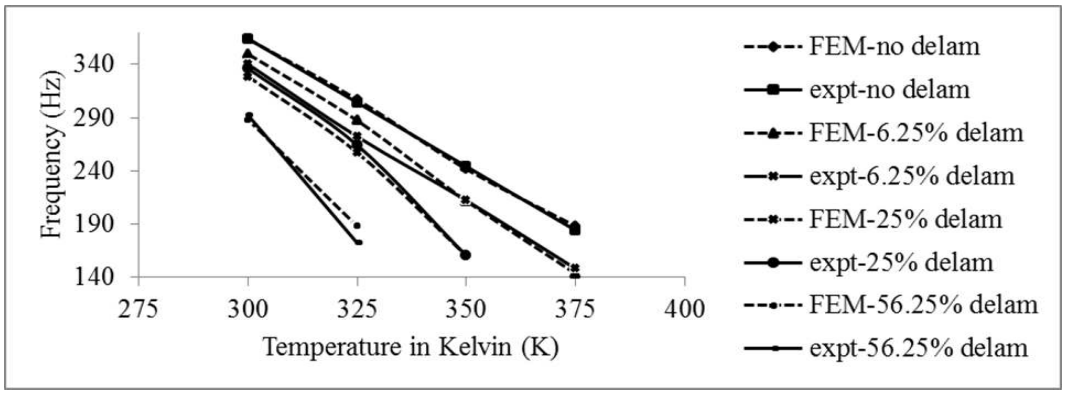

Figure 5.4: Effect of temperature on fundamental frequencies of vibration for composite plates with different delamination areas under $C-F-C-F$ boundary condition.

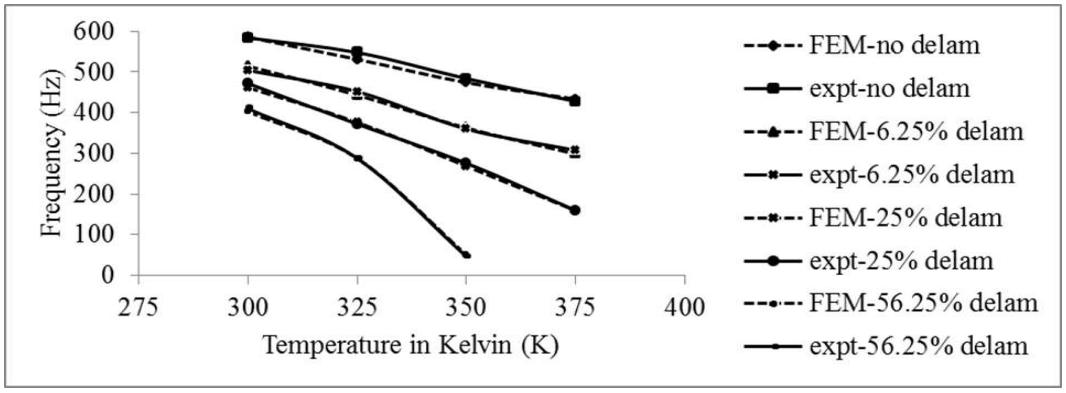

Figure 5.5: Effect of temperature on fundamental frequencies of vibration for composite plates with different delamination areas under $C-S-C-S$ boundary condition.

5.2.1.3 Delaminated plates with moisture concentrations

FEM and experimental results of fundamental frequencies of free vibration for woven fiber $[0/0]_{8s}$ Glass /Epoxy composite plates are shown in Fig. 5.6 against moisture concentrations (%) for different delamination areas with S-S-S-S boundary condition.

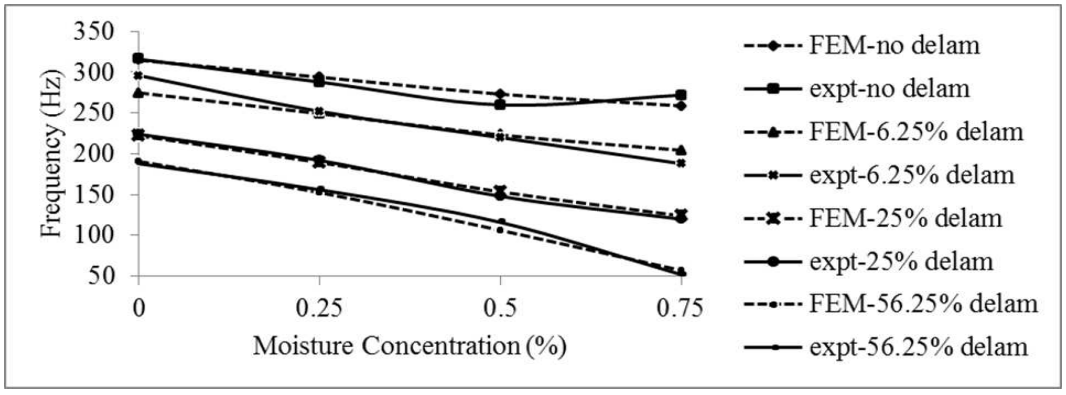

Figure 5.6: Effect of moisture on fundamental frequencies of vibration for composite plates with different delamination areas under $S-S-S-S$ boundary condition.

The first mode frequencies reduce in the range 18% for intact plate, 25% for 6.25% delamination, 44% for 25% delamination and 70% for 56.25% delamination areas respectively as the moisture concentration is raised from 0% to 0.75%. In comparison with the S-S-S-S boundary condition for temperature (Fig. 5.1), the frequencies are affected more by increment in moisture concentrations. At reference moisture concentration, 12%, 29% and 39% reduction and at 0.75% moisture concentration, 21%, 52%

and 78% reduction in frequencies is seen for 6.25%, 25% and 56.25% delaminations from that of the intact plate. In this case, delamination as well as moisture absorption play almost equal role in diminishing the stiffness of the composite plate, thereby affecting the frequencies of vibration.

Fig. 5.7 gives a plot of frequencies as found from the FEM and experiments with rise in moisture concentrations for fully clamped woven fiber $[0/0]_{8s}$ Glass /Epoxy composite plates. Fundamental frequencies of the composite plates reduce up to 48% for C-C-C-C case with rise in moisture from 0% to 0.75% for the intact plate. But, as the delamination size increases to and beyond 6.25%, the plate becomes unstable at higher moisture concentrations due to drastic reduction in stiffness as well as the restraining effects of the boundary condition. It is found that the effect of moisture concentrations in reducing the frequencies is much more than that of the elevated temperature conditions (Fig. 5.2) for different delamination sizes of the plate.

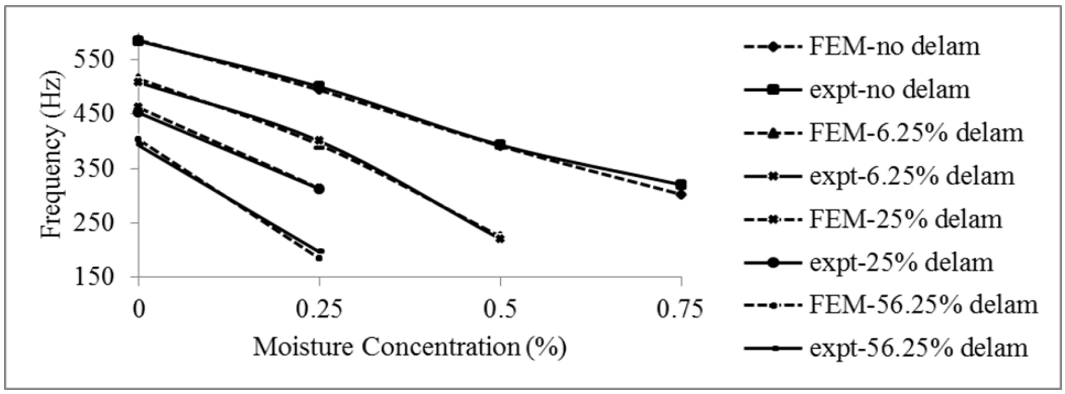

Figure 5.7: Effect of moisture on fundamental frequencies of vibration for composite plates with different delamination areas under $C-C-C-C$ boundary condition.

Frequencies of free vibration as obtained from FEM and experimental results are shown against the moisture concentrations for woven fiber $[0/0]_{8s}$ Glass /Epoxy cantilever composite plates as shown in Fig. 5.8. This boundary condition gives the lowest values of frequencies among all boundary conditions considered. Compared with Fig. 5.3, in this case also, there is no significant reduction in frequencies with increment in moisture. Here, the delamination area beyond 6.25% affects the natural frequencies more than the moist conditions of the plate. At reference moisture

content, the frequencies reduce up to 2% for 6.25% delamination, 10% for 25% delamination and 26% for 56.25% delamination area than that of the plate having no delaminations. Only, the delamination size governs the reduction in frequencies in this case as evident from Fig. 5.8.

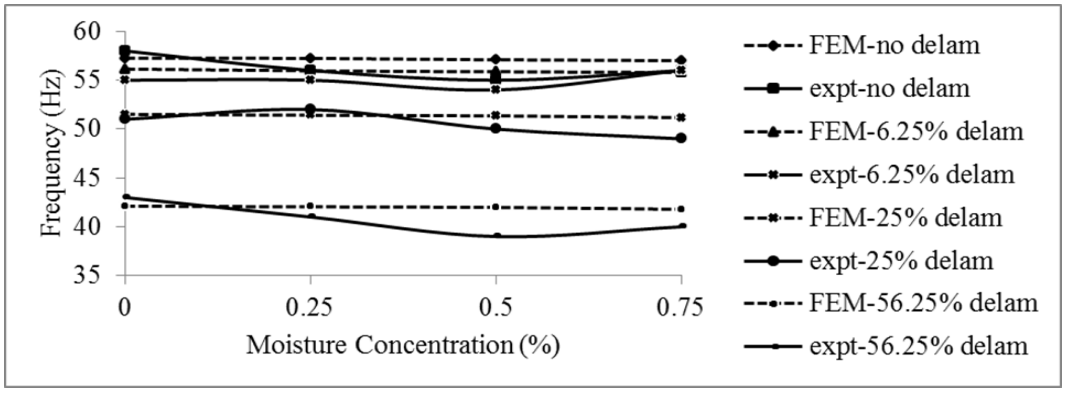

Figure 5.8: Effect of moisture on fundamental frequencies of vibration for composite plates with different delamination areas under $C - F - F - F$ boundary condition.

Results of present formulation and those found from experiments pertaining to the frequencies of free vibration of woven fiber $[0/0]_{8s}$ Glass /Epoxy composite plates are plotted against moisture percentages for C-F-C-F boundary condition in Fig. 5.9. The fundamental frequencies of plates with C-F-C-F boundary condition are the most affected i.e. up to 43% reduction in frequency is marked with no delamination at moisture concentration of 0.5% from that of the reference moisture concentration. As the delamination area increases and plate becomes moister, there is sudden reduction in frequencies and instability is marked. There is a good matching between the FEM and experimental values as seen from Fig. 5.9. A decrease of $4\%, 9\%$ and 21% in frequencies of the $6.25\%, 25\%$ and 56.25% delaminated plates from that of the intact plate at reference moisture concentrations is seen in this case. It is evident that the moisture content plays the dynamic role in reducing the frequencies in contrast to the effects of temperature as seen from Fig. 5.4.

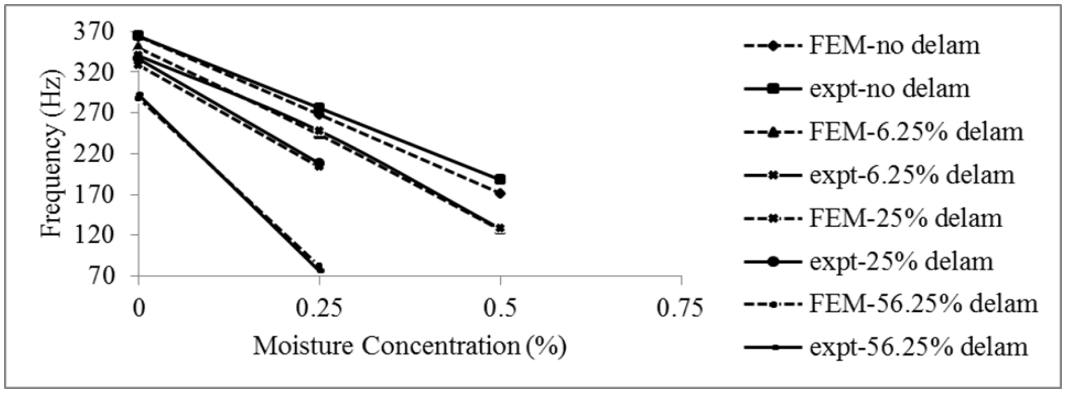

Figure 5.9: Effect of moisture on fundamental frequencies of vibration for composite plates with different delamination areas under $C-F-C-F$ boundary condition.

A comparison of fundamental frequencies of free vibration of woven fiber $[0/0]_{8s}$ Glass /Epoxy composite plates against moisture percentages for different delamination areas is shown in Fig. 5.10 with C-S-C-S boundary condition. It can be seen that there is 48% reduction in frequencies of the composite plates having no delamination at 0.75% moisture concentration from that of the reference moisture in C-S-C-S case. At elevated moisture concentrations with increase in delamination area, the frequencies drastically decrease due to reduction in stiffness and also the restraining effects of the boundary conditions as seen from Fig. 5.10. A comparison with Fig. 5.5 shows that the effects of moisture concentration on frequencies of free vibration are more than that of the temperature for different delaminated plates in C-S-C-S boundary condition.

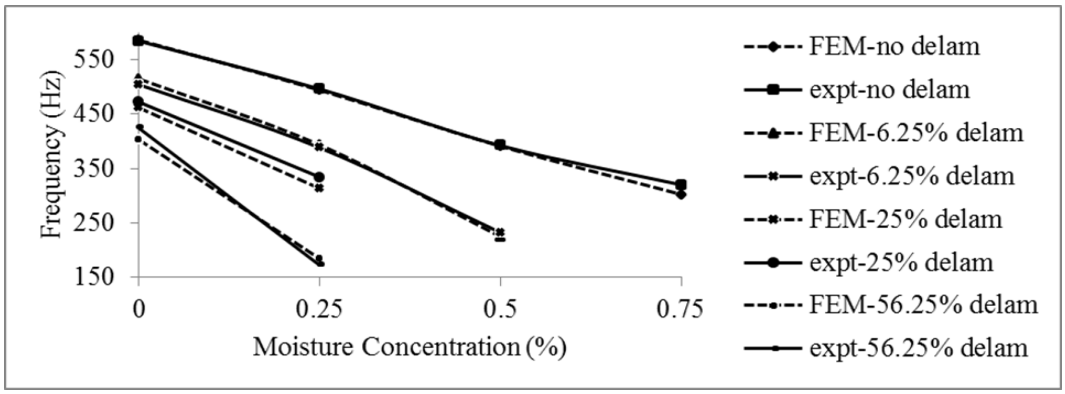

Figure 5.10: Effect of moisture on fundamental frequencies of vibration for composite plates with different delamination areas under $C-S-C-S$ boundary condition.

5.2.2 Delaminated composite shells in moist environment

The numerical (FEM) results of frequencies of vibration for 16 layer bidirectional woven fiber Glass/Epoxy composite panels are presented for various composite curved panels in moist environment for different strip delaminations with variety of boundary conditions. The boundary conditions (B.C.) for the present numerical analysis considered are: S-S-S-S, C-C-C-C and C-F-C-F. In the present dynamic analysis in moist environment, moisture content varies in the range 0% to 1%. The material properties of 16 layer bidirectional woven fibre Glass/Epoxy composite panels considered in this study at different moisture contents are presented in Table 5.7.

5.2.2.1 Comparison with previous studies

To validate the frequencies of vibration of composite shells subjected to moist environment based on present formulation are compared with the FEM results of Nanda and pradyumna [2011] and Naidu and Sinha [2007] as shown in Table 5.8. There exists excellent agreement based on present FEM with that of literature.

5.2.2.2 Moisture effects on vibration of cylindrical panels

The variations of fundamental frequencies of vibration of 16 layer bidirectional woven fibre cylindrical composite panels with moisture content are presented in Fig. 5.11 through Fig. 5.13 under various boundary conditions for different strip delaminations.

Table 5.7: Elastic moduli of Glass/Epoxy lamina at different moisture contents

Elastic	Moisture Content C (%)					
Moduli(GPa)	0.0	0.2	0.4	0.6	0.8	1.0
E_1	15.4	15.38	14.9	14.5	13.1	12.9
G_{12}	3.56	3.54	3.51	3.48	3.46	3.33

Table 5.8: Comparison of non-dimensional fundamental frequencies $\varpi = \sqrt{[\omega a^2(\rho/E_2h^2)]}$ of composite simply supported $[0/0/30/-30]_2$ spherical shells

$R/a = 10$, $a/h = 10$, $E_1 = 130\ GPa$, $E_2 = 9.5\ GPa$, $\nu_{12} = 0.3$, $G_{12} = G_{13} = 6.0\ GPa$, $G_{23} = 3.0\ GPa$

Source	Moisture Content C (%)		
	0.0	0.5	1.0
Present FEM	12.45	12.316	12.099
Nanda and Pradyumna[2011]	12.4667	12.3225	12.1894
Naidu and Sinha[2007]	12.32	12.238	12.13

For simply supported composite $[0]_{16}$ cylindrical panels ($R_y/b = 25$), the variation of fundamental mode frequencies of vibration against moisture contents are shown in Fig. 5.11 having different strip delaminations. There is a general trend in reduction

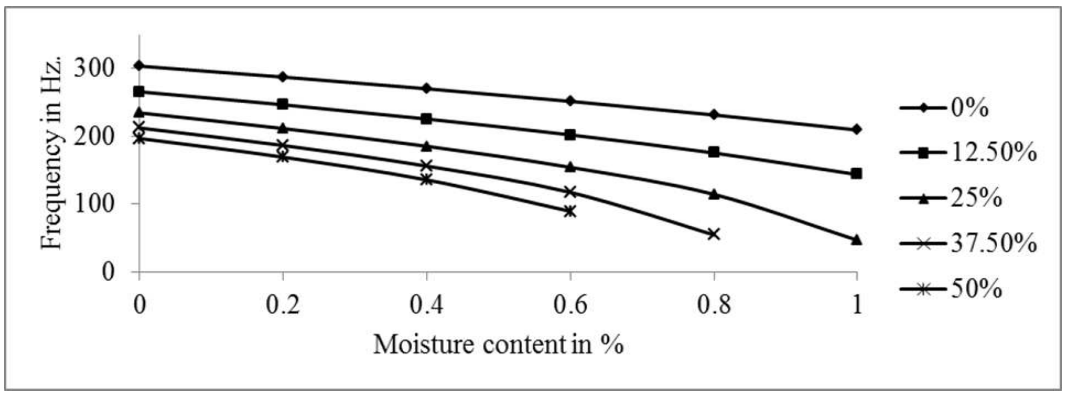

Figure 5.11: Variations of fundamental frequencies of $S-S-S-S$ composite $[0]_{16}$ cylindrical panel ($R_y/b = 25$) with moisture contents for different strip delaminations.

of frequencies with increase of moisture. The reduction in frequencies between 0% and 1% moisture contents are in the range $31\%, 46\%$ and 80% for intact, 12.5% and 25% strip delaminated composite panels. For 37.5% and 50% delaminated panels, instability is marked beyond a moisture content of 0.6%. This is due to the development of complex stress patterns in the composite panels under moist environment. At moisture content of 0.6%, the composite panels having $12.5\%, 25\%.37.5\%$ and 50% delamination suffer a degradation of frequencies of $19.8\%, 38.9\%, 53.6\%$ and 64.5% respectively from that of the intact ones. The rate of decrease of natural frequencies

is more pronounced with increasing area of delamination.

The variations of first mode frequencies of vibration against moisture contents for fully clamped composite $[0]_{16}$ cylindrical panels ($R_y/b = 25$) having different strip delaminations are shown in Fig. 5.12. Instability of composite panels are clearly marked soon after 0.2% moisture content for 37.5% and 50% strip delaminations for this boundary condition. At 0.4% moisture content, the frequencies of 12.5% and 25% delaminated panels reduce by 20% and 58% from that of the intact panels. Beyond this moisture content, the composite structures develop a drastic degradation of frequencies which may lead to instability. Even the intact panels become unstable at 1% moisture content under this boundary condition and between 0% and 0.8%, the frequency reduction is marked as 80%.

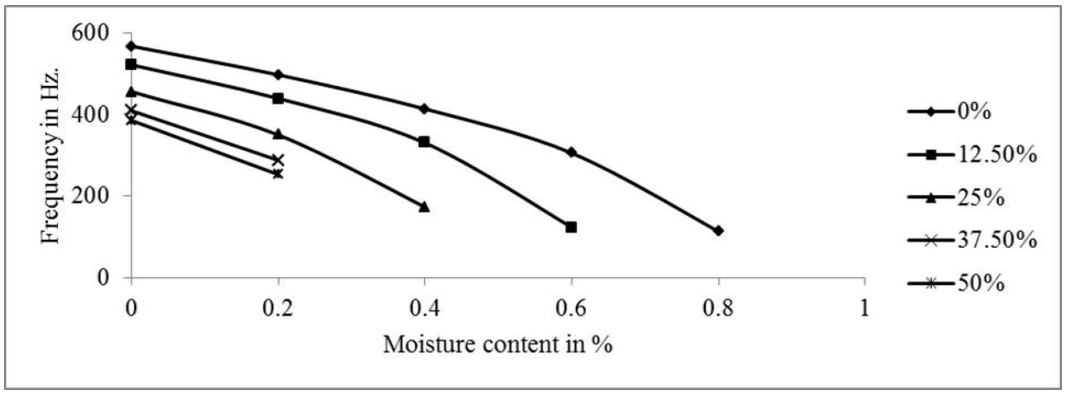

Figure 5.12: Variations of fundamental frequencies of clamped composite $[0]_{16}$ cylindrical panel ($R_y/b = 25$) with moisture contents for different strip delaminations.

The frequencies of vibration of composite $[0]_{16}$ cylindrical panel ($R_y/b = 25$) under C-F-C-F boundary conditions against moisture concentrations are shown in Fig. 5.13 for different strip delaminations. Between 0% and 4% moisture contents, the intact and 12.5% delaminated panels suffer a reduction of frequencies as 41% and 55.6%. As evident from the figure, a moisture content of 0.4% or more creates instability for intact and 12.5% delaminated panels; whereas, with higher strip delaminations, the composite spherical shell panels cannot continue to remain stable after a gain of 0.2% moisture concentration for this curvature and boundary condition. As seen from Fig. 5.11 through Fig. 5.13, the moisture concentrations and boundary conditions play

an important role in the vibration characteristics of composite $[0]_{16}$ cylindrical panel $(R_y/b = 25)$ with different strip delaminations.

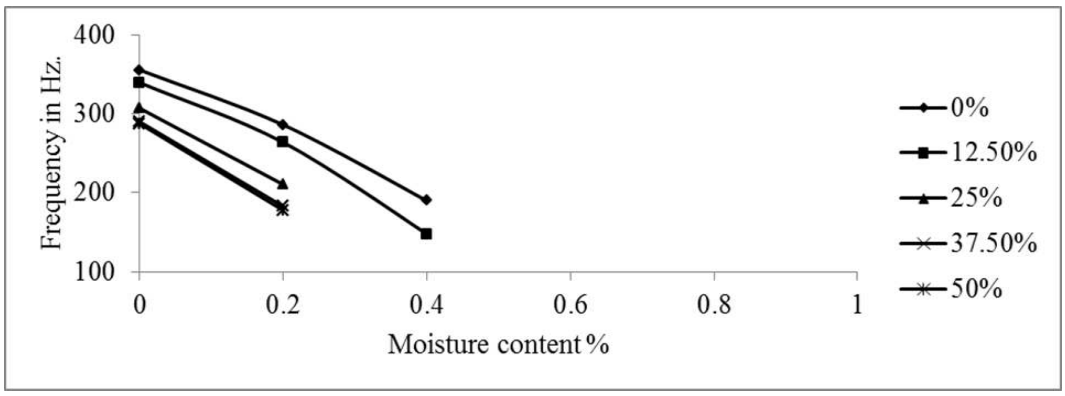

Figure 5.13: Variations of fundamental frequencies of $C-F-C-F$ composite $[0]_{16}$ cylindrical panel $(R_y/b = 25)$ with moisture contents for different strip delaminations.

5.2.2.3 Moisture effects on vibration of spherical panels

The variation of natural frequencies of 16 layer bidirectional woven fibre spherical composite panels are plotted against moisture contents under various boundary conditions in Fig. 5.14 through Fig. 5.16 with different strip delaminations.

The frequencies of vibration of simply supported composite $[0]_{16}$ spherical shell $(R_x/b = 5, R_y/b = 5)$ against moisture concentrations are plotted in Fig. 5.14 for various strip delaminations. Reduction of frequencies between 0% and 1% moisture uptake of the panels are in the range $4\%, 3.6\%, 3\%, 2.7\%$ and 2% for panels having delaminations as $0\%, 12.5\%, 25\%, 37.5\%$ and 50% respectively. At 0.2% moisture content, the composite panels with $12.5\%, 25\%, 37.5\%$ and 50% delamination suffer from the lowering of frequencies as $5\%, 9\%, 12\%$ and 13% respectively from that of the intact panel. This clearly shows that for the specific panel mentioned above, strip delamination plays dominant role in vibration analysis than moist environment under simply supported boundary condition.

The variation of fundamental frequencies of vibration with moisture uptake are shown in Fig. 5.15 for fully clamped composite $[0]_{16}$ spherical shell $(R_x/b = 5, R_y/b = 5)$ having different strip delaminations. At 1% moisture content, the frequencies

of vibration of composite spherical panels having 12.5%, 25%, 37.5% and 50% delaminations reduce in the range 10%, 16%, 27% and 39% respectively from that of the intact panel. Between ambient and 1% moist conditions, the composite panels of 0%, 12.5%, 25%, 37.5% and 50% delaminations show a reduction of frequencies as 14%, 19%, 21%, 27% and 38% respectively. At early stages of moisture contents, there is marginal variation in the frequencies for all types of strip delaminated panels; whereas, beyond 0.6% moisture uptake, the frequencies degrade significantly with higher delaminations.

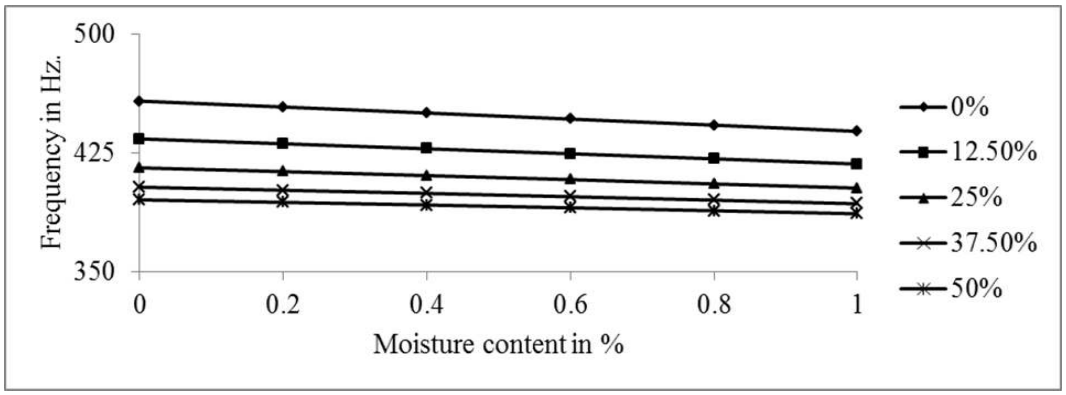

Figure 5.14: Variations of fundamental frequencies of $S-S-S-S$ composite $[0]_{16}$ spherical shell ($R_x/b = 5$, $R_y/b = 5$) with moisture contents for different strip delaminations.

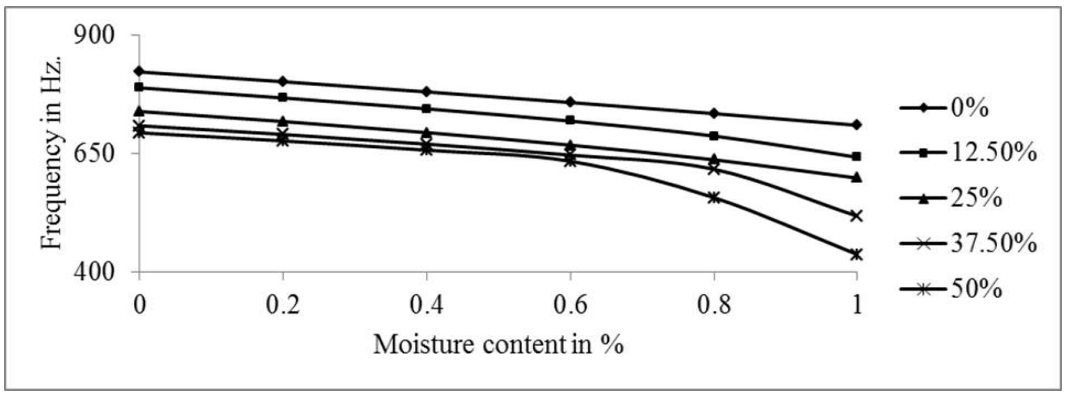

Figure 5.15: Variations of fundamental frequencies of $C-C-C-C$ composite $[0]_{16}$ spherical shell ($R_x/b = 5$, $R_y/b = 5$) with moisture contents for different strip delaminations.

For C-F-C-F composite $[0]_{16}$ spherical shell ($R_x/b = 5, R_y/b = 5$) having various strip delaminations, the frequencies of vibration against moisture contents are plotted

in Fig. 5.16. At different moisture concentrations starting from ambient conditions up to 0.6%, no significant reductions in frequencies are marked for all delaminated panels. The lowering of frequencies is observed in the range 4%, 18%, 25% and 32% for the composite panels having 12.5%, 25%, 37.5% and 50% delaminations respectively at 0.8% moist condition. Between ambient and 1% moisture concentrations, the composite panels with 0%, 12.5%, 25% and 37.5% strip delaminations suffer frequency reduction as 30%, 35%, 46% and 61% respectively. This clearly shows the importance of moist environment in the vibration analysis of C-F-C-F composite $[0]_{16}$ spherical shells ($R_x/b = 5, R_y/b = 5$). Fig. 5.14 and Fig. 5.15 show no sign of instability in the moisture concentration between $0\% - 1\%$ for the composite $[0]_{16}$ spherical panel ($R_x/b = 5, R_y/b = 5$) having different strip delaminations under S-S-S-S and C-C-C-C boundary conditions; but with C-F-C-F boundary condition in Figure 5.16, 50% delaminated panel shows a sign of instability at moisture uptake of 0.8% and more.

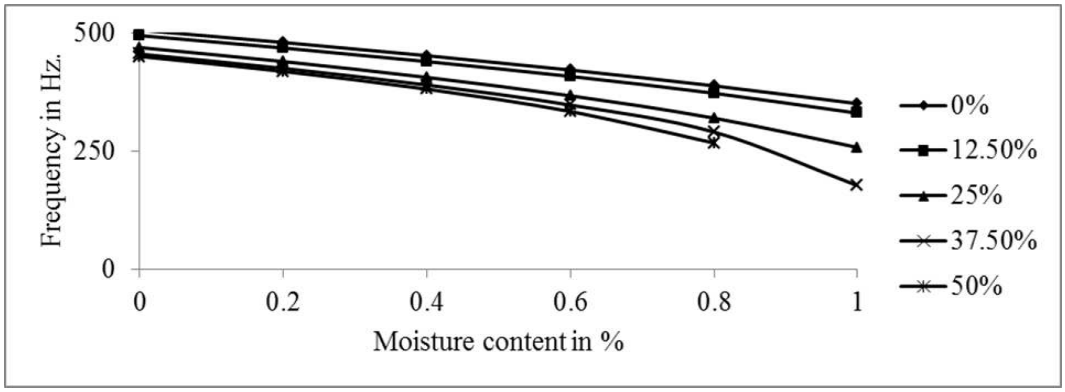

Figure 5.16: Variations of fundamental frequencies of $C - F - C - F$ composite $[0]_{16}$ spherical shell ($R_x/b = 5,\ R_y/b = 5$) with moisture contents for different strip delaminations.

5.2.2.4 Moisture effects on vibration of hyperbolic paraboloidal panels

The variation of fundamental frequencies of vibration against moisture contents are shown in Fig. 5.17 through Fig. 5.19 for various boundary conditions with strip delaminations of 16 layer bidirectional woven fibre hyperbolic paraboloidal composite panels.

The variations of fundamental frequencies of vibration against moisture concentra-

tions of S-S-S-S composite $[0]_{16}$ hyperbolic paraboloidal shell ($R_x/R_y = -1, R_y/b = -10$) with different strip delaminations are shown in Fig. 5.17. At ambient conditions, the frequency reduction for $12.5\%, 25\%, 37.5\%$ and 50% delaminated composite panels is in the range $11\%, 20\%, 27\%$ and 32% respectively; whereas, at 0.8% moisture uptake, the lowering of frequencies is observed in the range $18\%, 35\%, 49\%$ and 58% respectively from those of the intact panels. Beyond 0.8% moist condition, the 50% strip delaminated panels show sign of instability. Between 0% and 1% moisture concentrations, the frequencies of vibration of $0\%, 12.5\%, 25\%$ and 37.5% strip delaminated panels reduce as $26\%, 35\%, 49\%$ and 63% respectively.

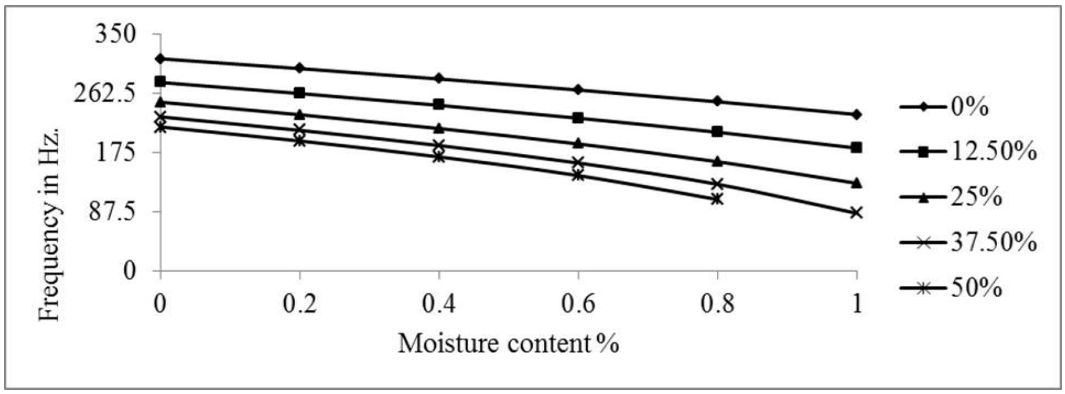

Figure 5.17: Variations of frequencies of $S-S-S-S$ composite $[0]_{16}$ hyperbolic paraboloidal shell ($R_x/R_y = -1, R_y/b = -10$) with moisture content for different strip delaminations.

For fully clamped composite $[0]_{16}$ hyperbolic paraboloidal shell ($R_x/R_y = -1, R_y/b = -10$), the frequencies of vibration are plotted with moisture contents for various strip delaminations as shown in Fig. 5.18. The intact panel at 1% moisture content shows a frequency degradation of 73% from that under ambient conditions. Up to 0.2% moisture uptake, all strip delaminated composite panels show a marginal change of frequencies; whereas beyond 0.4%, delaminated panels move to region of instability. At ambient conditions, $12.5\%, 25\%, 37.5\%$ and 50% delaminated composite panels show a lowering of frequencies as $6\%, 14\%, 20\%$ and 23% respectively; whereas at 0.4% moisture, the reduction of frequencies is in the range $12\%, 30\%, 42\%$ and 50% respectively from that of the intact panels.

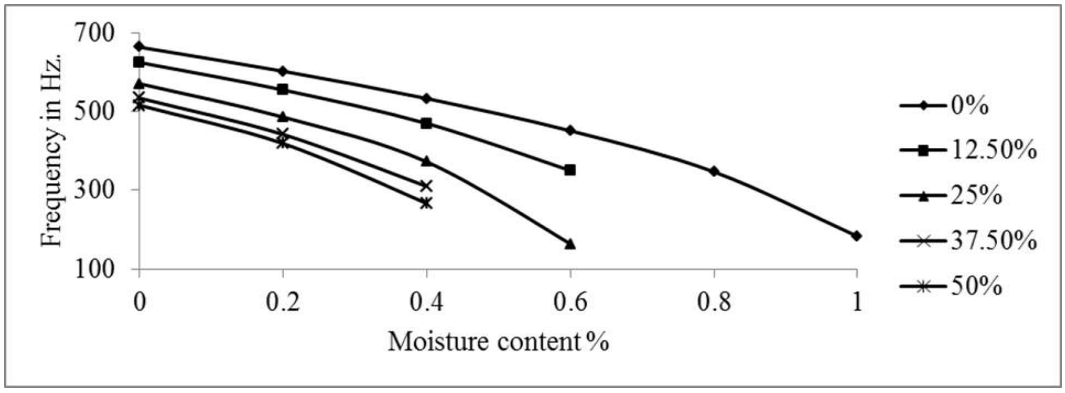

Figure 5.18: Variations of frequencies of clamped composite $[0]_{16}$ hyperbolic paraboloidal shell ($R_x/R_y = -1$,$Ry/b = -10$) with moisture content for different strip delaminations.

The variations of vibration frequencies of C-F-C-F composite $[0]_{16}$ hyperbolic paraboloidal shells ($R_x/R_y = -1, R_y/b = -10$) against moisture contents are shown in Fig. 5.19 with different strip delaminations. As seen from the figure, at lower

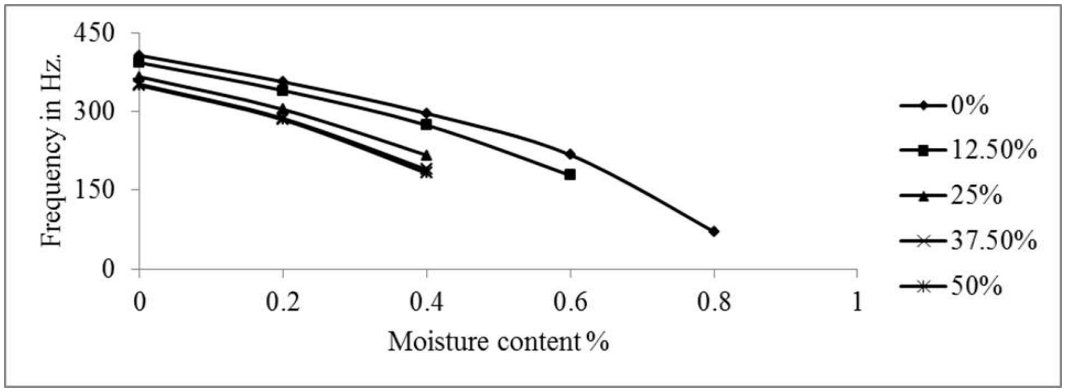

Figure 5.19: Variations of frequencies of $C-F-C-F$ composite $[0]_{16}$ hyperbolic paraboloidal shell ($R_x/R_y = -1$,$R_y/b = -10$) with moisture content for different strip delaminations.

moisture concentrations i.e. up to 0.2%, the variation of frequencies of composite panels are marginal. Beyond 0.2% moisture uptake, the frequency reduction is significant in this case and after 0.6%, almost all the delaminated panels show signs of instability. Between 0% and 0.4% moisture contents, the composite panels having $0\%, 12.5\%, 25\%, 37.5\%$ and 50% strip delaminations suffer from the frequency reduction in the range $27\%, 30\%, 41\%, 46\%$ and 48% respectively. As evident from Fig.

5.17 through Fig. 5.19, the composite panels under C-C-C-C and C-F-C-F boundary conditions show signs of instability at higher moisture concentrations; whereas under the simply supported boundary condition, the frequencies of the panels reduce more with moisture uptake than the strip delaminations.

5.2.2.5 Moisture effects on vibration of elliptic paraboloidal panels

For 16 layer bidirectional woven fibre elliptic paraboloidal composite panels, the fundamental frequencies of vibration are plotted against moisture contents under various boundary conditions in Fig. 5.20 through Fig. 5.22 with different strip delaminations.

The frequencies of vibration against moisture contents are plotted for simply supported composite $[0]_{16}$ elliptic paraboloidal shells ($R_x/R_y = 0.5, R_y/b = 5$) having different strip delaminations as shown in Fig. 5.20. For this particular curvature and boundary condition, the delamination plays dominant role in lowering the frequencies than the moisture content of the composite panels. At ambient conditions, frequencies of the panels having $12.5\%, 25\%, 37.5\%$ and 50% strip delaminations degrade in the range $3\%, 5\%, 6.5\%$ and 7.5% respectively from that of the intact panels. Between 0% and 1% moisture uptake, the frequencies of the panels having $0\%, 12.5\%, 25\%, 37.5\%$ and 50% strip delaminations reduce as $1.2\%, 1\%, 1\%, 0.9\%$ and 0.8% respectively.

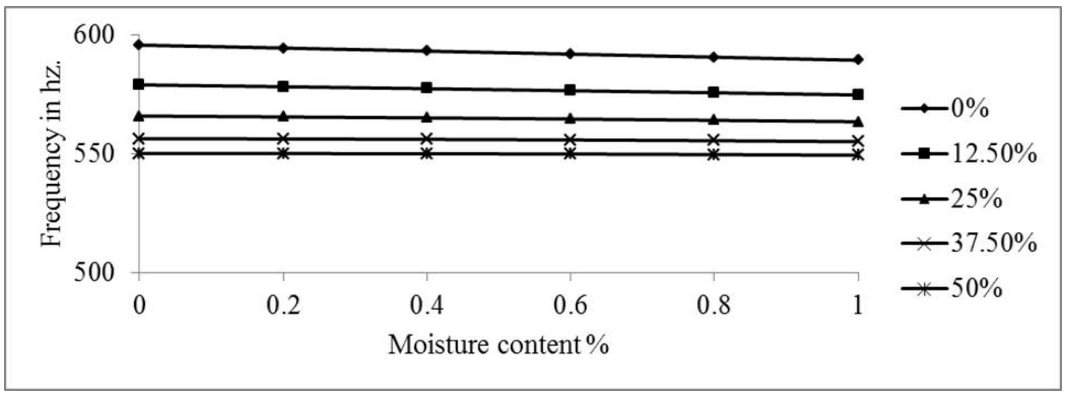

Figure 5.20: Variations of frequencies of $S-S-S-S$ composite $[0]_{16}$ elliptic paraboloidal shells ($R_x/R_y = 0.5$, $R_y/b = 5$) with moisture content for different strip delaminations.

The variations of fundamental frequencies of vibration of fully clamped composite $[0]_{16}$ elliptic paraboloidal shells ($R_x/R_y = 0.5, R_y/b = 5$) against moisture contents for different strip delaminations in Fig. 5.21. At 1% moisture, the frequencies of the panels having $12.5\%, 25\%, 37.5\%$ and 50% strip delaminations lower in the range $8\%, 12\%, 23.5\%$ and 29% respectively from that of the intact panels. The composite panels having 37.5% and 50% strip delaminations suffer more in the reduction of frequencies at high moisture concentrations, as evident from Fig. 5.21. Lower moisture concentrations up to 0.6% do not have significant effects on the vibration frequencies of composite panels.

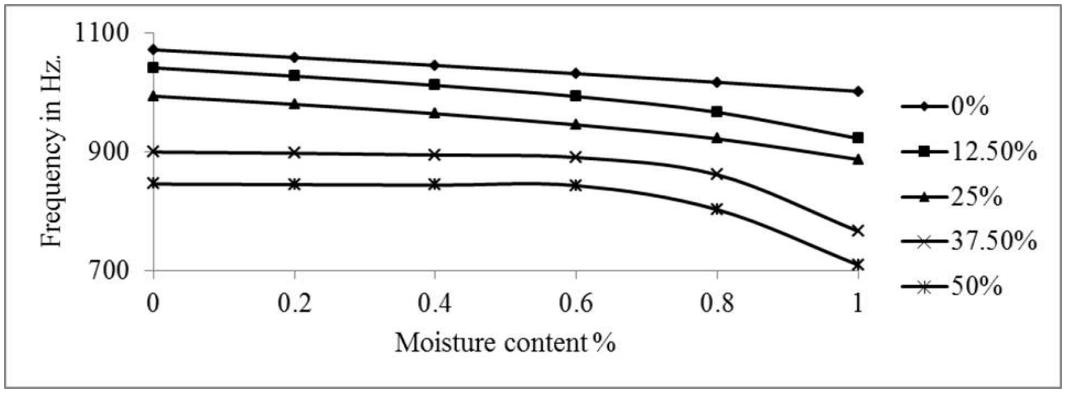

Figure 5.21: Variations of frequencies of $C-C-C-C$ composite $[0]_{16}$ elliptic paraboloidal shells ($R_x/R_y = 0.5$,$R_y/b = 5$) with moisture content for different strip delaminations.

For C-F-C-F composite $[0]_{16}$ elliptic paraboloidal shells ($R_x/R_y = 0.5, R_y/b = 5$), Figure 5.22 shows a plot of frequencies of vibration against moisture contents with different strip delaminations. As evident from the figure, the strip delamination has marginal role in reducing the vibration frequencies of composite panels than the moisture concentrations, which play a dominant role. Between 0% and 1% moisture uptake, the frequencies of the panels having $0\%, 12.5\%, 25\%$ and 37.5% strip delaminations reduce as $29\%, 32\%, 48\%$ and 81% respectively. The composite shell having 50% delamination becomes unstable after it gains a moisture content of 0.8%. From Fig. 5.20 through Fig. 5.22, it is evident moisture effects are significant in vibration analysis of elliptic paraboloidal shells under fully clamped and C-F-C-F conditions in exception of S-S-S-S boundary condition, where the strip delamination plays domi-

nant role.

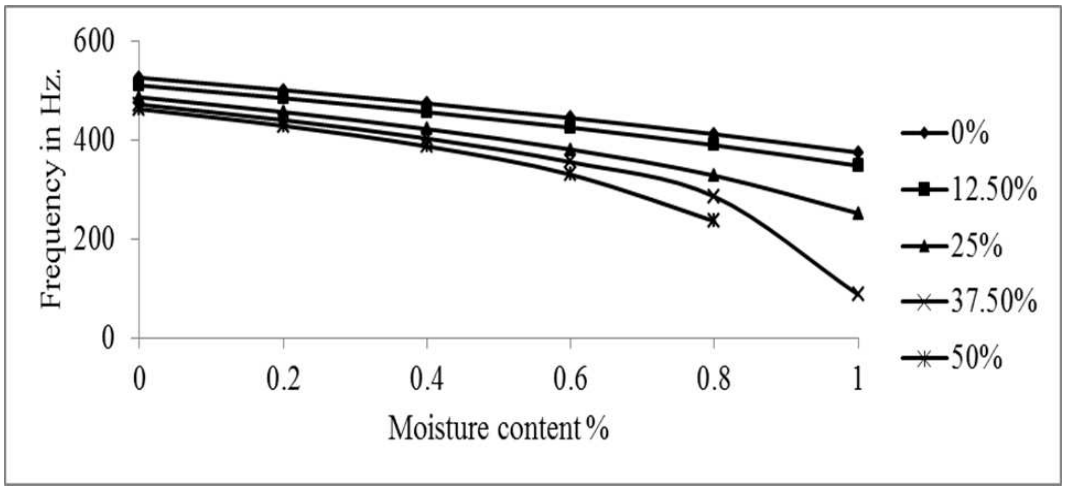

Figure 5.22: Variations of frequencies of $C-F-C-F$ composite $[0]_{16}$ elliptic paraboloidal shells ($R_x/R_y = 0.5$,$Ry/b = 5$) with moisture content for different strip delaminations.

5.2.3 Delaminated composite shell panels in thermal field

Numerical (FEM) results of frequencies of vibration for 16 layer bidirectional woven fibre Glass/Epoxy composite panels are presented for various composite curved panels in thermal environment for different strip delaminations with variety of boundary conditions. The boundary conditions for the present numerical analysis considered are: C-C-C-C, S-S-S-S and C-F-C-F. Temperature (T) varies in the range from sub-zero temperature from cryogenic range of 123K, 150K, 200K, 250K, 300K (ambient temperature), 350K and 400K, where 'K' stands for Kelvin. The material properties of 16 layer bidirectional woven fibre Glass/Epoxy composite panels considered in this study at different temperatures are presented in Table 5.9.

Table 5.9: Elastic moduli of woven fibre Glass/Epoxy lamina at different temperatures

Elastic	Temperature, T(K)						
Moduli(GPa)	123	150	200	250	300	350	400
E_1	15.4	15.4	15.4	15.4	15.4	14.93	14.7
G_{12}	3.56	3.56	3.56	3.56	3.56	3.51	3.48

5.2.3.1 Comparison with previous studies

To validate the frequencies of vibration of composite shells subjected to thermal field based on present formulation are compared with the FEM results of Nanda and pradyumna [2011] and Naidu and Sinha [2007] as shown in Table 5.10. There exists excellent agreement based on present FEM with that of literature.

Table 5.10: Comparison of non-dimensional fundamental frequencies $\varpi = \sqrt{[\omega a^2(\rho/E_2h^2)]}$ of composite $[0/0/30/-30]_2$ spherical shells

$R/a = 10$, $a/h = 10$, $E_1 = 130\ GPa$, $E_2 = 9.5\ GPa$, $\nu_{12} = 0.3$, $G_{12} = G_{13} = 6.0\ GPa$, $G_{23} = 3.0\ GPa$

Source	Temperature, T(K)		
	300	350	400
Present FEM	12.33	12.106	11.832
Nanda and Pradyumna[2011]	12.4667	12.2023	11.8901
Naidu and Sinha[2007]	12.32	12.078	11.803

5.2.3.2 Thermal effects on vibration of cylindrical panels

The effects of temperature on the frequencies of four sides simply supported (S-S-S-S) composite cylindrical panels ($R_y/b = 5$) are presented in Fig. 5.23 for various percentages of strip delaminations ($0 - 50\%$). The effects of temperature on the fundamental frequencies are studied from sub-zero temperature in cryogenic range of 123K up to 400K to simulate flight and ground conditions of aerospace vehicles. With respect to the ambient temperature, the frequencies of vibration decrease with increase of temperature from 300K to 400K as shown in Fig. 5.23 due to reduction of stiffness. This might be due to degradation of matrix used in composites. However, the fundamental frequencies increase with decrease of temperature from ambient to sub-zero temperatures up to cryogenic range of the order of 123K (-150^0 Celsius) due to presence of residual compressive stresses developed in the composite cylindrical panel.

For a composite panel with 0% delamination, the frequencies reduce by 9.8%

with increase of temperature from 300K to 400K. The frequencies of vibration of laminated cylindrical panel increase by 12.9% with decrease of temperature from 300K to 123K. At cryogenic temperature of 123K, the variations of frequencies of composite cylindrical panels, as shown in Fig. 5.23, are as $7\%, 14\%, 19\%$ and 23% for the delaminated panels of $12.5\%, 25\%, 37.5\%$ and 50% respectively from that of the intact shells. At 400K, a reduction of frequencies of $11\%, 20\%, 25\%$ and 28% is observed for the delaminated panels of $12.5\%, 25\%, 37.5\%$ and 50% respectively from that of the intact composite shells. Between cryogenic temperature 123K and 400K temperature range, the frequency reduction is as $21\%, 24\%, 26\%, 27.5\%$ and 28% for the shell panels having $0\%, 12.5\%, 25\%, 37.5\%$ and 50% strip delaminations respectively which shows the dominance of thermal field in the degradation of frequencies.

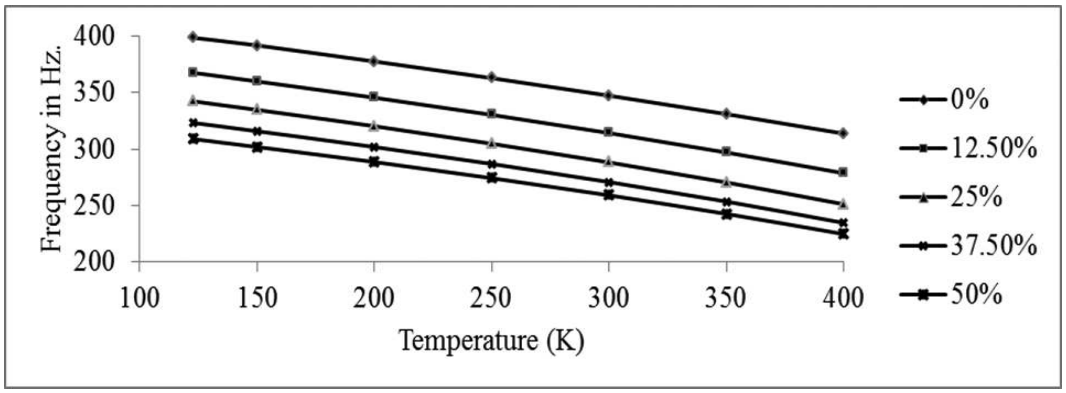

Figure 5.23: Variation of frequencies of $S-S-S-S$ composite $[0]_{16}$ cylindrical shell $(R_y/b = 5)$ with temperature for different percentages of strip delaminations.

The variations of frequencies of fully clamped cylindrical shell panels $(R_y/b = 5)$ in thermal environment for different strip delaminations are shown in Fig. 5.24. Between the cryogenic (123K) and 400K temperature range, it is observed that $38\%, 43\%, 50\%, 52\%$ and 54% reduction in frequencies of vibration take place for $0\%, 12.5\%, 25\%, 37.5\%$ and 50% delaminated cylindrical composite panels respectively. The 50% delaminated panel suffers $17.5\%, 23\%$ and 37% frequency reduction at cryogenic(123K), ambient and 400K temperatures respectively from that of the intact panel; whereas, for the 25% strip delaminated cylindrical panel, the reduction in frequencies is in the range $9.6\%, 19.6\%$ and 27% from that of the laminated panel

at 123K, 300K and 400K temperatures.

The fundamental frequencies of vibration against temperatures are plotted for C-F-C-F cylindrical composite panels ($R_y/b = 5$) with different strip delaminations in Fig. 5.25. Between 123K and 400K temperature range, there is a reduction of frequencies of $34\%, 35\%, 39\%, 40.5\%$ and 42% C-F-C-F composite panels with $0\%, 12.5\%, 25\%, 37.5\%$ and 50% strip delaminations respectively. It is marked that up to 25% strip delamination, composite panels show more reduction in frequencies at all thermal exposures including cryogenic temperature of 123K than the laminated panel; whereas, higher percentages of delamination shows a marginal variation in frequencies at all temperatures for the composite cylindrical panels.

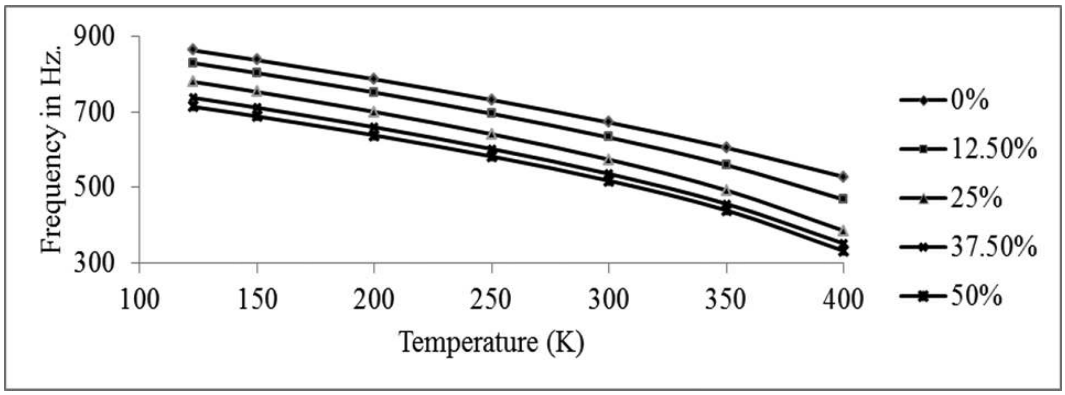

Figure 5.24: Variation of frequencies of $C-C-C-C$ composite $[0]_{16}$ cylindrical shell ($R_y/b = 5$) with temperature for different percentages of strip delaminations.

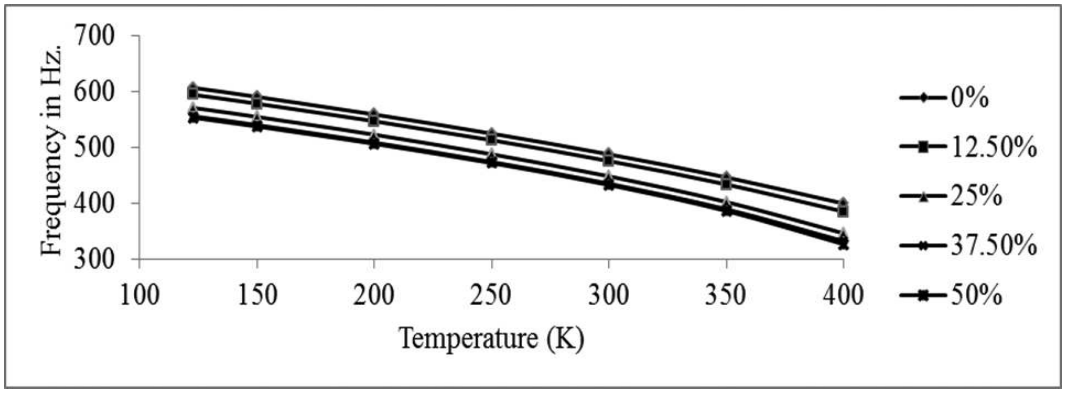

Figure 5.25: Variation of frequencies of $C-F-C-F$ composite $[0]_{16}$ cylindrical shell ($R_y/b = 5$) with temperature for different percentages of strip delaminations.

5.2.3.3 Thermal effects on vibration of spherical panels

For 16 layer bidirectional woven fiber composite spherical shell panels, the fundamental frequencies of vibration are plotted against temperatures including cryogenic at 123K for different strip delaminations, variety of boundary conditions and curvatures in Fig. 5.26 through Fig. 5.28.

The variation of the fundamental natural frequencies of vibration against the temperatures for simply supported doubly curved spherical ($R_x/b = 5, R_y/b = 5$) composite panels with various percentages of strip delaminations are shown in Fig. 5.26. The variation of frequencies is in the range $6.7\%, 4.9\%$ and 3.2% for strip delaminated panels of $0\%, 25\%$ and 50% respectively between cryogenic and 400K temperature ranges. It is observed that the spherical composite shell having 50% strip delamination suffers a reduction in frequencies 16% at cryogenic temperature, 13.5% at ambient temperature and 12% at 400K than those of the intact shell panel. This clearly shows that at higher values of strip delaminations the reduction percentage of frequencies is less than the intact panel in thermal environment for simply supported (S-S-S-S) spherical shell of this curvature.

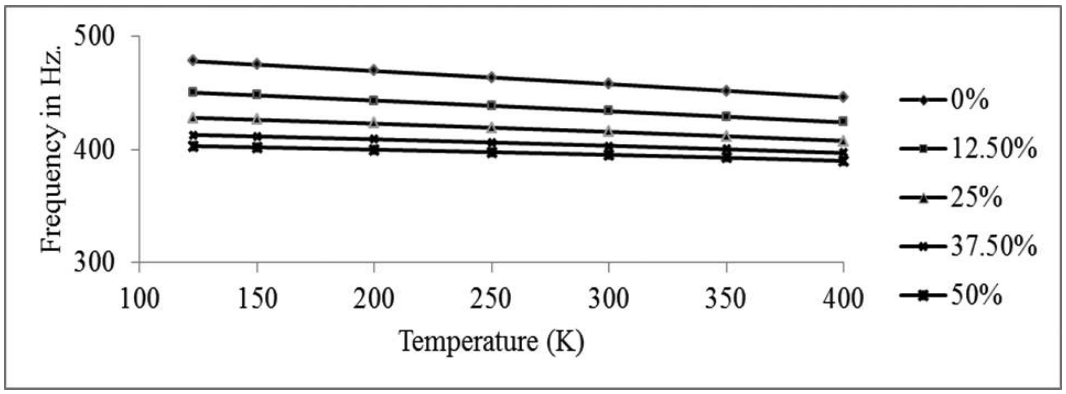

Figure 5.26: Variation of frequencies of $S-S-S-S$ composite $[0]_{16}$ spherical shell ($R_x/b = 5$, $R_y/b = 5$) with temperature for different percentages of strip delaminations.

The variation of fundamental frequencies of vibration of fully clamped (C-C-C-C) composite spherical panels having curvature ratio of $R_x/b = R_y/b = 5$ with temperatures are presented in Fig. 5.27 for a variety of percentages of strip delam-

inations. The reduction of frequencies in the range $18.6\%, 19.8\%, 20.7\%, 18.9\%$ and 17.8% is observed for $0\%, 12.5\%, 25\%, 37.5\%$ and 50% strip delaminated shells respectively between cryogenic (123K) and 400K temperatures. At ambient temperature, the $12.5\%, 25\%, 37.5\%$ and 50% strip delaminated spherical composite panels shows a percentage reduction in frequencies in the range $4\%, 10\%, 13.7\%$ and 18.5% from that of the panels without delaminations. Higher percentages of strip delaminations than 25% show a marginal reduction in frequencies at all thermal exposures than the laminated composite panels.

The variation of fundamental frequencies of vibration with temperature for C-F-C-F spherical ($R_x/b = 5, R_y/b = 5$) composite panels with a variety of strip delaminations are shown in Fig. 5.28. Elevated temperatures up to 400K from cryogenic (123K) degrades the frequencies as $33\%, 35\%, 39\%, 42\%$ and 43% for the strip delaminations of $0\%, 12.5\%, 25\%, 37.5\%$ and 50% respectively of all the composite shell panels. At cryogenic (123K), ambient and 400K temperatures, frequency reduction in the range $6\%, 7\%$ and 14% respectively for 25% delaminated shell and $9\%, 11\%$ and 23% respectively for 50% delaminated shells than the intact panel. Role of temperature is dominant in this case than the delaminations in decreasing the stiffness resulting in lowering of frequencies of free vibration of the spherical composite panels.

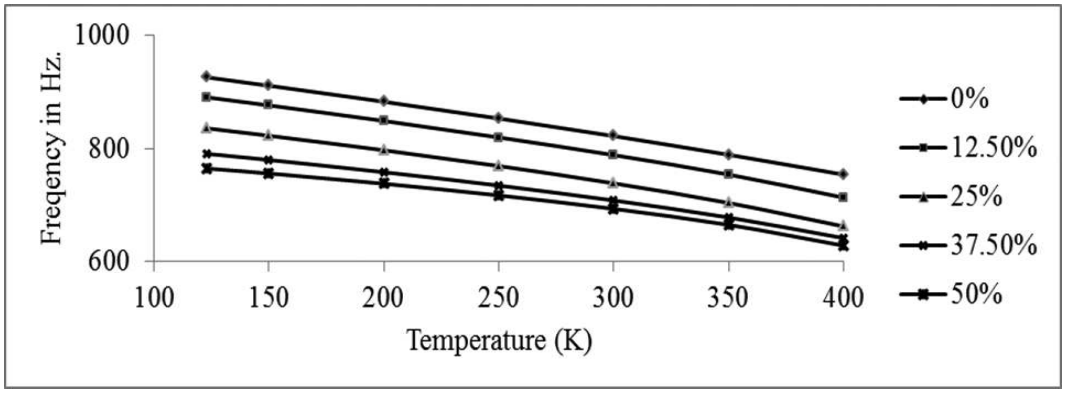

Figure 5.27: Variation of frequencies of $C-C-C-C$ composite $[0]_{16}$ spherical shell ($R_x/b = R_y/b = 5$) with temperature for different percentages of strip delaminations.

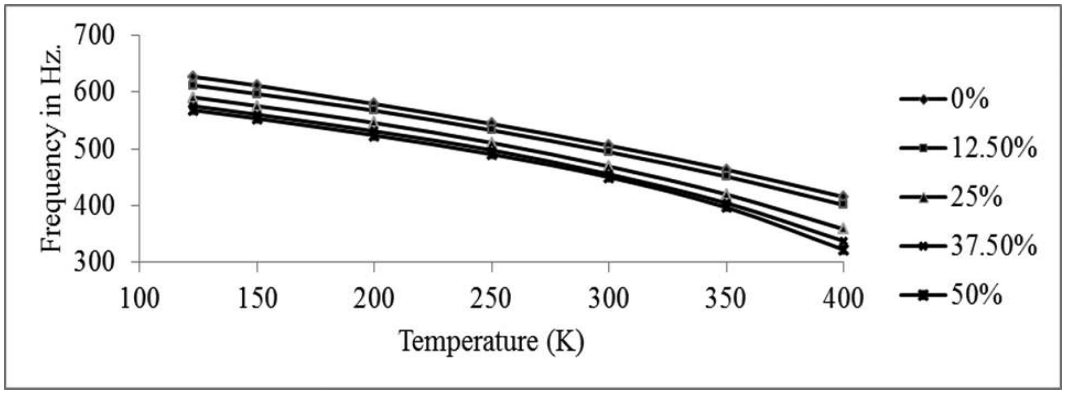

Figure 5.28: Variation of frequencies of $C-F-C-F$ composite $[0]_{16}$ spherical shell ($R_x/b = R_y/b = 5$) with temperature for different percentages of strip delaminations.

5.2.3.4 Thermal effects on vibration of hyperbolic paraboloidal panels

The variation of fundamental frequencies of vibration against temperatures including cryogenic at 123K for various strip delaminations, different boundary conditions and curvatures of 16 layer bidirectional woven fibre composite hyperbolic paraboloidal shell panels in Fig. 5.29 through Fig. 5.34.

The first lowest mode vibration frequencies of all sides simply supported composite hyperbolic paraboloidal panels of curvature ratio $R_x/R_y = -1, R_x/b = 5, R_y/b = -5$ against temperatures are shown in Fig. 5.29 for different strip delaminations. For the intact shell, the frequency of vibration at cryogenic (123K) temperature reduces by 36% when exposed to 400K; whereas, 80% reduction in frequency is marked for 50% delaminated panel between 123K and 400K temperatures. It is observed from Fig. 5.29 that at 123K, the delamination does not play important role in degrading the frequencies. At 300K, $12\%, 22.3\%, 30\%$ and 35.7% lowering in frequencies are marked for $12.5\%, 25\%, 37.5\%$ and 50% strip delaminated panels from that of the intact panel. At 400K, the reduction in percentages of frequencies is in the range $20.5\%, 41.5\%, 59.6\%$ and 76% for the panels having $12.5\%, 25\%, 37.5\%$ and 50% strip delaminations from that of the laminated panel. This shows the role of thermal field in reducing the frequencies of vibration for hyperbolic paraboloidal composite shell panels in simply supported boundary conditions.

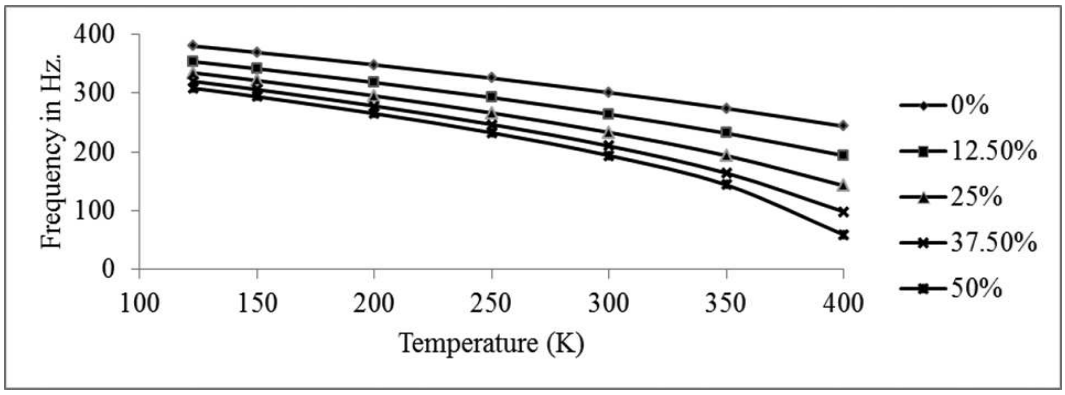

Figure 5.29: Variation of frequencies of $S-S-S-S$ composite $[0]_{16}$ hyperbolic paraboloidal panel ($R_x/R_y = -1$,$R_x/b = 5$,$R_y/b = -5$) with temperature for various strip delaminations.

The variations in frequencies of vibration with temperature are shown in Fig. 5.30 for a simply supported composite hyperbolic paraboloidal shell panel ($R_x/R_y = -0.5, R_x/b = 5, R_y/b = -10$) with different strip delaminations. Between 123K and 400K, the frequency degradation is observed in the range $21\%, 22\%, 22\%, 25\%$ and 27% for the composite panels of $0\%, 12.5\%, 25\%, 37.5\%$ and 50% strip delaminations respectively. At ambient temperature, the frequencies reduce by $8.5\%, 15.4\%, 21\%$ and 25% for the strip delaminated hyperbolic paraboloidal shell panels of $12.5\%, 25\%, 37.5\%$ and 50% delaminations from that of the intact plate. As shown in Fig. 5.30, between the intact panel and 50% delaminated panel, the frequencies reduce in the range 22% at cryogenic (123K) temperature and 27% at 400K.

For a fully clamped hyperbolic paraboloidal composite shell panel ($R_x/R_y = -1, R_x/b = 5, R_y/b = -5$), the variation in frequencies of vibration against temperatures are shown in Fig. 5.31 for different percentages of strip delaminations. A variation range of $48\%, 56\%, 71\%$ and 87% in frequencies is observed for $0\%, 12.5\%, 25\%$ and 37.5% delaminated shells between cryogenic (123K) and 400K temperature. Beyond 350K, the 50% delaminated panel shows instability. The reduction in frequencies between the laminated panel and 50% delaminated panel is 8% at 123K temperature and 33% at 350K temperature. In C-C-C-C composite hyperbolic paraboloidal shell panels, temperature plays an important role in degrading the frequencies of vibration than the strip delamination.

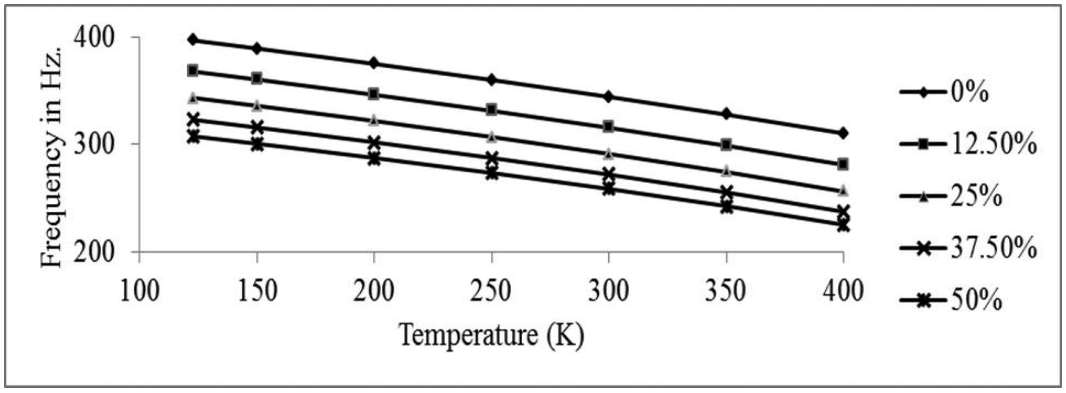

Figure 5.30: Variation of frequencies of $S-S-S-S$ composite $[0]_{16}$ hyperbolic paraboloidal shell ($R_x/R_y = -0.5$, $R_x/b = 5$, $R_y/b = -10$) with temperature for various strip delaminations

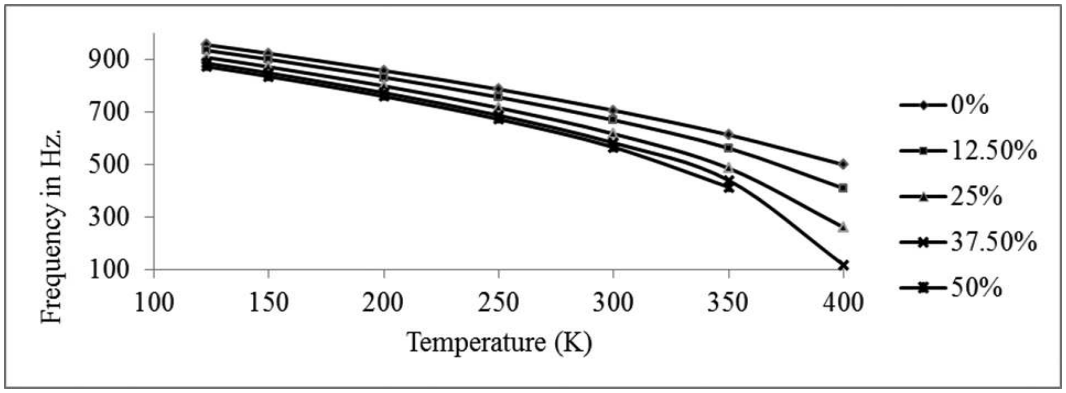

Figure 5.31: Variation of frequencies of $C-C-C-C$ composite $[0]_{16}$ hyperbolic paraboloidal shell ($R_x/R_y = -1$, $R_x/b = 5$, $R_y/b = -5$) with temperature for various strip delaminations.

For curvature ratio of $R_x/R_y = -0.5, R_x/b = 5, R_y/b = -10$, the variation in frequencies against temperature of fully clamped hyperbolic paraboloidal shell panels are shown in Fig. 5.32 having strip delaminations. Between the cryogenic and 400K temperatures; a variation of $33\%, 39\%, 50\%, 67\%$ and 82% in frequencies is observed for $0\%, 12.5\%, 25\%, 37.5\%$ and 50% strip delaminated shells. Between the 123K and 400K temperatures; a variation of $33\%, 39\%, 50\%, 67\%$ and 82% in frequencies is observed for $0\%, 12.5\%, 25\%, 37.5\%$ and 50% strip delaminated shells. It is observed that the frequencies of 50% delaminated composite panel comes down by 6% at cryogenic temperature, 13% at ambient temperature and 74% at 400K from that of the

intact panel. In this case, the role of temperature is predominant than the strip delaminations in reduction of the frequencies of vibration.

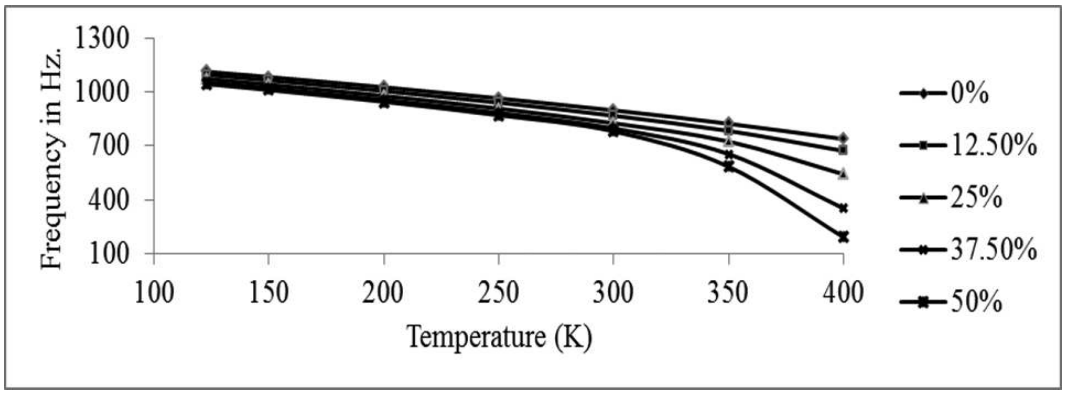

Figure 5.32: Variation of frequencies of $C-C-C-C$ composite $[0]_{16}$ hyperbolic paraboloidal shell ($R_x/R_y = -0.5$, $R_x/b = 5$, $R_y/b = -10$) with temperature for various strip delaminations.

The variation of frequencies of vibration with temperature for the C-F-C-F woven fibre composite hyperbolic paraboloidal shell ($R_x/R_y = -1, R_x/a = 5, R_y/a = -5$) having different delaminations in Fig. 5.33. There is deviation of $34\%, 41\%$ and 45%

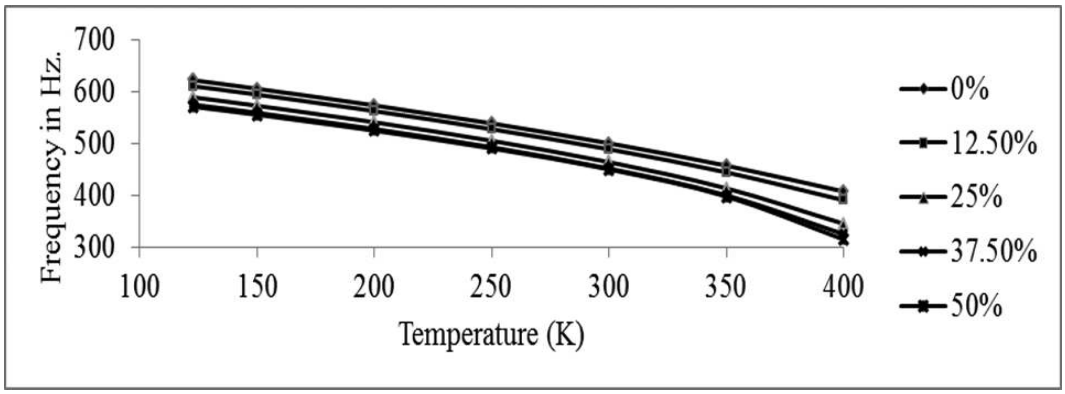

Figure 5.33: Variation of frequencies of $C-F-C-F$ composite $[0]_{16}$ hyperbolic paraboloidal shell ($R_x/R_y = -1$, $R_x/b = 5$, $R_y/b = -5$) with temperature for various strip delaminations.

in frequencies are marked for $0\%, 25\%$ and 50% strip delaminated shells between 123K and 400K temperatures from that of the laminated panels. As evident from Fig. 5.33, there is marginal role of delamination in reducing the stiffnesses in a wide range of temperatures including the cryogenic temperature at 123K and elevated

temperature at 400K. It is clearly evident that the thermal environment plays a vital role in decreasing the frequencies of vibration than the strip delamination in C-F-C-F hyperbolic paraboloidal composite shell panels also.

Fig. 5.34 represents the variation of frequencies of vibration of composite hyperbolic paraboloidal shell ($R_x/R_y = -0.5, R_x/a = 5, R_y/b = -10$) with temperature under C-F-C-F boundary conditions having different delaminations. Between the thermal exposure of 123K and 400K, the $0\%, 12.5\%, 25\%, 37.5\%$ and 50% strip delaminated composite hyperbolic paraboloidal shell panels suffer the decay of frequencies in the range $34\%, 37\%, 42\%, 45.5\%$ and 48% . It is observed that 50% delaminated shell panel suffers a reduction of frequencies in the range 8.5% at 123K, 12% at ambient and 28% at 400K temperatures respectively than the intact shell panel, which indicates the role of thermal field in affecting the frequencies of vibration.

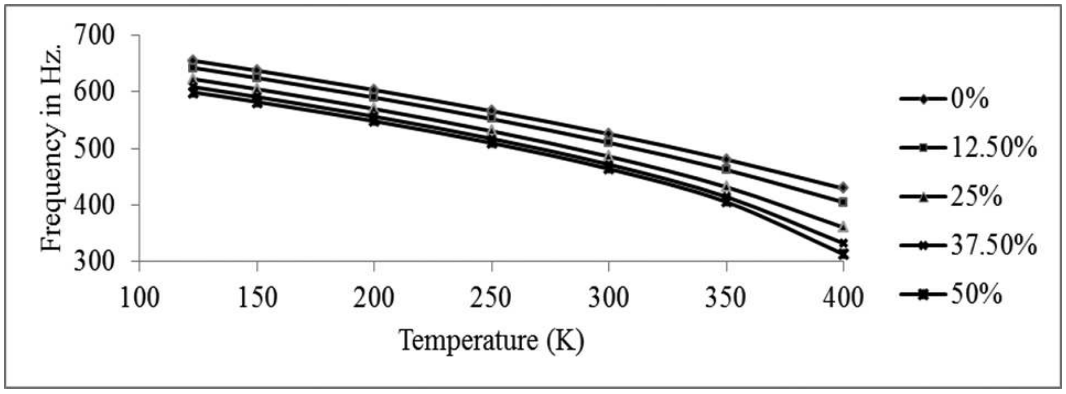

Figure 5.34: Variation of frequencies of $C-F-C-F$ composite $[0]_{16}$ hyperbolic paraboloidal shell ($R_x/R_y = -0.5$, $R_x/b = 5$, $R_y/b = -10$) with temperature for various strip delaminations.

5.2.3.5 Thermal effects on vibration of elliptic paraboloidal panels

The variation of fundamental frequencies of vibration against thermal exposure of 16 layer bidirectional woven fiber composite elliptic paraboloidal shell panels including cryogenic at 123K for different strip delaminations, various boundary conditions and curvatures of are shown in Fig. 5.35 through Fig. 5.37.

The variation of fundamental frequencies of simply supported composite elliptic paraboloidal shell panel having curvature ratio $R_x/R_y = 0.5, R_y/a = 5$ with strip delaminations with temperatures are shown in Fig. 5.35. The thermal exposure of 123K and 400K temperature range, frequencies of vibration of the elliptic paraboloidal shell panel reduce by 1.9%, 1.5%, 1.3%, 1.1% and 1% for the strip delamination sizes of 0%, 12.5%, 25%, 37.5% and 50% respectively. At cryogenic temperature, 7.8% variation in frequency is observed between the intact and 50% delaminated panels; whereas, at 400K temperature, 7.1% variation is marked. This shows that for this case in S-S-S-S panels, the strip delamination governs the reduction in stiffness and resulting frequencies than the thermal range.

For C-C-C-C composite elliptic paraboloidal shell ($R_x/R_y = 0.5, R_y/a = 5$), the variation of fundamental frequencies with temperature are shown in Fig. 5.36 for various delaminations. Between 123K and 400K temperatures, the 0%, 12.5%, 25%, 37.5% and 50% delaminated elliptic paraboloidal composite panels show reduction of frequencies by 9.5%, 10.67%, 7.4%, 1.8% and 1.3% respectively. At 400K, ambient and 123K temperatures, the 25% delaminated shell shows the frequency reduction by 8.4%, 7.2% and 10.5% respectively; whereas, the 50% delaminated shell shows reduction in the range 18%, 21% and 25% respectively from that of the intact panels.

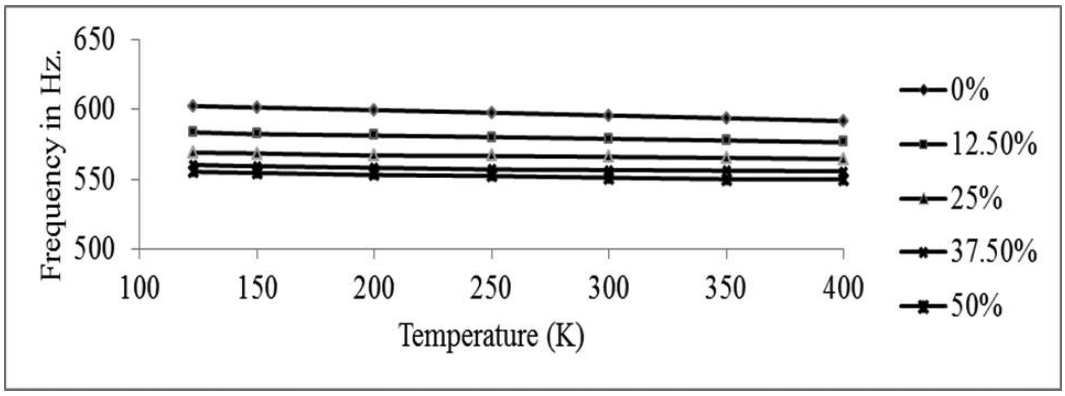

Figure 5.35: Variation of frequencies of $S-S-S-S$ composite $[0]_{16}$ elliptic paraboloidal shell ($R_x/R_y = 0.5$,$R_y/b = 5$) with temperature for different strip delaminations.

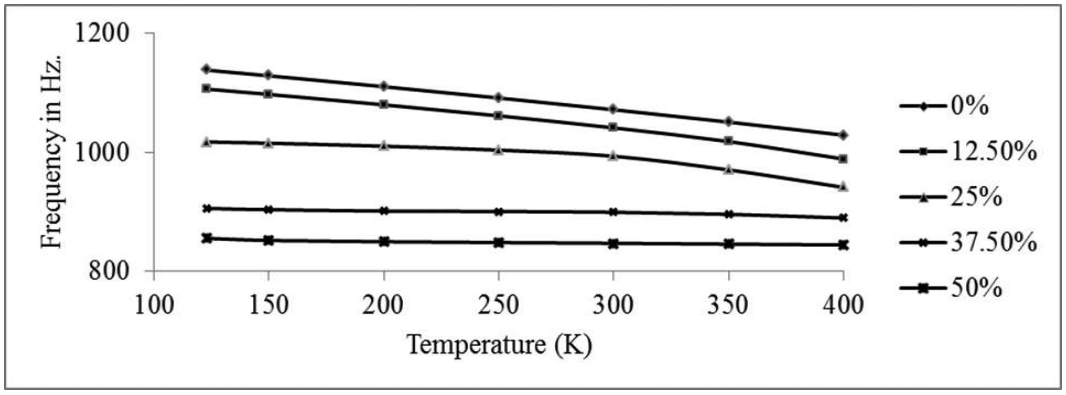

Figure 5.36: Variation of frequencies of $C-C-C-C$ composite $[0]_{16}$ elliptic paraboloidal shell ($R_x/R_y = 0.5,\ R_y/b = 5$) with temperature for different strip delaminations.

Fig. 5.37 shows the variation of vibration frequencies of woven fibre composite elliptic paraboloidal shell ($R_x/R_y = 0.5, R_y/a = 5$) with temperature under C-F-C-F boundary conditions for various delaminations. Between 123K and 400K temperature range, $31.5\%, 33\%, 39\%, 42\%$ and 46% reduction in frequencies is indicated for $0\%, 12.5\%, 25\%, 37.5\%$ and 50% strip delaminated composite panels respectively. The percentage of decay in frequencies of vibration is significant when the C-F-C-F elliptic paraboloidal shell panels are exposed beyond ambient temperature than in a range between 123K and ambient temperatures.

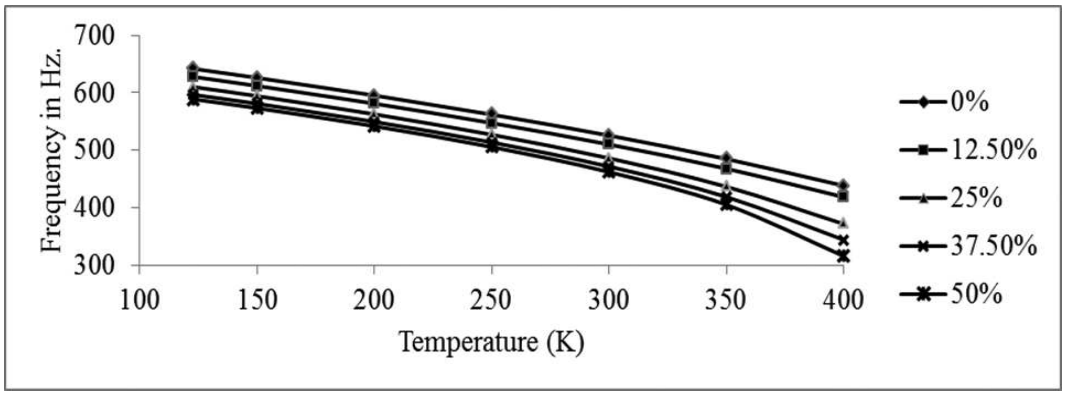

Figure 5.37: Variation of frequencies of $C-F-C-F$ composite $[0]_{16}$ elliptic paraboloidal shell ($R_x/R_y = 0.5,\ R_y/b = 5$) with temperature for different strip delaminations.

5.3 Buckling Analysis

Presence of delamination and hygrothermal environment may significantly reduce the stiffness and strength of the composite structures and may affect the design parameters such as the buckling strength. In the present study, the buckling load of delaminated Glass/Epoxy composite plates in hygrothermal field were determined both numerically and experimentally. The effects of various parameters like delamination area, boundary conditions, fiber orientations, stacking sequence, temperature and moisture concentrations were studied.

5.3.1 Delaminated composite flat panels in hygrothermal field

Numerical (fem) and experimental (exp) results of critical buckling loads for $[0/0]_{8s}$, $[30/-30]_8$ and $[45/-45]_8$ woven fiber Glass/Epoxy composite plates are obtained with elevated temperatures and moisture concentrations for different delamination areas as well as for different boundary conditions. In the present static analysis in hygrothermal environment, moisture concentration is varied from 0% to 0.8% and temperature from 300K to 400K. For computing the results, centrally located single mid plane delaminations of three different sizes like $6.25\%, 25\%$ and 56.25% of the total plate area are considered for composite plates.

The geometry and material properties of the composite plates at elevated temperatures and moisture concentrations used in the present study are shown in Tables 5.11 and 5.12 respectively.

Table 5.11: Elastic moduli of woven fiber Glass/Epoxy lamina at different temperatures

Elastic	Temperature, T(K)				
Moduli(GPa)	300	325	350	375	400
E_1	15.4	15.39	14.93	13.21	13.01
G_{12}	3.56	3.54	3.51	3.48	3.42

Table 5.12: Elastic moduli of Glass/Epoxy lamina at different moisture concentrations

Elastic	Moisture, C(%)				
Moduli(GPa)	0.0	0.2	0.4	0.6	0.8
E_1	15.4	15.38	14.69	13.17	13.0
G_{12}	3.56	3.53	3.49	3.47	3.41

5.3.1.1 Comparison with previous studies

To validate the critical buckling loads of laminated composite plates subjected to hygrothermal field based on present formulation are compared with the FEA results of Sairam and Sinha [1992] and Whitney and Ashton [1971] as shown in Table 5.13. There exists excellent agreement of results based on present FEM with that of literature.

For validation of the program results, buckling load of delaminated composite plates using the present formulation are compared with the FEM results of Pekbey and sayman [2006] as shown in Table 5.14. It is observed that there is good agreement between the two results.

The buckling loads for delaminated composite plates from present numerical analysis are compared with those of Radu and Chattopadhyay [2002] as shown in Table 5.15, wherein good agreement is witnessed.

Table 5.13: Validation of normalized buckling load [$\lambda_{nbl} = \lambda/(\lambda)_{C=0\%,T=300Kand0\%delamination}$] under hygrothermal conditions, $a/b = 1$, $a/h = 100$, [0/90/90/0], simply supported.

Moisture, $C = 0.1\%$			Temperature, $T = 325K$		
Present FEM	Sai Ram and Sinha[1992]	Whitney and Ashton[1971]	Present FEM	Sai Ram and Sinha[1992]	Whitney and Ashton[1971]
0.6093	0.6099	0.6091	0.4481	0.4488	0.4477

Table 5.14: Validation of buckling load of delaminated composite plates

$E_1 = 27.0$ GPa, $E_2 = 21.5$ GPa, $G_{12} = 7.5$ GPa, $\nu_{12} = 0.15$

Plate Dimensions (mm)	Fiber Orientation	Present FEM	Pekbey and Sayman[2006]
$200 \times 160 \times 1.7$	$[0/0]_8$	6.87	6.42
$200 \times 160 \times 1.7$	$[30/-30]_{2s}$	5.93	5.64
$200 \times 160 \times 1.7$	$[45/-45]_{2s}$	5.56	5.38

Table 5.15: Comparison of buckling load in Newton (N) for delaminated cantilever plates

Delamination Length	Buckling Load (N)	
(mm)	Present FEM	Radu and Chattopadhyay[2002]
0	16.29	16.336
25.4	15.91	16.068
50.8	14.87	15.054
76.2	12.52	12.712
101.6	9.81	9.934

Numerical (fem) and experimental (exp) results of normalized buckling loads $[\lambda_{nbl} = \lambda/(\lambda)_{C=0\%,T=300K\ and\ 0\%\ delamination}]$ for [0/0]8s , [30/-30]8 and [45/-45]8 woven fiber Glass/Epoxy composite plates are plotted with temperatures in Kelvin (K) and moisture concentrations (%) for different delamination areas as well as for C-F-C-F and C-C-C-C boundary conditions.

5.3.1.2 Effect of temperature on buckling loads

Fig. 5.38 shows the variations in predicted and experimental results of normalised buckling load against temperature for $[0/0]_{8s}$ delaminated woven fiber composite plates under C-F-C-F boundary condition. There is a good matching of numerical and experimental results. At ambient temperature, the deviations of normalized buckling loads for $6.25\%, 25\%$ and 56.25% delaminations are observed in the range

16%, 44% and 62% respectively from that of the intact plate due to reduction in stiffness. At 400K, reductions of normalized buckling loads are 73% and 80% for un-delaminated and 6.25% delaminated plates respectively from that of the intact plate at ambient temperature. This might be the due to the degradation of matrix used in composites. The 56.25% delaminated plate becomes highly unstable at temperatures more than 325K. The 25% delaminated plate shows a decrement of 40% in normalized buckling load at 375K from that of the reference temperature.

The normalized buckling loads resulting from FEA and experiments are plotted against temperatures in Fig. 5.39 for $[30/-30]_8$ woven roving asymmetric composite plates under C-F-C-F boundary conditions. Except the intact plate, all the delaminated composite plates show instability beyond 375K temperature with 56.25% delaminated plate showing high degree of instability even beyond 325K. At 375K, 45%, 68% and 90% reductions in normalized buckling loads are marked for 0%, 6.25% and 56.25% delaminated composite plates from that of the intact plate at ambient temperature. For the intact plate, normalized buckling loads decrease by 78% at 400K from that of the reference temperature. This shows that the temperature plays a dominant role in degrading the matrix of the composite plates at higher temperatures finally affecting the buckling load under C-F-C-F boundary condition.

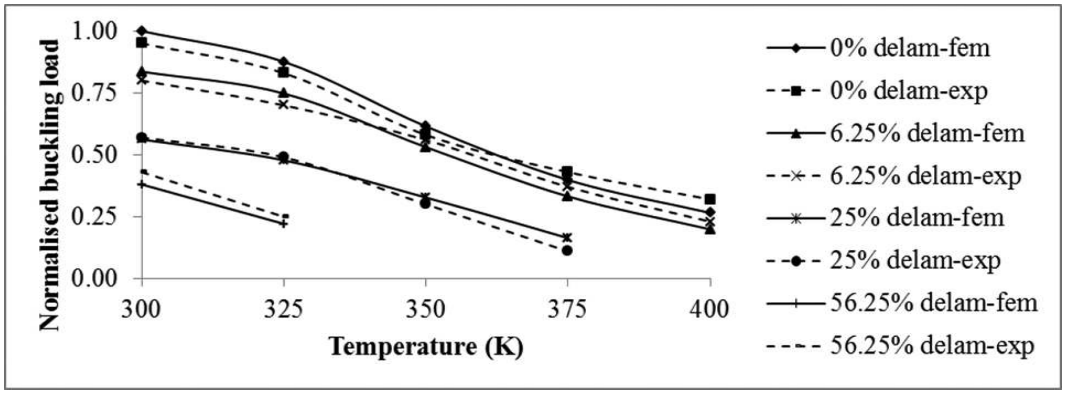

Figure 5.38: Effect of temperature on normalized buckling load of $[0]_{8s}$ woven fiber delaminated composite plates under $C-F-C-F$ boundary condition.

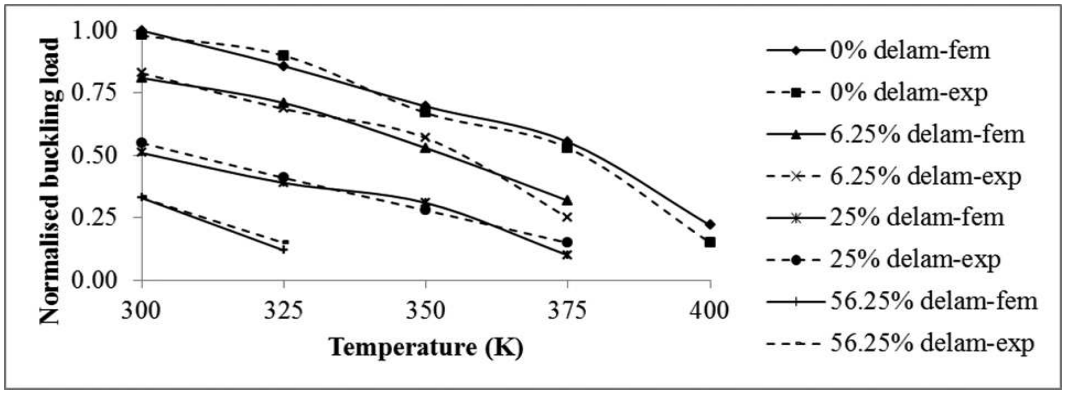

Figure 5.39: Effect of temperature on normalized buckling load of $[30/-30]_8$ woven fiber delaminated composite plates under $C-F-C-F$ boundary condition.

The variations of normalized buckling loads against temperatures are shown in Fig. 5.40 for $[45/-45]_8$ woven fiber delaminated unsymmetric composite plates under C-F-C-F boundary conditions. Here, all the plates (laminated as well as delaminated) show a sign of instability at temperatures beyond 375K highlighting the importance of thermal analysis in plate buckling. At 350K, a reduction of normalized buckling load in the range $27\%, 45\%$ and 82% is marked for $0\%, 6.25\%$ and 25% delaminated composite plates from that of the intact plate at reference temperature. At ambient temperature, 9% and 28% decrease in normalized buckling loads are observed for 6.25% and 25% delaminated composite plates from that of the laminated plate.

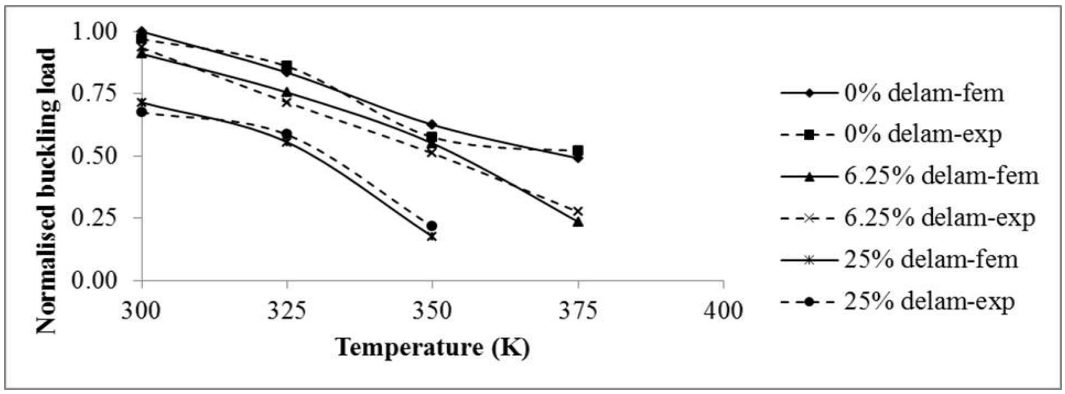

Figure 5.40: Effect of temperature on normalized buckling load of $[45/-45]_8$ woven fiber delaminated composite plates under $C-F-C-F$ boundary condition.

The variations in normalized buckling loads against temperature for $[0]_{8s}$ delaminated woven fiber composite plates under C-C-C-C boundary conditions are shown

in Fig. 5.41. Between 300K and 400K, buckling loads reduce in the range 60%, 65% and 74% for 0%, 6.25% and 25% delaminated composite plates respectively from that of the intact plate. At 375 K, 44%, 52%, 60% and 86% decrease in buckling loads are marked for 0%, 6.25%, 25% and 56.25% delaminated plates respectively from that of the intact plate at ambient temperature. Plates under C-C-C-C boundary conditions seem to be stable even at elevated temperatures and higher delamination percentages of area.

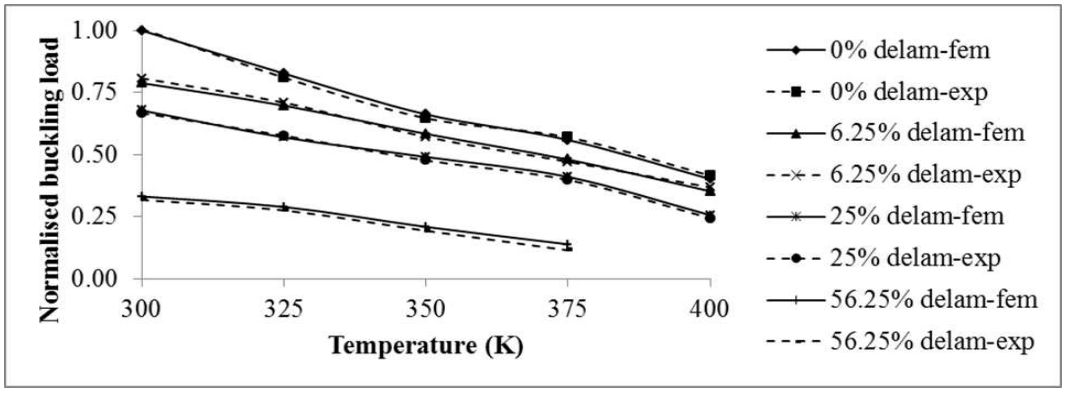

Figure 5.41: Effect of temperature on normalized buckling load of $[0]_{8s}$ woven fiber delaminated composite plates under $C-C-C-C$ boundary condition.

The FEM and experimental results of normalized buckling loads are plotted against temperature in Fig. 5.42 for $[30/-30]_8$ delaminated, unsymmetric woven roving composite plates under fully clamped boundary condition. At ambient

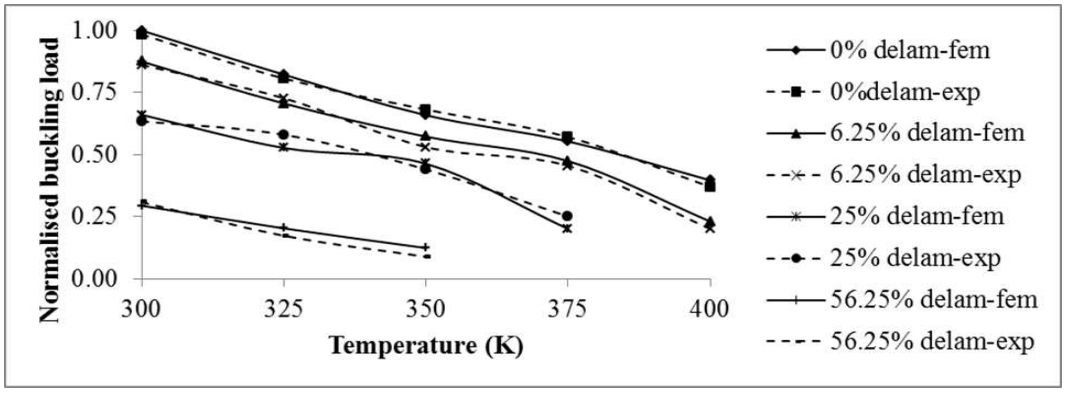

Figure 5.42: Effect of temperature on normalized buckling load of $[30/-30]_8$ woven fiber delaminated composite plates under $C-C-C-C$ boundary condition.

temperature, 12%, 34% and 70% decrease in buckling loads are marked for 6.25%, 25%

and 56.25% plate area delaminations respectively from that of the intact plate. At 375K, the buckling loads for $0\%, 6.25\%$ and 25% delaminated plates reduce in the range $45\%, 53\%$ and 80% respectively from that of the intact plate at reference temperature condition. Here, elevated temperature plays the key role in reducing the buckling loads than the delamination.

The effects of temperature on normalized buckling loads for $[45/-45]_8$ delaminated, asymmetric woven fiber composite plates under fully clamped boundary conditions are shown in Fig. 5.43. Between 300K and 400K, the intact plate suffers as high as 72% reduction in buckling load. At reference temperature, $30\%, 57\%$ and 75% decrease in buckling loads are marked for $6.25\%, 25\%$ and 56.25% delaminated plates respectively from that of the intact plate. Between reference temperature and 350K, the $0\%, 6.25\%$ and 25% delaminated plates suffer reduction in buckling loads in the range $35\%, 58\%$ and 83% respectively from the intact plate at ambient temperature. The buckling loads for particular stacking sequence and fiber orientation of this plate decrease in higher percentages at elevated temperatures than the other two plates.

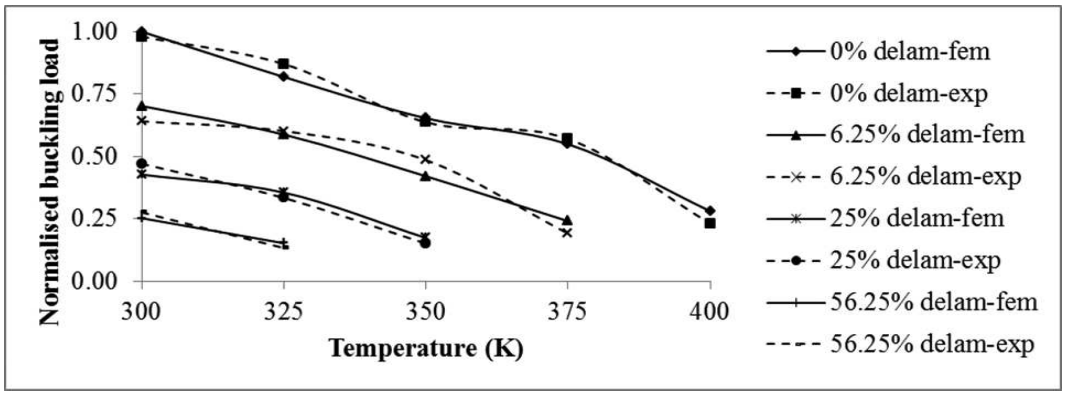

Figure 5.43: Effect of temperature on normalized buckling load of $[45/-45]_8$ woven fiber delaminated composite plates under $C-C-C-C$ boundary condition.

5.3.1.3 Effect of moisture on buckling loads

The normalized buckling loads as found from FEM and experimental results vs moisture content for $[0]_{8s}$ woven fiber delaminated composite plates under C-F-C-F boundary conditions are plotted as shown in Fig. 5.44. The 25% and 56.25% delaminated

plates become unstable beyond 0.4% and 0.2% moisture contents respectively for high reduction in stiffness due to moist environment. At 0.6% moisture content, reductions of 57% and 87% in normalized buckling load are observed for 0% and 6.25% delaminated composite plates respectively from that of the intact plate at reference moisture content. At reference moisture content, 18%, 34% and 78% reduction in normalized buckling loads is marked for 6.25%, 25% and 56.25% delaminated composite plates respectively from that of the intact plate. It seems that the moist environment plays a critical role as compared to the thermal field in degrading the matrix of the composites.

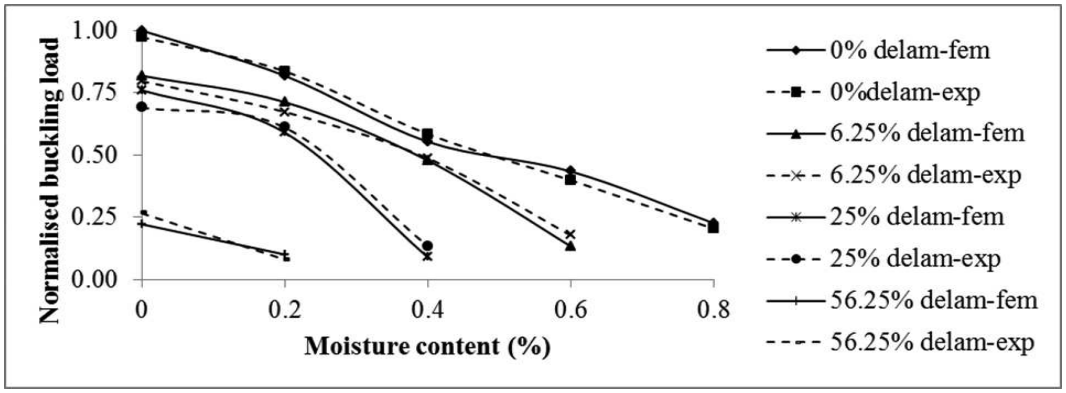

Figure 5.44: Effect of moisture on normalized buckling load of $[0]_{8s}$ woven fiber delaminated composite plates under $C-F-C-F$ boundary condition.

Fig. 5.45 represents the variations in normalized buckling loads against moisture concentrations as calculated from numerical and experimental results for $[30/-30]_8$ delaminated, unsymmetric woven fiber composite plates under C-F-C-F boundary conditions. At ambient temperature, huge difference of 79% on normalized buckling load is marked between intact and 56.25% delaminated plates; whereas 14% and 27% difference in buckling load are marked for 6.25% and 25% delaminated plates respectively from that of the intact plates. At 0.4% moisture content, 38%, 47% and 87% reduction in buckling loads are observed for 0%, 6.25% and 25% delaminated plates respectively from that of the intact plate at reference moisture content. As compared to $[0]_{8s}$ plate, this stacking sequence and fiber orientation suffers more in regard to buckling load calculations at higher moisture concentrations.

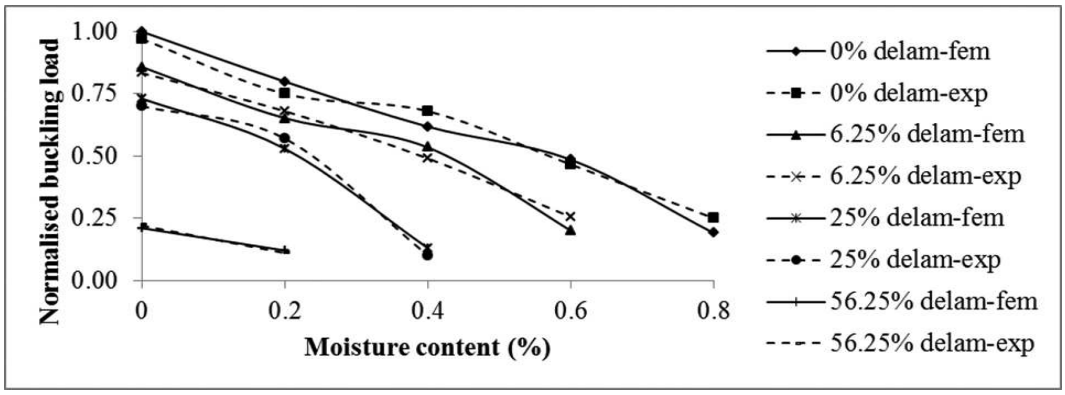

Figure 5.45: Effect of moisture on normalized buckling load of $[30/-30]_8$ woven fiber delaminated composite plates under $C-F-C-F$ boundary condition.

The predicted and experimental values of normalized buckling loads against moisture uptake for $[45/-45]_8$ delaminated, asymmetric woven roving composite plates under C-F-C-F boundary conditions are plotted as shown in Fig. 5.46. It is observed that all the composite plates show a sign of instability beyond 0.6% moisture uptake with 56.25% delaminated plate having instability beyond 0.2%. Here, moisture concentration plays the dominant role in degrading the buckling loads than the delamination. At 0.4% moisture uptake, $40\%, 55\%$ and 82% reduction in buckling loads are marked for $0\%, 6.25\%$ and 25% delaminated composite plates respectively from that of the intact plate at ambient moisture content. Between 0% and 0.6% moisture uptake, 68% and 80% reduction in buckling load are observed for intact and 6.25% delaminated plates respectively.

Moist environmental effects on normalized buckling loads for $[0]_{8s}$ delaminated woven fiber composite plates under fully clamped boundary conditions are shown in Fig. 5.47. At 0.6% moisture uptake, the reduction in buckling loads are observed in the range $65\%, 71\%$ and 77% for plates of $0\%, 6.25\%$ and 25% delaminations respectively from that of the intact plate at reference moisture content. The composite plate having 56.25% delamination seems to be unstable at 0.4% moisture uptake. Moist environment plays a critical role in reducing the buckling loads for composite plates than the delamination as seen from Fig. 5.47 under fully clamped boundary condition.

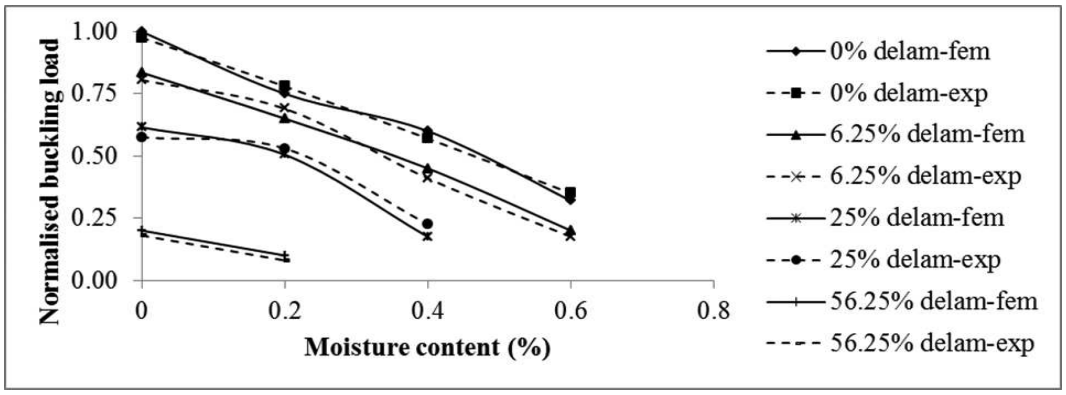

Figure 5.46: Effect of moisture on normalized buckling load of $[45/-45]_8$ woven fiber delaminated composite plates under $C-F-C-F$ boundary condition.

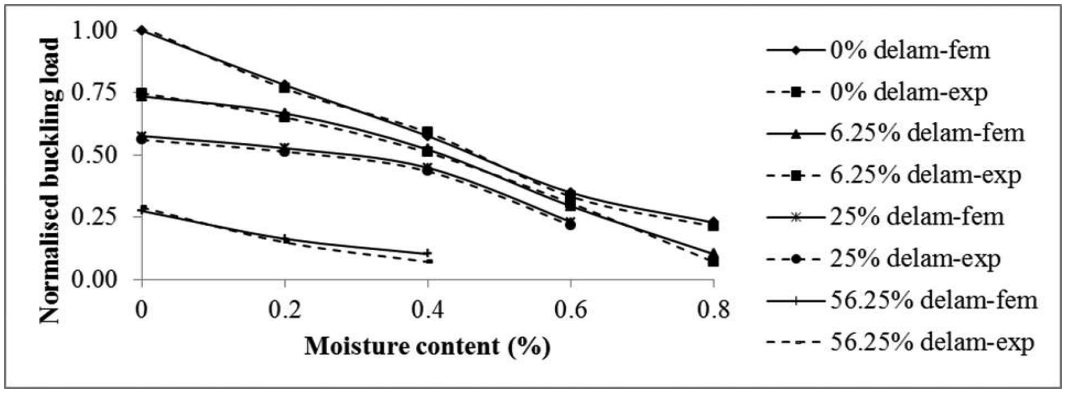

Figure 5.47: Effect of moisture on normalized buckling load of $[0]_{8s}$ woven fiber delaminated composite plates under $C-C-C-C$ boundary condition.

The variations of normalized buckling load against moisture uptake for $[30/-30]_8$ delaminated, asymmetric woven roving composite plates under C-C-C-C boundary conditions are presented in Fig. 5.48. The buckling load for intact plate is decreased by 82% at 0.8% moisture uptake from that of the reference moisture, which shows the importance of hygrothermal response in calculating buckling loads of delaminated composite plates. At 0.4% moisture concentration, $43\%, 48\%$ and 73% reduction in buckling loads are observed for $0\%, 6.25\%$ and 25% delaminated composite plates respectively than that of the reference moisture content.

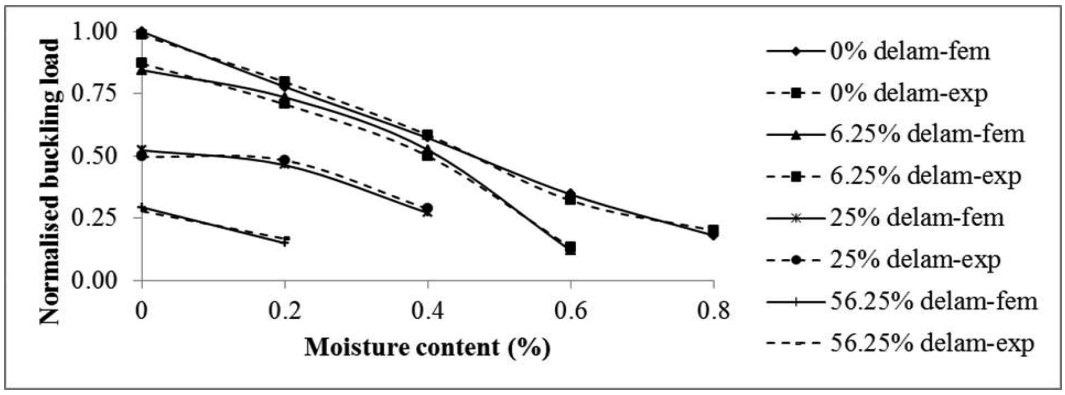

Figure 5.48: Effect of moisture on normalized buckling load of $[30/-30]_8$ woven fiber delaminated composite plates under $C-C-C-C$ boundary condition.

Effects of moisture uptake on normalized buckling loads of $[45/-45]_8$ delaminated, asymmetric woven fiber composite plates under C-C-C-C boundary condition are shown in Fig. 5.49. It is observed that this particular stacking sequence and fiber orientation of the composite plate suffers much in buckling at elevated moisture concentrations. The buckling load of the intact plate is reduced by 90% at 0.8% moisture uptake from that of the reference moisture. Instability is marked for the delaminated composite plates at higher moisture concentrations. At 0.4% moisture uptake, $43\%, 74\%$ and 91% reduction in buckling loads are observed for $0\%, 6.25\%$ and 25% delaminated plates respectively from that of the intact plate at reference moisture. This figure highlights the importance of hygrothermal analysis on buckling of delaminated composite plates.

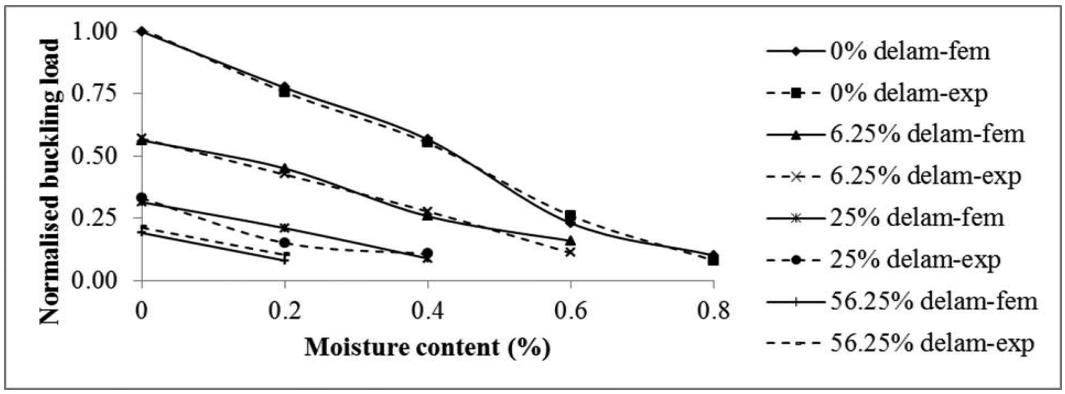

Figure 5.49: Effect of moisture on normalized buckling load of $[45/-45]_8$ woven fiber delaminated composite plates under $C-C-C-C$ boundary condition.

5.4 Parametric Instability Analysis

The bidirectional Glass/Epoxy delaminated composite flat and curved panels are chosen for numerical evaluation of dynamic instability regions in hygrothermal field. The temperature variations are preferred between 300K and higher range of 375K, whereas, the moisture variations are taken in the range 0% to 0.6%. The delaminated portion considered in the analysis is mid-plane square delamination having 12.5% of the total panel area (unless otherwise stated). Three boundary conditions are considered in the present study as: S-S-S-S, C-C-C-C and C-F-F-F.

Non-dimensional excitation frequencies ($\bar{\Omega}$) are calculated using the computer program by taking the above material properties of delaminated bidirectional Glass/Epoxy composite flat panels in hygrothermal environment. For dynamic stability analysis, the essential analyses of free vibration and buckling are done with the help of FEM based code. The effects of static load factor and dynamic load factor, delamination, temperature, moisture, stacking sequence and boundary conditions on the dynamic instability regions (DIR) of composite flat and curved panels in hygrothermal field are established.

5.4.1 Delaminated composite flat panels in hygrothermal field

The composite flat panels chosen are symmetric, asymmetric, cross ply and angle ply having stacking sequences as $[0/0]_8$, $[30/-30]_8$ and $[45/-45]_8$. Static load factor 'L_S' is varied between 0 and 0.6, whereas, dynamic load factor 'L_D' is varied between 0 and 0.8.

The material properties (unless otherwise mentioned) under hygrothermal conditions used in the present example are as per Tables 5.2, 5.7 and 5.9.

5.4.1.1 Comparison with previous studies

For validation of current FE formulation, the boundary excitation frequencies for delaminated square plates under simply supported boundary condition without hy-

grothermal environment obtained by Noh and Lee [2014] are compared with the predicted numerical results. The present finite element results match well with the results published in the literature for boundary frequencies as shown in Table 5.16.

Table 5.16: Boundary excitation frequencies (rad/sec) of delaminated SS [0/90/90/0] square plates

Boundary Frequencies	'L_S'	'L_D'	Delamination size			
			0%		50%	
			Present FEM	Noh and Lee [2014]	Present FEM	Noh and Lee [2014]
ω^U	0	0	142.81	143.54	128.92	129.79
	0	0.6	162.93	163.57	141.88	142.77
	0.2	0.06	130.51	131.01	120.97	121.52
	0.8	0.24	81.19	81.82	86.98	87.77
ω^L	0	0	142.81	143.54	128.92	129.79
	0	0.6	119.87	120.32	113.93	114.55
	0.2	0.06	125.87	126.23	117.79	118.38
	0.8	0.24	41.08	41.69	51.26	51.99

5.4.1.2 Effect of Static Load factor

The variations of DIRs are shown in Fig. 5.50 for delaminated S-S-S-S $[0/0]_8$ bidirectional composite flat panels for different values of L_S at 325K temperature exposure. The onset of instability starts at for $L_S = 0$ starts at non-dimensional excitation frequency of 9 and shifts towards lower side with increase in L_S. At high values of L_D, more widening of the DIRs is observed for L_S increments. At 0.6 L_S, the onset of instability is marked with a reduction of 56% excitation frequency than the value at zero (0) L_S. The composite flat panels show a sign of dynamic instability in regard to the lower boundary frequencies at 0.4 L_S and above with L_D values at 0.4. This is attributed to the reduction in stiffness at higher values of L_S and L_D.

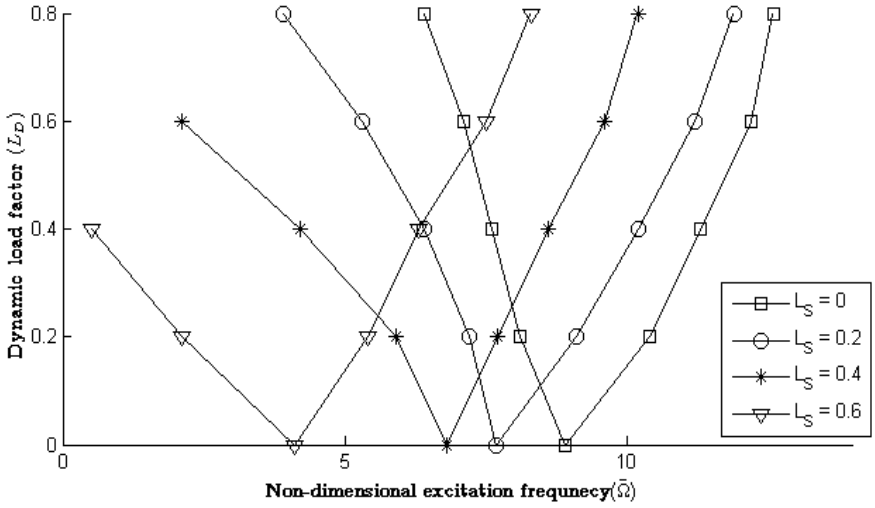

Figure 5.50: Variations of instability regions for delaminated $S-S-S-S$ $[0/0]_8$ bidirectional composite panels with different values of 'L'_S at 325K.

Non-dimensional excitation frequencies observed from the present numerical analysis are plotted against $L_D$as in Fig. 5.51 for delaminated asymmetric C-C-C-C

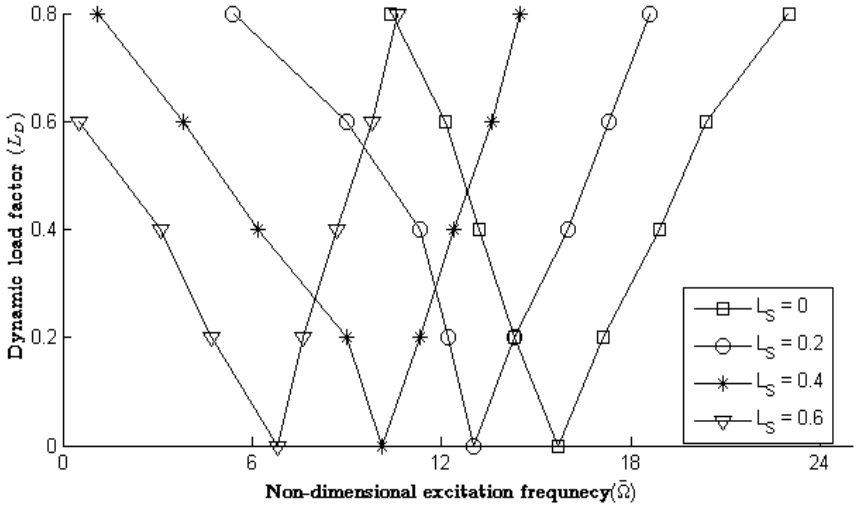

Figure 5.51: Variations of instability regions for delaminated $C-C-C-C$ $[30/-30]_8$ bidirectional composite panels with different values of 'L'_S at 325K.

$[30/-30]_8$ bidirectional composite angle ply flat panels at 325K with variation in L_S. The onset of instability region starts with non-dimensional excitation frequency of 16.4 and with increase in L_S as 0.2, 0.4 and 0.6, this value reduces in the range $21\%, 35\%$ and 58% respectively in this case, which shows a premature parametric

resonant frequency as compared to the case of symmetric cross ply laminates in S-S-S-S boundary condition as in Fig. 5.50. But, at higher values of L_D, better stability regions are located in this case than the simply supported one (Fig. 5.50) with increment in L_S from 0.2.

5.4.1.3 Effect of Delamination size

For different delamination percentages, the variations of instability regions for completely clamped $[0/0]_8$ bidirectional composite laminates at 0.2% moist condition with L_S as 0.2 are shown in Fig. 5.52. The onset of instability region starts at 19.2 non-dimensional excitation frequency for intact flat panels. With $6.25\%, 12.5\%$ and 25% delaminations of composite flat panels, the parametric resonant frequency shifts towards lower side as $8\%, 34\%$ and 55% respectively. Better stability is marked at delaminations of 6.25% and 12.5% but still higher values of delaminations affect the lower boundary frequencies significantly at raised L_D.

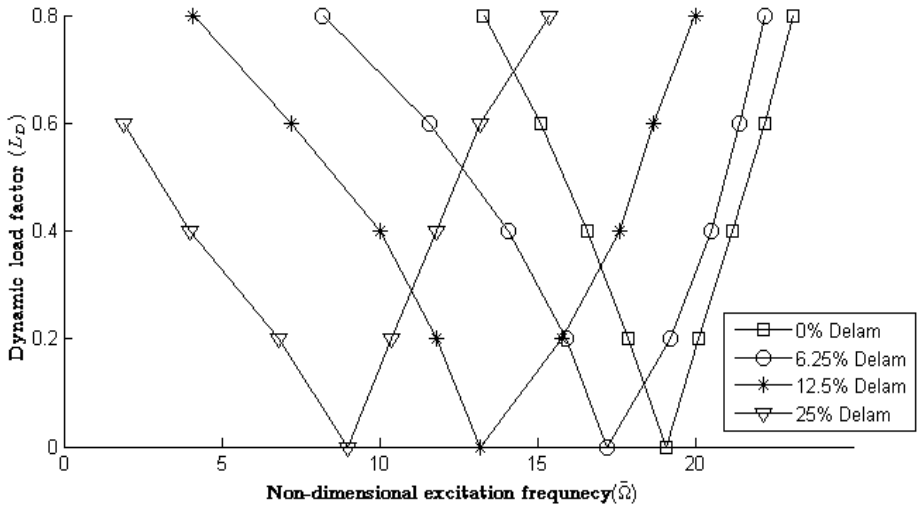

Figure 5.52: Variations of instability regions for delaminated $C-C-C-C$ $[0/0]_8$ bidirectional composite panels at 0.2% moisture content with 0.2 'L'_S.

5.4.1.4 Effect of Boundary Conditions

The non-dimensional excitation frequencies vs. L_D are plotted for $[0/0]_8$ composite flat panels having 6.25% delamination at 325K with L_S 0.2 as shown in Fig. 5.53

having different boundary conditions. The clamped boundary condition shows highest value of parametric resonant frequency 16 at the onset of instability whereas the S-S-S-S and C-F-F-F boundary conditions show the values at 9 and 3.4 respectively. Wider DIR is seen in C-C-C-C case at higher $L_D$than the other two. The C-F-F-F boundary condition shows the least width of DIR at higher L_D values when exposed to thermal environment at 325K.

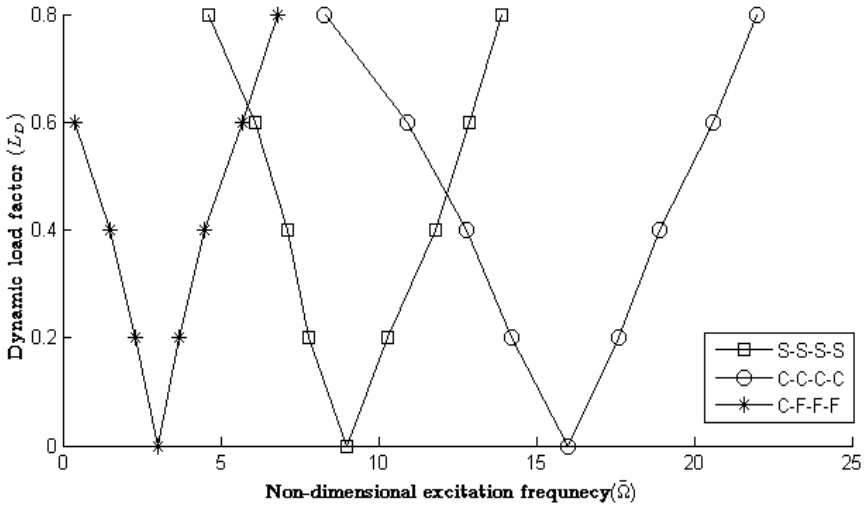

Figure 5.53: Variations of instability regions for 6.25% delaminated $[0/0]_8$ bidirectional composite panels at 325K with 'L'_S 0.2.

5.4.1.5 Effect of Thermal Environment

Thermal influence on non-dimensional excitation frequencies of delaminated S-S-S-S $[0/0]_8$ bidirectional composite flat panels for 0.2 L_S against L_D are shown in Fig. 5.54. The non-dimensional excitation frequency comes down to as low as 4 at 375K, which is 52% less than the value at ambient conditions for this boundary condition. Wider DIRs are observed at elevated temperatures with increase in dynamic load factor. Particularly, the lower boundary frequencies reduce significantly with rise in temperature for composite panels.

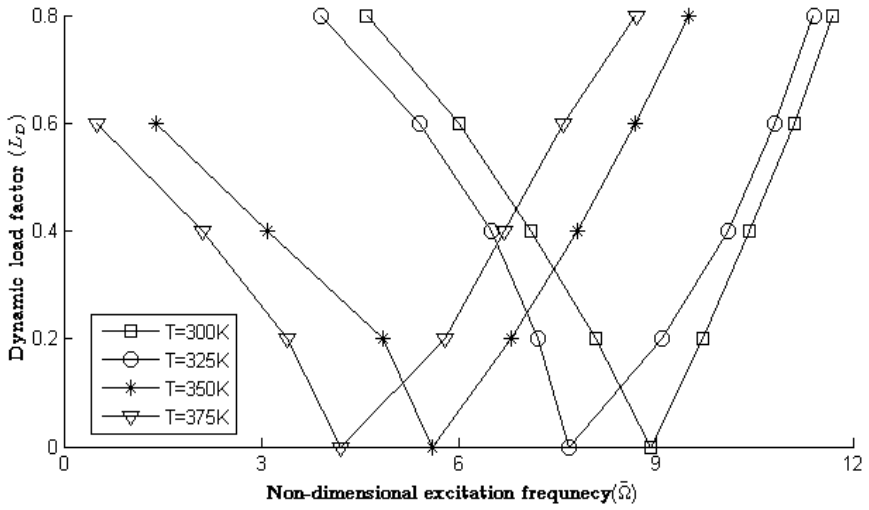

Figure 5.54: Variations of instability regions for delaminated $S-S-S-S$ $[0/0]_8$ bidirectional composite panels with 0.2 'L'_S at elevated temperatures.

At elevated temperatures, the excitation frequencies vs L_D is shown in Fig. 5.55 for delaminated $[0/0]_8$ bidirectional composite panels under fully clamped condition

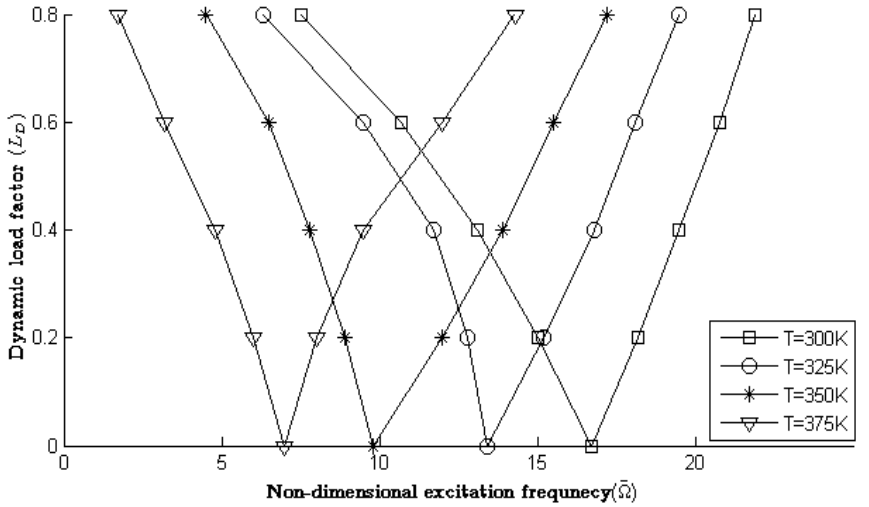

Figure 5.55: Variations of instability regions for delaminated $C-C-C-C$ $[0/0]_8$ bidirectional composite panels with 0.2 'L'_S at elevated temperatures.

with 0.2 L_S. Widening of DIRs is observed at higher L_D for all variations of temperature in thermal environment. More than 50% reduction in excitation frequencies is marked at temperature of 375K than that of the ambient condition. The onset of instability starts at non-dimensional frequency of 17 for the delaminated composite

panels at 300K temperature in thermal environment which reduces to 13, 10 and 7 respectively at temperatures 325K, 350K and 375K in the thermal field.

For asymmetric delaminated $[30/-30]_8$ bidirectional composite panels, the effects of temperature on excitation frequencies are shown in Fig. 5.56 against L_D for 0.2 static load factor. Lowering of excitation frequencies is observed at higher temperatures to 6.1 at 375K that is 53% less than the value at ambient conditions. This shows the influence of thermal field in dynamic stability analysis of delaminated composite panels. Lower boundary excitation frequencies are more influenced at higher L_D than the upper boundary values in thermal field for this specific ply orientation of composite panels in clamped condition.

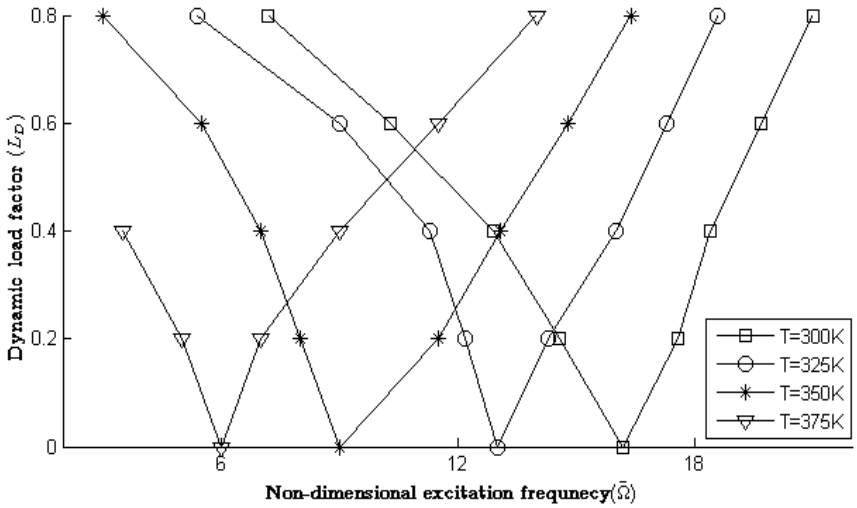

Figure 5.56: Variations of instability regions for delaminated $C-C-C-C$ $[30/-30]_8$ bidirectional composite panels with 0.2 'L'_S at elevated temperatures.

Non-dimensional excitation frequencies vs. L_D for asymmetric delaminated $[45/-45]_8$ composite panels under clamped condition in thermal field are shown in Fig. 5.57 with 0.2 L_S. Widening of DIRs at higher L_D in this case is more significant than that shown in Figs. 5.55 and 5.56 for all temperature conditions. The lower boundary frequencies are drastically reduced at 350K and higher temperatures for greater L_D. 67% reduction in excitation frequency at the onset of instability region is observed at 375K than that under ambient condition for this particular ply orientation, which highlights the influence of thermal environment in dynamic stability studies of

delaminated composite panels.

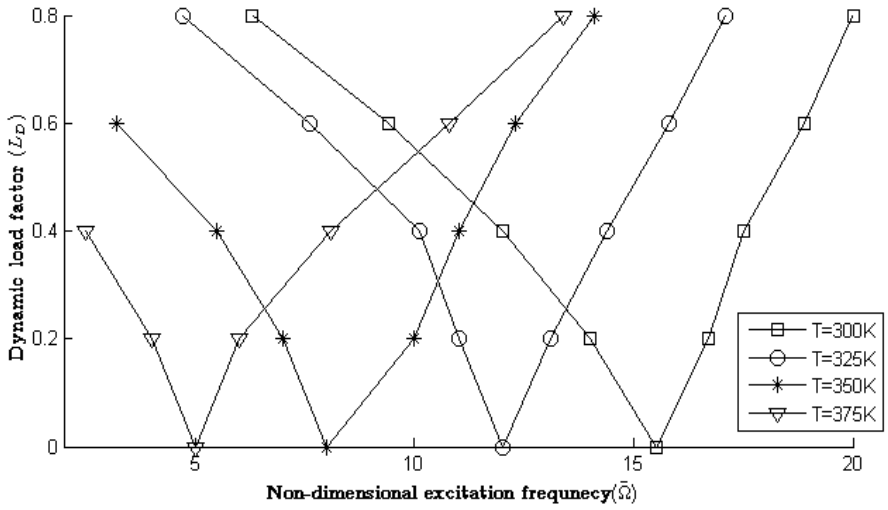

Figure 5.57: Variations of instability regions for delaminated $C-C-C-C$ $[45/-45]_8$ bidirectional composite panels with 0.2 'L'_S at elevated temperatures.

5.4.1.6 Effect of Moist Environment

Moisture effects on non-dimensional excitation frequencies against L_D for delaminated S-S-S-S $[0/0]_8$ bidirectional composite panels with 0.2 L_S are plotted as shown in Fig. 5.58. There is a frequency reduction of $9\%, 44\%$ and 75% is observed for delaminated composite plates exposed to moisture contents of $0.2\%, 0.4\%$ and 0.6% respectively in hygrothermal environment from the frequency value at ambient conditions at the onset of instability region. Beyond 0.4% moisture concentration in hygrothermal environment, the lower boundary frequencies of delaminated composite panels are much affected at higher L_D resulting in wider DIRs.

Influence of moisture concentrations on instability regions of fully clamped $[0/0]_8$ delaminated bidirectional composite flat panels having 0.2 L_S are shown in Fig. 5.59 as a plot between non-dimensional excitation frequency and dynamic load factor. The plates are better stabilized up to 0.4% moisture uptake in hygrothermal field than those in Fig. 5.58. But at 0.6% moisture content, the lower boundary frequencies show sign of instability at higher L_D. The onset of instability region of composite panels starts at excitation frequency of 17 for ambient conditions and the reduction in this

is observed as $24\%, 48\%$ and 62% for moisture of $0.2\%, 0.4\%$ and 0.6% respectively.

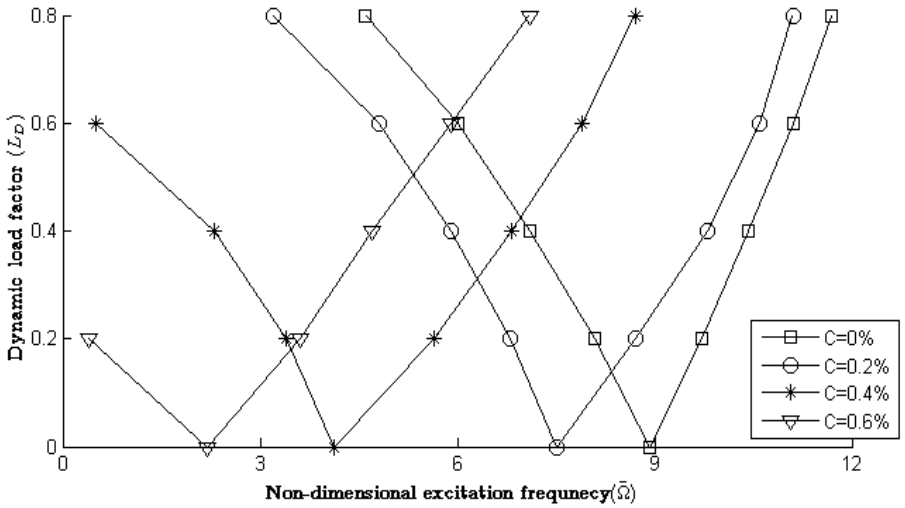

Figure 5.58: Variations of instability regions for delaminated $S-S-S-S$ $[0/0]_8$ bidirectional composite panels with 0.2 'L'_S at higher moisture contents.

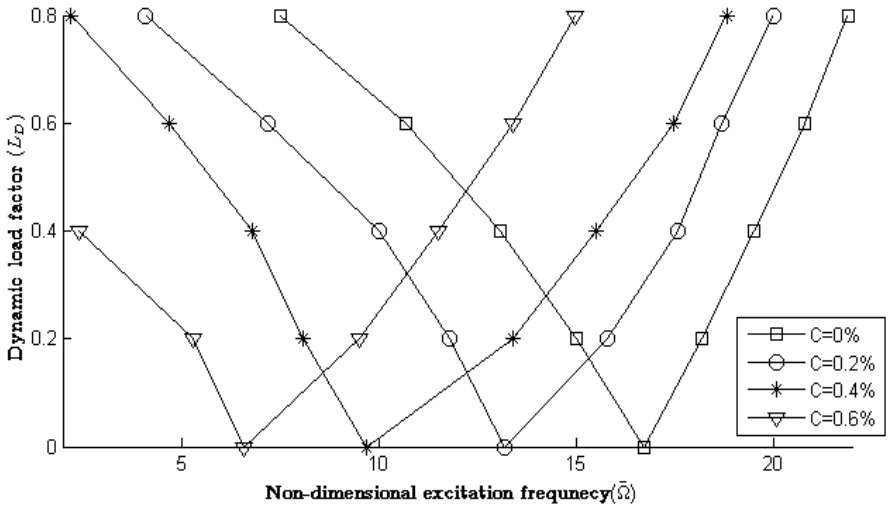

Figure 5.59: Variations of instability regions for delaminated $C-C-C-C$ $[0/0]_8$ bidirectional composite panels with 0.2 'L'_S at higher moisture contents.

The variations in excitation frequency against dynamic load factors in the moist environment for fully clamped delaminated $[30/-30]_8$ asymmetric bidirectional composite panels at 0.2 L_S are shown in Fig. 5.60. The onset of instability starts at non-dimensional frequency of 16 for delaminated composite panels at ambient moisture conditions, which reduces to $12.5, 8$ and 4.7 respectively at moisture contents of

$0.2\%, 0.4\%$ and 0.6% in moist environment. However, the lower boundary frequencies degrade more at moisture contents higher than 0.2% showing instability of delaminated composite flat panels in hygrothermal field at higher values of dynamic load factor.

The variations of excitation frequencies against L_D values are shown in Fig. 5.61 for completely clamped asymmetric [45/-45]8 bidirectional delaminated composite panels with 0.2 L_S in moist environment. Excitation frequencies reduce in the range $27\%, 60\%$ and 74% for delaminated composite panels having moisture uptake of $0.2\%, 0.4\%$ and 0.6% respectively as against the values at ambient conditions. This highlights the influence of moist environment in the dynamic stability analysis of delaminated composite panels. Beyond 0.2% moisture uptake, the lower boundary frequencies suffer much degradation at higher L_D. This particular panel suffers much in dynamic stability requirements at elevated moisture contents than $[0/0]_8$ and $[30/-30]_8$ panels for clamped boundary condition.

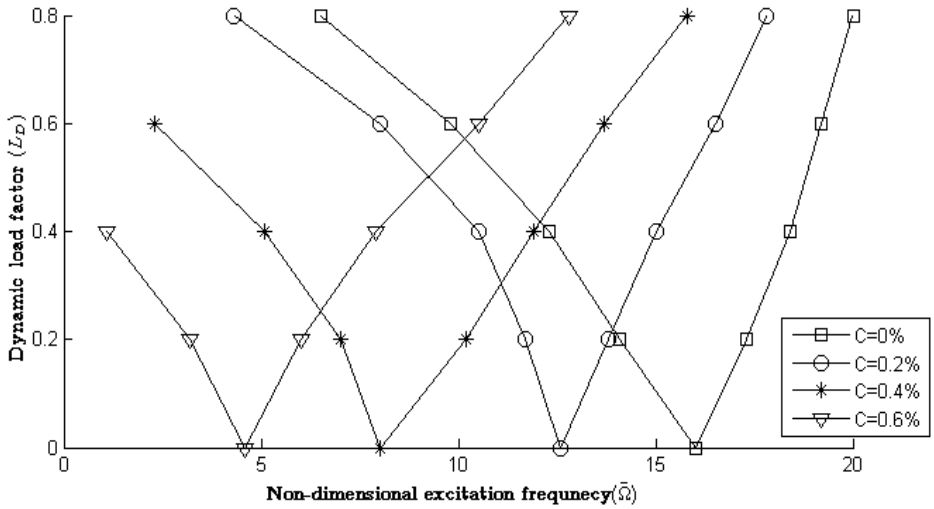

Figure 5.60: Variations of instability regions for delaminated $C-C-C-C$ $[30/-30]_8$ bidirectional composite panels with 0.2 'L'_S at higher moisture contents.

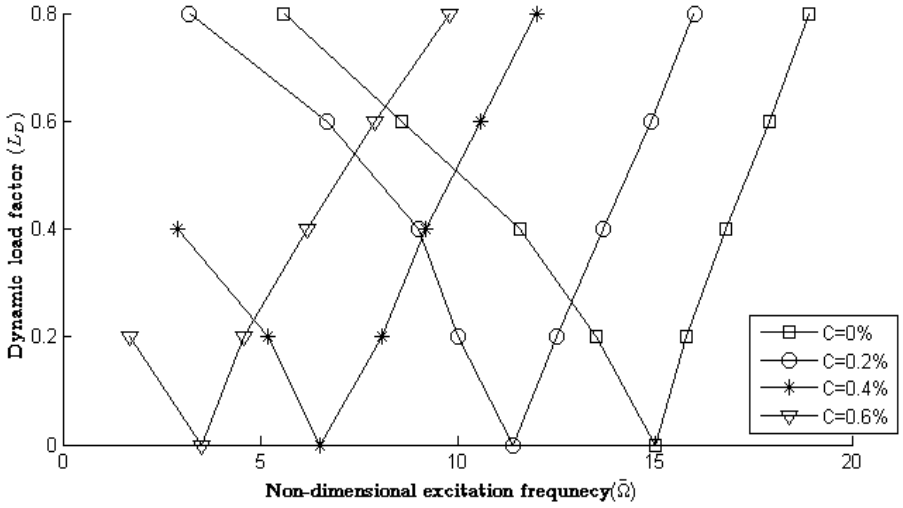

Figure 5.61: Variations of instability regions for delaminated $C-C-C-C$ $[45/-45]_8$ bidirectional composite panels with 0.2 'L'_S at higher moisture contents.

5.4.2 Delaminated composite shell panels in hygrothermal field

The composite doubly curved panels i.e. cylindrical ($R_y/b = 5$), spherical ($R_y/b = R_x/b = 5$) , hyperbolic paraboloidal ($R_y/b = -5, R_x/b = 5$) and elliptic paraboloidal ($R_y/b = 5, R_x/R_y = 0.5$) are chosen for the present numerical study. Static load factor 'L_S' is varied between 0 and 0.6, whereas, dynamic load factor 'L_D' is varied between 0 and 0.8. The delamination percentage chosen for the study is 6.25% (unless otherwise stated).

The material properties (unless otherwise mentioned) under hygrothermal conditions used in the present numerical investigation are as per Tables 5.2 and 5.7.

5.4.2.1 Comparison with previous studies

The non dimensional fundamental frequencies os spherical shell panels obtained from the numerical analysis are compared with those available in literature as per Table 5.8.

Non dimensional compressive buckling loads from the present numerical analysis at ambient conditions for square simply supported symmetric cross ply [0/90/0/90/0]

cylindrical shell panels are validated with the results of Sciuva and Carrera [1990] and Ravi Kumar et al. [2003] as shown in Table 5.17.

Table 5.17: Validation of non dimensional compressive buckling loads for square simply supported symmetric cross ply [0/90/0/90/0] cylindrical shell panels.

$a/b = 1$, $R/a = 20.0$, $E_{11} = 40E_{22}$, $G_{12} = G_{13} = 0.5E_{22}$, $G_{23} = 0.6E_{22}$, $\nu_{12} = \nu_{12} = 0.25$

b/h	10	20	50	100
Ravi Kumar et al. [2003]	23.9655	31.7944	35.3974	36.8474
Sciuva and Carrera [1990]FSDT	24.19	31.91	35.42	36.86
Sciuva and Carrera [1990]CST	35.84	35.88	36.13	37.04
Present	23.92	31.74	35.02	36.51

5.4.2.2 Effect of Static Load factor

Fig. 5.62 shows the variations of non-dimensional excitation frequencies of 6.25% delaminated S-S-S-S $[0/0]_8$ cylindrical ($Ry/b = 5$) composite shells against dynamic load factors at ambient conditions of temperature and moisture for different values of static load factor 'L_S'. The onset of instability region starts at 12.31 non-dimensional excitation frequency having zero 'L_S' and decrease in the range $13.5\%, 29.6\%$ and 50% for 0.2, 0.4 and 0.6 values of 'L_S' respectively from that of zero 'L_S'. Widening of DIR is seen at higher static load factors and at 0.6 'L_S', the cylindrical composite shell panels become unstable with 0.6 dynamic load factor or more.

The non-dimensional excitation frequencies of 6.25% delaminated S-S-S-S $[0/0]_8$ spherical ($R_y/b = R_x/b = 5$) composite shells are plotted against dynamic load factors at ambient conditions for different values of 'L_S' as observed from Fig. 5.63. Here, the onset of instability region starts at a value of non dimensional frequency of 16.72 for zero 'L_S' and at higher values of 'L_S', this particular composite shell panel shows better stability than cylindrical panel even at higher values of dynamic load factors. At 0.6 'L_S', the onset of instability occurs at 23% less than that of the zero 'L_S' for this composite panel.

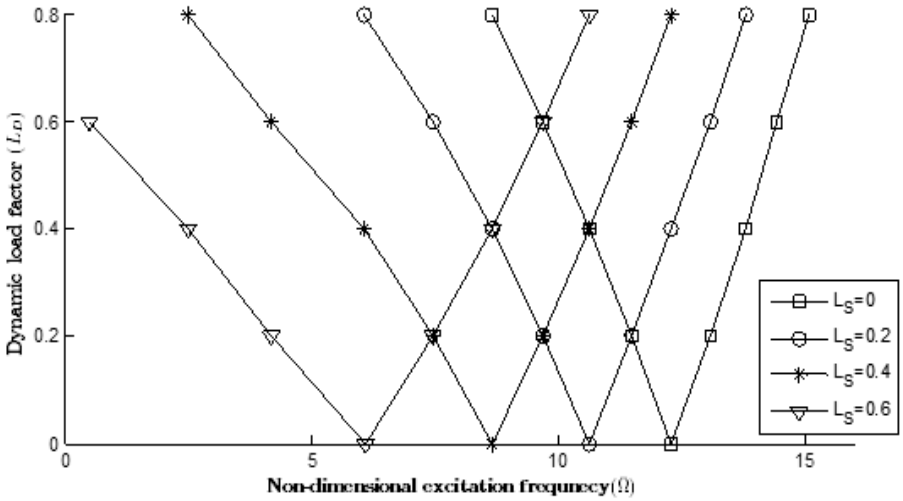

Figure 5.62: Variation of instability regions of delaminated S-S-S-S $[0/0]_8$ cylindrical ($Ry/b = 5$) composite shells with different values of 'L_S' at ambient conditions.

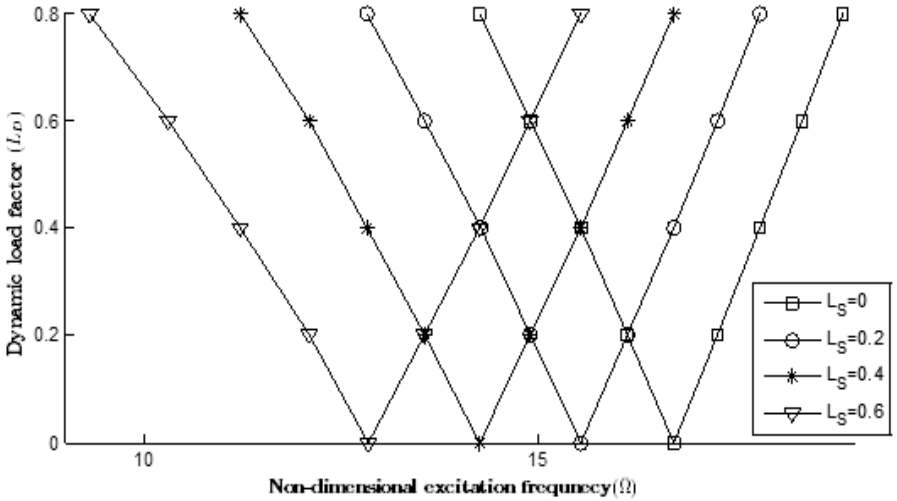

Figure 5.63: Variation of instability regions of delaminated S-S-S-S $[0/0]_8$ spherical ($R_y/b = R_x/b = 5$) composite shells with different values of 'L_S' at ambient conditions.

The variations of non-dimensional excitation frequencies of delaminated S-S-S-S $[0/0]_8$ hyperbolic paraboloidal ($R_y/b = -5, R_x/b = 5$) composite shells are plotted against dynamic load factors at ambient conditions, as seen from Fig. 5.64, at different values of 'L_S'. In this case, wider DIRs are observed even at zero static load factor. This composite shell becomes highly unstable at 0.4 and more value of 'L_S'

even at very low values of dynamic load factors. The onset of instability starts at 10.41 excitation frequency for zero 'L_S' and at 0.6 'L_S', it reaches a value of 1.28 as evident from Fig. 5.64. This shell panel is extremely vulnerable in case of parametric instability at higher values of static as well as dynamic load factors. The designers are to take utmost care in designing these composite panels at higher in-plane periodic forces.

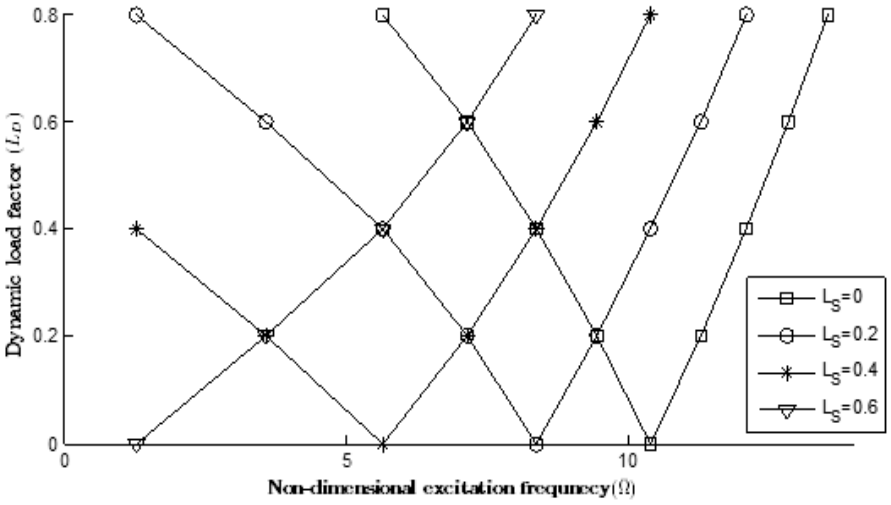

Figure 5.64: Variation of instability regions of delaminated S-S-S-S $[0/0]_8$ hyperbolic paraboloidal ($R_y/b = -5, R_x/b = 5$) composite shells with different values of 'L_S' at ambient conditions.

Influence of static load factors on non dimensional excitation frequencies of delaminated S-S-S-S $[0/0]_8$ elliptic paraboloidal ($R_y/b = 5, R_x/R_y = 0.5$) composite shells at ambient conditions are shown in Fig. 5.65. The onset of instability for this panel at zero 'L_S' starts at 22.13 excitation frequency and is reduced by $4\%, 8\%$ and 12.5% for 0.2, 0.4 and 0.6 'L_S' respectively. At higher values of dynamic load factors, better DIRs are available in this case. Almost same widening of DIRs are observed for different values of 'L_S' even at 0.8 dynamic load factor. Among all four composite doubly curved panels mentioned here, this panel shows the least influence of static load factor.

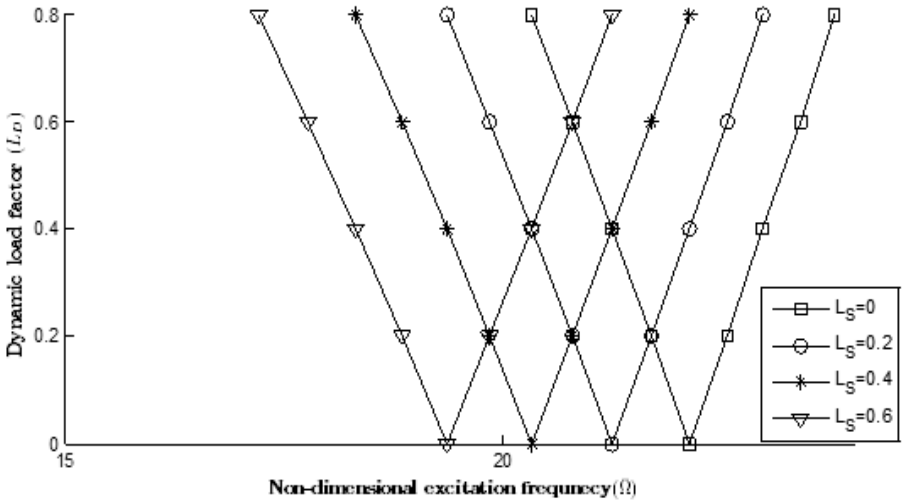

Figure 5.65: Variation of instability regions of delaminated S-S-S-S $[0/0]_8$ elliptic paraboloidal ($R_y/b = 5, R_x/R_y = 0.5$) composite shells with different values of 'L_S' at ambient conditions.

5.4.2.3 Effect of Delamination size

Effect of delamination sizes on non dimensional excitation frequencies of S-S-S-S $[0/0]_8$ cylindrical ($R_y/b = 5$) composite shells at 0.2 'L_S' and 325 K are shown in Fig. 5.66.

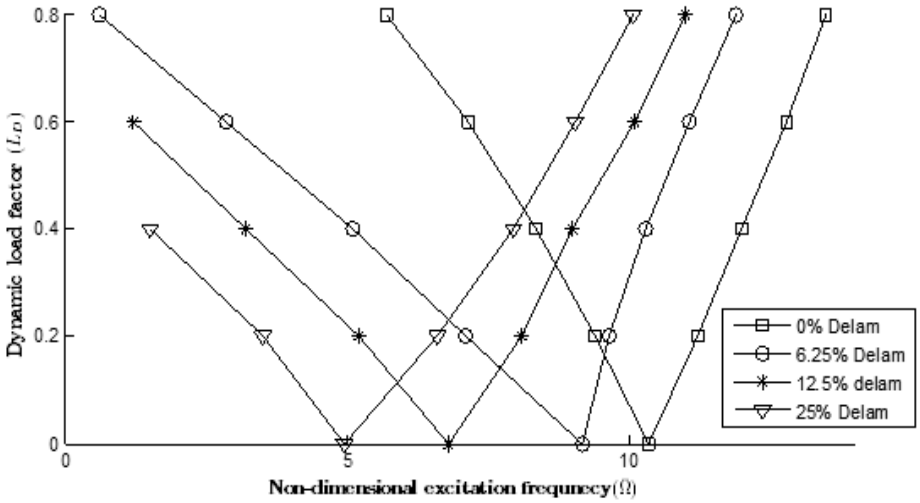

Figure 5.66: Variation of instability regions of S-S-S-S $[0/0]_8$ cylindrical ($R_y/b = 5$) composite shells with various delaminations at 0.2 'L_S' and 325 K.

Wider DIRs are observed at a value 6.25% delamination and the shell panels become

unstable at higher values of dynamic load factors. The onset of instability starts at a value of 10.37 excitation frequency at zero delamination and is reduced by 52% at delamination area of 25%. This shows the vulnerability towards the parametric instability of the cylindrical shell panel at higher percentages of delamination under S-S-S-S boundary condition only.

The variations of non dimensional excitation frequencies of S-S-S-S $[0/0]_8$ spherical ($R_y/b = R_x/b = 5$) composite shells with various delaminations at 0.2 'L_S' and 325 K are plotted against dynamic load factors in Fig. 5.67. The 25% delaminated spherical shell becomes more unstable at higher values of dynamic load factors showing wider DIR. The onset of instability for intact panel starts at 15.35 excitation frequency and is reduced in the range as $9.4\%, 14.6\%$ and 19.4% for delaminations of $6.25\%, 12.5\%$ and 25% respectively from that of the intact panel. At zero dynamic load factor, the delaminations do not show any drastic effect on the instability, but at higher values of dynamic load factors, the wider DIRs evidently hint the delamination effects for this composite panel.

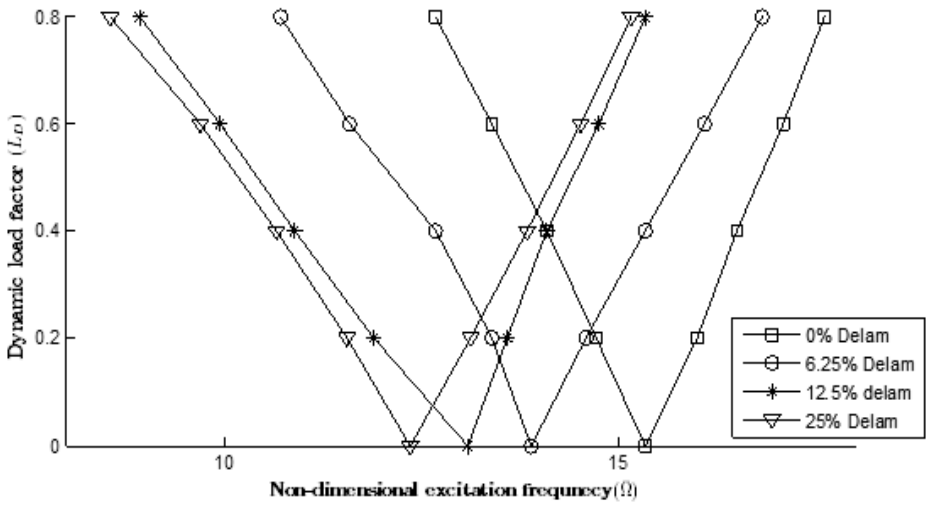

Figure 5.67: Variation of instability regions of S-S-S-S $[0/0]_8$ spherical ($R_y/b = R_x/b = 5$) composite shells with various delaminations at 0.2 'L_S' and 325 K.

Delamination effects on non dimensional excitation frequencies of simply supported $[0/0]_8$ hyperbolic paraboloidal ($R_y/b = -5, R_x/b = 5$) composite shells at 0.2 'L_S' and 325 K are shown in Fig. 5.68. The onset of instability starts at excitation

frequency of 8 for the intact panel and drastically decreases by 76% from that of the intact one at 25% delamination area. The particular shell becomes highly unstable beyond 12.5% delamination at even lower dynamic load factors showing wider DIRs. The designer has to be very cautious while designing these composite panels at higher in-plane periodic forces.

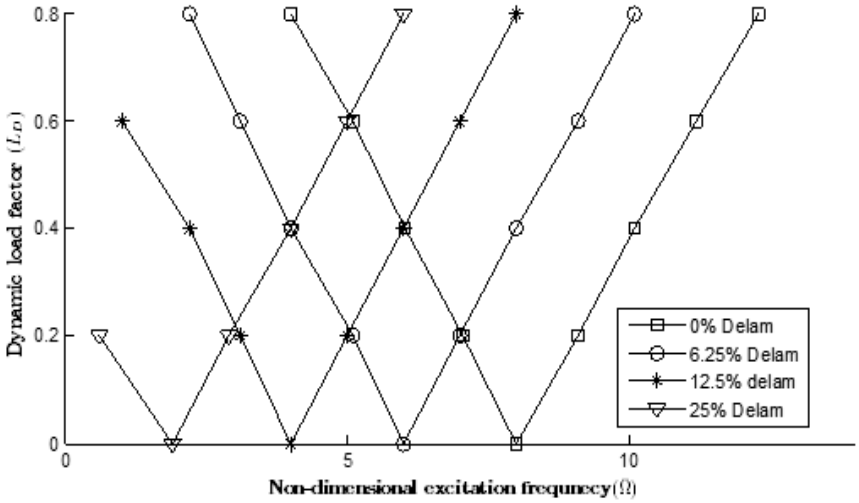

Figure 5.68: Variation of instability regions of S-S-S-S $[0/0]_8$ hyperbolic paraboloidal $(R_y/b = -5, R_x/b = 5)$ composite shells with various delaminations at 0.2 'L_S' and 325K.

The non dimensional excitation frequencies are plotted against dynamic load factors for simply supported $[0/0]_8$ elliptic paraboloidal $(R_y/b = 5, R_x/R_y = 0.5)$ composite shells having various delaminations at 0.2 'L_S' and 325 K in Fig. 5.69. The onset of instability occurs at 21.1 excitation frequency for the intact panel and is reduced by 9% only for delamination area of 25%. This shows the minimal effect of delamination in zones having dynamic load factors less than 0.4. But at higher 'L_D' , wider DIRs are marked for 12.5% delaminations. Among all other composite doubly curved panels under discussion, this panel shows better stability in higher delamination areas.

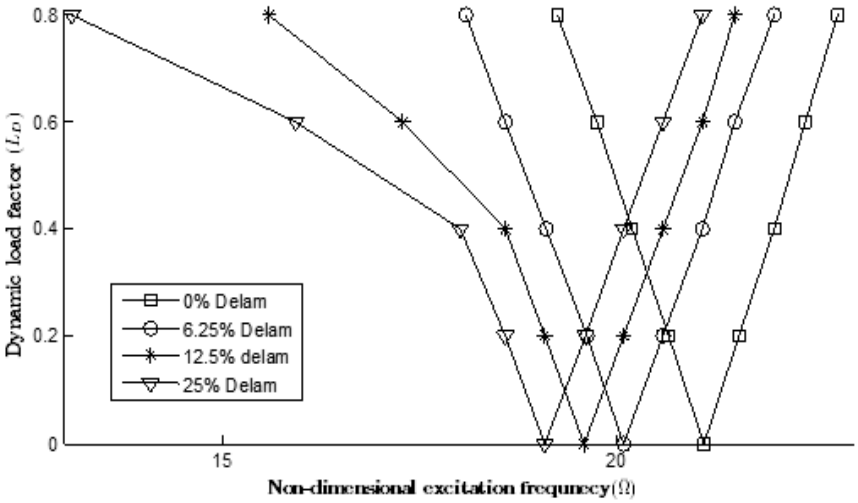

Figure 5.69: Variation of instability regions of S-S-S-S $[0/0]_8$ elliptic paraboloidal ($R_y/b = 5, R_x/R_y = 0.5$) composite shells with various delaminations at 0.2 'L_S' and 325 K.

5.4.2.4 Effect of Boundary Conditions

The non-dimensional excitation frequencies of delaminated $[0/0]_8$ cylindrical ($R_y/b = 5$) composite shells at at 0.2 'L_S' and 325 K are plotted against dynamic load factors having different boundary conditions in Fig. 5.70. For clamped boundary condition, the onset of instability starts at an excitation frequency of 20.37, whereas for simply supported shells starting point of instability is 8.06. The composite cylindrical shell under S-S-S-S case shows wider DIR than C-C-C-C case at higher values of dynamic load factors. Better stability is marked in completely clamped case than simply supported one.

For delaminated spherical composite shells at 0.2 'L_S' and 325 K, the non dimensional excitation frequencies are plotted against dynamic load factors in Fig. 5.71 with different boundary conditions. Though better stability regions are marked under both boundary conditions for spherical shells even at higher dynamic load factors, the onset of instability starts at excitation frequency of 26.69 for completely clamped one, whereas for simply supported case it starts at 50% lower excitation frequency.

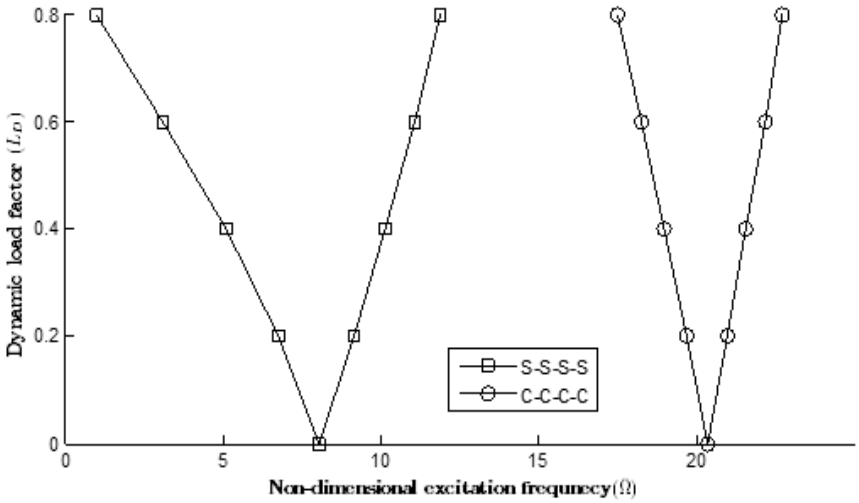

Figure 5.70: Variation of instability regions of delaminated $[0/0]_8$ cylindrical ($R_y/b = 5$) composite shells with different boundary conditions at at 0.2 'L_S' and 325 K.

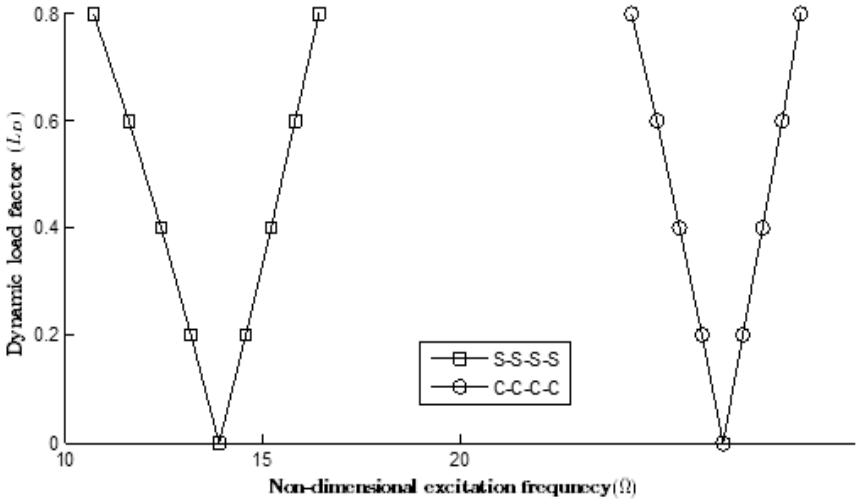

Figure 5.71: Variation of instability regions of delaminated $[0/0]_8$ spherical ($R_y/b = R_x/b = 5$) composite shells with different boundary conditions at 0.2 'L_S' and 325 K.

Fig. 5.72 shows the variations of non dimensional excitation frequencies of delaminated [0/0]8 hyperbolic paraboloidal ($R_y/b = -5, R_x/b = 5$) composite shells at 0.2 'L_S' and 325 K for various boundary conditions. The shell with S-S-S-S case becomes highly unstable with lower boundary frequencies at 0.4 'L_D' or more. The onset of instability for simply supported shell starts at excitation frequency of 4.75 which is 78% less than that of completely clamped one. Better stability is marked for this

shell under clamped condition.

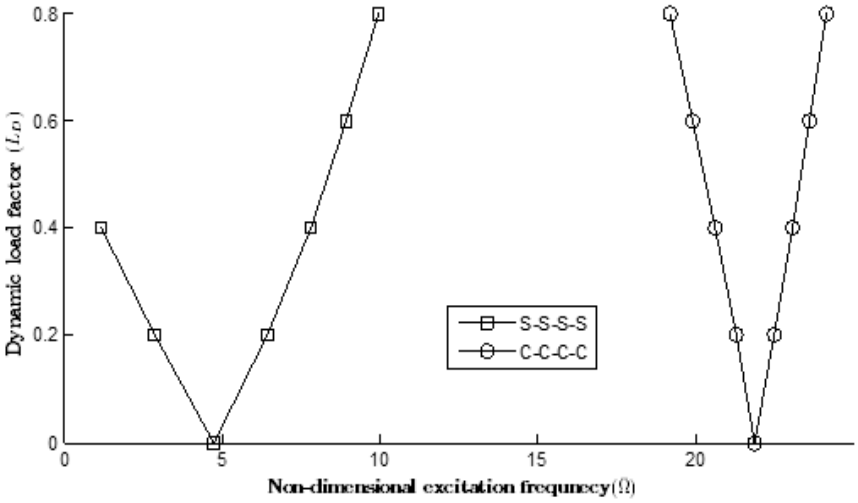

Figure 5.72: Variation of instability regions of delaminated $[0/0]_8$ hyperbolic paraboloidal ($R_y/b = -5, R_x/b = 5$) composite shells with different boundary conditions at 0.2 'L_S' and 325 K.

The effects of various boundary conditions on the non dimensional excitation frequencies of delaminated $[0/0]_8$ elliptic paraboloidal ($R_y/b = 5, R_x/R_y = 0.5$) composite shells at 0.2 'L_S' and 325 K are shown in Fig. 5.73. The onset of instability

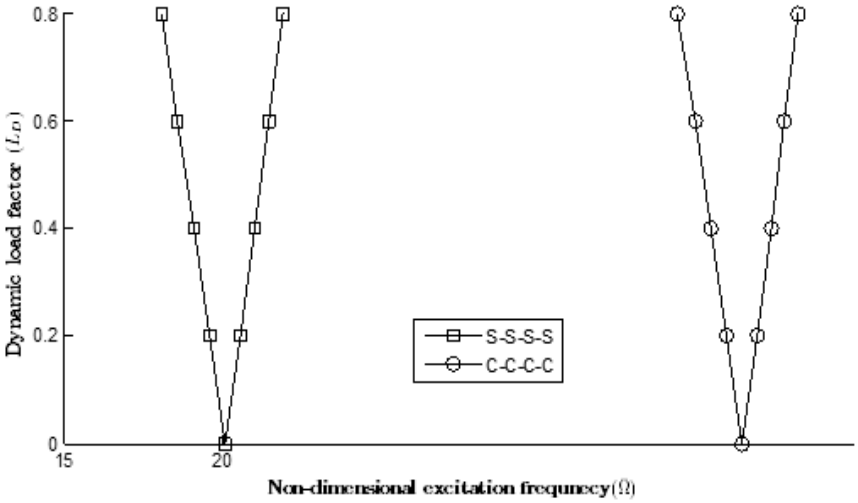

Figure 5.73: Variation of instability regions of delaminated $[0/0]_8$ elliptic paraboloidal ($R_y/b = 5, R_x/R_y = 0.5$) composite shells with different boundary conditions at 0.2 'L_S' and 325 K.

for simply supported shell is marked at 20.12 excitation frequency which is 45% less than that of the fully clamped shell. Besides this, better stability regions are marked in both the boundary conditions of the composite shell even at higher dynamic load factors. This particular shell gives better stability regions under both the boundary conditions among all the shell panels under discussion.

5.4.2.5 Effect of Thermal Environment

Thermal effects on non dimensional excitation frequencies of delaminated S-S-S-S $[0/0]_8$ cylindrical ($R_y/b = 5$) composite shells having 0.2 'L_S' and zero moisture content are shown in Fig. 5.74. The shell at ambient temperature shows the onset of instability at 10.65 with wider DIR at higher values of dynamic load factors. The rise of temperature shows a decay in excitation frequency at the onset of instability of the shells in the range $24\%, 50\%$ and 67% for 325K, 350K and 375K respectively than that of the shells at ambient conditions. The lower boundary frequencies degrade much beyond temperature of 350K with higher values of dynamic load factors.

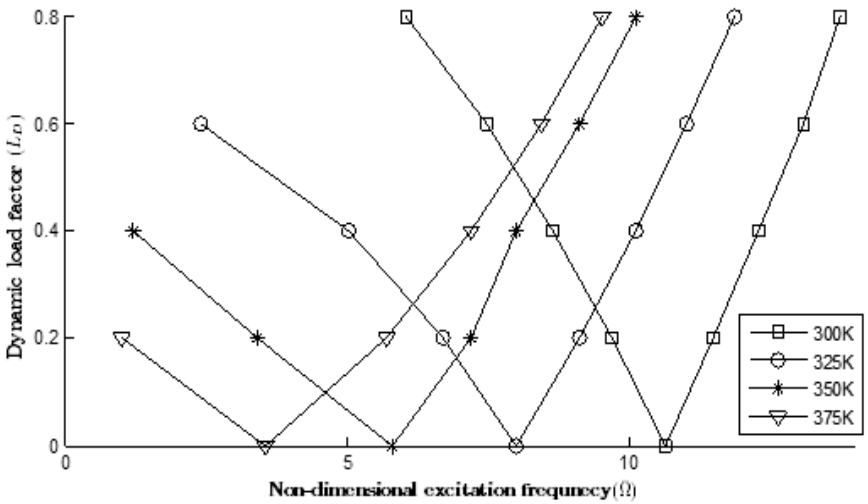

Figure 5.74: Variation of instability regions of delaminated S-S-S-S $[0/0]_8$ cylindrical ($R_y/b = 5$) composite shells at different temperatures having 0.2 'L_S'.

The variations of non dimensional excitation frequencies of delaminated S-S-S-S $[0/0]_8$ spherical ($R_y/b = R_x/b = 5$) composite shells having 0.2 'L_S' at different tem-

peratures are shown in Fig. 5.75. With rise in temperature, wider DIRs are marked for these shells at higher dynamic load factors. The onset of instability for the shells at ambient conditions starts at 15.54 and degrades in the range $10.6\%, 23.4\%$ and 33.6% from that of the ambient one at temperatures of 325K, 350K and 375K respectively. Comparatively, this shell shows better stability regions than the cylindrical one under discussion in Fig. 5.74.

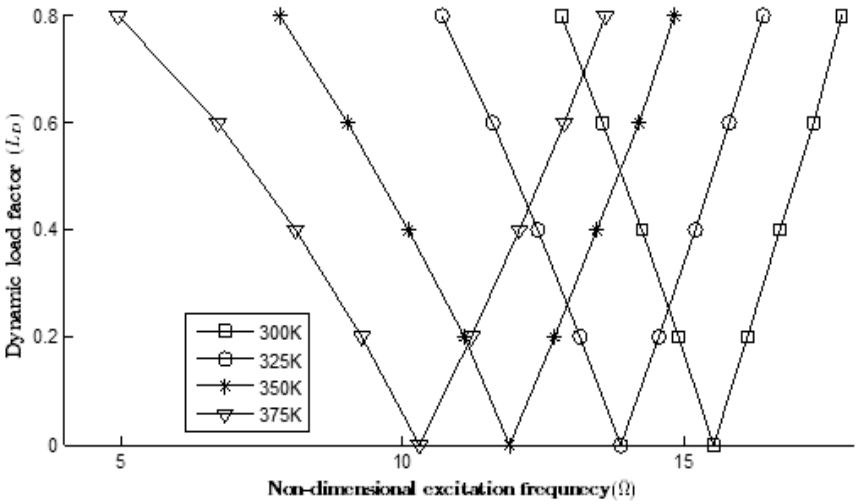

Figure 5.75: Variation of instability regions of delaminated S-S-S-S $[0/0]_8$ spherical $(R_y/b = R_x/b = 5)$ composite shells at different temperatures having 0.2 'L_S'.

Temperature effects on instability regions of delaminated S-S-S-S $[0/0]_8$ hyperbolic paraboloidal $(R_y/b = -5, R_x/b = 5)$ composite shells having 0.2 'L_S' and zero moisture content are shown in Fig. 5.76. The stability regions of this shell are much more affected by the thermal environment, which is evident from the lower boundary frequencies at higher temperatures and with increment of dynamic load factors. The onset of instability for the shell at ambient conditions starts at an excitation frequency of 8.38 and at temperatures 325K, 350K and 375K, this value of frequency for onset of instability remain at 6.3, 4.67 and 2.1 respectively.

For delaminated S-S-S-S $[0/0]_8$ elliptic paraboloidal $(R_y/b = 5, R_x/R_y = 0.5)$ composite shells having 0.2 'L_S', the variations of non dimensional frequencies against dynamic load factors with rise in temperature are plotted as shown in Fig. 5.77. Among all composite shell panels discussed in this section, this panel shows better

stability regions even at elevated temperatures and higher dynamic load factors. The onset of instability for this shell at ambient conditions starts at 21.25 excitation frequency and decays in the range $5.3\%, 11.4\%$ and 15.7% from that of the ambient one, at temperatures 325K, 350K and 375K respectively. Wider DIRs are observed at elevated temperatures with increment in dynamic load factors.

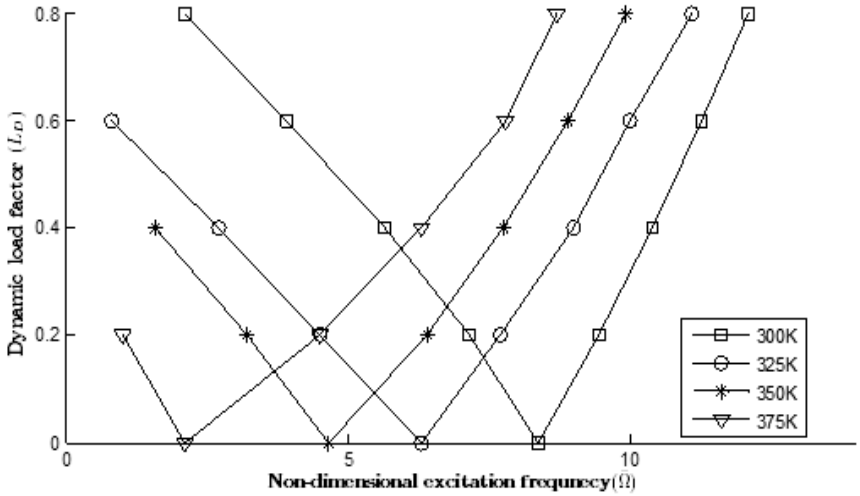

Figure 5.76: Variation of instability regions of delaminated S-S-S-S $[0/0]_8$ hyperbolic paraboloidal ($R_y/b = -5, R_x/b = 5$) composite shells at different temperatures having 0.2 'L_S'.

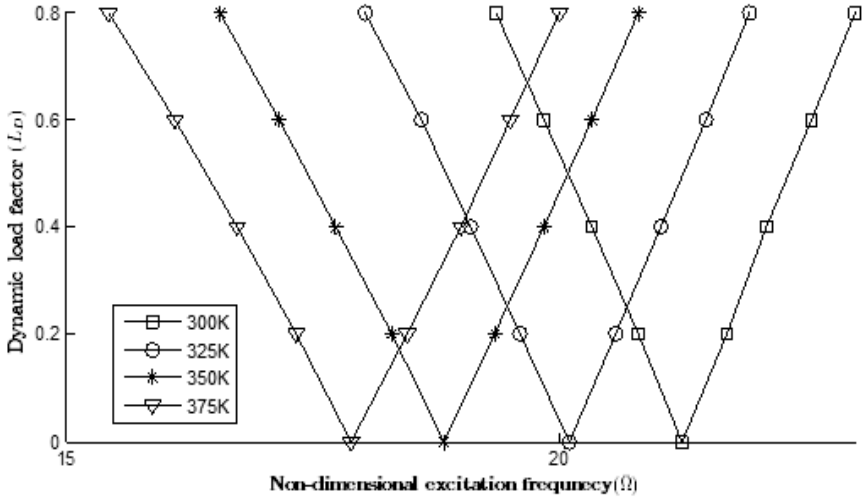

Figure 5.77: Variation of instability regions of delaminated S-S-S-S $[0/0]_8$ elliptic paraboloidal ($R_y/b = 5, R_x/R_y = 0.5$) composite shells at different temperatures having 0.2 'L_S'.

5.4.2.6 Effect of Moist Environment

For delaminated S-S-S-S $[0/0]_8$ cylindrical ($R_y/b = 5$) composite shells having 0.2 'L_S' at ambient temperature, the variations of non dimensional excitation frequencies against dynamic load factors are plotted in Fig. 5.78 with different moisture concentrations. It is clear from the figure that the shell panel becomes highly unstable beyond 0.2% moisture content with increase in dynamic load factors. The lower boundary frequencies degrade much more in the presence of 0.4% or high moisture content. This shows the effect of moist environment on dynamic stability of cylindrical shell panels under simply supported boundary conditions. The onset of instability at ambient conditions starts at 10.65 excitation frequency and degrade by 50% when exposed to a moisture content of 0.6%.

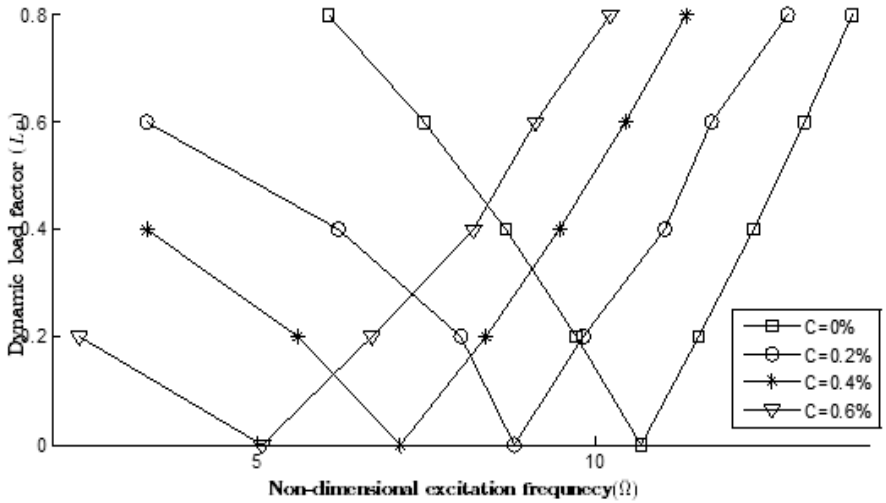

Figure 5.78: Variation of instability regions of delaminated S-S-S-S $[0/0]_8$ cylindrical ($R_y/b = 5$) composite shells at different moisture concentrations having 0.2 'L_S'.

Fig. 5.79 represents the moisture effects on the stability regions of delaminated S-S-S-S $[0/0]_8$ spherical ($R_y/b = R_x/b = 5$) composite shells having 0.2 'L_S' at ambient temperature. The onset of instability in this case starts at 15.54 excitation frequency under ambient conditions and is reduced in the range $13.8\%, 31.6\%$ and 50% at moisture concentrations of $0.2\%, 0.4\%$ and 0.6% from that of the ambient conditions. Wider DIRs are observed at moisture concentrations of 0.4% or more with higher

dynamic load factors. The spherical composite panels show better stability than the cylindrical panels discussed above under moist conditions.

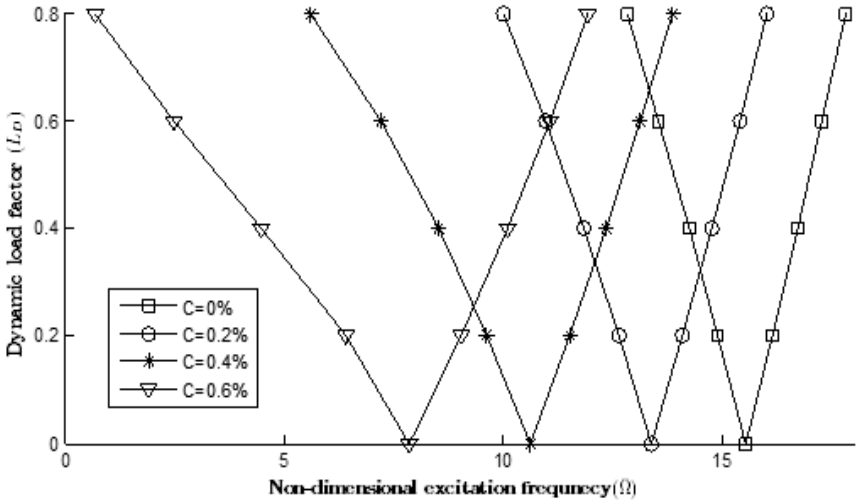

Figure 5.79: Variation of instability regions of delaminated S-S-S-S $[0/0]_8$ spherical ($R_y/b = R_x/b = 5$) composite shells at different moisture concentrations having 0.2 'L_S'.

Variations of non dimensional excitation frequencies of delaminated S-S-S-S hyperbolic paraboloidal ($R_y/b = -5, R_x/b = 5$) composite shells having 0.2 'L_S' at ambient temperature are shown in Fig. 5.80 for various moisture contents. It is clear from the figure that even at ambient conditions the lower boundary frequencies of this shell degrade much showing wider DIR. Beyond 0.2% moisture concentration; the composite panels become highly unstable showing the catastrophic effects of moist environment. The onset of instability of these shells under ambient conditions starts at 8.38 excitation frequency and is reduced by 64% when exposed to a moisture content of 0.4% only.

Moisture effects on the instability regions of delaminated S-S-S-S $[0/0]_8$ elliptic paraboloidal ($R_y/b = 5, R_x/R_y = 0.5$) composite shells having 0.2 'L_S' are shown in Fig. 5.81 exposed to different moisture concentrations. As evident from the figure, this particular doubly curved panel shows better stability regions even at higher moisture contents and dynamic load factors among all the four composite doubly curved panels discussed in this section. The onset of instability for these shells at ambient

conditions starts at 21.25 excitation frequency and the value comes down to 19.78, 18.1 and 16.69 when exposed to moisture content of 0.2%, 0.4% and 0.6%. These values are less than their counterparts for the same composite panel exposed to elevated temperatures as shown in Fig. 5.77; highlighting the effects of moist environment on dynamic instability regions under simply supported boundary conditions only.

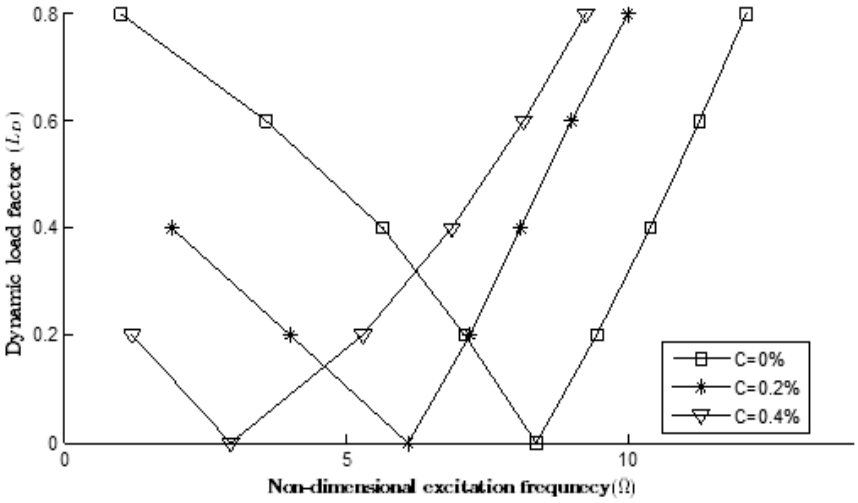

Figure 5.80: Variation of instability regions of delaminated S-S-S-S $[0/0]_8$ hyperbolic paraboloidal ($R_y/b = -5, R_x/b = 5$) composite shells at different moisture concentrations having 0.2 'L_S'.

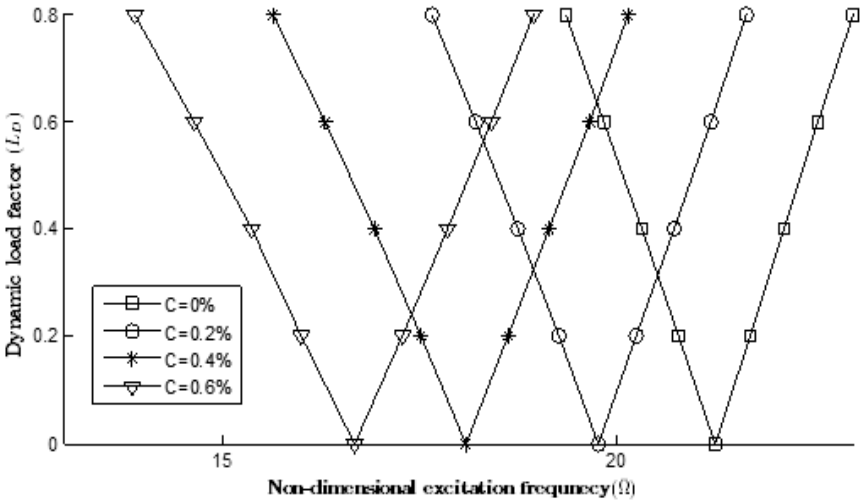

Figure 5.81: Variation of instability regions of delaminated S-S-S-S $[0/0]_8$ elliptic paraboloidal ($R_y/b = 5, R_x/Ry = 0.5$) composite shells at different moisture concentrations having 0.2 'L_S'.

The fibers in cross ply laminates remain in the direction of in-plane harmonic loading causing parametric resonance showing more stiffness than the fibers in angle ply laminates in which fibers are not in direction of load. Hence, the onset of instability comes at a lower range in case of angle ply than cross ply as marked from the DIRs. The worst behavior of angle ply laminates to axial in-plane harmonic loads may be attributed to this.

Chapter - 6

Conclusions

6.1 Overview

The present research work deals with the study of the vibration, buckling and dynamic stability characteristics of delaminated composite panels in hygrothermal field. The investigation on vibration and buckling of delaminated composite panels subjected to varieties of temperature and moisture is studied by both numerical approach using FEM and experimentally. The development of regions of instability arises from Floquet's theory developed by Bolotin (1964) for homogeneous structures and the boundaries of the primary instability regions have been determined to study the effect of various parameters on the dynamic instability regions of the delaminated composite panels in hygrothermal environment.

A general formulation dealing with vibration, buckling and parametric instability of delaminated composite flat and curved panels subjected to hygrothermal changes is presented. The effects of various geometrical parameters like delamination size, boundary conditions, fiber orientations, ply sequence, temperature and moisture concentrations and static load factor on the free vibration and stability characteristics of delaminated woven fiber composite panels have been analyzed. The conclusions drawn in respect of different studies are presented below.

6.2 Vibration of delaminated composite panels in hygrothermal field

The main thrust of the present study is the modal analysis of delaminated woven fiber composite panels in hygrothermal environment, because of its inherent link with dynamic stability analysis. The effect of different parameters on the frequencies of free vibration of composite panels are observed and compared with numerical predictions using FEM.

Based on first order shear deformation theory, a dynamic finite element analysis of single mid plane delaminated square composite plates exposed to hygrothermal environment is investigated taking into account the changes in thermo-mechanical properties due to temperature and moisture effect. The accuracy of the formulation has been verified using sample problems available in literature. At the same time, the numerical results of natural frequencies of vibration obtained from the above formulation are also experimentally checked in the laboratory by casting 16 layered woven fiber $[0/0]_{8s}$ Glass /Epoxy composite plates with a wide variety of boundary conditions, percentage of delaminations subjected to temperature and moisture. The broad conclusions that can be made from the above study are as follows:

- The natural frequencies of free vibration of composite plates decrease with increase in uniform moisture content and temperature due to reduction of stiffness for all laminates.

- The reduction in the fundamental frequencies is non-linear and the problem may become one of instability depending on the value of moisture concentration and temperature.

- The delamination of composite laminates plays an important role in degrading the natural frequencies of the laminates and in hygrothermal environment it offers a challenge to the designer of composite structures.

- The effects of delamination and hygrothermal environment on natural frequen-

cies are greatly dependent on the boundary conditions, that is, the more strongly the plate is restrained, the greater the effects on the natural frequencies.

- The frequencies of vibration are the lowest in $C-F-F-F$ boundary condition and the highest in $C-C-C-C$ cases for all laminates as observed here with several boundary conditions.

- The composite plate with $C-F-C-F$ boundary condition is the worst affected among all boundary conditions at elevated temperatures and moistures with delamination area 25% or more with reference to frequency of vibration.

- The percent reductions of natural frequencies of composite plates at elevated moisture concentrations with increase in delamination area for all types of boundary conditions studied here are higher than those at elevated temperatures.

A general formulation is presented for vibration analysis of woven fiber laminated composite curved panels with strip delaminations in moist environment covering any moisture range. The concluding remarks based on range of geometry, materials, boundary conditions and moisture effects are listed below.

- Natural frequencies of free vibration of woven fibre composite panels decrease with increase in moisture content and delamination area due to reduction of stiffness for all laminates.

- Complex stresses develop in moist environment which show reduction in stiffness resulting in degradation of frequencies of vibration for composite panels of different curvatures.

- Effects of strip delamination and moist environment on natural frequencies are greatly dependent on the boundary conditions.

- The woven fiber composite panels with $C-F-C-F$ boundary condition are the most affected in moist environment.

- Moisture effects on free vibration are more significant than percentage of strip delaminations for all composite panels.

A finite element vibration analysis of woven fiber laminated composite panels of various curvatures with strip delaminations in thermal field is presented which can handle any temperature range including sub-zero temperatures up to cryogenic range and elevated temperatures. The following conclusions are based on range of boundary conditions, geometry, materials and thermal effects.

- The natural frequencies of free vibration of woven fibre composite shells decrease with increase in temperature and delamination area due to reduction of stiffness for all laminates.
- The effects of delamination and thermal environment on natural frequencies are greatly dependent on the boundary conditions.
- Woven fiber composite shell panels with $C - F - C - F$ boundary condition are the most affected in thermal environment.
- Shells of different curvatures also show the reduction in stiffness resulting in reduction of frequencies of vibration due to development of complex stress system in thermal field.
- At sub-zero temperatures up to cryogenic range, the frequencies of free vibration increase than those at ambient temperature conditions due to the presence of residual compressive stresses in the woven fiber composite curved panels.
- The effect of thermal field is more significant than percentage of delaminations for all composite panels.

6.3 Buckling of delaminated composite panels in hygrothermal field

The present study highlights the effects of several parameters as temperature and moisture contents, delamination area, stacking sequence, boundary conditions and fiber orientations on the buckling load of bidirectional composite flat panels. Based on predicted and numerous test results, the broad conclusions are as follows:

- The buckling loads decrease with increase in temperature, moisture concentrations as well as delamination area.
- Variations in buckling loads are significant in $C-F-C-F$ BC than fully clamped condition for all stacking sequence and fiber orientations of the panels.
- Composite delaminated panels having $[45/-45]_8$ stacking sequence suffer much compared to other panels in both the boundary conditions in hygrothermal environment.
- It is observed that moisture uptake plays a key role in reducing the buckling loads than temperature for all delaminated composite panels under both boundary conditions.
- Curvilinear variations in buckling loads are marked more in moist cases than elevated temperatures for all stacking sequence and boundary conditions.

6.4 Parametric instability of delaminated composite panels in hygrothermal field

A finite element dynamic stability analysis is conducted to study the influences of various parameters like static load factor, dynamic load factor, delamination percentage, temperature, moisture, ply orientation, stacking sequence and different boundary

conditions on the excitation frequencies of symmetric, asymmetric, cross ply as well as angle ply bidirectional delaminated composite flat and doubly curved panels in hygrothermal field. Some of the broad conclusions from the above numerical investigation are:

- A general FEM based formulation is presented for vibration, buckling and parametric resonance characteristics of delaminated composite plates subjected to hygrothermal environment.
- The widening of DIRs is more with higher values of dynamic load factor for all composite laminates under different boundary conditions of the range of examples considered and is significant for $[45/-45]_8$ bidirectional composite flat panels than $[0/0]_8$ and $[30/-30]_8$ laminates.
- The influence of static load factor on the lower boundary frequencies is remarkable even in completely clamped boundary conditions for delaminated bidirectional composite panels.
- Significant thermal effects on the onset of instability are observed for all laminates with parabolic DIRs and the composite panel having $[45/-45]_8$ ply sequence is the worst affected among all varieties.
- Noteworthy influences of moist environment on dynamic stability characteristics are witnessed among all types of bidirectional delaminated composite flat panels under variety boundary conditions with exceptionally more parabolic DIRs than those in thermal field. High moisture concentrations degrade the excitation frequencies more than rise in temperature for all composite laminates.
- The lower boundary frequencies are drastically affected in moist environment than in thermal field at higher static and dynamic load factors for all bidirectional delaminated composite flat panels.

The above finite element parametric instability analysis of composite flat panels is extended to include doubly curved delaminated composite shell panels of various

curvature ratios exposed to hygrothermal field under various boundary conditions. The concluding remarks of this numerical investigation are:

- Effect of static load factor is seen much more in hyperbolic paraboloidal composite shells as compared to others under simply supported boundary conditions as discussed.

- Delamination plays a key role in degrading the excitation frequencies in almost all composite shell panels under simply supported boundary conditions at higher dynamic load factors affecting the instability regions more in case of cylindrical as well as hyperbolic paraboloidal shells.

- Among the two boundary conditions i.e. simply supported and completely clamped, considered in the numerical analysis; clamped boundary conditions shows better stability regions than the other one for all doubly curved shell panels. Only the hyperbolic paraboloidal composite panels become unstable at 0.4 dynamic load factor under simply supported condition.

- The instability regions of cylindrical and hyperbolic paraboloidal composite shell panels with higher dynamic load factors are highly affected at elevated temperatures than the other two panels showing the effects of thermal field.

- Moisture concentration plays a vital role for parametric instability of delaminated doubly curved composite panels highlighting the effects on DIRs of cylindrical, spherical and hyperbolic paraboloidal shells. Only the elliptic paraboloidal shell is comparatively more stable in moist environment than the other ones.

6.5 Final outcome of present work

Significant impact of delamination, temperature and moisture is observed on the vibration of laminated woven fibre composite flat and curved panels. These results can be used as a technique for structural health monitoring or testing of structural

integrity, performance and safety. The buckling response of delaminated bidirectional composite flat panels is highly influenced by stacking sequence, ply orientations, boundary conditions, size of delaminations in hygrothermal field. The parametric variations dealing with normalized buckling loads can be recommended as design aids for delaminated bidirectional composite flat panels under hygrothermal conditions. The variations of excitation frequencies are observed with symmetric, asymmetric, cross ply as well as angle ply delaminated bidirectional composite flat and doubly curved panels under different boundary conditions that can be utilized as good and bad vibration regimes for analysis and design of the composite structures under dynamic in-plane loads. These properties can be utilized to tailor the design of woven fiber delaminated composite flat and curved panels in hygrothermal environment. The above recommendations for design of composite panels are valid within the range of materials, hygrothermal and geometrical parameters utilized in the study.

6.6 Future scope of research

Possible extensions to the present work are:

- Forced vibration of delaminated panels in hygrothermal environment.
- Dynamic stability of stiffened composite panels subjected to hygrothermal field.
- Dynamic stability of hybrid composite panels with cutouts in hygrothermal field.
- Damping effects on instability regions of composite panels.
- Material nonlinearity formulation for vibration and stability of composite panels.
- Experimental investigations on dynamic instability of composite panels in hygrothermal environment.

Bibliography

Abot, J.L., Yasmin, A. and Daniel, I.M. (2005): Hygroscopic behavior of woven fabric carbon epoxy composites, *Journal of Reinforced Plastics and Composites*, Vol. **24**(2), pp. 195-207.

Acharya, A.K., Chakraborty, D. and Karmkar, A. (2007): *Free vibration of delaminated composite cylindrical shell roofs*, Vibration Problems ICOVP-2007. Publisher: Springer, Netherlands.

Acharyya, A.K. (2010): Natural frequencies and mode shapes of composite cylindrical delaminated shells by finite element, *Journal of Reinforced Plastics and Composites*, Vol. **29** (2), pp. 226-237.

Alijani, F., Amabili, M. and Bakhtiari-Nejad, F. (2011): Thermal effects on nonlinear vibrations of functionally graded doubly curved shells using higher order shear deformation theory, *Composite Structures*, Vol. **93**, pp. 2541-2553.

Alijani, F. and Amabili, M. (2013): Nonlinear dynamic instability of functionally graded plates in thermal environments, *International Journal of Non-Linear Mechanics*, Vol. **50**, pp. 109-126.

Allahbakhsh, H. and Shariati, M. (2013): Buckling of cracked laminated composite cylindrical shells subjected to combined loading, *Applied Composite Materials*, Vol. **20**, pp. 761-772.

Anderson, T.J. and Nayfeh, A.H. (1996): Natural frequencies and mode shapes of laminated composite plates: Experiments and FEA, *Journal of Vibration and Control*, Vol. **2**(4), pp. 381-414.

Alnefaie, K. (2009): Finite Element modeling of composite plates with internal delamination, *Composite Structures*, Vol. **90**, pp. 21-27.

Argento, A and Scott, R.A. (1993): Dynamic instability of laminated anisotropic circular cylindrical shells part II numerical results, *Journal of Sound and Vibration*, Vol.**162** (2), pp. 323-332.

Asha, A. V. and Sahu, S. K. (2011): Parametric instability of twisted cross ply laminated panels, *Aerospace Science and Technology*, Vol. **15**, pp. 465-475.

ASTM Standard: D3039/D 3039 M (2008): *Standard Test Method for Tensile Properties Of Polymer Matrix Composite Materials.*

ASTM Standard: D5687/D5687M-07 (2007): *Standard Guide for Preparation of Flat Composite Panels with Processing Guidelines for Specimen Preparation.*

ASTM Standard: D5229/D5229M-04 (2004): *Standard Test Method for Moisture Absorption.*

Asadi, E. and Qatu, M.S. (2012): Free vibration of thick laminated cylindrical shells with different boundary conditions using general differential quadrature, *Journal of Vibration and Control*, Vol.**19**(3), pp. 356-366.

Aslan, Z. and Sahin, M. (2009): Buckling behavior and compressive failure of composite laminates containing multiple large delaminations, *Composite structures*, Vol. **89**, pp. 382-390.

Baba, B.O. (2007): Buckling behavior of laminated composite plates, *Journal of Reinforced Plastics and Composites*, Vol.**26**, pp1637-1655.

Baba, B.O. and Baltaci, A. (2007): Buckling characteristics of symmetrically and antisymmetrically laminated composite plates with central cutout, *Applied Composite Materials*. Vol. **14**, pp. 265-276.

Babu, C.S. and Kant, T. (2000): Refined higher order finite element models for thermal buckling of laminated Composite and sandwich plates. *Journal of Thermal Stresses*, Vol.**23**, pp.111-130.

Bert, C.W. and Birman, V. (1987): Dynamic instability of shear deformable antisymmetric angle-ply plates, *International Journal of Solids and Structures*, Vol.**23**, pp. 1053-61.

Bert, C.W, and Birman, V. (1988): Parametric instability of thick, orthotropic, circular cylindrical shells, *Acta Mechanica*, Vol.**71**, pp. 61-76.

Birman, V, and Bert, C.W. (1990): Dynamic stability of reinforced composite cylindrical shells in thermal fields, *Journal of Sound and Vibration*, Vol. **142(2)**, pp. 183-190.

Bolotin, V.V. (1964): *The Dynamic stability of elastic systems*. Holden-Day, San Francisco.

Bolotin, V.V. (1996): Delaminations in composite structures: its origin, buckling, growth and stability, *Composites: Part B*, Vol. **27**(B), pp 129-145.

Bullions, T.A., Jungk, J.M. and Loos, A.C. (2000): Moisture sorption effects on Carbon fiber-reinforced Phenyl ethynyl-terminated $Ultem^{TM}$ composites. *Journal of Thermoplastic Composite Materials*, Vol. **13**, pp. 460-480.

Cappello, F. and Tumino, D. (2006): Numerical Analysis of Composite Plates with Multiple Delaminations Subjected to Uniaxial Buckling Load, *Composites Science and Technology*, vol. **66**(2), pp. 264-272.

Cawley, P. and Adams, R. D. (1978): The predicted and experimental natural modes of free-free CFRP plates. *Journal of Composite Materials*, Vol. **12**, pp. 336-347.

Cederbaum, G. (1991): Dynamic stability of shear deformable laminated plates, *AIAA Journal*, Vol. **29**, pp. 2000-2005.

Chai, G.B. (1994) : Free vibration of generally laminated composite plates with various edge support conditions. *Composite Structures*, Vol. **29**, pp. 249-258.

Chai, G. B., Chin, S. S., Lim, T. M. and Hoon, K. H. (1993): Vibration analysis of laminated composite plates: TV-holography and finite element method, *Composite Structures*, Vol. **23**, pp. 273-283.

Chai, G. B and Khong, P. W. (1993): The Effect of Varying the Support Conditions on the Buckling of Laminated Composite Plates, *Composite Structures*. Vol. **24**, pp. 99-106.

Chakraborty, S. and Mukhopadhyay, M. (2000): Free vibration responses of FRP composite plates, Experimental and Numerical studies. *Journal of Reinforced plastics and Composites*, Vol.**19** (7), pp.535- 551.

Chakrabarti, A. and Sheikh, A. H. (2006): Dynamic instability of laminated sandwich plates subjected to in-plane partial edge loading, *Journal of Ocean Engineering*, Vol.**33**, pp. 2287-2309.

Champanelli R.W. and Engblom, J.J. (1995): The effect of delaminations in graphite/PEEK composite plates on modal dynamic characteristics, *Composite Structures*, Vol. **31**, pp. 195-202.

Chandrashekhara, K. (1989): Free vibrations of anisotropic laminated doubly curved shells, *Computers and Structures*, Vol.**33**(2), pp.435-440.

Chang, T.P., Hu, C.Y. and Jane, K.C. (1998): Vibration of delaminated composite plates under axial load, *Mech. Structure*, Vol. **26**, pp. 195-218.

Chatterjee, S.N. and Kulkarni, S.V. (1979): Effects of environment, damping and shear deformations on flutter of laminated composite panels, *International Journal of Solids and Structures*, Vol. **15**, pp. 479-491.

Chattopadhyay, A. and Radu, A.G. (2000): Dynamic instability of composite laminates using a higher order theory, *Computers and Structures*, Vol. **77**, pp. 453-460.

Chattopadhyay, A., Radu, A.G. and Dragomir-Daescu, D. (2000): A high order theory for dynamic stability analysis of delaminated composite plates, *Computational Mechanics*, Vol. **26**, pp. 302-308.

Chattopadhyay, L. and Murthy, S.S. (2011): Analytical and finite element modeling and simulation of buckling and post buckling of delaminated orthotropic plates,*International Journal of Modeling and Scientific Computing*, Vol.**2**, pp. 97-104.

Chen, L. W. and Chen, Y.M. (1989): Vibration of hygrothermal elastic composite Plates, *Journal of Engineering Fracture Mechanics*, Vol.**31**(2), pp. 209-220.

Chen, L-W and Chen, L-Y. (1987): Thermal buckling of laminated composite plates,*Composite Structures*, Vol.**8**, pp.189-205.

Chen, W, Chen, C. and Shyu, J. (2013): Stability of parametric vibrations of laminated composite plates, *Applied Mathematics and Computations*, Vol. **223**, pp.127-138.

Chen, H., Hong, M., and Liu, Y. (2004): Dynamic Behavior of Delaminated Plates Considering Progressive Failure Process,*Composite Structures*, Vol. **66**, pp.459-466.

Chen, L. W. and Lee J. H. (1988): Vibration of thermal elastic orthotropic plates, *Journal of Applied Acoustics*, Vol. **27** (4), pp.287-304.

Chen, L.W. and Yang, J.Y. (1990): Dynamic stability of laminated composite plates by the finite element method.*Computers and Structures*, Vol.**36**, pp.845-851.

Cho, M., and Kim, J-S. (2001): Higher-Order Zig-Zag Theory for Laminated Composites With Multiple Delaminations,*Journal of Applied Mechanics*, Vol. **68**, pp. 869-877.

Cook, R.D., Malkus, D.S., Plesha, M.E. and Witt, R.J. (2007): *Concepts and applications of finite element analysis*, Fourth Edition, John Wiley and Sons, Singapore.

Damghani, M., Kennedy, D. and Featherston, C. (2011): Critical buckling of delaminated composite plates using exact stiffness analysis,*Computers and Structures*, Vol. **89**, pp. 1286-94.

Damghani, M., Kennedy, D. and Featherston, C. (2014): Global buckling of composite plates containing rectangular delaminations using exact stiffness analysis and smearing method,*Computers and Structures*, Vol. **134**, pp. 32-47.

Della, C.N. and Shu, D. (2007): Vibration of delaminated composites: A Review,*Applied Mechanics Reviews*, Vol. **60**, pp. 1-20.

Deolasi, P.J. and Datta, P.K. (1995): Parametric instability of rectangular plates subjected to localized edge compressing (compression or tension), *Computers and Structures*, Vol. **54**, pp.73-82.

Deolasi, P.J. and Datta, P.K. (1997): Experiments on the parametric vibration response of plates under tensile loading.*Experimental Mechanics*, Vol. **37**, pp. 56-61.

Dey, S. and Karmakar, A. (2012): Free vibration analyses of multiple delaminated angle ply composite conical shells - A finite element approach, *Composite Structures*, Vol. **94**, pp. 2188-2196.

Dey, S. and Karmakar, A. (2012): Natural frequencies of delaminated composite rotating conical shells: A finite element approach, *Finite Elements in Analysis and Design*, Vol. **56**, pp. 41-51.

Dey, S. and Karmakar, A. (2013): Effect of multiple delamination on free vibration behavior of quasi-isotropic composite conical shells, *Journal of Institution of Engineers India Sec C*, Vol. **94**(1), pp. 53-63.

Dey, P. and Singha, M.K. (2006): Dynamic stability analysis of composite skew plates subjected to periodic in-plane load, *Thin-Walled Structures*, Vol. **44**, pp. 937-942.

Dey, T. and Ramachandra, L. S. (2014): Static and dynamic instability analysis of composite cylindrical shell panels subjected to partial edge loading, *International Journal of Non-Linear Mechanics*, Vol. **64**, pp. 46-56.

Ding, K. and Tang, L. (1999): Three dimensional free vibration of thick laminated cylindrical shells with clamped edges, *Journal of Sound and Vibration*, Vol. **220** (1), pp.171-177.

DiSciuva, M. (1986): Bending, Vibration and Buckling of Simply Supported Thick Multilayered Orthotropic Plates: An Evaluation of the New Displacement Model, *Journal of Sound and Vibration*, Vol. **105**, pp. 425-442.

Eslami H and Maerz, S. (1995): Thermally induced vibration of asymmetric cross-ply plate with hygrothermal effects. *American Institute of Aeronautics of Astronautics Journal*, Vol.**33** (10), pp. 1986-1988.

Fakhari, V. and Ohadi, A. (2010): Nonlinear vibration control of functionally graded plate with piezoelectric layers in thermal environment,*Journal of Vibration and Control*, Vol. **17**(3), pp. 449-469.

Fazilati, J. and Ovesy, H.R. (2010): Dynamic instability analysis of composite laminated thin-walled structures using two versions of FSM, *Composite Structures*, Vol. **92**, pp. 2060-2065.

Fazilati, J. and Ovesy, H.R. (2012): Finite strip dynamic instability analysis of perforated cylindrical shell panels, *Composite Structures*, Vol. **94**, pp.1259-1264.

Fazzolari, F.A., Banerjee, J.R. and Boscolo, M. (2013): Buckling of composite plate assemblies using higher order shear deformation theory-an exact method of solution, *Thin Walled Structures*, Vol. **71**, pp. 18-34.

Fazzolari, F.A. and Carrera, E. (2013): Advances in the Ritz formulation for free vibration response of doubly curved anisotropic laminated composite shallow and deep shells,*Composite Structures*, Vol.**101**, pp. 111-128.

Flaggs, D. L. and Vinson, J. R. (1978): Hygrothermal effects on the buckling of laminated composite plates, *Fibre Science and Technology*, Vol. **11**(5), pp. 353-365.

Frostig, Y. and Thomsen, O.T. (2011): Nonlinear thermo mechanical behavior of delaminated curved sandwich panels with a compliant core,*International Journal of Solids and Structures*, Vol. **48**, pp. 2218-2237.

Gaiotti, M., Rizzo, C.M., Branner, K. and Berring, P. (2014): An high order Mixed Interpolation Tensorial Components (MITC) shell element approach for modeling the buckling behavior of delaminated composites, *Composite Structures*, Vol. **108**, pp. 657-666.

Gallego, A., Moreno-Garcia, P. and Casanova, C.F. (2013): Modal analysis of delaminated composite plates using the finite element method and damage detection via combined Ritz/2D-wavelet analysis,*Journal of sound and Vibration*, Vol. **332**, pp. 2971-2983.

Gandhi, M.V., Usman, M and Chao, L. (1988): Nonlinear vibration of laminated composite plates in hygrothermal environments,*Journal of Engineering Material Technology*, Vol.**110** (2), pp. 140-146.

Ganapathi, M. (1998): Dynamic instability of laminates subjected to temperature field,*Journal of Engineering Mechanics*, Vol.**124**, pp.1166- 1168.

Ganapathi, M., Boisse, P. and Solaut, D. (1999): Nonlinear dynamic stability analysis of composite laminates under periodic in-plane compressive loads. *International Journal for Numerical Methods in Engineering*, Vol. **46**, pp. 943-956.

Ganapathi, M. Patel, B.P. and Pawargi, D.S. (2002): Dynamic analysis of laminated cross-ply composite non-circular thick cylindrical shells using higher-order theory, *International Journal of Solids and Structures*, Vol.**39**, pp. 5945-5962.

Ganapathi, M., Varadan, T.K., and Balamurugan, V. (1994): Dynamic instability of laminated composite curved panels using finite element method, *Computers and Structures*, Vol. **53**(2), pp. 335-342.

Gim, C.K. (1994): Plate finite element modeling of laminated plates, *Composite Structures*, Vol. **52**, pp.157-168.

Gu, H. and Chhatopadhyay, A. (1999): An experimental investigation of delamination buckling and post buckling of composite plates, *Composites Science and Technology*, Vol. **59**, pp. 903-910.

Hadi, N.H. and Ameen, K.A. (2011): Nonlinear free vibrations of cylindrical shells with delamination using high order shear deformation theory: A finite element approach,*American Journal of Scientific and Industrial Research*, Vol. **2** (2), pp.251-277.

Hajlaoui, A., Jarraya, A., Kallel-Kamoun, I. and Dammak, F. (2012): Buckling analysis of laminated composite plate with delaminations using the enhanced assumed strain solid shell element, *Journal of Mechanical Science and Technology*, Vol. **26**(10), pp. 3213-3221.

Han, W. and Petyt, M. (1996): Linear vibration analysis of laminated rectangular plates using the hierarchical finite element method, *Computers and Structures*, Vol. **61**(4), pp.705-712.

Hosseini-Toudeshky, H., Hosseini, S. and Mohammadi, B. (2010): Buckling and delamination growth analysis of composite laminates containing embedded delaminations, *Applied Composite Materials*, Vol. **17**, pp. 95-109.

Hou, J.P. and Jeronimidis, G. (1999): Vibration of delaminated thin composite plates, *Composites, Part A*, Vol. **30**, pp. 989-995.

Hu, N., Fukunaga, H., Sekine, H. and Ali, K.M. (1999): Compressive buckling of laminates with an embedded delamination, *Composites Science and Technology*, Vol.**59**, pp. 1247-1260.

Hu, N., Fukunaga, H., Kameyama, M., Aramaki, Y. and Chang, F. K. (2002): Vibration Analysis of Delaminated Composite Beams and Plates Using

Higher-Order Finite Element, *International Journal of Mechanical Sciences*, Vol. **44**, pp. 1479-1503.

Huang, X. L., Shen, Hui-Shen and Zheng, Jian-Jun. (2004): Nonlinear vibration and dynamic response of shear deformable laminated plates in hygrothermal environments, *Composites Science and Technology*, Vol.**64**, pp. 1419-1435.

Hwang, S.F. and Liu, G.H. (2002): Experimental study for buckling and post buckling behaviours of composite materials with multiple delaminations, *Journal of Reinforced Plastics and Composites*, Vol. **21**, pp. 333-349.

Hwang, S.F. and Mao, C.P. (2001): Failure of delaminated carbon/epoxy composite plates under compression, *Journal of Composite Materials*, Vol.**35**, pp.1634-165.

Jansen, E.L. (2007): The effect of geometric imperfections on the vibrations of anisotropic cylindrical shells, *Thin Walled Structures*, Vol. **45**, pp. 274-282.

Jeyaraj, P., Ganesan, N and Padmanabhan, C. (2009): Vibration and acoustics response of a composite plate with inherent material damping in a thermal environment, *Journal of Sound and Vibration*, Vol.**320**, pp. 322-338.

Jones, R.M. (1975): *Mechanics of Composite Materials*, McGraw Hill, New York.

Jones, R. M. (2005): Thermal buckling of uniformly heated unidirectional and symmetric cross-ply laminated fiber-reinforced composite uniaxial in-plane restrained simply supported rectangular plates, *Composites: Part-A*, Vol. **36**, pp. 1355-1367.

Jinho, O., Maenghyo, C. and Kim, J. (2005): Dynamic analysis of composite plate with multiple delaminations based on higher order zigzag theory, *International Journal of Solids and Structures*, Vol. **42**, pp. 6122-6140.

Ju, F., Lee, H.P. and Lee, K.H. (1995): Finite element analysis of free vibration of delaminated composite plate, *Composites Engineering*, Vol. **5**(2), pp. 195-209.

Ju, F., Lee, H. P., and Lee, K. H. (1995): Free Vibration of Composite Plates with delaminations around Cutouts, *Composite Structures*, Vol. **31**, pp. 177-183.

Kant, T. and Mallikarjuna, A. (1989): A higher-order theory for free vibration of unsymmetrically laminated composite and sandwich plates. *Computers and Structures*, Vol. **32**, pp. 1125-1132.

Kang, C., Han, Z., Lu, G. and Zhang, S. (2011): Compressive buckling of composite plates with delamination, *Advanced Materials Research*, Vol. **150-151**, pp. 235-238.

Karmakar, A., Roy, H. and Kishimoto, K. (2005): Free vibration analysis of delaminated composite pre-twisted shells, *Aircraft Engineering and Aerospace Technology*, Vol. **77**(6), pp.486-490.

Kharazi, M. and. Ovesy, H.R. (2008): Post buckling behavior of composite plates with through-the-width delaminations, *Thin Walled Structures*, Vol.**46**, pp. 939-946.

Kim, H.J. and Hong, C.S. (1997): Buckling and postbuckling behaviors of composite laminates with a delamination, *Composites Science and Technology*, Vol.**57**, pp. 557-564.

Kim, H. and Kedward, K.T. (1999): A method for modeling the local and global buckling of delaminated composite plates, *Composite Structures*, Vol. **44**, pp. 43-53.

Kim, S. H., Chattopadhyay, A., and Ghoshal, A. (2003): Dynamic Analysis of Composite Laminates With Multiple Delaminations Using Improved Layerwise Theory,*AIAA Journal*, Vol. **41**, pp. 1771-1779.

Krawezuk, M., Zak, A. and Ostachowicz, W. (1997): Dynamics of cracked composite material structure, *Computational Mechanics*, Vol. **20**, pp. 79?83.

Kucuk, M. (2004): An investigation on buckling behaviour of simply supported woven steel reinforced thermoplastic laminated plates with lateral strip delamination, *Journal of Reinforced Plastics and Composites*, Vol. **23**, pp.209-216.

Kumar, N. J., Babu, P. R. and Pandu, R. (2013): Investigations on buckling behavior of laminated curved composite stiffened panels. *Applied Composite Materials*, doi 10.1007/s10443-013-9337-4

Kumar, S.K. and Singh, B .N. (2008): Thermal buckling analysis of SMA fiber reinforced composite plates using layer wise Model, *Journal Aerospace Engineering*, Vol.**53** (1), pp. 1-7.

Kumar, A., Bhargava, P. and Chakrabarti, A. (2013): Vibration of laminated composite skew hypar shells using higher order theory, *Thin Walled Structures*, Vol. **63**, pp. 82-90.

Kumar, A., and Shrivastava, R. P. (2005): Free Vibration of Square Laminates with Delamination around a central cutout using HSDT, *Composite Structures*, Vol. **70**, pp. 317-333.

Kumar, S.K., Cinefra, M., Carrera, E., Ganguli, R. and Harursampath, D. (2014): Finite element analysis of free vibration of delaminated composite plate with variable kinematic multilayer plate elements, *Composites: Part B*, http://dx.doi.org/10.1016/j.compositesb.2014.05.031

Kundu, C.K. and Han. J.H. (2009): Vibration characteristics and snapping behavior of Hygro-thermo-elastic composite doubly curved shells, *Composite Structures*, Vol.**91**, pp. 306-317.

Kundu, C.K and Han, Jae-Hung. (2009): Nonlinear buckling analysis of hygrothermoelastic composite shell panels using finite element method, *Composites Part- B*, Vol.**40**, pp. 313-328.

Kutlu, Z. and Chang, F.K. (1992): Modeling compression failure of laminated composites containing multiple through-the-width delaminations,*Journal of Composite Materials*, Vol. **26**, pp. 350-387.

Kwon, Y.W. (1991): Finite element analysis of dynamic instability of layered

composite plates using a high-order bending theory, *Computers and Structures*, Vol.**38**(1), pp. 57-62.

Lai, J. Y. and Young, K. F. (1995): Dynamics of graphite/epoxy composite under delamination fracture and environmental effects,*Composite Structures*, Vol. **30**, pp 25-32.

Lal, A. and Singh, B. N. (2010): Stochastic free vibration of laminated composite plates in thermal environments, *Journal of Thermoplastic Composite Materials*, Vol.**23**, pp. 57-77.

Lal, A., Singh, B. N. and Kumar, R. (2009): Effects of random system properties on the thermal buckling analysis of laminated composite plates. *Computers and Structures*, Vol.**87**, pp.1119-1128.

Lal, A. and Singh, B. N. (2010): Effect of uncertain system properties on thermo elastic stability of laminated Composite Plates under nonuniform temperature distribution, *International Journal of Applied Mechanics*, Vol.**2** (2), pp. 399-420.

Lal, A. Singh, B.N and Kale, S. (2011): Stochastic post buckling analysis of laminated composite cylindrical shell panel subjected to hygrothermomechanical loading, *Computers and Structures*, Vol. **93**, pp. 1187-1200.

Lam, K.Y, and Ng, T.Y. (1998) Dynamic stability analysis of laminated composite cylindrical shells subjected to conservative periodic axial loads, *Composites Part B: Engineering*, Vol.**29(6)**, pp. 769-785.

Lanhe, Wu. , Hangjur, W. Daobin. (2007): Dynamic stability analysis of functionally graded material plates by the moving square differential quadrature method, *Composite Structures*, Vol.**77**, pp. 383-394.

Lee, S.Y. (2010): Finite element dynamic stability analysis of laminated composite skew plates containing cutouts based on HSDT, *Composites Science and Technology*, Vol.**70**(8), pp.1249-1257.

Lee, C. Y. and Kim, J. H. (2013): Hygrothermal post buckling behavior of functionally graded plates, *Composite Structures*, Vol. **95**, 278-282.

Lee, Sang-Youl , Park, Dae-Yon. (2007): Buckling analysis of laminated composite plates containing delaminations using the enhanced assumed strain solid element, *International Journal of Solids and Structures*, Vol. **44**(24), pp. 8006-8027.

Lee, Sang-Youl, Chung, Dae-Seouk. (2010): Finite element delamination model for vibrating composite spherical shell panels with central cutouts,*Finite Elements in Analysis and Design*, Vol. **46**, pp 247-256.

Lee, S.Y and Yen, W.J. (1989): Hygrothermal effects on the stability of cylindrical composite shell panel, *Computers and Structures*, Vol. **33**(2), pp.551-559.

Lee, Sang-Youl. (2010): Finite element dynamic stability analysis of laminated composite skew plates containing cutouts based on HSDT, *Composites Science and Technology*, Vol. **70**, pp. 1249-1257.

Leissa, A. W. (1987): Recent studies in plate vibrations: 1981-1985, part-i, classical theory. *Shock and Vibration Digest*, Vol. **19**(2), pp. 11-18.

Leissa, A. W. (1987): Recent studies in plate vibrations: 1981-1985, part-ii, classical theory.*Shock and Vibration Digest*, Vol. **19**(3), pp. 10-24.

Leissa, A. W. (1983): Buckling of composite plates, *Composite Structures*, Vol.**1**, pp. 51-66.

Leissa, A.W. (1987): A review of laminated composite plate buckling, *Applied Mechanics Reviews*, Vol.**40**(5), pp. 575-591.

Leissa, A.W. and Narita, Y. (1984): Vibrations of completely free shallow shells of rectangular planform, *Journal of Sound and Vibration*, Vol. **96** (2), pp. 207-218.

Liao, C.L and Cheng, C.R. (1994): Dynamic stability of stiffened laminated composite plates and shells subjected to in-plane pulsating forces,*Journal of Sound and Vibration*, Vol.**174**(3), pp. 335-351.

Librescu, L and Lin,W. (1996): Vibration of geometrically imperfect panels subjected to thermal and mechanical loads,*Journal of Spacecraft Rockets*, Vol. **33**(2), pp.285-91.

Li, D., Tang, G., Zhou, J. and Lei, Y. (2005): Buckling analysis of a plate with built-in rectangular delamination by strip distribute transfer function method, *Acta Mechanica*, Vol.**176**, pp.231-245.

Li, D., Xu, J. and Qing, G. (2011): Free vibration analysis and eigenvalues sensitivity analysis for the composite laminates with interfacial imperfection, *Composites: Part B*, Vol. **42**, pp.1588-95.

Liew, K.M., Lim, C.W. and Kitipornchai, S. (1997): Vibration of shallow shells: a review with bibliography,*Applied Mechanics Reviews*, Vol. **50**, pp. 431-444.

Liew, K.M, Hu, Y.G. Zhao, X and Ng, T.Y. (2006): Dynamic stability analysis of Composite laminated Cylindrical Shells via the mesh-free kp-Ritz method, *Computer Methods in Applied Mechanics and Engineering*, Vol.**196**, pp.147-160.

Liew, K.M., Lee, Y.Y., Ng, T.Y. and Zhao, X. (2007): Dynamic stability analysis of composite cylindrical panels,*International Journal of Mechanical Sciences*, Vol.**49**, pp. 1156-1165.

Liew, K.M., Yang, J. and Wu, Y.F. (2006): Nonlinear vibration of a coating-FGM-substrate cylindrical panel subjected to a temperature gradient. *Computer Methods in Applied Mechanics and Engineering*, Vol.**195**, pp.1007-1026.

Liu, C-F and Huang, C-H. (1995): Free vibration of composite laminated plates Subjected to temperature changes, *Computers and Structures*, Vol.**60** (1), pp. 95-101.

Liu, P. F. and Zheng, J. Y. (2013): On the through-the-width multiple delamination, and buckling and postbuckling behaviors of symmetric and unsymmetric composite laminates,*Applied Composite Materials*, Vol. **20**, pp. 1147-1160.

Lo, S.H., Zhen, W., Cheung, Y.K. and Wanji, C. (2010): Hygrothermal effects on multilayered composite plates using a refined higher order theory, *Composite Structures*, Vol. **92**, pp. 633-646.

Luo, H. and Hanagud, S. (1996): Delamination modes in composite plates, *Journal of Aerospace Engineering*, Vol. **9**, pp. 106-113.

Marjanovic, M. and Vuksanovic, D. (2014): Layerwise solutions of free vibrations and buckling of laminated composite and sandwich plates with embedded delaminations, *Composite Structures*, Vol. **108**, pp. 9-20.

Matsunaga, H. (2007): Free vibration and stability of angle-ply laminated composite and Sandwich plates under thermal loading, *Composite Structures*, Vol. **77**(2), pp. 249-262.

Mohsen, F. and Amin, S. (2010): Analysis of delamination buckling and post buckling of composite structures by generalised differential quadrature method, *International Journal of Advanced Engineering Sciences and Technologies*, Vol. **1**, pp. 030-037.

Mond, M. and Cederbaum, G. (1992): Dynamic instability of antisymmetric laminated Plates, *Journal of Sound and Vibration*, Vol.**154**, pp.271-279.

Moorthy, J., Reddy, J.N. and Plaut, R.H. (1990): Parametric instability of laminated composite plates with transverse shear deformation,*International Journal of Solids and Structures*, Vol.**26**, pp.801-811.

Muggleton, J.M., Brennan, M.J and Rogers, C.D.F. (2014): Point vibration measurements for the detection of shallow-buried objects, *Tunnelling and Underground Spacwe Technology*, Vol. **39**, pp.27-33.

Nagai, K and Yamaki, N. (1988): Dynamic stability of circular cylindrical shells, *Acta Mechanica*. Vol. **71**, pp. 61-76.

Naidu, N.V.S and Sinha, P.K. (2007): Nonlinear free vibration of laminated Composite Shells in Hygrothermal condition, *Composite Structures*, Vol.**77**, pp. 475-483.

Nanda, N., Sahu, S.K. and Bandyopadhyay, J. (2010): Effect of delamination on the non-linear transient response of composite shells in hygrothermal environment,*International Journal of Structural Integrity*, Vol. **1**(3), pp. 259-279.

Nanda, N. and Sahu, S.K. (2012): Free vibration analysis of delaminated composite shells using different shell theories, *International Journal of Pressure Vessels and Piping*, Vol. **98**, pp. 111-118.

Nanda, N. and Pradyumna, S. (2011): Nonlinear dynamic response of laminated shells with imperfections in hygrothermal environments,*Journal of Composite Materials*, Vol. **45**(20), pp. 2103-2112.

Narita, Y. and Leissa, A.W. (1992): Frequencies and mode shapes of cantilever laminated composite plates. *Journal of Sound and Vibration*, Vol. **54**, pp.161-172.

Natarajan, S., Deogekar, P. S., Manickam, G. and Belouettar, S. (2014): Hygrothermal effects on the free vibration and buckling of laminated composites with cutouts, *Composite Structures*, Vol. **108**, pp. 848-855.

Ng, T.Y., Lam, K.Y and Reddy, J.N. (1998): Dynamic stability of cross-ply laminated composite cylindrical shells, *International Journal of Mechanical Sciences*, Vol. **40**(8), pp. 805-823.

Ng, T.Y., Lam, K.Y and Reddy, J.N. (1999): Dynamic stability of cylindrical panels with transverse shear effects, *International journal of Solids and Structures*, Vol. **36**, pp. 3483-96.

Nguyen, H., Ostiguy, G.L. and Samson, L.P. (1989): Effect of Boundary conditions on the Dynamic Instability and Non-linear Response of Rectangular plates II: Experiments, *Journal of sound and vibration*, Vol. **133**(3), pp. 401-422.

Noh, M. and Lee, S. (2012): free vibration of composite shells containing embedded delaminations based on the third order shear deformation theory, *KSCE Journal of Civil Engineering*, Vol. **16**(7), pp. 1193-1201.

Noh, Myung-Hyun and Lee, Sang-Youl. (2014): Dynamic instability of delaminated composite skew plates subjected to combined static and dynamic loads based on HSDT, *Composites Part B: Engineering*, Vol. **58**, pp. 113-121.

Noor, A. K and Burton, W. S. (1992): Three-dimensional solutions for the free Vibrations and buckling of thermally stressed multilayered angle-ply composite Plates, *Journal of Applied Mechanics*, Vol.**59** (4), pp. 868-877.

Obdrzalek, V. and Vrbka, J. (2010): Buckling of a plate with multiple delamination, *Engineering Mechanics*, Vol.**17**, pp. 37-47.

Oh, J., Maenghyo, C. and Kim, J.S. (2005): Dynamic analysis of composite plate with multiple delaminations based on higher-order zigzag theory, *International Journal of Solids and Structures*, Vol.**42**, pp. 6122-6140.

Oh, J., Cho, M. and Kim, J-S. (2008): Buckling analysis of composite shell with multiple delaminations based on a higher order zig-zag theory, *Finite Elements in Analysis and Design*, Vol. **44**, pp. 675-685.

Ostachowicz, W. M. and Kaczmarczyk, S. (2001): Vibrations of Composite Plates With SMA Fibres in a Gas Stream With Defects of the Type of Delamination, *Composite Structures*, Vol. **54**, pp. 305-311.

Ovesy, H.R., Ghannadpour, S. A. M. and Sherafat, M. H. (2010): Buckling analysis of laminated composite plates using higher order semi-analytical finite strip method, *Applied Composite Materials*, Vol.**17**, pp. 69-80.

Ovesy, H.R. and Fazilati, J. (2014): Parametric instability analysis of laminated composite curved shells subjected to non-uniform in-plane load, *Composite Structures*. Vol. **108**, pp. 449-455.

Ozben, T. (2009): Analysis of Critical Buckling Load of Laminated Composite Plates With Different Boundary Conditions using FEM and Analytical Methods, *Computational Materials Science*, Vol. **45**, pp.1006-1015.

Ramachandra, L.S. and Panda, S.K. (2012): Dynamic instability of composite plates subjected to non-uniform in-plane loads, *Journal of Sound and Vibration*, Vol. **331**, pp. 53-65.

Panigrahi, S.K. (2013): Structural design of single lap joints with delaminated FRP composites adherends, *Composites: Part B*, Vol. **51**, pp.112-120.

Parhi, P.K., Bhattacharyya, S.K. and Sinha, P.K. (2000): Finite element dynamic analysis of laminated composite plates with multiple delaminations, *Journal of Reinforced Plastics and Composites*, Vol. **19**, pp. 863-882.

Parhi, P.K., Bhattacharyya, S.K. and Sinha, P.K. (2001): Hygrothermal effects on the dynamic behavior of multiple delaminated composite plates and shells, *Journal of Sound and Vibration*, Vol. **248**(2), pp. 195-214.

Park, T. and Lee, S-Y. (2009): Parametric instability of delaminated composite spherical shells subjected to in-plane pulsating forces, *Composite Structures*, Vol. **91**, pp. 196-204.

Patel, B.P., Ganapati, M. and Makhecha, D.P. (2000): Hygrothermal effect on the structural behavior of thick composite laminates using higher order theory, *Composite Structures*, Vol. **56**, pp. 25-34.

Pavier, M.J. and Chester, W.T. (1990): Compression failure of carbon fiber reinforced coupons containing central delaminations, *Composites*, Vol.**21**, pp. 23-31.

Peck, S.C. and Springer, G.S. (1991): The behavior of delaminations in composite plates- Analytical and Experimental results. *Journal of Composite Materials*, Vol. **25**, pp. 907-929.

Pekbey,Y. and Sayman, O. (2006): A numerical and experimental investigation of critical buckling load of rectangular laminated composite plates with strip delamiantion, *Journal of Reinforced Plastics and Composites*, Vol. **25**, pp.685-697.

Petyt, M. (2010): *Introduction to finite element vibration analysis*, Second Edition, Cambridge University Press.

Pietropaoli, E. and Riccio, A. (2012): Finite element analysis of the stability (buckling and post-buckling) of composite laminated structures: well established procedures and challenges, *Applied Composite Materials*, Vol. **19**, pp. 79-96.

Prabhakara, D.L. and Datta, P.K. (1993): Parametric instability characteristics of rectangular plates with localized damage subjected to in-plane periodic load, *Structural Engineering Review*, Vol. **5**(1), pp. 71-79.

Pradyumna, S. and Bandyopadhyay, J. N. (2011): Dynamic instability behavior of laminated hypar and conoid shells using a higher order shear deformation theory, *Thin Walled Structures*, Vol. **49**, pp. 77-84.

Pradyumna, S. and Gupta, A. (2011): Nonlinear dynamic stability of laminated composite shells integrated with piezoelectric layers in thermal environment, *Acta Mechanica*, Vol. **218**, pp. 295-308.

Qatu, M.S., Sullivan, R.W. and Wang, W. (2010): Recent research advances on the dynamic analysis of composite shells: 2000-2009 Review, *Composite structures*, Vol. **93**, pp. 14-31.

Qatu, M.S. (1993): Vibration of doubly cantilevered laminated composite thin shallow shells, *Thin Walled Structures*, Vol. **15**(3), pp. 235-248.

Qatu, M.S. (1999): Theory and vibration analysis of laminated barrel thin shells, *Journal of Vibration and Control*, Vol. **5**, pp. 851-889.

Qinkai, H, and Fulei, C. (2013): Parametric instability of a rotating truncated conical shell subjected to periodic axial loads, *Mechanics Research Communications*, Vol. **53**, pp. 63-74.

Ravi Kumar, L., Datta, P.K. and Prabhakara, D.L. (2003): Tension buckling and dynamic stability behaviour of laminated composite doubly curved panels subjected to partial edge loading, *Composite Structures*, Vol. **60**(2), pp. 171-181.

Radu, A.G. and Chattopadhyay, A. (2002): Dynamic stability analysis of composite plates including delaminations using a higher order theory and transformation matrix approach, *International Journals of Solids and Structures*, Vol.**39**(7), pp.1949-1965.

Rao, V.V.S. and Sinha, P.K. (2004): Dynamic response of multi directional composites in hygrothermal environments, *Composite Structures*, Vol. **64**, pp. 329-338.

Rath, M.K. and Sahu, S.K. (2011): Vibration of woven fiber laminated composite plates in hygrothermal environment, *Journal of Vibration and Control*, Vol. **18**(13), pp. 1957-1970.

Reddy, J.N. (1979): Free vibration of anti-symmetric angle ply laminated plates including transverse shear deformation theory by finite element method, *Journal of Sound and Vibration*, Vol. **66**, pp. 565-576.

Reddy, J.N. (1990): A review of refined theories of laminated composite plates,*Shock and Vibration Digest*, Vol. **22**, pp. 3-17.

Ribeiro, P. and Jansen, E. (2008): Nonlinear vibrations of laminated cylindrical shallow shells under thermomechanical loading, *Journal of Sound and Vibration*, Vol. **315**, pp. 624-640.

Sahu, S.K. and Datta, P.K. (2007): Research Advances in the dynamic stability behaviour of plates and shells, 1987-2005, *Applied Mechanics Reviews*, Vol.**60**, 65-75.

Sahu, S.K., and Datta, P.K. (2003): Dynamic stability of laminated composite curved panels with cutouts, *Journal of Engineering Mechanics*, Vol.**129**(11), pp.1245-1253.

Sahu, S.K. and Datta, P.K. (2001): Parametric resonance characteristics of laminated composite doubly curved shells subjected to non-uniform loading, *Journal of Reinforced Plastics and Composites*, Vol. **20**(18), pp. 1556-1576.

Sahu, S.K. and Datta, P.K. (2001): Parametric instability of doubly curved panels subjected to non-uniform harmonic loading, *Journal of Sound and Vibration*, Vol. **240**(1), pp. 117-129.

Sairam, K.S. and Sinha, P.K. (1992): Hygrothermal effects on the free vibration of laminated composite plates, *Journal of Sound and Vibration*, Vol. **158**(1), pp. 133-148.

Sairam, K. S. and Sinha, P. K. (1992): Hygrothermal effects on the buckling of laminated composite plates, *Composite Structures*, Vol. **21**, pp. 233-247.

Salim, S., Iyengar, N. G. R. and Yadav, D. (1998): Buckling of laminated composite plates with random material characteristics, *Applied Composite Materials*, Vol. **5**, pp.1-9.

Sallam, S. and Simitses, G.J. (1985): Delamination buckling and growth of flat cross-ply laminates, *Composite Structures*, Vol. **4**, pp. 361-381.

Sciuva, M.D. and Carrera, E. (1990): Static buckling of moderately thick, anisotropic, laminated and sandwich cylindrical shell panels, *AIAA Journal*, Vol. **28**, pp. 1782-93.

Shan, B. and Pelegri, A.A. (2003): Approximate analysis of the buckling behavior of composites with delamination, *Journal of Composite Materials*, Vol. **37**(8), pp. 673-685.

Shen, H-S., Zheng, J-J. and Huang, X-L. (2004): The effects of hygrothermal conditions on the dynamic response of shear deformable laminated plates resting on elastic foundations, *Journal of Reinforced Plastics and Composites*, Vol. **23**(10), pp.1095-1113.

Shiau, L.C. and Zeng, J.Y. (2010): Free vibration of rectangular plate with delaminations, *Journal of Mechanics*, Vol. **26**(1), pp. 87-93.

Shukla, K. K., Nath, Y., Kreuzer, E. and Sateesh, K.V. (2005): Buckling of Laminated Composite Rectangular Plates, *Journal of Aerospace Engineering*, Vol.**18** (4), pp.215-223.

Simitses, G.J. (1987): Instability of dynamically loaded structures, *Applied Mechanics Reviews*, Vol. **40**(10), pp. 1403-1408.

Singh, B. N. and Verma, V. K. (2009): Hygrothermal effects on the buckling of laminated composite plates with random geometric and material properties, *Journal of Reinforced Plastics and Composites*, Vol. **28**(4), pp. 409-427.

Sofiyev, A.H. (2015): Influences of shear stresses on the dynamic instability of exponentially graded sandwich cylindrical shells, *Composites Part B: Engineering*, doi: http://dx.doi.org/10.1016/j.compositesb.2015.03.040.

Srivastava, A.K.L., Datta, P.K. and Sheikh, A.H. (2003): Dynamic instability of stiffened plates subjected to non-uniform harmonic edge loading, *Journal of Sound and Vibration*, Vol. **262**, pp.1171-1189.

Strozzi, M. and Pellicano, F. (2013): Nonlinear vibrations of functionally graded cylindrical shells,*Thin Walled Structures*, Vol. **67**, pp. 63-77.

Suemasu, H. (1993): Effects of multiple delaminations on compressive buckling behaviors of composite panels, *Journal of Composite Materials*, Vol. **27**, pp 1172-1192.

Suzuki, K., Kimpara, I. and Kageyama, K. (2004): Non-linear vibration and damping characterization of delaminated composite laminates by using multilayered finite element,*ICAS, 24th International Congress of the Aeronautical Sciences*, pp. 1-10.

Tauchert, T.R. (1991): Thermally induced flexure, buckling and vibration of plates, *Applied Mechanics Reviews*, Vol. **44**(8), pp 347-360.

Tenek, L. H., Hennekke, E. G., II and Gunzburger, M. D. (1993): Vibration of Delaminated Composite Plates and Some Applications to Non-Destructive Testing, *Composite Structures*, Vol. **23**, pp. 253?262.

Thornburg, R.P. and Chattopadhyay, A. (2003): Combined delamination and matrix cracking in adaptive composite laminates. *Proceedings of the 44th AIAA/ASME/ASCE/AHS/ASC structures, Structural dynamics and materials conference*, Norfolk,VA,7-10 April, pp.3395-3405.

Tsai, S.W. and Hahn, H.T. (1980): *Introduction to composite materials*, Technomic, Stanford, Connecticut, 1980.

Tsouvalis, N.G. and Garganidis, G.S. (2011): Buckling strength parametric study of composite laminated plates with delaminations, *Ships and Offshore Structures*, Vol. **6**, pp. 93-104.

Tumino, D., Cappello, F. and Rocco, D. (2007): 3D buckling analysis of delaminated composite specimens, *Science and Engineering of Composite Materials*, Vol.**14**, pp. 181-188.

Udar, R. S. and Datta, P. K. (2007): Parametric combination resonance instability characteristics of laminated composite curved panels with circular cutout

subjected to non-uniform loading with damping, *International Journal of Mechanical Sciences*, Vol. **49**, pp. 317-334.

Viola, E., Tornabene, F. and Fantuzzi, N. (2013): General higher order shear deformation theories for the freee vibration analysis of completely doubly curved laminated shells and panels, *Composite Structures*, Vol. **95**, pp. 639-666.

Wang, S. and Dawe, D.J. (2002): Dynamic instability of composite laminated rectangular plate and prismatic plate structures, *Computer Methods and Applied Mechanics Engineering*, Vol.**191**, pp. 1791-1826.

Wang, X., Yang, W.D. and Sheng, G. G. (2014): Non-linear buckling for the surface rectangular delamination of laminated piezoelectric shells, *Applied Mathematical Modeling*, Vol. **38**, pp. 374-383.

Whitney, J. M. and Ashton, J. E. (1971): Effect of environment on the elastic response of layered composite plates, *AIAA Journal*, Vol. **9**, pp. 1708-1713.

Wu, C. P. and Chiu, S. J. (2002): Thermally induced dynamic instability of laminated composite conical shells, *International Journal of Solids and structures*, Vol. **39**, pp. 3001-3021.

Yam, L.H., Wei, Z., Cheng, L. and Wong, W.O. (2004): Numerical analysis of multi-layer composite plates with internal delamination,*Computers and Structures*, vol.**82**, pp. 627-637.

Yang, J and Fu, Y. (2007): Analysis of dynamic stability for composite laminated cylindrical shells with delaminations, *Composite Structures*, Vol. **78**, pp. 309-315.

Yang, W.D., Zhang, W., Wang, X. and Lu, G. (2014): Non-linear delamination buckling and expansion of functionally graded laminated piezoelectric composite shells, *International Journal of Solids and Structures*, Vol. **51**, pp. 894-903.

Yeh, M. and Tung, K. (2006): Dynamic instability of delaminated composite plates under parametric excitation, *Key Engineering Materials*, Vol. **326-328**, pp. 1765-1768.

Yeh, M.K. and Tan, C.M. (1994): Buckling of elliptically delaminated composite plates, *Journal of Composite Materials*, Vol. **28**(1), pp. 36-52.

Zak, A., Krawczuk, M. and Ostachowicz, W. (2000): Numerical and Experimental Investigation of Free Vibration of Multilayer Delaminated Composite Beams and Plates, *Computational Mechanics*, Vol. **26**, pp. 309-315.

Zak, A., Krawezuk, M. and Ostachowicz, W. (2001): Vibration of a laminated composite plate with closing delamination, *Journal of International Material Systems and Structures*,Vol. **12**, pp. 545-551.

Zhang, Y., Fu, H. and Wang, Z. (2013): Effect of moisture and temperature on the compressive failure of CCF300/QY8911 unidirectional laminates, *Applied Composite Materials*, Vol. **20**, pp. 857-872.

Zhang, Y., Wang. S. and Loughlan, J. (2006): Free vibration analysis of rectangular composite laminates using a layer wise cubic B-spline finite strip method, *Thin Walled Structures*, Vol. **44**, pp. 601-622.

Zhang, Y.X. and Yang, C.H, (2009): Recent developments in finite element analysis for laminated composite plates, *Composite Structures*, Vol. **88**, pp.147-157.

Zheng, S. and Sun, C.T. (1998): Delamination interaction in laminated structures, *Engineering Fracture Mechanics*, Vol. **59**(2), pp. 225-240.

Zor, M. (2003): Delamination width effect on buckling loads of simply supported woven fabric laminated composite plates made of carbon/epoxy, *Journals of Reinforced Plastics and Composites*, Vol. **22**, pp. 1535-1546.

Zor, M., Sen, F. and Toygar, M. E. (2005): An investigation of square delamination effects on buckling behavior of laminated composite plates with a square hole by using three-dimensional FEM analysis, *Journal of Reinforced Plastics and Composites*, Vol.**24**, pp. 1119-1130.

Chapter - 7

Appendix

7.1 Convergence Studies

Convergence study is carried out for free vibration of composite plates under hygrothermal conditions without delamination and also the results are validated with available literature as shown in Table 7.1. Based on this convergence study and for convenience of calculation of particular percentage of delamination (i.e. $6.25\%, 25\%$ and 56.25%), 8×8 mesh is used throughout the studies.

Table 7.1: Convergence study of non-dimensional frequency $\varpi = \sqrt{[\omega a^2(\rho/E_2h^2)]}$ of simply supported [0/90/90/0] laminated Graphite/Epoxy plate

$a/b = 1, a/h = 100$
$E_1 = 130\ GPa$, $E_2 = 9.5\ GPa$, $G_{12} = 6.0\ GPa$,$G_{12} = G_{13}$, $G_{23} = 0.5G_{12}$
$\nu_{12} = 0.3$, $\alpha_1 = -0.3 \times 10^{-6}/K$, $\alpha_2 = 28.1 \times 10^{-6}/K$, $\beta_1 = 0$, $\beta_2 = 0.44$

Mesh Size	Non-dimensional Frequency	
	$T = 325K$	$C = 0.1\%$
4×4	8.079	9.422
6×6	8.039	9.387
8×8	8.036	9.384
10×10	8.036	9.384
Sairam and Sinha [1992] mesh 4×4	8.088	9.429